UNIVERSITA' DEGLI STUDI DI VERONA

DEPARTMENT OF

Neurosciences, Biomedicine and Movement Sciences

GRADUATE SCHOOL OF

Life and Health Sciences

DOCTORAL PROGRAM IN

Applied Life and Health Sciences

WITH THE FINANCIAL CONTRIBUTION OF

University of Verona

Cycle / year XXXVI/ 2020

TITLE OF THE DOCTORAL THESIS

The use of SARS-CoV-2 Pseudoviruses to investigate the neutralizing immunity and the pathogenesis of COVID-19

S.S.D. BIO/11

Coordinator: Prof. Simone Accordini

Signature _____

Tutor: Prof. Donato Zipeto

Signature _____

Doctoral Student: Dott. Tobia Fantoni

Signature _____

ABSTRACT

The Coronavirus Disease – 19 (COVID-19) occurs following SARS-CoV-2 infection with a wide spectrum of symptoms, which degenerate into severe acute respiratory syndrome (SARS) in susceptible patients or those with comorbidities. Although innovative vaccine technologies have been developed, the mutability of the virus, coupled with the natural decrease of neutralising antibodies (nAbs) that protect the organism by blocking the viral glycoprotein-human receptor interaction, has led to the administration of a booster dose of vaccine to increase the levels of protection against the newer variants (Omicron variants). nAbs targeting a virus are measured by enzymatic or cell-based serological tests. Among these, neutralisation assays that use pseudoviruses (PVNA) contributed to the investigation of anti-SARS-CoV-2 humoral immunity. PVs borrow the core from a known virus, engineered to be safe, whose envelope is replaced with that of a virus of interest. In this way, the infection mechanism is replicated in a safe, measurable and standardised manner. The PVNA on serum samples from 17 subjects receiving the third dose revealed that A) the vaccine stimulates the production of high specific antibody titres against the Spike protein, which wane after 4 months, B) these antibodies protect against the Omicron variants, C) older people produce fewer antibodies than younger people, D) hybrid immunity (having contracted the virus before or after the administration of the vaccine) provides better protection. These results are in line with what the literature reported. Although the technology of PVs contributed to the research on neutralization of SARS-CoV-2, it still suffers from the problems of using a cell line. An alternative strategy is to couple an enzymatic serological assay with the quantification of other biomarkers, such as circulating microRNAs, which are involved in the regulation of multiple processes, including the production of nAbs. The overexpression of miR-155-5p and downregulation of miR-148a-3p in serum are studied in the context of infections or following vaccination. Both are valuable candidates as potential biomarkers within a panel for the rapid assessment of the neutralising responses. Unfortunately, miR-155-5p was present in a few samples but its trend was similar to that of the literature. The analysis of miR-148a-3p also reflected what the literature reported. Despite this, no difference in expression over time was observed, nor did a direct correlation with specific antibody titre or protection levels emerge. PVs are also used to study cellular mechanisms, if they depend on the viral protein-host receptor interaction. Most severe COVID-19 patients show high levels of the SARS-CoV-2 receptor, ACE2, in soluble form in the circulation. ACE2 is normally released in circulation

by proteases, such as ADAM17. However, excessive levels of ACE2 occur in cardiovascular diseases. A study from 2021found that the SARS-CoV-2 spike-induced reduction in intracellular miR-28-3p expression corresponded to altered ADAM17 expression levels. This mechanism could explain one of the main causes of the pathogenesis of COVID-19. The experiments I performed showed that A) the original variant (Wuhan) and the BA.5 induce the reduction of miR-28-3p; B) the Wuhan variant does not induce alteration of ACE2 or ADAM17, C) the Omicron BA.5 variant appears to reduce both the number of ACE2-positive and ADAM17-positive cells at 12 h incubation, although the alteration is minimal and not significant, D) there is no correlation between miR-28-3p expression levels and the number of ACE2- and ADAM17-positive cells. In conclusion, this thesis presents the advantageous aspects and limitations of using SARS-CoV-2 PVs technology to study neutralising immunity, in comparison to other serological tests, proposing an alternative approach, and understanding the pathogenesis of COVID-19.

INDEX

ABBREVIATIONS

96WP	96-well plate
ACE	Angiotensin-converting enzyme
ACE2	Angiotensin-converting enzyme 2
ADAM17	A Disintegrin and Metalloprotease 17
Ang	Angiotensin
AIDS	Acquired Immune Deficiency Syndrome
BNT1626b2	BioNTech 162b2 vaccine
BSL	Biosafety Level
BuHV-1	Bubaline alpha herpesvirus – 1
CDC	Centre for Disease Control
CHO	Chinese Hamster Ovary
CMIA	Chemiluminescent Microparticle Immunoassay
CTRL	Control
CoV	Coronavirus
COVID-19	Coronavirus Disease – 2019
CPE	Cytopathic Effect
DMEM	Dulbecco's Modified Eagle Medium
DNA	Deoxyribonucleic Acid
ELISA	Enzyme-Linked Immunosorbent Assay
ER	Endoplasmic Reticulum
FACS	Fluorescence Activated Cell Sorting
FBS	Foetal Bovine Serum
HCoVs	Human Coronaviruses
HCW	Healthcare Worker
HEK293T	Human Embryonic Kidney 293T
HIV-1	Human Immunodeficiency Virus – 1
HR1/HR2	Heptad repeats 1/2
HRP	Horseradish Peroxidase
IC50	Inhibitory concentration 50
IgG	Immunoglobulin G

IgM	Immunoglobulin M
KO	Knockout
MERS	Middle-East Respiratory Syndrome
miR	microRNA
miRNA	microRNA
MLV	Murine Leukaemia Virus
MNA	Microneutralization Assay
mRNA	Messenger-Ribonucleic Acid
nAbs	Neutralizing Antibodies
Nsp	Non-structural proteins
NTD	N-terminal Domain
PBMCs	Peripheral Blood Mononuclear Cells
PBS	Phosphate Buffered Saline
PEI	Polyethyleneimine
PI	Previously Infected
PMA	phorbol myristate aspartate
PV	Pseudotyped virus
PVNA	Pseudotyped virus Neutralization Assay
RAS	Renin-angiotensin system
RBD	Receptor-Binding Domain
RBM	Receptor-Binding Motif
RLU	Relative Luminescence Units
RNA	Ribonucleic Acid
rpm	revolution per minute
RT	Room temperature
RT-qPCR	Real-time – quantitative Polymerase Chain Reaction
SARS	Severe Acute Respiratory Syndrome
TACE	Tumour Necrosis Factor-alpha converting enzyme
$TCID_{50}$	Tissue culture infectious dose 50
TMB	3,3',5,5' -tetramethylbenzidine
TMPRSS2	transmembrane protease, serine 2
UT	Untreated
VBM	Variant Being Monitored

VOC	Variant of Concern
VOHC	Variant of Hich Consequence
VOI	Variant of Interest
VSV-G	Vesicular Stomatitis Virus - Glycoprotein
WHO	World Health Organization

1. INTRODUCTION

1.1. The emergency of COVID-19

Human history is littered with the mysterious appearance of new, seemingly unexplainable diseases, which put the unprepared population under socio-political and healthcare threats. From the Plague of Athens (430 B.C.ca) (Thucydides, "History of the Peloponnesian War"), through the “Black Death” during the Middle Ages (Benedictow, 2021) and Spanish influenza (Taubenberger and Morens, 2006), to the contemporary pandemic of Acquired Immune Deficiency Syndrome (AIDS) (Sharp and Hahn, 2010), invisible pathogens contributed to the development of new containment strategies, potent detection methods and innovative therapies to reduce their spread and effects on the population. During the past four years, the propagation of the Coronavirus Disease 2019 (COVID-19) changed the known proportion and spreading rates of pandemics, the perception of infectious diseases in the population and the importance of detecting and investigating viruses to prevent future spillovers.

At the end of the first trimester of 2020, the COVID-19 pandemic spread worldwide six months after the registration of the first cases of a novel respiratory disease in Wuhan, Hubei, China (Zhou et al., 2020). Patients suffered from symptoms similar to those induced by severe acute respiratory syndrome (SARS) Coronavirus (SARS-CoV) of the first threatening epidemic at the beginning of the third millennium (Hui et al., 2003). Later identified as a *Betacoronavirus*, it was named SARS-CoV-2 due to the similarities with the first SARS Coronavirus of 2003 (Wan et al., 2020).

At the time of writing, more than 700 million cases of SARS-CoV-2 infection were registered and severe COVID-19 was responsible for almost 7 million deaths (WHO Coronavirus (COVID-19) dashboard). COVID-19 manifests itself in a wide spectrum of symptoms, starting from fever, cough, fatigue and dyspnoea (Alimohamadi et al., 2020). The patients that develop the most severe form present hyperinflammatory responses that degenerate in lung disfunction and multi-organ failure (Nagy et al., 2021). These people usually suffer from coexisting pathological conditions, such as cardiopathies, pulmonary disease, cancer and many others (Silaghi-Dumitrescu et al., 2023). Subsequently, the virus mutated and adapted to the human organism, generating a series of variants (Tosta, 2022). The development of innovative vaccine technologies allowed to manage and contain the onset of severe symptoms, also protecting most fragile patients. However, although the vaccination across the whole population caused

the apparent loss of aggressiveness of the virus, the infectious properties of SARS-CoV-2 increased, making the most recent variants easily escape the vaccine-induced immunity (Malik et al., 2022). This thesis will discuss the importance of studying the molecular characteristics of humoral immunity against COVID-19 and the pathogenesis of SARS-CoV-2, taking advantage of the viral pseudotyping technology.

1.2. SARS-CoV-2: origins, evolution, and main features

Human Coronaviruses (HCoVs) belong to the subfamily of *Coronavirinae* of the *Coronaviridae* family, which is divided into four genera, named after the first letters of the Greek alphabet (*Alpha-*, *Beta-*, *Gamma-*, *Delta- coronavirus*). The former two groups, *Alpha-* and *Betacoronavirus,* are of peculiar interest because they also infect humans. Alpha-CoVs include the HCoV-229E and -NL63, whereas -HKU1 and -OC43 belong to the Beta-CoV group. These are called seasonal HCoVs, as they are usually responsible for common colds since they infect the respiratory tract. SARS-CoV, Middle East Respiratory Syndrome (MERS)-CoV and SARS-CoV-2 are also included in this same group. These viruses are of paramount importance since they have led to epidemics and pandemics during the past two decades. HCoVs are RNA positive-sense viruses that share several features: the structure, the length of the genome (~27-32 kbs), the mechanism of entry and the replication cycle (Cui et al., 2019; Koma et al., 2020; Lim et al., 2016; Nassar et al., 2021). The analysis of the Receptor-Binding Domain (RBD) region on the Spike protein, which mediates the viral entry and will be discussed later in this thesis, revealed that SARS-CoV-2 may have originated from the recombination of bat Coronaviruses RaTG13 and MP789 (Flores-Alanis et al., 2020).

Because of their ribonucleic nature, which implies a more pronounced tendency to accumulate mutations, Coronaviruses quickly evolve, generating multiple variants as an effect (Cosar et al., 2022). Mutation events include substitutions, insertions and deletions (indels), and recombination. Several factors naturally impact the process of generating and acquiring mutations, and consequently new features, such as the replication mechanisms and immune system of the host, the environment, and the mechanism and rate of transmission (Qin et al., 2022). The intervention of therapeutics (intensive care, drugs, vaccines, etc.) could further influence the evolution of the virus. Three major hypotheses could explain the origin, spreading and alternate switching of dominant mutants in humans. First,

the slow variant detection program could not sustain the rapid evolution of the virus. Second, the presence of other permissive mammals could have predisposed several animal reservoirs, from which the virus could have spilt again into humans because of multiple zoonotic events (reverse zoonoses) (Pramod et al., 2021). Lastly, chronic COVID-19 patients (cancer, immunocompromised patients, etc.) could have been the major reservoir for SARS-CoV-2 for progressive accumulation of mutations. To date, these hypotheses are still under debate; however, the possibility of prolonged accumulation of mutations that could happen in long-term immunodeficient patients remains the most plausible, especially for the most recent variants (Bahadur Shrestha et al., 2022; Markov et al., 2023).

SARS-CoV-2 variants have been classified into four categories by the Centre for Disease Control (CDC): Variants of High Consequence (VOHCs), Variants of Concern (VOCs), Variants of Interest (VOIs), and Variants Being Monitored (VBMs). From the VOHC to VBM evaluation grade, variants are included and recorded whether the diagnostic and clinical characteristics are satisfied, from reduced response to available drugs/treatments to low circulating/extinct variants. For this reason, VOHCs and VOCs are the most studied and monitored. As one variant surpasses the others, those are then classified as VBMs (CDC, 2020). The major former VOCs will be partially discussed in this manuscript and are listed in the table below (Table 1).

The genome of all HCoVs is organized into genes encoding for structural, non-structural (Nsp) and accessory proteins. The genome of SARS-CoV-2 presents 26 of them, grouped as 4 structural, 16 Nsps and 6 accessory ones (Justo Arevalo et al., 2023). Nsps are important for the suppression of the host cell processes by reorienting its metabolism towards viral replication. Therefore, Nsps can induce cellular mRNA and protein degradation, interfering with antiviral responses, whereas they guide viral protein translation, maturation and localization, vesicle formation, and many other functions (Tam et al., 2023). On the other hand, structural proteins determine the morphology, the attachment and the infection of SARS-CoV-2. HCoVs are known for the typical “crown-shaped” structures observed with the electron microscope. SARS-CoV-2 also harbours disproportionately large, trimeric structures protruding from the envelope, called Spikes (Spike protein, or S). The main function of the S protein is the attachment to the target cell and the fusion of the viral envelope to the cellular membrane to mediate the entrance into the host’s cellular machinery (Verma and Subbarao,

2021). The E (envelope) and M (membrane) proteins are also anchored in the viral phospholipid double-leaflet. These proteins are mainly deputed to ionic flux and envelope shaping, respectively (Kakavandi et al., 2023). Lastly, the N (nucleocapsid) protein is fundamental for the assembly of the viral RNA-based genome into the virion (Justo Arevalo et al., 2023; Naqvi et al., 2020). Because of its importance in driving the initiation of the infection and stimulating efficient, protective humoral immunity, a deeper description of the Spike protein is discussed in the following paragraph.

Variant Name	**Origin**	**First detected**
Wuhan	China	Sep/Oct 2019
Alpha (B.1.1.7)	United Kingdom	Sept 2020
Beta (B.1.351)	South Africa	Sept 2020
Gamma (P.1)	Brazil	Dec 2020
Delta (B.1.617.2)	India	Dec 2020
Omicron BA.1	South Africa	Nov 2021
Omicron BA.2	South Africa	Nov 2021
Omicron BA.3	South Africa	Nov 2021
Omicron BA.4	South Africa	Jan 2022
Omicron BA.5	South Africa	Feb 2022
Omicron BA.2.75	India	Feb 2022
Omicron BA.2.86	Denmark/Israel	July 2023

Table 1. *List of SARS-CoV-2 more important VOCs, now de-escalated, from the original strain from Wuhan to the Omicron BA.2.86 (CDC, 2020).*

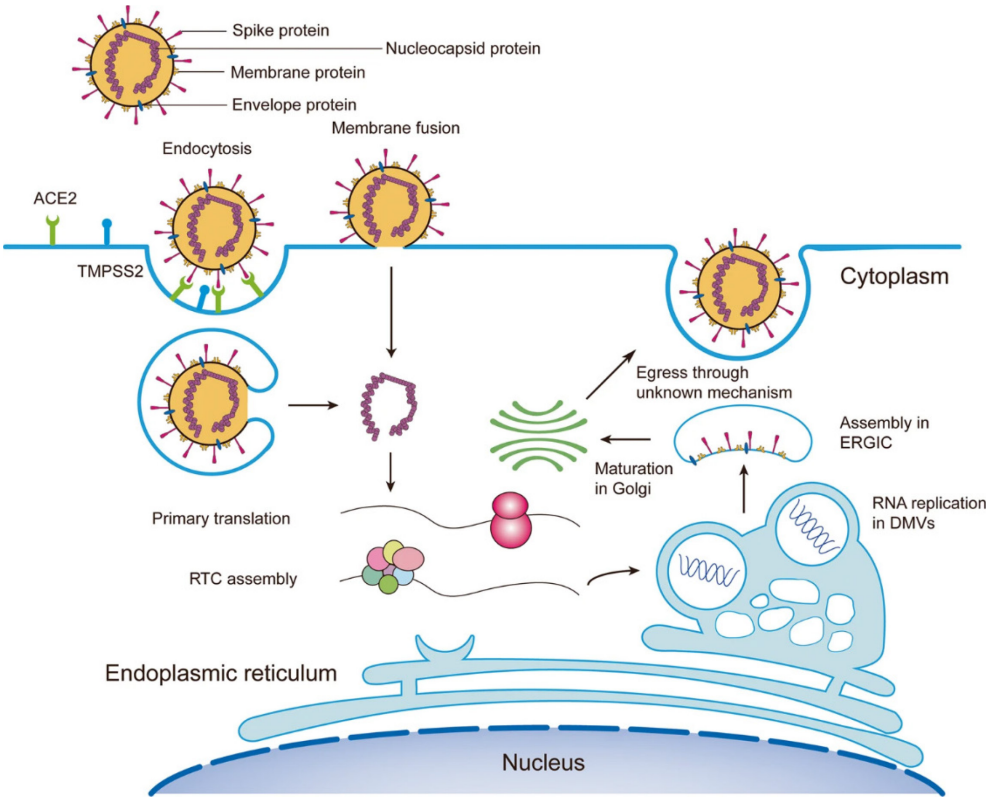

Figure 1. The life cycle of SARS-CoV-2. *The virus enters the target cells by binding to the receptor (ACE2) and the co-receptor (TMPRSS2), a process that leads to the fusion of membranes and the release of the viral genome into the cytoplasm. Next, the virus genome is translated into mature, functional proteins that contribute to the replication. The virion is then assembled in proximity to the Endoplasmic Reticulum (ER) and released by budding through the secretory pathway involving the Golgi apparatus. The schematic representation of the structure of SARS-CoV-2 is also shown (top left). Image adapted from P. Chen et al., 2023.*

1.3. The Spike protein

The entry of SARS-CoV-2 into human pulmonary cells occurs in two main phases: the attachment and the fusion processes. Both are mediated by the S protein on the virus side; many proteins could mediate the entrance on the cellular side (Baggen et al., 2021; Barthe et al., 2023). The highly-glycosylated Spike protein on the viral envelope is a trimeric complex, consisting of single-chain segments which belong to the class I fusion proteins (Wrapp et al., 2020). The S trimers on the surface of mature virions exist in a pre-fusion state, that requires activation induced by the host's proteases to initiate the fusion process (Benhaim and Lee, 2020; Colman and Lawrence, 2003).

The S protein monomer is divided into two main domains, S1 and S2, connected by the hinge region. Each one could be further distinguished into regions and

subdomains. S1 includes the signal peptide region for protein localization, the N-terminal domain (NTD), and the Receptor-Binding Domain (RBD) for attachment and binding to the receptor, the Angiotensin-converting enzyme 2 (ACE2) (Hoffmann et al., 2020b). Within the RBD, the receptor-binding motif (RBM) is included and it is necessary for attaching to the receptor (Lan et al., 2020). On the other side of the protein, the S2 domain includes the fusion-mediating heptad repeats (HR1 and HR2), and the C-terminal portion, which harbours the transmembrane region and the cytoplasmic tail (Jun Zhang et al., 2021).

Since the beginning of the pandemic, ACE2 has been defined as the main receptor of SARS-CoV-2. The transmembrane protease, serine 2 (TMRPSS2) was thereafter identified as the priming protease that triggers the activation of the fusion process, by splitting the protein at the S2' cleavage site, within the S2 domain. In addition, furin has been pointed out as a fundamental enzyme. It is necessary for cleaving the Spike protein at the S1/S2 interface during the virus replication, rendering it accessible to TMPRSS2 (Hoffmann et al., 2020a; Walls et al., 2020; Wrobel et al., 2020; Zhang et al., 2023). Due to the ubiquitous expression of furin-like proteases, the presence of the furin cleavage site into the Spike protein broadens the tropism of SARS-CoV-2 (Lu et al., 2015).

The infection is a complex succession of processes that begins with the attachment phase (Fig. 2). The trimeric Spike binds to the ACE2 receptor through the RBM within the RBD. It has been found that the single monomers are in alternate open/close conformations (namely, also "up"/"down" states) (Evans and Liu, 2021; Wrapp et al., 2020; Wrobel et al., 2020; Xu et al., 2023): this mechanism allows for maximum attachment/affinity rate, without excessive exposure of the RBD. Also, the presence of the cleaved furin site promotes more dynamic interchangeable conformations (from a more closed conformational state to a more open one) (Wrobel et al., 2020). The second phase, the fusion, is triggered by the RDB-ACE2 contact, which exposes the S2' site, which is furtherly cleaved by TMPRSS2; this process results in the shedding of the S1 domain (Sinha et al., 2023; Walls et al., 2020). This event causes the stretching of the S2 region, which binds to the host membrane and completes the fusion by exploiting the presence of the HR1/HR2 region (Sinha et al., 2023). The more prominent aspect surrounding the Spike protein is the tendency to accumulate mutations. Specifically, the region which mediates attachment (RBD) is more prone to acquire alterations (Mengist et al., 2021). The modification of its

structure could lead to the transition to other entry mechanisms. In fact, with the emergence of the Omicron sub-lineage, the main entry pathway moved from the ACE2/TMPRSS2 fusion mechanism to the endosomal cathepsin-mediated route (Bruel et al., 2022; Pather et al., 2023). Therefore, it is the most studied SARS-CoV-2 protein, since it is implied in immune escape, for vaccine design and development (Gaspersic and Dolzan, 2022; Le et al., 2023; Malik et al., 2022). Future studies investigating the main entrance mechanism and indirect infection mechanisms will be helpful in the discovery of drugs and the understanding of the maintenance of adaptive immunity against the spike protein to confer more robust protection (Evans and Liu, 2021).

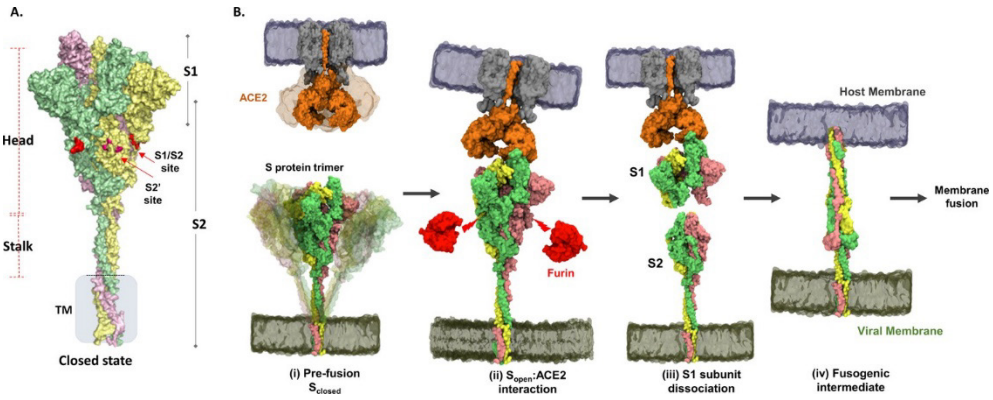

Figure 2. The structure of the Spike protein of SARS-CoV-2 (A) and the molecular representation of the attachment and fusion processes (B). *The Spike is a trimeric glycoprotein protruding from the envelope of the SARS-CoV-2 virion. The "head" portion includes the S1 and S2 regions, and it is connected to the membrane through a "stalk" (A). The attachment phase is initiated as the S1, proximal to the ACE2 receptor, switches from the closed (i) to the open state (ii). Human proteases process the ACE2/Spike complex and release the S1 portion (iii), leaving the S2 accessible for the fusion phase (iv) (B). Image from a published article (Raghuvamsi et al., 2021).*

1.3.1. Anti-SARS-CoV-2 neutralizing activity elicited by vaccination

If molecular drugs are intended to cure a disease or a pathological state, vaccination is a specific type of drug that can prevent the onset of harmful, infectious diseases long-term, by stimulating the immune system in recognizing the external agent. The more the population is protected by the vaccine, the more limited the circulation of the virus and the lower the onset of the life-threatening infectious disease (Clemente-Suárez et al., 2020). In addition, limiting the circulation of the virus in immunocompromised individuals could reduce the

emergence of new, fugacious variants, which could become more virulent VOCs (Carabelli et al., 2023).

Several vaccine technologies were proposed in response to the COVID-19 pandemic, including inactivated virus, viral vectors, DNA/mRNA-based and protein vaccines (Fathizadeh et al., 2021). Next-generation vaccines, like mRNA-based ones and adenoviral vectors, were preferred over other conventional technologies because of the timing and costs of production, testing, and safety profile. Also, conventional (based on live attenuated or inactivated viruses, and viral proteins) vaccines usually require multiple administrations to mount a durable response (Khare et al., 2023).

The administration of mRNA-based (BNT162b2 and mRNA-1273) and adenoviral vector (ChAdOx1) vaccines was approved in Italy at the end of 2020 (Bellino, 2021). At that time, available data suggested the administration of two doses within 21 days, 28 days and 4 weeks for BNT162b2, mRNA-1273 and ChAdOx1, respectively, from the first injection to induce a sustained level of protection against the circulating variants (Khare et al., 2023). Later, the ChAdOx1 platform was abandoned due to reported adverse effects (Greinacher et al., 2021), also in favour of the more efficient immune protection induced by the mRNA-based vaccines (Bellino, 2021). All these vaccines included the optimized and/or modified sequence of the Spike protein because it is the first viral target that is physically exposed to the immune system (Castruita et al., 2023). The infection, and therefore the onset of COVID-19, could be blocked by interfering with the entry of the virus.

A few months later, the emergency of new variants raised a new debate on the effectiveness of the available vaccine platforms. More and more studies highlighted and suggested the necessity of administering a third booster dose to enhance and preserve a sustained protective effect induced by the vaccine (Yue et al., 2022). Investigating and understanding the multiple mechanisms that allow the virus to evade the immune reaction and pharmacological treatments will contribute to developing more efficient vaccines. Mechanical and structural features that promote evasion are the elevated number of glycosylation sites, the alternation of open/closed conformational states, and the switching to other preferential entry routes (Casalino et al., 2020; Wrapp et al., 2020; S. Zhang et al., 2021). These can be influenced by the accumulation of mutations, because of the absence of an efficient proof-reading activity. Also, the immune system itself, potentially with the support of vaccination, exerts selective pressure on the virus

(Andreano et al., 2021; Malik et al., 2022). As a result, the Spike protein becomes less accessible to the primary participants in the blockade of direct virus-host interactions, which are antibodies, specifically neutralizing antibodies (nAbs) (Pastorio et al., 2022; von Bülow et al., 2023). These are defined as those glycoproteins produced by humoral immunity that specifically target receptor-binding and/or fusion-activating sites, the binding of the viral glycoprotein to its cellular target is abrogated, and the pathogen could be regularly eradicated (Srinivasan et al., 2016). In the case of SARS-CoV-2, nAbs target the RBD, the NTD and the S2 regions (Y. Chen et al., 2023; Sinha et al., 2023; Xia, 2021). nAbs are produced by activated, mature plasma cells and circulate into the bloodstream. Because of these properties, nAbs can be easily isolated, processed and analyzed, with the minimum invasiveness. The study of anti-SARS-CoV-2 nAbs, how they are stimulated and produced, can also contribute to the development of therapeutic tools against, to date, uncurable viral disease (AIDS, C hepatitis) (Y. Chen et al., 2023; Srinivasan et al., 2016).

The progressive decay of nAbs after vaccination emerged early after the first doses were administered (Ibarrondo et al., 2021; Vicenti et al., 2021). From the Alpha to the Delta variants in 2021, several studies highlighted and suggested the necessity to induce stronger protection in the population by administering a booster dose (Cele et al., 2022; Furukawa et al., 2022). Later, the emergency of the Omicron VOC family required the administration of multiple doses to stimulate a more robust immunity (Choi et al., 2022). The reasons for the progressive decay of nAbs are several. First, as mentioned before in this thesis, the elevated mutational rate of the virus promotes its immune evasion (Chakraborty et al., 2022; Sun et al., 2022). Second, some factors are associated with a worse response to the virus and the vaccine. For example, ageing and the consequent loss of efficiency of the immune system influence the process (Xu et al., 2020). Also, female subjects appear to be more prone to produce highly specific anti-Spike IgGs (Piubelli et al., 2023). In general, several studies identified that hybrid immunity, that is, exposure to the virus and the vaccine, produces stronger, long-term protection against upcoming variants (Cameroni et al., 2022). The analysis of the humoral reaction to the vaccine can help monitor the necessity of receiving the vaccine, the development of new vaccines and saving people who suffer the most severe form of the disease.

1.3.2. Serological assays for evaluating anti-SARS-CoV-2 protection

Nowadays, the comprehension of all the participants in the immune system and the extremely complex network of cells and molecules that protect the organism requires the application of multiple, high-throughput technologies, resulting in laborious, expensive analysis (Goldblatt et al., 2022). Testing the presence of antigen-specific antibodies with serological assays is one first, rapid approach to analysing the actual response to the vaccine (Dalle Carbonare et al., 2021; Plotkin, 2010). However, the mere measure of the antibody titre is reductive, as it only partially allows for outlining the complete picture of the neutralizing response. For this reason, by knowing that the nAbs have a first-line protective role, measuring their titre allows for a screening of the protection level against the pathogen, to evaluate the prioritization of vaccination (Y. Chen et al., 2023; Du et al., 2021; Kitikoon and Vincent, 2014; Mishra et al., 2021; Walker and Burton, 2018).

A series of cell-free and cell-based assays were developed for this purpose. The first method presented here is the titration of Spike-targeting IgMs and IgGs using the SARS-CoV-2 IgM and IgG II Quant Assays developed for the Abbott ARCHITECT platform. Also, IgGs targeting the N protein can be measured using the SARS-CoV-2 IgG Quant Assay, to test previous exposure to the virus. These chemiluminescent microparticle immunoassays (CMIA) utilise magnetic nanoparticles to capture Spike (RBD)-specific antibodies in a suspension and label them with a luciferase-conjugated secondary antibody. Using a calibration curve, the relative luminescence units (RLU) emitted by the microparticle complex allow for quantification of the titre of the RBD-binding antibodies (Hemken et al., 2023; Narasimhan et al., 2021; Takahashi et al., 2023). The described CMIA is an automated, diagnostic test, requiring the dedicated device to be run. This platform is usually inaccessible to most laboratories that are not directly involved in diagnostics.

A more accessible assay is the cPass SARS-CoV-2 Neutralization Antibody Detection Kit (Ferrari et al., 2024; Lester et al., 2024). This test is based on a competitive Enzyme-Linked Immunosorbent Assay (ELISA), which employs an HRP-RBD bait to capture serum or plasma anti-RBD antibodies. If nAbs are present, they will prevent the binding to the recombinant human ACE2, immobilized on the bottom of the microplate wells. The higher the signal, the lower the titre of neutralizing antibodies in the sample. This assay allows for both qualitative and semi-quantitative measures of antibodies. The neutralization

activity can be measured as the percentage of the reduction of the colourimetric signal (Jung et al., 2021). This assay is cost-effective and requires low handling skills, in comparison to the previous one. However, both the CMIA and the cPass assay only measure RBD-binding nAbs and, therefore, do not include those targeting the NTD and the S2 regions, resulting in a misrepresentation of the actual neutralizing capabilities of the tested samples.

Cell-based assays can overcome this major hurdle. Both the Microneutralization Assay (MNA) and the Pseudotyped Virus Neutralization Assay (PVNA) rely on the titration of serum samples for calculating the concentration that corresponds to the blockade of half population of virus that enters a defined number of cells. In this setup, the inhibitory concentration (IC) is calculated as a relative neutralization value. Both the assays share the principles to calculate the IC and both require A) the propagation or production of the viral particle in a replication-permissive cell line, B) the titration, and C) a suitable target cell line that allows for the virus entry. However, they differ in the setup and reliability of the actual virus features.

In the case of the MNA (Vergori et al., 2022), Vero E6 cells are usually employed to propagate the real virus and as the target cell line for SARS-CoV-2. Next, once the harvested virus is titrated, it is temporarily exposed to the human serum sample and left in incubation with the target cell line, to let the virus infect the cells. After the proper incubation time (a few days), the cytopathic effect (CPE) is observed through light microscopy and the dilution at which CPE is abrogated is defined. Because the MNA uses the real virus, it is the most reliable method to test the neutralizing activity of serum samples. Several are, however, the limitations to this technique: 1) elevated safety and containment requirements, for preventing any outbreak of the pathogen, 2) highly specialized personnel, 3) high building and maintenance costs, and 4) it is time-consuming and laborious (Bewley et al., 2021).

A preferrable alternative to the MNA is the PVNA, which uses pseudotyped viruses (PVs), instead of the real virus. A PV is an enveloped viral particle whose tropism can be modified at will by exchanging the external glycoprotein, thus mimicking the actual host-virus interaction. The nucleocapsid core of the PV belongs to a donor virus, whose genome has been modified to prevent autonomous replication and to harbour a reporter gene, coding for a fluorescent or chemiluminescent protein (Temperton, 2009a). Therefore, PVs are the perfect surrogate of real, enveloped viruses, since they are easily handled, safe and

measurable (Fantoni et al., 2023). PVs are produced by co-transfecting a highly replicating cell line, like the human embryonic kidney 293T cell line (HEK293T) and its derivatives, with the expression plasmids encoding the viral structural proteins. Several PV platforms are available (Carnell et al., 2015; Ferrara et al., 2021; Nie et al., 2020); however, retroviral and lentiviral PVs, are more frequently employed. Lentiviruses, like the human immunodeficiency virus – 1 (HIV-1), integrate into the genome of the infected cell, allowing for the stable, continuous expression of a transgene. Also, their genome can be split into multiple plasmids, increasing the safety handling conditions. Major advantages of SARS-CoV-2 PVs over the other presented assays are the production of VOCs PVs by changing the surface glycoprotein, working in biosafety level 2 (BSL2) laboratories, and the requirement for minimum practical skills to handle PVs. On the other hand, the main disadvantage of using PVs is the unreliability of the structure of the glycoprotein since the original core is replaced. In fact, in many cases, the glycoprotein sequence must be modified and optimized to enhance the budding and the infectivity of the PVs (Zhang et al., 2023). As for the MNA, the results are obtained according to the time of growth of the target cell line.

SARS-CoV-2 PVs were extensively employed to study humoral reaction to the infection and vaccination, because of the advantages mentioned above. Recently, a published meta-analysis compared the correlation of results obtained using both the presented cell-based serological assays. The analysis revealed that MNA and PVNA tests are strongly correlated because of structural similarities and infection dynamics of the real virus and SARS-CoV-2 PVs, although the work was restricted to SARS-CoV-2 research (Cantoni et al., 2023b).

1.4. The role of microRNAs in the immunology and pathogenesis of COVID-19

Since their discovery in 1993 (Lee et al., 1993), microRNAs (miRNAs) gained increasing clinical and therapeutic value in the scientific community. miRNAs belong to the family of non-coding RNAs that regulate the expression of messenger RNA (mRNA) at the cellular level: as the expression levels of a miRNA increase, the translation of target mRNAs is reduced. This causes modulation of the corresponding proteins (Ying et al., 2021). Mature miRNAs result from a series of processing steps, starting from the early transcript of genomic DNA to the precursor miRNAs (pre-miRNAs) through primary

miRNAs (primiRNA). This is called the canonical pathway, which requires the interaction of the miRNA being processed with several complexes, including Drosha, Dicer, exportin 5 and the Argonaute protein family. Other non-canonical pathways are classified as Drosha- and Dicer-independent (Fig. 3) (O'Brien et al., 2018; Shang et al., 2023; Shukla et al., 2011).

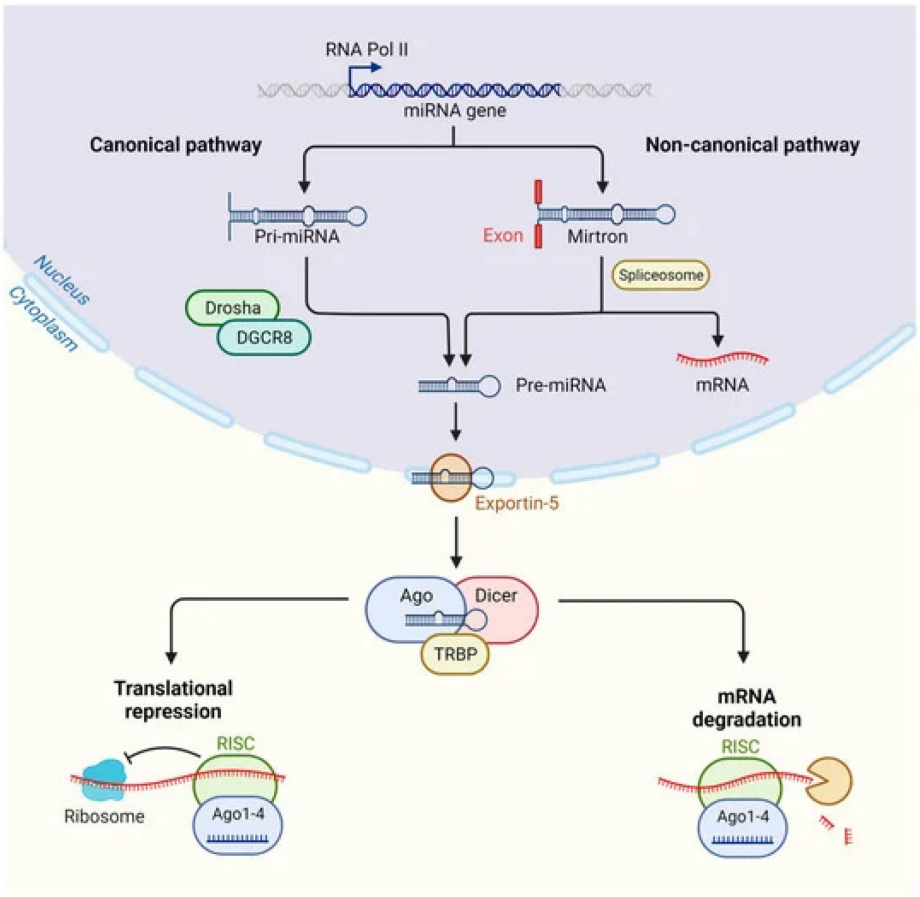

Figure 3. The maturation of microRNAs. *miRNAs are first transcribed by RNA polymerase II. The first processing step follows the canonical pathway (Drosha-dependent) or the non-canonical pathway (Drosha-independent), to obtain the pre-miRNA. This one is further processed into the mature form. Image from published review (Luna Buitrago et al., 2023).*

miRNAs are involved in various physiological and pathological processes (cardiovascular diseases, lung diseases, cancer, etc.) and are therefore considered valuable biomarkers (Condrat et al., 2020). Some miRNAs have an intracellular function, while others can be released into the bloodstream (circulating miRNAs). The latter, which can be isolated from serum and plasma, can be reliable markers discriminating the outcome of a disease. They are therefore advantageous in the diagnostic and prognostic fields as their collection is minimally invasive, replicable over the disease's progression and they can be quantified within a short

timeframe. Moreover, they may prove to be candidates for therapeutic purposes (Narożna and Rubiś, 2021). miRNAs are also involved in viral infections and regulate host-virus interaction (Mao et al., 2023). A viral agent stimulates miRNAs involved in different processes (direct interaction with the viral genome, inflammation, cell damage, etc.). Recent studies are focusing on finding specific miRNA panels to determine disease progression and patient recovery (Giannella et al., 2022; Narożna and Rubiś, 2021). The following paragraphs will present three potential miRNAs involved in the pathogenesis and immunity of COVID-19.

1.4.1. miR-155-5p

miR-155-5p is a multifunctional miRNA involved in several pathological processes induced by viruses, such as influenza virus (Woods et al., 2020), herpes simplex virus 1 (Wang et al., 2019), Epstein-Barr virus (Wood et al., 2018). miR-155-5p is also endowed with antiviral properties, involved in the activation and maintenance of an efficient humoral and cellular immune response (Hu et al., 2021; Jafarzadeh et al., 2021). Because of these studies, miR-155-5p has been pointed out as a major participant in SARS-CoV-2 infections (Gasparello et al., 2021). Nonetheless, the actual mechanism by which this miRNA functions is still under debate.

High miR-155-5p expression levels have been measured in the plasma or peripheral blood mononuclear cells (PBMCs) of severe COVID-19 patients (Donyavi et al., 2021; Eyileten et al., 2022; Garg et al., 2021; Soni et al., 2020; Ying et al., 2021). From these studies, miR-155-5p emerged to be involved in thrombosis, cardiovascular disease, inflammation, and several other processes. However, other studies report that miR-155-5p in peripheral blood appears to be expressed at low levels in very severe patients with an adverse outcome (Aboulela et al., 2024; Giannella et al., 2022; Kassif-Lerner et al., 2022). This discrepancy suggests that, in addition to being a marker of mortality, it is potentially related to the patient's levels of immune protection at the time of hospitalization. The trend of miR-155-5p in the blood could reflect the activity of neutralizing anti-CoV-2 antibodies and could potentially act as a marker of correlates of protection.

1.4.2. miR-148a-3p

Another possible participant in the regulation of nAbs production and humoral immunity maintenance is miR-148a-3p. Its upregulation is responsible for B-cell autoimmune disease in mouse models. Therefore, its fine regulation is important for the selection, differentiation, maturation and proliferation of B lymphocytes (Gonzalez-Martin et al., 2016; Porstner et al., 2015). In a recent study, miR-148a-3p isolated from nasal swabs of buffaloes vaccinated against Bubaline alpha herpesvirus 1 (BuHV-1) was significantly upregulated in comparison to the control, unvaccinated group. Also, the same vaccinated group presented neutralizing antibodies against the virus, leading the group to suppose it could be a marker for protective immunity, and potentially, associated with neutralizing responses (Lecchi et al., 2023). Also, the absence of this miRNA causes a reduction of 50% in the production of antibodies by activated B cells in a mouse model (Pracht et al., 2021).

Previous studies found the involvement of this miRNA in the infection of human coronaviruses. For example, miR-148a-3p directly targets the genome of SARS-CoV (Hu et al., 2021; Mallick et al., 2009). miR-148a-3p is emerging as a biomarker for survival discrimination of COVID-19 patients (de Gonzalo-Calvo et al., 2021; Pollet et al., 2023). Analysis of the expression levels of circulating miR-148a-3p in people receiving the BNT162b2 vaccine revealed that its reduction positively correlates with the increased production of Spike-specific antibodies (Y. Liang et al., 2023; Miyashita et al., 2022). Therefore, miR-148a-3p represents an interesting candidate for monitoring the neutralizing humoral immune response, together with miR-155-5p.

1.4.3. miR-28-3p and its implications in COVID-19 pathogenesis

A relevant topic in COVID-19 infection is the impairment of the renin-angiotensin system or RAS. The role of RAS is to maintain cardiovascular function by regulating blood pressure and vascular tension (Imai et al., 2005; König et al., 2023). Specific enzymes and their substrate participate in this process. Angiotensin I (AngI) is produced from angiotensinogen by renin. AngI is thereafter converted to AngII by ACE. AngII induces the contraction of the vasculature and the myocardial tissue and promotes inflammation (Anguiano et al., 2017). To counterbalance the effects of AngII, ACE2 intervenes to reduce both AngI and AngII into Ang1-9 and Ang1-7. These products promote

vasodilation and minimize inflammation (Anguiano et al., 2017; Fountain et al., 2024; Patel et al., 2014). In particular, early studies on ACE2, in both its cell-bound and cell-free forms, highlighted its essential role in maintaining cardiovascular function (Crackower et al., 2002; Shao et al., 2019).

The mechanism by which ACE2 is released into circulation (Donoghue et al., 2000) and accomplishes its function is only partially understood. AngII is responsible for this process: high AngII levels in blood induced over-transcription of ACE2 mRNA and reduced ACE2 levels on cardiomyocytes in both *in vivo* and *in vitro* models. It has been shown that the activity of surface proteases is necessary for the shedding of ACE2 (Patel et al., 2014). Among these proteases, ADAM17, also known as TACE has gained importance due to its involvement in many diseases, such as cancer and cardiovascular ones. ADAM17 is a transmembrane protein of the first type, consisting of an extracellular region, divided into several subdomains, including the catalytic one, the transmembrane region and a cytoplasmic tail (Lorenzen et al., 2016). Membrane-bound ACE2 is a substrate of ADAM17 (Lambert et al., 2005; Lorenzen et al., 2016; Patel et al., 2014).

A common feature of severe COVID-19 patients is the increment of the soluble form of ACE2 in plasma (Elemam et al., 2022; Kuba et al., 2005; Mariappan et al., 2022; Nagy et al., 2021). Although soluble ACE2 is a physiologically protective factor for lung integrity (Imai et al., 2005), excessive levels of the protein in the circulation are associated with ageing, diabetes, and cardiovascular diseases (Kunvariya et al., 2023; Narula et al., 2020). The administration of the soluble form of the Spike protein of SARS-CoV to *wild-type* (*wt*) and ACE2-knockout (KO) mice gave similar results. Reduced lung injury was detected in the KO model compared to the *wt* ones (Kuba et al., 2005). Moreover, an *in vitro* study revealed that the treatment of Vero E6 cells with SARS-CoV PVs induced the release of a soluble form of ACE2 (Haga et al., 2008)

A recent study (Xu and Li, 2021) found the simultaneous increase and decrease of ADAM17 and ACE2, respectively, from cell isolates when incubation with the RBD of the SARS-CoV-2 Spike occurred. Also, the expression levels of a miRNA, miR-28-3p, were reduced upon treatment. The study proposed a model to explain the phenomenon. The direct binding of ACE2 by the RBD of the Spike protein induces structural and conformational changes in the receptor, activating its signal-transmitting cytoplasmic tail. This way, the signal reduces the expression of miR-28-3p. In turn, ADAM17 mRNA, which is targeted by the

miRNA, is translated, and its product is translocated to the membrane, where it can accomplish the shedding of ACE2 (Fig. 4) (Xu and Li, 2021). Still, the study suffered from a dependable model for investigating the actual interaction and its consequences. A potential experimental layout to achieve this will be presented here.

miR-28-3p has been previously identified as a valid biomarker of pulmonary embolism (Zhou et al., 2016) and diabetes (Zampetaki et al., 2010) due to its overexpression in plasma. It is also dysregulated in many types of cancer (Almeida et al., 2012; Liu et al., 2013; Wang et al., 2015). Another study highlighted the overexpression of miR-28-3p in peripheral blood mononuclear cells (PBMCs) as a potential biomarker to distinguish severe patients from patients with mild symptoms (Khatami et al., 2023). miR-28-3p is known as a circulating miRNA in plasma (Silva et al., 2021), although the complete picture of its role in COVID-19 is unknown. For these reasons, it is a miRNA of interest in the context of COVID-19 and SARS-CoV-2 research (Zipeto et al., 2020).

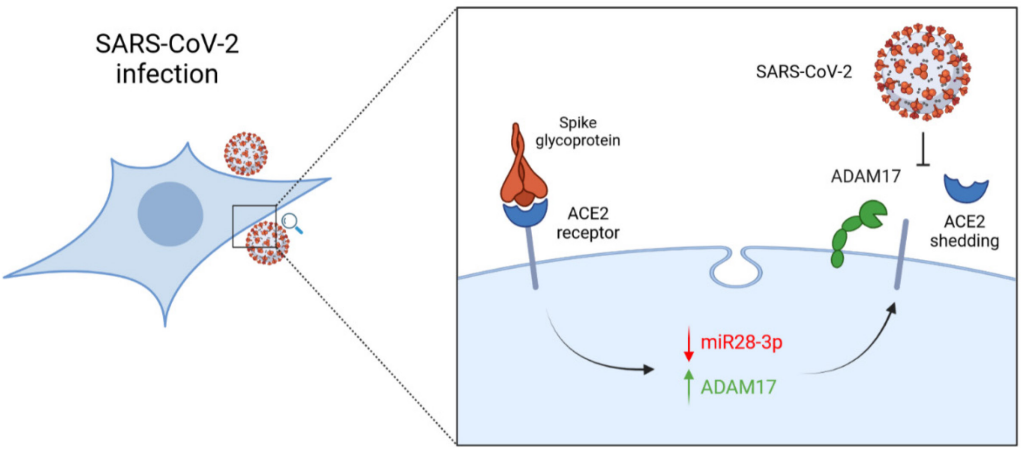

Figure 4. SARS-CoV-2 induces ACE2 shedding via miR-28-3p and ADAM17 alternate deregulation. *According to the hypothesis of Xu and Li, 2021, the RBD of the Spike protein induces conformational changes in the membrane-bound ACE2 receptor, which alternatively downregulates miR-28-3p and upregulates ADAM17. The overexpression of ADAM17 causes the shedding of ACE2 into its soluble form. Image created with Biorender.*

2. AIM OF THE THESIS

The major aim of this thesis is to show the potential applications of the technology of PVs applied to SARS-CoV-2 and COVID-19 research, with a particular focus on the serology and the pathogenesis of the disease. Secondarily, this work aims to investigate molecular processes potentially involved in the maintenance of a durable protective immunity against SARS-CoV-2 and the onset of severe COVID-19 in the early stages of infection.

First, this work will present the results obtained in serological assays in subjects receiving the third booster dose against SARS-CoV-2. The protective neutralizing immunity has been investigated against SARS-CoV-2 Omicron VOCs that emerged during the time or after the vaccine administration. Also, four different serological assays are compared, to valorise the use of PVs in serological assays. Second, the work presents the potential role of circulating microRNAs in the support of strong, long-term anti-SARS-CoV-2 humoral immunity. Third, SARS-CoV-2 PVs are presented as a model to investigate molecular mechanisms induced by the direct virus-cell surface interaction, which implies the involvement of intracellular mediators.

3. MATERIALS AND METHODS

3.1. Study population

Sample collection was performed at the section of Respiratory and Sports Medicine at the Azienda Ospedaliera Universitaria Integrata (Verona, Italy), with the supervision of Prof. L. Dalle Carbonare and Dr. M. T. Valenti. Serum samples of 17 healthcare workers (HCW) volunteers were collected before (T3), 1 month (T4) and 4 months (T5) after the administration of the third booster dose with either the BNT162b2 (13/17) or mRNA-1273 (4/17) vaccines. The time of collection will be referred to as T3, T4 and T5 since they are considered from the beginning of the vaccination program (T0, before the first dose; T1, before the second dose; T2, three weeks after the second dose) (Ruggiero et al., 2022). General data are reported in Table 1. Serum was harvested from whole blood after leaving it to coagulate at room temperature (RT) and centrifugating collection tubes at 3000 rpms for 5 minutes. Harvested serum was stored at -80°C until use. All the participants signed the informed consent before the collection of samples.

Characteristic (n=17)	Data
Age (median), Range of age (min-max)	51(26-65)
Male, % (vs female)	53%
Previously infected (PI) % (vs. Naive)	24%
Third dose, vaccine type, BNT162b2, % (vs. mRNA-1273)	76%
First collection (T3): days after first dose (mean, number of weeks)	289, 30 dd, 72w
Second collection (T4), days after first dose (mean, number of weeks)	318,80 dd, 80w
Third collection (T5), days after first dose (mean, number of weeks)	409,60 dd, 102w

Table 2. *Report of general characteristics of the study population.*

3.2. Cell cultures and plasmids for PV production

Human Embryonic Kidney 293T cells (HEK293T) and ACE2-overexpressing hepatocellular carcinoma HuH.7 cells (a kind gift from Prof. M. Pizzato, University of Trento, Italy) were maintained in Dulbecco's Modified Eagle Medium (DMEM) (P04-036001, PAN Biotech; 11965092, Gibco). Chinese Hamster Ovary cells, stably expressing ACE2 and TMPRSS2 (CHO/A2/T2) cells were cultured in either DMEM or Ham's F12 medium (P04-14559, PAN Biotech). All cell culture media were added with 10% heat-inactivated Foetal Bovine Serum (FBS) (A5256701, Gibco), 5% L-glutamine (BEBP17-605E, Lonza), 1% penicillin/streptomycin (15070063, Gibco). These media will be referred to as "complete" throughout the thesis. The following plasmids were used to produce the SARS-CoV-2 PVs: packaging plasmid, pCMV-dR8.91; backbone plasmid, pCSFLW; SARS-CoV-2 VOCs envelope-encoding plasmid; VSV-G expression plasmid (Di Genova et al., 2021). Plasmids were amplified in the TOP10 *E. coli* strain (C404010, Thermo Fisher Scientific), cultured in Luria-Bertani's liquid broth (LB broth). Plasmid extraction was performed using a Midiprep Extraction kit (12143) or Maxiprep EndoFree Plasmid kit (12362) (Qiagen).

3.3. Cell cultures and plasmids for flow cytometry experiments

HEK293T/ACE2 cells for flow cytometry experiments were prepared as follows. The human ACE2 receptor was overexpressed by transducing the cell line with a lentiviral vector (RRL.sin.cPPT.SFFV/Ace2.IRES-puro.WPRE, AddGene). The vector was prepared by co-transfecting HEK293T cells with the ACE2-coding lentiviral plasmid, a second-generation packaging plasmid (psPAX2, AddGene), and a plasmid coding for the vesicular stomatitis virus glycoprotein (VSV-G)

(pCMV-VSV-G, Addgene). Cells were incubated with the lentiviral vector for 48 hours before selection with puromycin (0.6 μg/mL). After the selection, surviving cells were detached and stained with anti-ACE2-PE antibody (10108-MM36-P, SinoBiological) for further cell sorting with FACSAria Fusion (Beckman Dickison) at the Centro Piattaforme Tecnologiche, which is in convention with the University of Verona. Cells with PE signals ranging from 10^4 and 10^5 were sorted to homogenize the population.

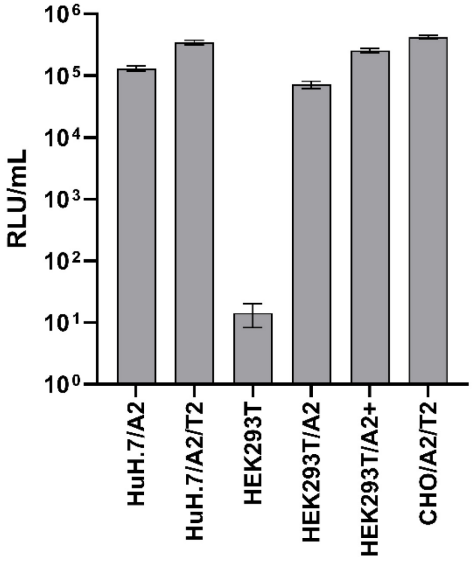

Figure 5. Different transduction rates of SARS-CoV-2 Wuhan PVs on multiple cell lines (bar plot). *ACE2-overexpression is critical for the virus to enter. The overexpression of TMRPSS2 further increases the entry rate. Data are presented as RLU per millilitre (RLU/mL) of PV-containing medium.*

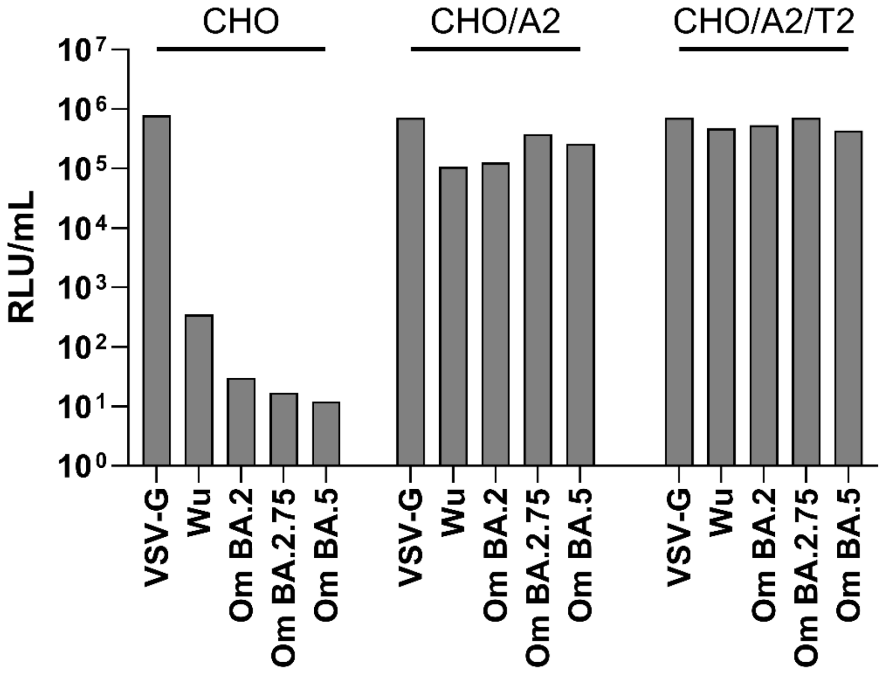

Figure 6. Different transduction rates of SARS-CoV-2 VOCs PV (bar plot). *Wild-type CHO cells show low entry of SARS-CoV-2 PVs. On the contrary, the presence of ACE2, and also of TMPRSS2, increases the infection rate. Data are presented as RLU per millilitre (RLU/mL) of PV-containing medium.*

3.4. IgG quantification

IgGs anti-Spike (RBD) (IgG-S) and anti-N protein (IgG-N) were quantified via SARS-CoV-2 IgG II Quant Assay and SARS-COV-2 IgG-N Assay (Abbott), respectively. The iARCHITECT system was used to perform these serologic assays. A signal-to-noise ratio cut-off of 1,4 was determined to identify positive samples. Antibody titres were converted to natural logarithms for the correlation analyses.

3.5. Pseudotyped virus production and titration

SARS-CoV-2 PVs were produced following previously published protocols (Di Genova et al., 2021; Fantoni et al., 2023). Briefly, HEK293T cells were co-transfected with the plasmids for producing PVs (pCMV-dR8.91, pCSFLW and Envelope plasmid for each variant) using either FugeneHD (E2311, Promega) or polyethyleneimine (PEI) (408727, Sigma-Aldrich) at 1 mg/mL in PBS 1X. 72 hours after transfection, the cell medium containing the pseudotypes was harvested in a Falcon tube, centrifuged at 3000 rpms for 5 min and filtered through a 0.45 μm filter. The filtered medium was aliquoted and frozen at -80°C before use. For titration of the PVs stocks, 100 μL in duplicate of the PV preparation was serially two-fold diluted in a 96-well plate (96WP), and $2*10^4$ HEK293T/ACE2 or CHO/A2/T2 cells per well were added. After 48 hours of incubation at 37°C, 5% CO_2, Luciferase assay was performed by adding Bright-Glo reagent (E2610, Promega) for the VPU experiments and steadylite plus (6066759, Perkin Elmer). The readout was obtained with a GloMax 96WP reader (Promega) or Victor3 96WP reader (1420-032, Perkin Elmer). The titre of single PV stocks was calculated as RLU/mL, after multiplication to the corresponding dilution factor.

3.6. Pseudotyped Virus Neutralization Assay (PVNA)

PVNAs were performed at the Viral Pseudotype Unit laboratory, Medway School of Pharmacy, University of Kent, U.K., during my internationalization research program, as previously reported (Cantoni et al., 2023a; Di Genova et al., 2021; Fantoni et al., 2023). Heat-inactivated serum samples in duplicate were diluted ten-fold in a complete F12 medium. Next, seven two-fold dilutions were performed, and the excess medium was discarded. Neutralizing and non-

neutralizing human serum samples were used as controls. PV stocks were thawed and diluted to obtain ~10^6 RLU/mL. Diluted PV stock was distributed to each well and incubated at 37°C, 5% CO_2, for 60 minutes to let the neutralizing antibodies bind the PVs. After the incubation, $2*10^4$ CHO/A2/T2 cells per well were added. After 48 hours of incubation at 37°C, 5% CO_2, Luciferase assay was performed by adding Bright-Glo reagent (E2610, Promega). The readout was obtained with a GloMax 96WP reader (Promega). Data analysis to calculate the inhibitory concentration 50 (IC50) was performed with GraphPad Prism, according to published procedures (Ferrara and Temperton, 2018).

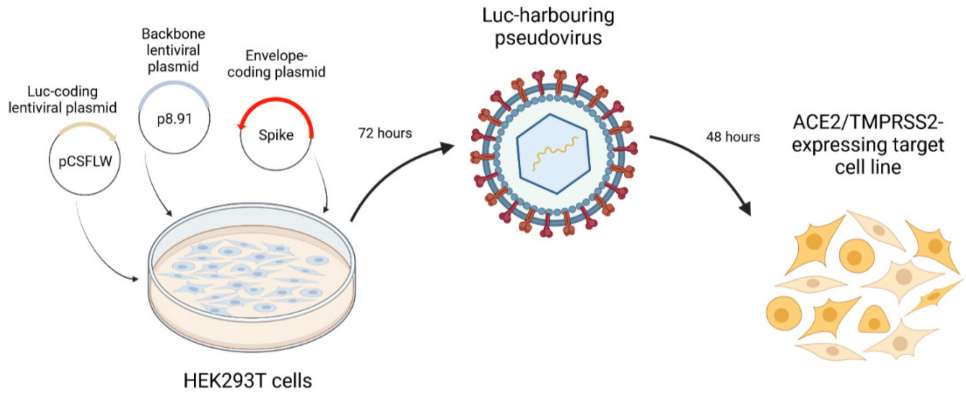

Figure 7. The production of SARS-CoV-2 PVs. *HEK293T cells are co-transfected with a three-plasmid lentiviral system to produce SARS-CoV-2 PVs. The medium containing the PVs is harvested after 72 hours of incubation. Luciferase assay is performed 48 hours after infecting the ACE2/TMPRSS2 expressing cell line.*

3.7. Microneutralization Assay (MNA)

Microneutralization assays (De Rienzo et al., 2021; Vergori et al., 2022) were performed at the Department of Infectious, Tropical Diseases and Microbiology, IRCCS Sacro Cuore Don Calabria Hospital, Negrar, Verona, Italy. Serum samples (n=12) were selected from the initial group of HCW volunteers. Samples collected before and 1 month after the vaccination were tested against the original SARS-CoV-2 Wuhan strain. The real virus was propagated in Vero E6 cells. Heat-inactivated (56°C for 30 min) samples were diluted two-folds seven times in duplicate in 96WP. The initial dilution started at 1:10. Next, an equal volume of the real virus at 100 tissue culture infectious dose 50 ($TCID_{50}$) was added and incubated with titrated serum samples at 37°C for 30 min. After the incubation, sub-confluent Vero E6 cells were added to each well. After 48 hours of incubation at 37°C, 5% CO_2, plates were checked by brightfield microscopy for the presence

of cytopathic effect (CPE). Positive and negative control samples were tested to verify inter-assay reproducibility. The cut-off was defined as $MNA_{90} \geq 1:10$.

3.8. cPass™ SARS-CoV-2 Neutralization Antibody Detection Kit

The cPass nAbs Detection kit (L00847, GenScript) is a blocking ELISA test that uses protein-protein interactions to detect the presence of anti-SARS-CoV-2 Spike protein neutralizing antibodies in serum samples (cPass™ SARS-CoV-2 Neutralization Antibody Detection Kit, GenScript; Jung et al., 2021). The experimental conditions (samples and SARS-CoV-2 variants) were the same tested in MNA. Serum samples were diluted 1:10 before incubation with the recombinant RBD of the Spike protein of the VOC of interest, conjugated with horseradish peroxidase, (RBD-HRP) in a 96WP at 37°C for 30 min. Calibration curves and positive and negative controls were included in each plate. Next, the serum – RBD-HRP mixtures were moved to the ACE2-coated ELISA microplate and left in incubation to let the free RBD-HRP bind the fixed ACE2 protein at 37°C for 15 min. After washing, TMB solution was added, and the microplate was read using an Enzo Absorbance 96 Plate reader (Byonoy). The antibody titre and the percentage of neutralization were calculated according to the manufacturer's instructions.

3.9. Flow cytometry analysis

Flow cytometry data acquisition was performed using FACS Fortessa LX-20 (Beckman Dickison) at the Centro Piattaforme Tecnologiche, (Verona, Italy), in collaboration with Dr. G. Finotti. HEK293T/A2 cells were infected with PVs of Wuhan and Omicron BA.5 PVs. Untreated (UT), incubated with phorbol myristate aspartate (PMA) and cells infected with VSV-G PVs were used as controls. $1*10^5$ target cells were incubated with PVs in a 48WP for 6 and 12 hours before detachment with 5 mM EDTA in PBS 1X. PVs were washed out at 3 hours after the beginning of incubation by replacing the culture medium with fresh cDMEM. Infected cells were washed twice with FACS buffer (PBS 1X with the addition of EDTA 2mM, FBS 2%), by centrifugation at 600 x g for 5 min at RT. Cells were incubated with fluorescent dye-labelled antibodies for 25-30 min, at +4°C, in the dark. After washing the cells with FACS buffer, the samples were fixed by incubating them in the presence of paraformaldehyde (PFA) 1% (420801, BioLegend), for 10 min, at +4°C, in the dark. Next, cells were washed

twice with FACS Buffer and resuspended with FACS buffer before analysis. The antibodies and dyes employed for labelling the cells are listed as follows: mouse anti-hACE2-PE (10108-MM36-P, SinoBiological); mouse anti-hADAM17-APC (NBP2-12018APC, NovusBio); LIVE/DEAD Fixable Near-IR Dead Cell Stain kit (L34975, Thermo Fisher Scientific).

3.10. microRNA extraction and Real-Time – quantitative PCR

The method for miRNA extraction from serum was adopted from a previous protocol (Khoury et al., 2014) and adapted to the available volume of serum from each sample. Briefly, total RNA from serum samples was extracted using TRIzol-LS reagent (10296010, Thermo Fisher Scientific). For miR-28-3p downmodulation experiments, infected cells were treated with Trizol for total RNA extraction, in parallel with flow cytometry experiments. Total RNA was isolated using TRIzol reagent (15596026, Thermo Fisher Scientific).

In both experiments, total RNA was copied to double-strand DNA (cDNA) using TaqMan™ Advanced miRNA cDNA Synthesis Kit (A28007). Circulating miR-155-5p (ID 483064_mir), miR-148a-3p (ID 477814_mir) and miR-28-3p (ID 477999_mir) levels (A25576, TaqMan™ Advanced miRNA Assay) were measured via RT-qPCR (4444556, TaqMan™ Fast Advanced Master Mix for qPCR, Thermo Fisher Scientific). Each sample was measured in triplicate and the relative expression of miRNAs of interest was normalized to miR-191-5p (ID 477952_mir) (Peltier and Latham, 2008).

3.11. Statistical analysis

For PVNA assays, the non-parametric Wilcoxon Test was applied to compare paired neutralization data overtime. For comparing different populations (PI vs. Naive, M vs. F, etc.) non-parametric unpaired Mann-Whitney test was employed. The correlation of neutralization capacity vs. IgG-S titre and neutralization vs. age were calculated using Spearman's correlation test. The non-parametric Wilcoxon Test was also applied to compare the paired data obtained from MNA and cPass assays. Linear regression was performed to analyse the output of serological assays.

For Flow Cytometry analyses, FACS data were gated using Flow Jo 10 (Becton Dickinson). The gating strategy is presented in Fig. 8. The median number of the

ACE2-positive (ACE2+) cell populations was calculated. For identifying the ADAM17-positive (ADAM17+) populations, the median number of the unstained, auto-fluorescent population was subtracted from the ADAM17+ cells to calculate the actual ADAM17+ cells. For miRNA assays, the expression levels were normalized to miR-191-5p expression using the $2^{(-\Delta\Delta Ct)}$ method. FACS expression and miRNA expression data were analyzed via unpaired t-test with Welch's correction and one-way ANOVA with Brown-Forsythe and Welch's tests in GraphPad Prism 10.

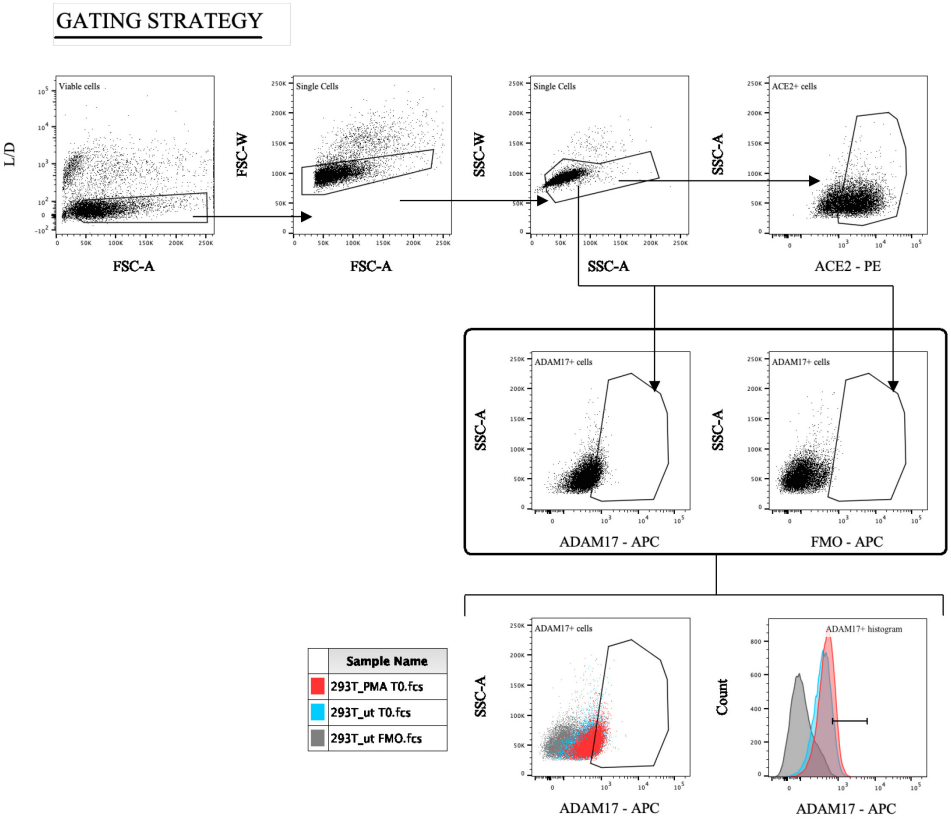

Figure 8. Dot plots and one histogram representing the gating strategy applied throughout the flow cytometry experiments. *The viable HEK293T/A2 cells (labelled as Live/Dead-negative population) were first gated and the singlets population were filtered. Once these have been identified, the ACE2+ and ADAM17+ cells were gated, and median numbers were analysed. To separate and distinguish the actual ADAM17+ population, ADAM17-unstained (light grey), unstimulated (light blue) and PMA-stimulated (red) populations were overlapped (see the dot plot and the histogram).*

4. RESULTS

4.1.1. Population data

17 HCWs from the University of Verona were enrolled in this study. The subjects were vaccinated with the third booster dose (BNT162b2 or mRNA-1273) 72 weeks (T3) after receiving the first dose. The subsequent samples were collected 4 weeks (T4) and 17 weeks (T5) after the booster dose injection. The 76% of subjects received the BNT162b2 vaccine. The participants were mainly males (53%). The mean age was 51 years (range = 25 – 65 yo). 3/17 subjects (18%) were previously diagnosed with SARS-CoV-2 infection via antigenic or PCR-based test at least once before the administration of the third dose. 1/17, supposed negative to the antigenic/molecular tests, resulted positive for anti-nucleoprotein (anti-N) IgG at the time of administration of the vaccine, and was therefore included in the previously infected (PI) HCW group (PI = 4/17). One participant of the PI group was IgG-N – negative at T3 and T4, but positive at T5.

4.1.2. The third booster dose stimulates the production of neutralizing IgG-S against the SARS-CoV-2 Omicron variants

PVNAs are progressively gaining importance in the evaluation of neutralizing activity of serum since this methodology is comparable to the tests based on the real virus (Cantoni et al., 2023b). In this part of the study, PVNAs were performed to test the trend of neutralizing activity of serum samples before (T3), 1 month (T4) and 4 months (T5) after the HCW received the booster dose. The SARS-CoV-2 VOCs were selected based on the emergence at the time of vaccination and the subsequent collection of serum samples (Omicron BA.1 and BA.2) or later (BA.4/5 and BA.2.75), to evaluate whether the booster dose could have stimulated strong immune responses also against the latter variants. In parallel, anti-S (RBD) (Wuhan) IgGs were measured at the three timepoints. All the subjects developed significantly high levels of IgGs-S (T3 vs. T4, $p<0.0001$; T4 vs. T5, $p<0.0001$; T3 vs. T5, $p<0.0001$). The titre of antibodies was almost halved at T5 (mean T4 = 532.8 BAU/mL; mean T5 = 249.2 BAU/mL) (Fig. 9).

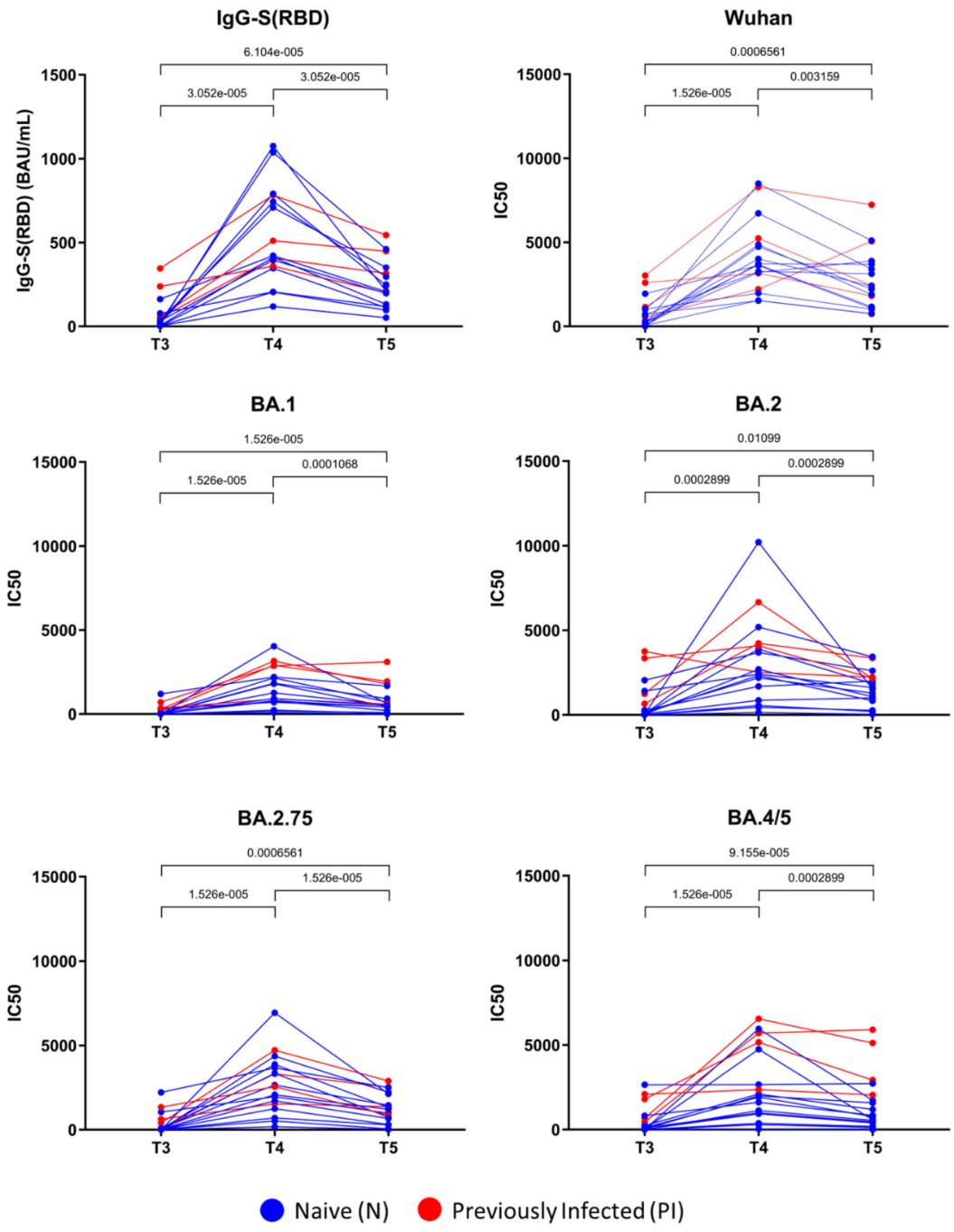

Figure 9. Overtime IgG-S titres and neutralizing activity against SARS-CoV-2 variants (before-after plots). *Overtime analysis of IgG-S titres and IC50 results against the original Wuhan strain and Omicron VOCs BA.1, BA.2, BA2.75 and BA.4/5 after administration of the booster dose. IgG-S titres were measured using the SARS-CoV-2 IgG II Quant Assay (Abbott). The neutralizing activity rate was measured via PVNA. The non-parametric Wilcoxon test was applied for statistical analysis. Blue dots: naive; ed dots: PI; T3: before administration; T4: one month after administration, T5: four months after administration of the booster dose.*

PVNAs revealed that all the subjects produced nAbs (T3 vs. T4, Wuhan $p<0.0001$, BA.1 $p<0.0001$, BA.2 $p=0.00029$; BA.4/5 $p<0.0001$, BA.2.75 $p<0.0001$). 4 months after the booster, the neutralization levels waned (T4 vs. T5, Wuhan $p=0.0032$, BA.1 $p=0.0001$, BA.2 $p=0.0003$; BA.4/5 $p=0.0003$, BA.2.75 $p<0.0001$), resulting in a halving of the median IC50 (T4 vs. T5, Wuhan 3664 vs. 2398; BA.1 1269 vs. 550,5; BA.2 2517 vs. 1617; BA.4/5 1993 vs. 843,9; BA.2.75 2559 vs. 1210). Subjects who contracted the virus before receiving the booster dose showed higher IC50 levels (previously infected, red dots) (Dalle Carbonare et al., 2021; Siracusano et al., 2022). The comparative analysis of Naive vs. Previously infected subjects highlighted that the presence of the infection in the clinical history of the subject confers an advantage in protection against further infections (Fig. 12). Unfortunately, no further collections of serum were performed after 4 months after vaccination due to the withdraw of subjects. This result is a bias in the evaluation of protection against the variants that emerged later in 2022 (BA.4/5, BA.2.75).

4.1.3. Sex and age could influence the antibody titre and neutralizing activity

IgG-S titres and IC50 responses were compared based on sex and age. No significant differences were observed, although males generally displayed higher median titres (M vs. F at T4; Wuhan, 3724 vs. 3642; BA.1, 1802 vs. 846,3; BA.2, 2692 vs. 2370; BA.2.75, 3350 vs. 2317; BA.4/5, 1993 vs. 2011; M vs. F at T5, Wuhan, 3417 vs 1495; BA.1 550,5 vs. 513; BA.2 1850 vs. 1574; BA.2.75 1323 vs. 1094; BA.4/5 1578 vs. 808,1) (Fig. 10). Also, correlation analysis of either IgG-S (RBD) or IC50 vs. age revealed no direct correlation, although the older population showed lower IgG-S titres and neutralization activity (Fig. 11).

4.1.4. IC50 is proportional to IgG-S titres before and after vaccination

IgG-S (anti-Wuhan S-RBD region) in serum samples of the 17 subjects at the three timepoints were quantified and the titres were correlated with the neutralizing activity against the Wuhan and Omicron VOCs PVs. A direct correlation was observed before the administration of the third dose (T3) ($p\leq0.0001$) for all the VOCs in the analysis. A significant correlation was also observed at T4 for VOCs Wuhan ($p=0.0436$) and BA.1 ($p=0.024$), whereas it was lost when analysing the BA.2 ($p=0.355$), BA.2.75 ($p=0.0642$) and BA.4/5 VOCs ($p=0.5486$). A direct correlation was observed for Wuhan ($p=0.0111$), BA.1

(p=0.012), BA.2.75 (p=0.0111) and BA.4/5 (p=0.03) at T5. Also, it was apparent that the range of IC50 expanded as the titre of antibodies against the RBD region did not vary at the second serum collection (Fig. 13).

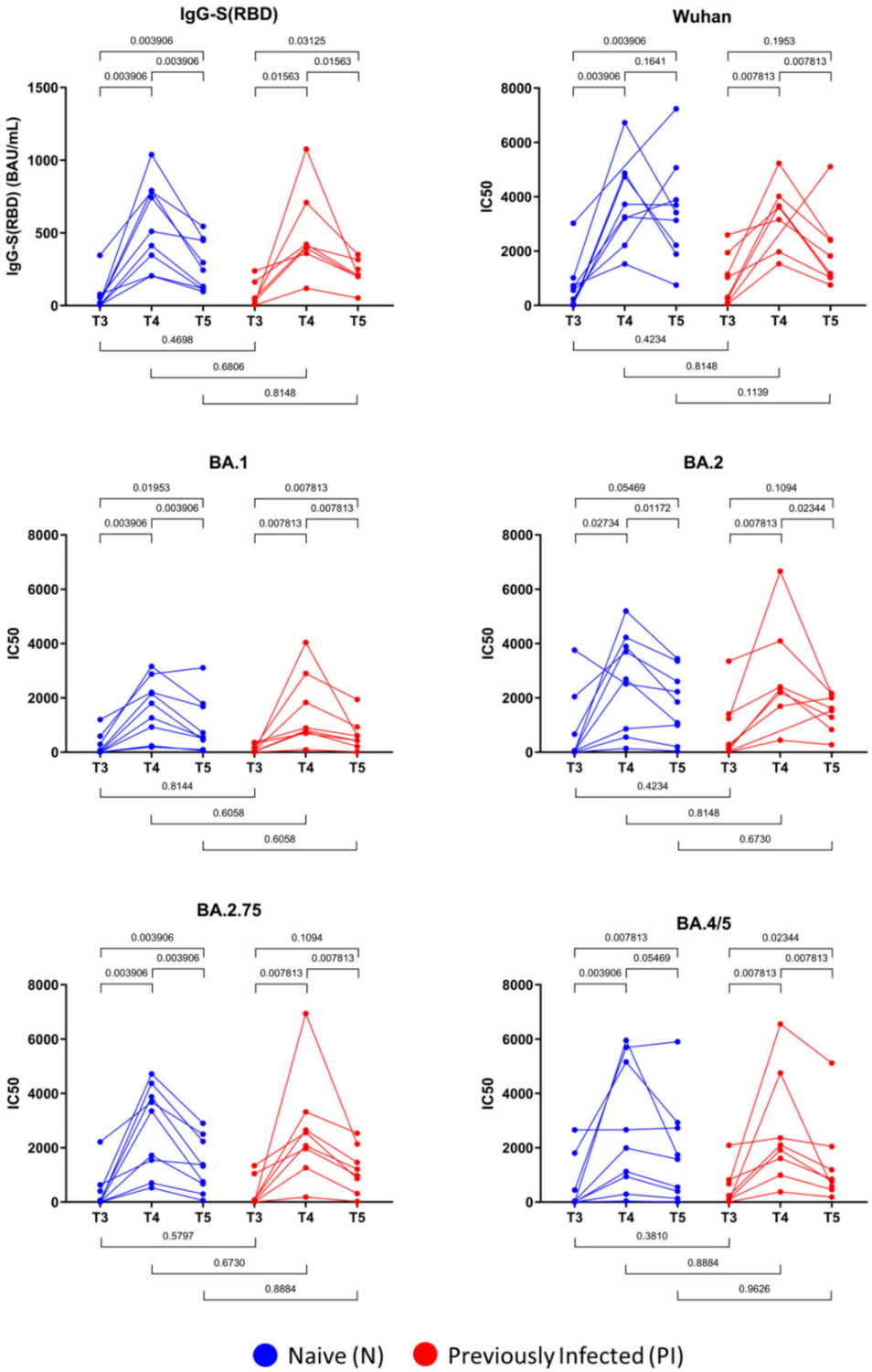

Figure 10. Comparison of the IgG-S titres and IC50 against the major SARS-CoV-2 VOCs between the male and female populations (before-after plots). *IgG-S titres were measured using the SARS-CoV-2 IgG II Quant Assay (Abbott). The neutralizing activity rate was measured via PVNA. The non-parametric Wilcoxon test and unpaired Mann-Whitney test were applied for*

statistical analysis. Blue dots and lines: male; red dots and lines: female; T3: before administration; T4: one month after administration; T5: four months after vaccine administration.

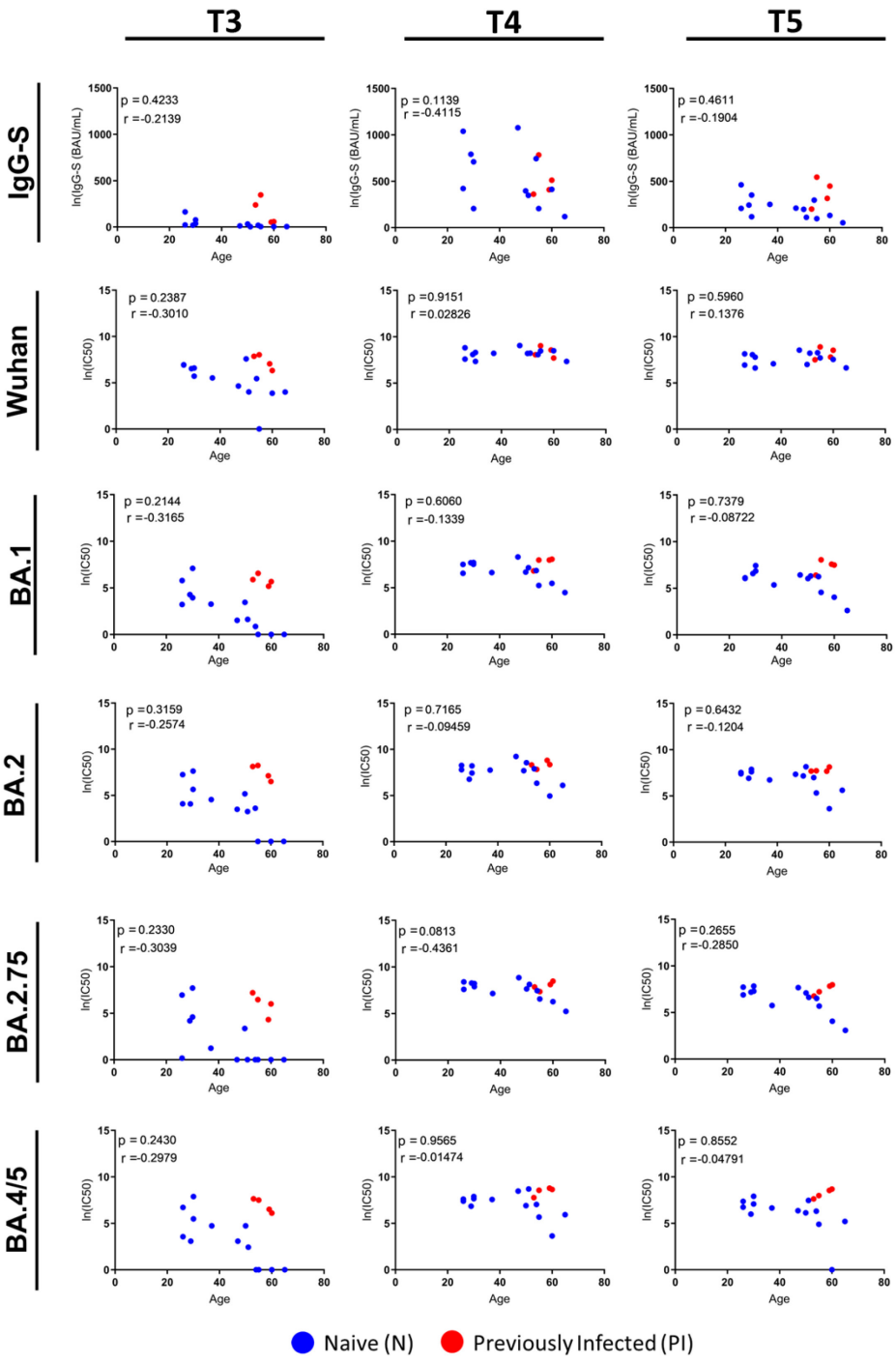

Figure 11. Spearman's correlation analysis between IgG-S or IC50 against age (dot plots). *The analysis suggests a negative trend that associates specific antibodies and neutralizing activity with increasing age. Blue dots: naive; red dots: PI; T3: before administration: T4: one month after administration; T5: four months after administration.*

4.1.5. Infections before vaccination could confer a better long-term protection against emerging variants

The literature reports that exposure to the pathogen before or after vaccination results in a stronger, more durable protective response against subsequent VOCs (Ruggiero et al., 2022). Therefore, investigating the effects of hybrid humoral immunity could contribute to understanding long-term immunity. The comparison of PI vs. N individuals after vaccination is shown in Fig. 12. No significant differences in the production of RBD-specific IgGs were observed between the two groups after the vaccination. Different titres were observed before vaccine administration (Fig. 12, IgG-S(RBD) N vs. PI at T3, p=0.01319). The neutralizing activity at T3 against all tested variants displayed a similar trend (IC50 of N vs. PI at T3, Wuhan, p=0.02269; BA.1, p=0.02185; BA.2, p=0.009664; BA.2.75, p=0.036655; BA.4/5, p=0.02101), which was also maintained at 17 weeks after vaccination against some Omicron VOCs (N vs. PI at T5, BA.1, p=0.01008; BA.2, p=0.0319, BA.4/5 p=0.001681).

4.2. PNVA is comparable to MNA and *in vitro* ELISA assays

12 among the 17 HCWs were selected to perform cell-based (MNA) and cell-free (cPass) serological assays for comparative analyses. All the tests revealed that a significant difference existed one month (T3 vs. T4; PVNA, p=0.0015; MNA, p=0.00098; cPass, p=0.00048) and 17 weeks (T3 vs. T5; PVNA, p=0.012; MNA, p=0.00098; cPass, p=0.00048) after the vaccination. None of the assays reported significant differences between T4 and T5 (Fig. 14).

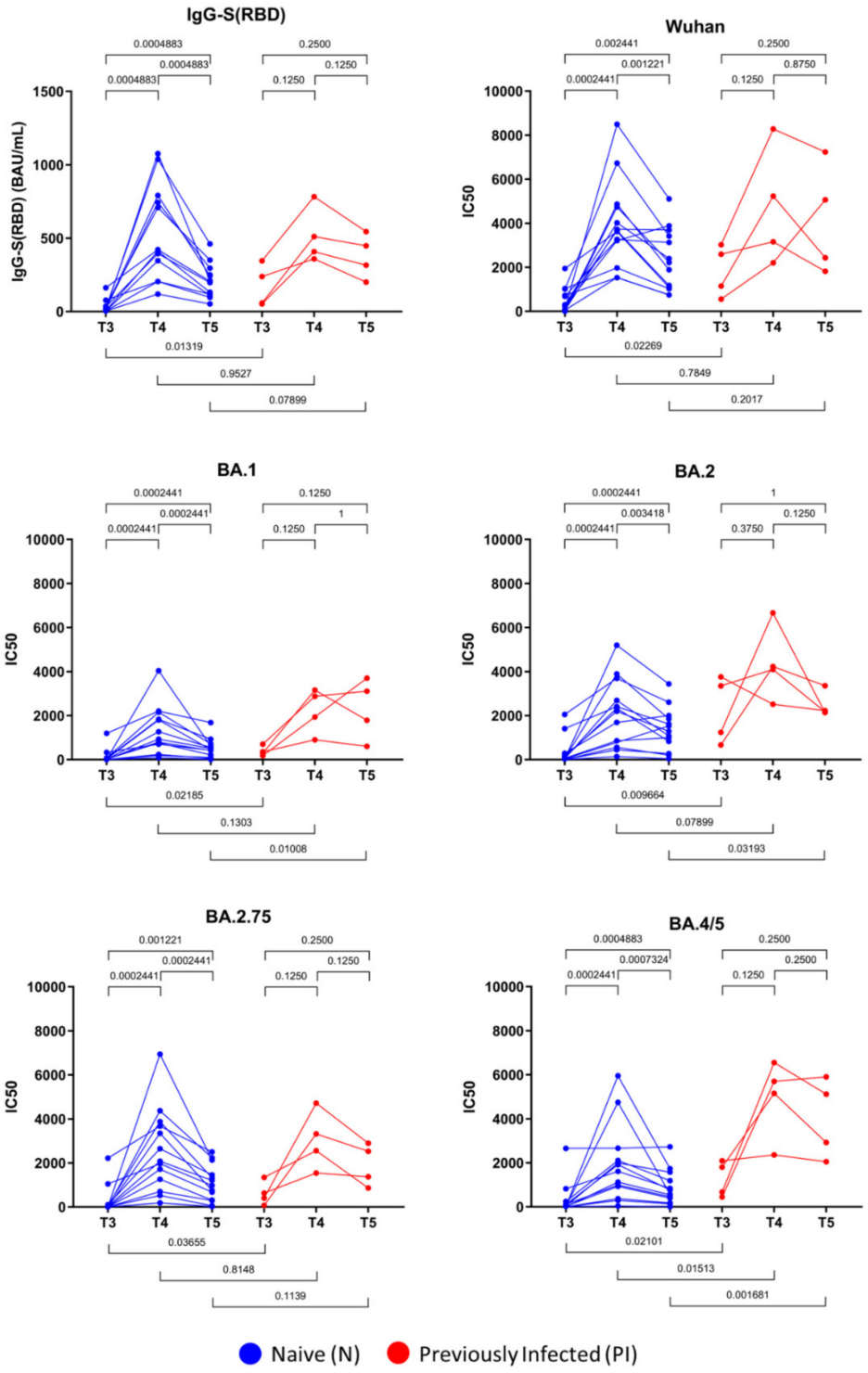

Figure 12. Comparison of IgG-S titres and IC50 between PI and N subjects (before-after plots). *The exposure to the virus results in a higher neutralizing activity. IgG-S titres were measured using the SARS-CoV-2 IgG II Quant Assay (Abbott). The neutralizing activity rate was measured via PVNA. The non-parametric Wilcoxon test and unpaired Mann-Whitney test were applied for statistical analysis. Blue dots and lines: naive; red dots and lines: PI; T3: before administration; T4: one month after administration; T5: four months after vaccine administration.*

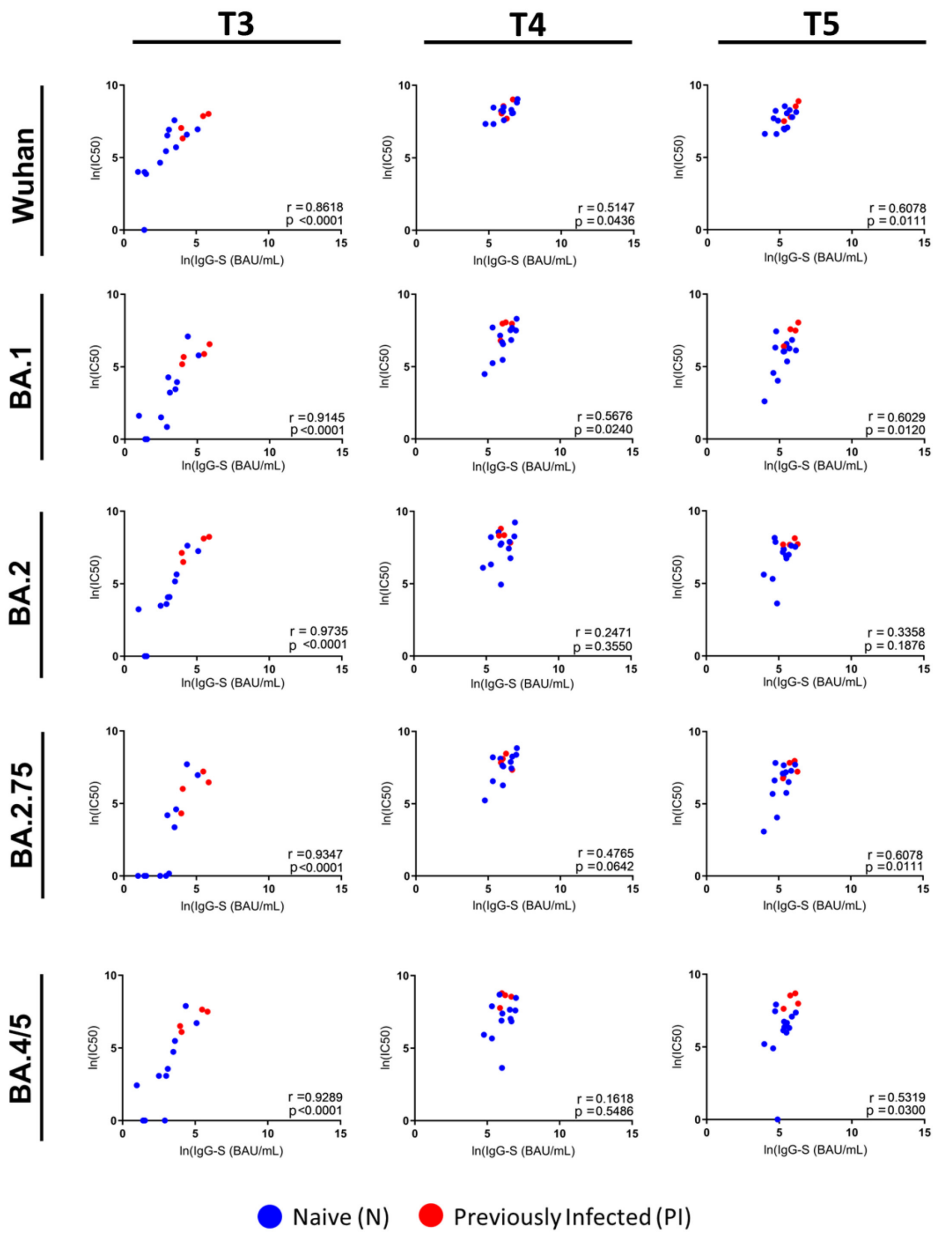

Figure 13. Dot plots representing Spearman's correlation analysis between the IgG-S titres vs. the neutralizing activity IC50. *A direct correlation is observed considering the Wuhan original strain, Omicron BA.1 and BA.2.75 at all timepoints. For Omicron BA.2 and BA.4/5, a direct correlation is observed before and four months after the vaccination. Blue dots: naive; red dots: PI; T3: before administration; T4: one month after administration; T5: four months after vaccine administration.*

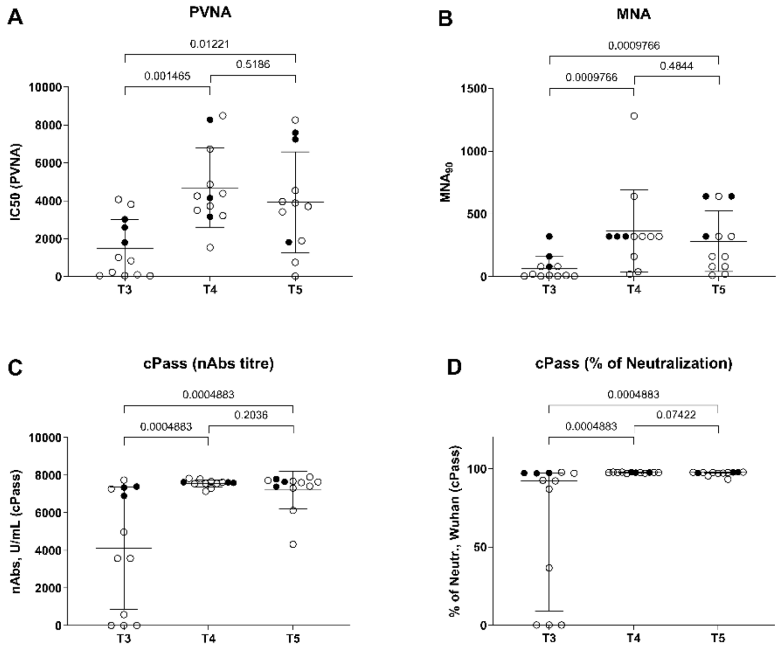

Figure 14. Dot plots comparing the results obtained from serological assays. *A reduced number of subjects (n=12) was tested because of practical reasons. PVNA (A), MNA (B), titration of nAbs using cPass (C), and calculation of the percentage of neutralization using cPass (D). Statistical analysis was carried out by applying the non-parametric Wilcoxon Test. Black circles: PI; white circles: naïve; T3: before administration; T4: one month after administration; T5: four months after administration.*

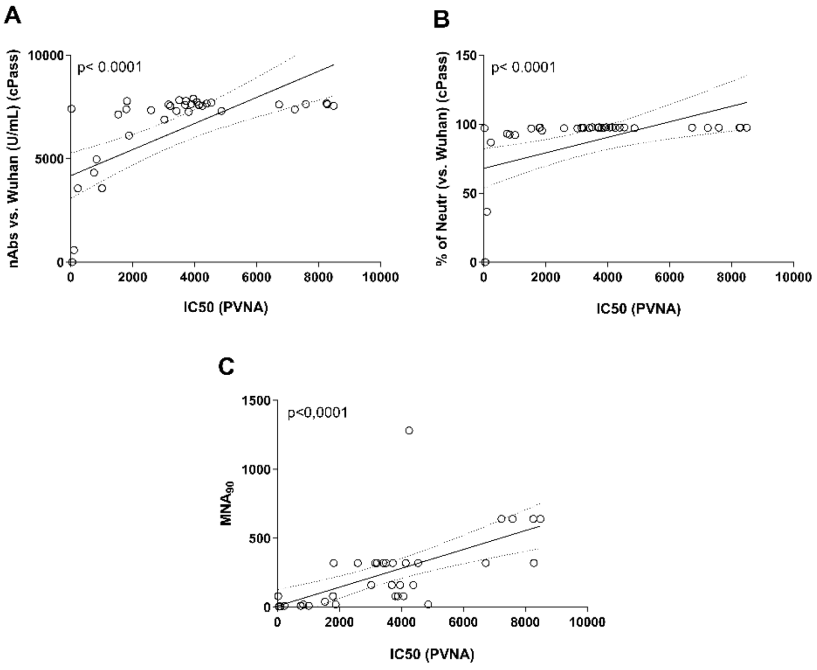

Figure 15. Dot plots representing the correlation analysis of cumulative results obtained with different serological assays. *nAbs titres (cPass) vs. PVNA (A), percentage of neutralization (cPass) vs. PVNA (B), PVNA vs. MNA (C). Linear regression analysis was performed.*

4.3. Circulating miR-155-5p and miR-148a-3p are altered in vaccinated subject

miR-155-5p and miR-148a-3p have been reported as critical participants in the onset of strong humoral immunity in COVID-19 patients (Giannella et al., 2022; Kassif-Lerner et al., 2022; Y. Liang et al., 2023; Miyashita et al., 2022). Therefore, they could be involved in the production of Spike-specific nAbs. The expression levels of miR-155-5p and miR-148a-3p were normalized to the expression levels of circulating miR-191-5p. 17 serum samples from unvaccinated, naive subjects were used as control (CTRL) (Fig.16).

While miR-191-5p was detected in all the subjects except for 1/17 in group T3 and 2/17 in the CTRL group, unfortunately, only a few, unpaired samples (CTRL: 5/17, T3: 5/17, T4: 4/17; T5: 6/17) showed clear detection of miR-155-5p. As for miR-155-5p, miR-148a-3p was detected in a few, unpaired samples (CTRL: 12/17, T3: 13/17, T4: 10/17, T5: 15/17). This dataset was not sufficiently large to support my thesis. More samples need to be collected and tested. The median detection cycles (Cq) of RT-qPCR are shown in Fig.16 (A, B, and C). The unpaired analyses of quantitative cycles (Cq) revealed no differences when comparing the different groups (CTRL vs. T3, CTRL vs. T4, CTRL, vs. T5, T3 vs. T4, T4 vs. T5, T3 vs. T5) expressing miR-155-5p or miR-148a-3p, although both appear reduced over time. For miR-191-5p, significant differences in the median Cq were observed when performing unpaired comparisons and paired comparisons of CTRL vs. T5 (p=0.0442) and T4 vs. T5 (p=0.011), respectively.

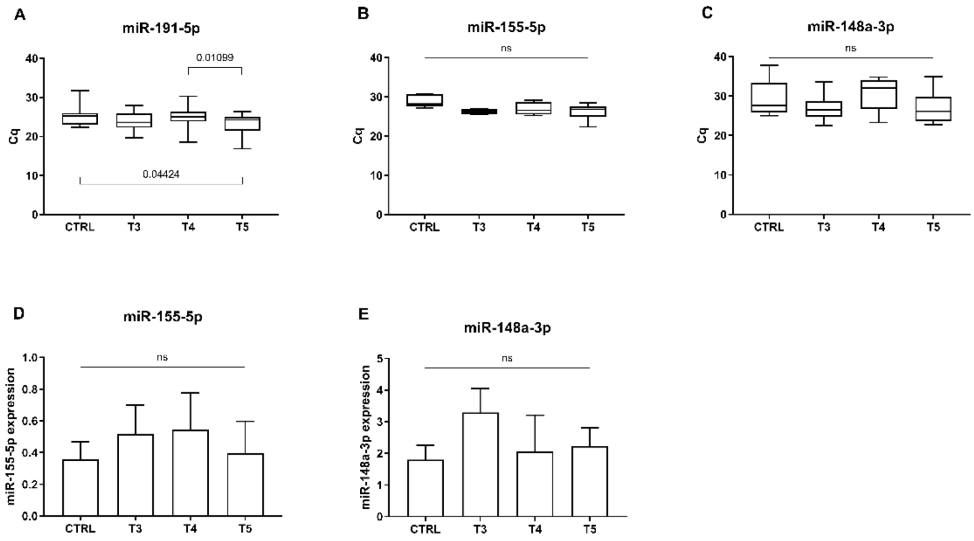

Figure 16. Bar plots of the circulating miRNAs analysis. *The quantitative cycles (Cq) of miR-191-5p (A), miR-155-5p (B), and miR-148a-3p are represented. miR-155-5p (D) and miR-148a-3p*

(E) normalized expressions are shown as bar plots. The non-parametric Wilcoxon and Mann-Whitney tests were performed to compare the miRNA expression levels.

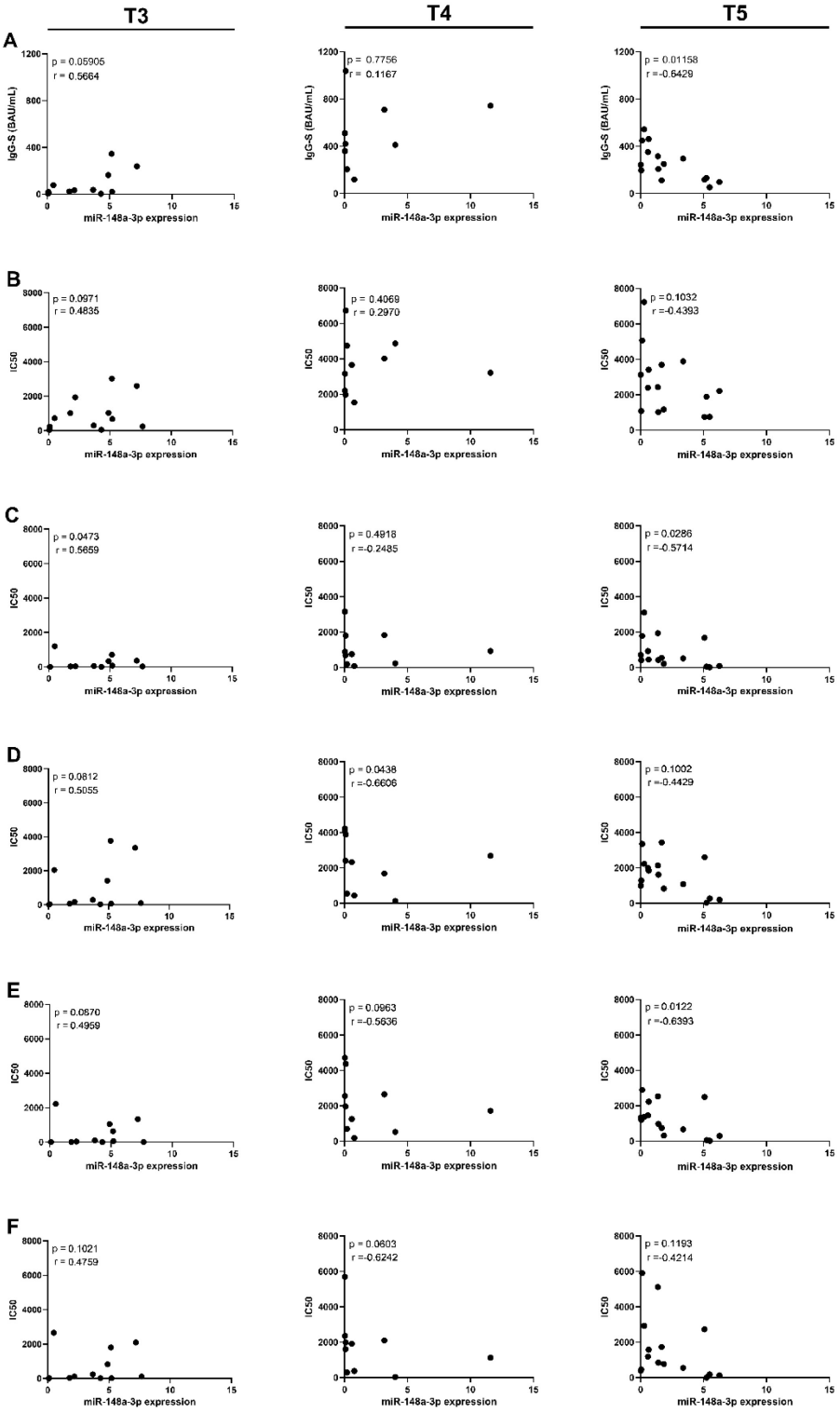

Figure 17. Spearman's correlation analysis of miR-148a-3p to IC50 (Wuhan) (dot plots). *The correlation of the expression levels of miR-148a-3p is reported against the titre of IgG-S (A) and the neutralizing activity against the original Wuhan strain (B), Omicron BA.1 (C), BA.2 (D), BA.2.75 (E), and BA.4/5 (F).*

The correlation between IC50 or IgG-S titre vs. miR-155-5p was impossible, due to the small amount of data. Nonetheless, Spearman's correlation of miR-148-3p with IC50 or IgG-S revealed an inverse association with the IgG-S titre at T5 (p=0.01158), with neutralizing activity against BA.1 at T3 (p=0.0473) and T5 (p=0.0286), against BA.2 ay T4 (p=0.0438), against BA.2.75 at T5 (p=0.0122) (Fig. 17).

4.4. SARS-CoV-2 PVs alter the expression of miR-28-3p

miR-28-3p has been identified as a major responsible for ADAM17 upregulation, with consequent ACE2 shedding, during SARS-CoV-2 infection (Xu and Li, 2021). Previous data on SARS-CoV showed that the incubation of ACE2-expressing cells with SARS-CoV PVs for 12 hours was sufficient to induce the reduction of ACE2 in cell isolates in Western Blot analyses (Haga et al., 2008). The same effect was not observed during the incubation with VSV-G PVs.

A preliminary experiment showed that the incubation with SARS-CoV-2 (Wuhan) for 6 hours induced a significant reduction in the relative expression of miR-28-3p (p=0.005601) in comparison to the control (UT, untreated) cell sample (Fig. 18). The same effect was not observed in the presence of VSV-G PVs. Although the expected effect was detected at 6 hours, the prolonged incubation (12 hours) with both the PVs caused a rise in the relative expression levels of miR-28-3p.

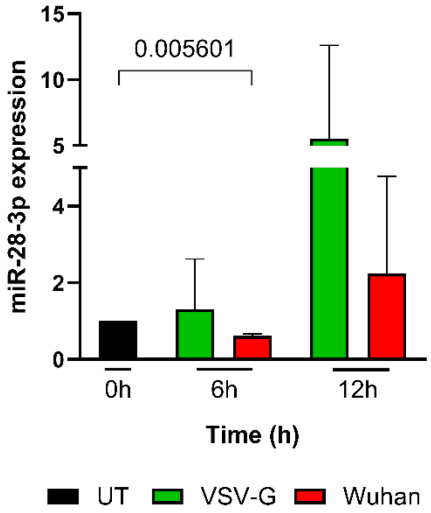

Figure 18. Bar plots showing reduced miR-28-3p expression after incubation with SARS-CoV-2 PVs. *miR-28-3p expression is significantly reduced when incubating CoV-2 PV for 6 hours (red bars). No alteration is induced by VSV-G (green bars). Higher expression is detected at 12 hours of incubation (UT, untreated; control sample). The unpaired t-test with Welch's correction was applied.*

4.5. ACE2 and ADAM17 expression levels after incubation with SARS-CoV-2 PVs

Previous studies demonstrated that A) ACE2 is shed from the cells surface of cells incubated with the RBD of SARS-CoV Spike or its lentiviral PVs (Haga et al., 2010, 2008), or the RBD of SARS-CoV-2 Spike, B) the simultaneous ADAM17 upregulation is responsible for sACE2 release, C) miR-28-3p contributes to this pathway (Xu and Li, 2021). To verify whether this mechanism occurs in the presence of SARS-CoV-2 PVs, HEK293T/A2 cells were incubated with Wuhan and Omicron BA.5 PVs for 6 and 12 hours, and the population expressing ACE2 and ADAM17 were analysed via FACS. The incubation of the cell line with phorbol-myristoyl aspartate (PMA) for 5-10 min was included as a control for ADAM17 upregulation (Lambert et al., 2005; Lorenzen et al., 2016). VSV-G PVs were also introduced as a control.

No alteration in the median number of ACE2+ cells was detected at 6 hours of incubation. A slight reduction of ACE2+ cells was observed after incubation with BA.5 PVs after 12 hours when compared to the untreated (UT) cell sample. A modest increase, although non-significantly different in comparison to the control (UT), was detected when the incubation with VSV-G and Wuhan PVs, respectively, occurred (Fig. 19A). The simultaneous detection of ADAM17 revealed a slight increase in the median number of ADAM17+ cells incubated with Wuhan PVs at 6 and 12 hours. The same effect was not detected for BA.5 and VSV-G at 6 hours of incubation. Conversely, the incubation with the BA.5 variant produced a visible reduction, although not significant, of ADAM17+ cells (Fig. 19B). Simultaneously, a duplicate of the same experiment was performed to extract total cellular RNA and measure miR-28-3p expression. A significant reduction in the relative expression levels of miR-28-3p was observed after 6 hours of incubation with the Wuhan PVs ($p=0.01984$) (Fig. 19C). No alteration was observed during the incubation with either VSV-G or Om BA.5, although the latter being visibly reduced. Surprisingly, a large increase of miR-28-3p was observed for all the incubation conditions at 12 hours.

Correlation analysis of miR-28-3p expression with ACE2+ or ADAM17+ cells after incubation with SARS-CoV-2 Wuhan and BA.5 PVs and VSV-G PVs at 6 and 12 hours are represented in Fig. 20. No significant correlation was detected.

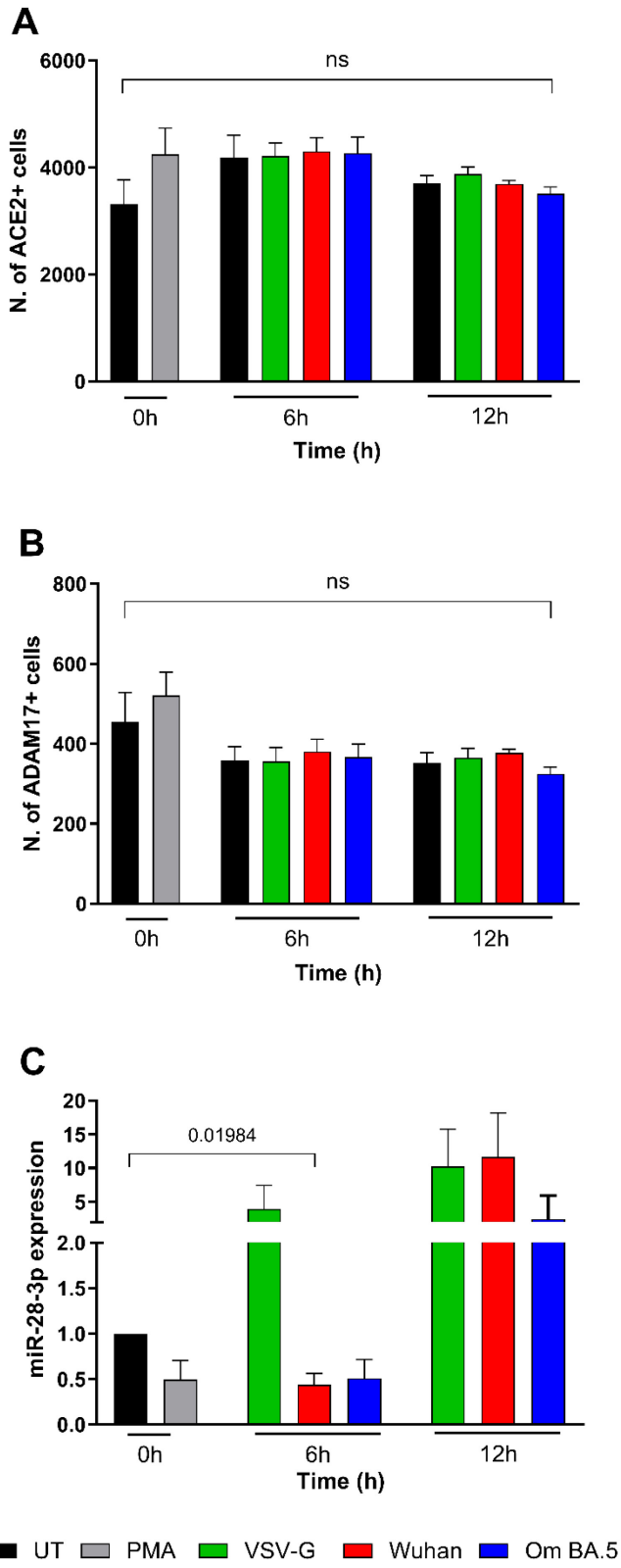

Figure 19. Bar plots representing the alteration of ACE2, ADAM17 and miR-28-3p after incubation with SARS-CoV-2 PVs. *ACE2+ median (A), ADAM17+ median (B) cell number, and miR-28-3p expression levels (C) are shown after 6 and 12 hours incubation with SARS-CoV-2 Wuhan (red bars), Omicron BA.5 (blue bars) and VSV-G PVs (green bars). Untreated (UT) (black*

bars) and PMA-treated (PMA) (grey bars) are considered controls. Unpaired t-test with Welch's correction and one-way ANOVA with Brown-Forsythe and Welch's were applied.

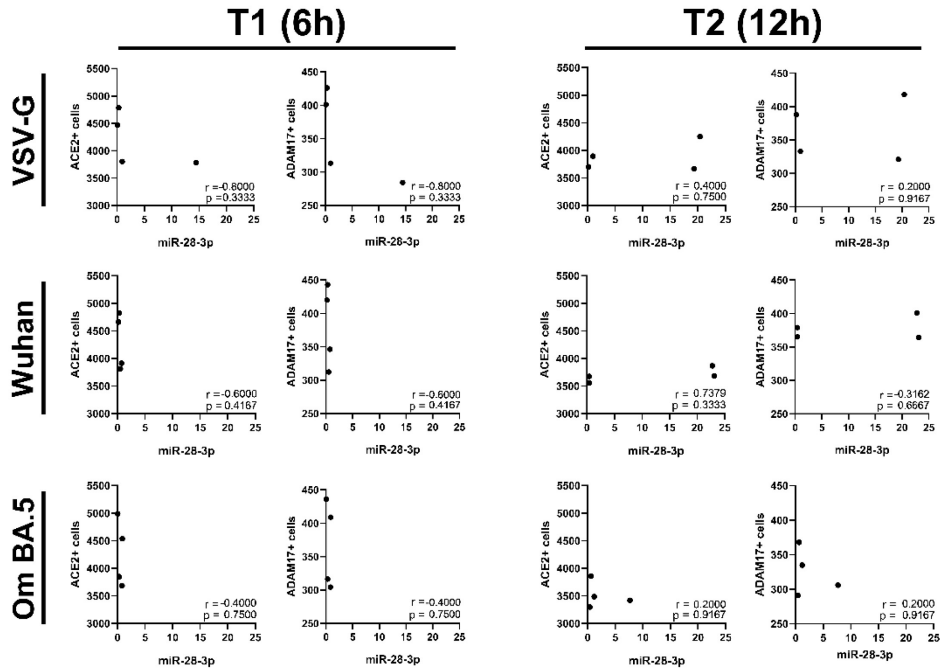

Figure 20. Dot plots representing the correlation analysis of miR-28-3p expression levels against the median number of ACE2+ or ADAM17+ cells after 6 and 12 hours incubation with VSV-G, SARS-CoV-2 Wuhan and Omicron BA.5 PVs. *No significant correlations were observed.*

5. DISCUSSION

5.1. The use of pseudotyped viruses in COVID-19 research

Since the beginning of my PhD course, I studied SARS-CoV-2 PVs, and the research experience abroad directly impacted my knowledge and my skills on this topic to adapt protocols for different applications. I explored different applications of SARS-CoV-2 PVs to study virus-cell surface interactions.

The technology of PVs offers advantages over other methods: PVs mimic the external surface of the real, enveloped virus interacting with the target cell; PVs are non-autonomously replicating; their infection rate can be measured; PVs require only biosafety level 2 (BSL2) containment conditions; the external glycoprotein can be easily switched to study different variants (Cantoni et al., 2023b; Carnell et al., 2015; Di Genova et al., 2021; Fantoni et al., 2023; Temperton, 2009b).

Several PV packaging systems exist (Tan et al., 2023; Xiang et al., 2022), including rhabdovirus-based (VSV-ΔG), lentiviral (HIV-1), and retroviral (MLV) platforms. Among these, lentiviral PVs are the preferable choice, since they are easily handled, highly replicating and more accessible. A major limitation to the use of PVs is that only enveloped viruses can be studied (Cantoni et al., 2023b; Xiang et al., 2022).

The critical step in the setup of different protocols and comparable results was the generation of SARS-CoV-2 permissive cell lines. The overexpression of ACE2 was necessary for the entrance of the PVs; infectivity rates were enhanced when the priming protease TMPRSS2 was overexpressed (Fig. 5) (Hoffmann et al., 2020b). Also, different SARS-CoV-2 variants showed different infectivity rates using the same permissive cell line (Fig. 6).

PVs have multiple applications, that include the investigation of direct receptor/coreceptors – viral glycoprotein interactions and drugs and monoclonal antibody discovery. Still, the principal application of PVs is the serological assay (PVNA) to measure the neutralizing rates of infected and/or vaccinated subjects (Li et al., 2018; Tan et al., 2023; Xiang et al., 2022). PVs have superior applications over other serological assays. MNA, a cell-based serological assay that uses the real virus of interest, requires highly trained and skilled personnel, a suitable and certified facility, and the assay lasts 2 up to 7 days (De Rienzo et al., 2021; Vergori et al., 2022). Alternatively, enzymatic cell-free assays overcome the necessity of a certified facility, and everyone with basic laboratory training can perform them. However, the model of the interaction is reduced to only the receptor and the viral protein. The cPass assay presented here uses only

the RBD-ACE2 interaction, further reducing the actual full-length viral glycoprotein-cell surface interaction (Jung et al., 2021).

Thus, PVs in the PVNA overcome several of these major issues: PVs allow for investigating both S1- and S2-targeting nAbs; PVs are produced and titred in less than two weeks and they are reproducible; PVs are easier to control, since their design prevents from accidental spread/spillover, reducing the risks of handling real viruses (Millet et al., 2019). Also, a recent study established that the results obtained from PVNA are comparable to those of the gold-standard MNA (Cantoni et al., 2023b).

Still, the major hurdle of SARS-CoV-2 PVs is the timeline for the results, as compared to cell-free assays. A period from 24 up to 48 hours is necessary to obtain the readout of the tests. To date, some systems that allow for automatic PVNA (Z. Liang et al., 2023) are being developed and commercialized. However, these platforms could be inaccessible to most laboratories due to the cost of purchase and maintenance. Strategies that could overcome this problem are the coupling of techniques that quantify biomarkers of the immune response.

This thesis also aims to show the use of SARS-CoV-2 PVs to investigate molecular processes that are initiated by the virus-cell interaction, since previous studies showed the possibility of studying the effects of intracellular or surface host factors that are initiated by the virus protein and cellular target interactions (Li et al., 2018).

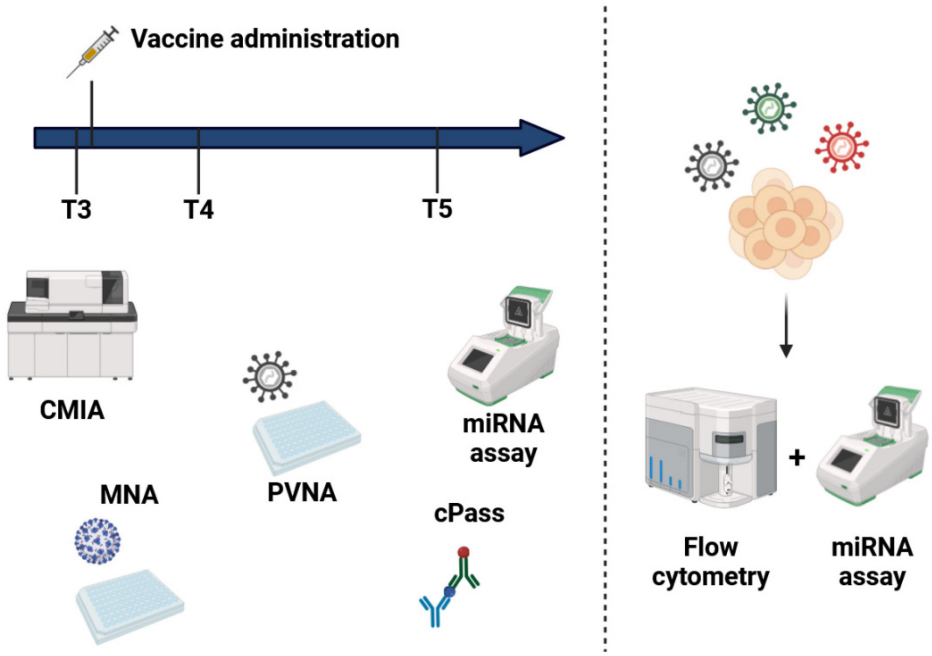

Figure 21. Graphical representation of the projects presented in this thesis. *On the left, the summary of the analysis of the humoral immunity. Three serum samples were collected from*

subjects receiving the third anti-SARS-CoV-2 vaccine. Samples were collected before (T3), one month (T4) and 4 months (T5) after the administration. Antibodies were quantified using CMIA assay or cPass assay. The potency of neutralizing antibodies was measured via MNA and PVNA. RT-qPCR for measuring circulating miRNAs involved in nAbs production was also performed. On the right, PVs of SARS-CoV-2 variants were used to analyse the role of miR-28-3p in regulating the expression of cell surface ADAM17 and ACE2. (Created with Biorender).

5.2. The efficacy of anti-SARS-CoV-2 third vaccination

At the end of 2020, innovative vaccine technologies were available for mass vaccination against SARS-CoV-2. Two platforms were mainly distributed in Italy: the mRNA-based and the adenoviral-based ones. The programme required the administration of two doses to sustain full protection against the virus (Zamagni et al., 2022). Simultaneously with the initiation of the vaccination programme, new SARS-CoV-2 variants, such as the Alpha and Beta VOCs, were already emerging (Stefanelli et al., 2022). The subsequent Gamma and Delta VOCs, and lately the subfamily of Omicron, showed increased escape rates, posing a new threat to the population, especially the elderly and more fragile people (La Rosa et al., 2022). The monitoring of the effective protection against new VOCs stimulated by the vaccine was essential for evaluating how to proceed with the vaccination. It appeared necessary to boost the immunity with a third dose to re-establish sufficient protection rates (Feikin et al., 2022).

A particular focus was dedicated to the humoral neutralizing immunity, which employs nAbs to block the onset of the infection by binding to the neutralizable sites on the Spike protein (Srinivasan et al., 2016). Nonetheless, vaccine-stimulated nAbs naturally decay after a few months, increasing the risk of recurrent infections (Levin et al., 2021; Morales-Núñez et al., 2021; Selvavinayagam et al., 2022).

A major part of my PhD project involved the setup, optimization, application and analysis of the technology of pseudotyped viruses to investigate the stimulation of the third booster dose. The data on the neutralizing activity against SARS-CoV-2 PVs in people receiving the third booster dose was presented in this thesis. Serum samples from 17 HCW volunteers were screened for IgG-S, IgG-N and neutralizing activity against the original SARS-CoV-2 strain and the Omicron variants, circulating early before and later during the vaccination follow-up. Serum samples were collected at the time of administration, four weeks and seventeen weeks after receiving the third booster vaccine. Since some of these HCWs participated in another project which investigated the effects of the first

two doses, the time of sample collection was referred to as T3, T4 and T5 (Dalle Carbonare et al., 2021). The studies on the first and second doses mainly focused on the trend in the generation of IgM-S and IgG-S in naive and PI subjects. It was reported that the presence of IgM-S immediately after vaccination and high titres of IgG-S are associated with stronger and prolonged protection (Dalle Carbonare et al., 2021; Piubelli et al., 2023; Ruggiero et al., 2022). In this study, only 2/17 subjects developed new Spike-specific IgM-S. All the participants produced IgG-S, showing that the booster vaccine still stimulated specific immunoglobulins. IgG-N were monitored to verify the presence of previous exposure to the virus. 4/17 experienced infection before the booster administration; one of these experienced a second infection between the second (T4) and the third (T5) sample collection.

The PVNAs revealed that some participants showed neutralizing activity against the analysed VOCs (16/17 against Wuhan, 8/17 against BA.1, 11/17 against BA.2, 8/17 against BA.2.75, 9/17 against BA.4/5) before receiving the booster dose. All the HCWs reacted positively to the vaccine, showing the blockade of all the analysed VOCs. These results confirm that the subjects were protected against variants that emerged after the vaccine administration. However, one subject has never shown efficient neutralizing activity only against BA.4/5; it would be interesting to study what factors are involved in the missing reaction to the vaccine. By comparing the neutralizing activity against Wuhan and Omicron VOCs, Wuhan was the best neutralized one (as expected, since the vaccine was designed on the original strain) (Girl et al., 2024). Interestingly, the Omicron BA.2, BA.2.75 and BA.4/5 were better neutralized than the Omicron BA.1. A similar result was obtained in another study (Hvidt et al., 2022). Both BA.2.75 and BA.4/5 originated from BA.2 (Chavda et al., 2023). Thus, one possible explanation is that PI subjects in this study contracted the BA.2 VOC, resulting in a higher, average protection level against the most recent variants. The halving of the median IC50 within 4 months after the vaccine administration was an observed trend (Brisotto et al., 2021). Unfortunately, none of the subjects donated other samples at 8 or 12 months to monitor the rate of loss of the neutralizing activity.

The measure of IgG-S and the corresponding neutralizing activity was another main topic of this thesis, since a direct association has been previously confirmed (Dalle Carbonare et al., 2021; Grunau et al., 2022; Tran et al., 2022). The Spearman's correlation analysis revealed that a direct correlation between IgG-S and IC50 existed before (T3) and 4 months (T5) after the booster dose for all the

variants, except for BA.2 (Fig. 13). A direct association between IC50 and the titre of IgG-S was observed at T4 only for Wuhan and BA.1. This effect could be attributed to the infected subjects that contracted the BA.2 VOC, as speculated above, although the literature reported the strong association between the titre of IgG-S and neutralization against multiple variants (Dalle Carbonare et al., 2021; Higashimoto et al., 2022).

The female population produced higher IgG-S antibodies in comparison to males after vaccine administration in a study from 2023. Only the antibody titres were analysed, excluding the neutralizing activity (Piubelli et al., 2023). In this thesis, sex did not influence either the production of specific antibodies or the protection level. The same study (Piubelli et al., 2023) also revealed that the proportion of IgG-S produced by the older population was generally lower if compared to the younger population. Similarly, Spearman's correlation analysis of neutralization capacity vs. age suggested that the elderly population struggles in producing and keeping highly neutralizing antibodies, although all the PI in these studies sat above the median age (> 51 yo). To sustain this assertion, the only subject that never developed nAbs against BA.4/5 aged 62 yo. Yet only one case is insufficient.

A major active debate in the literature is the previous exposure to SARS-CoV-2 infection, which guarantees prolonged protection (Crotty, 2021; Dalle Carbonare et al., 2021; Salgado et al., 2023). Generally, PI subjects produced higher median titres of IgG-S and average stronger neutralization against Omicron BA.1, BA.2 and BA.4/5 at T5, whereas no difference was observed against the BA.2.75. This could be attributable to the longer evolutionary distance of BA.275 from Wuhan, in comparison to the other Omicron VOCs in analyses. Since the number of PI (n=4/17) was insufficient, it was difficult to appreciate the immunological advantage of PI over the naive population.

Because of the natural waning of antibodies after the third booster dose, the international health organizations established to administer a fourth, and possibly a fifth booster, to induce better protection (Della Polla et al., 2023). A very recent study found that: A) both the PI and Naive populations suffer from the initial waning of the protective antibodies, B) the recurrent booster vaccination in the naive group raises the setpoint of specific antibody titres as high as those of PI, and C) a long-term stabilization of the specific antibodies exists in both groups (Srivastava et al., 2024).

The main limitation of this study is the limited number of enrolled HCWs, which is not sufficient to appreciate the multiple characteristics of the population.

5.3. Serological assays give similar readouts

In this study, the comparison of cell-based (MNA and PVNA) and cell-free (the cPass assay by GenScript) serological assays was tested. The characteristics of the single assays are commented on in paragraph 1.3.2. The advantages and limitations of the methods were also commented on in paragraph 5.1.

After the PVNAs were performed, I compared the obtained results to validate the use of PVNA over the other methods. A restricted number of subjects has been tested for the gold-standard MNA and the cell-free serological assay cPass. Correlation analyses revealed that all three methods efficiently detect the neutralizing activity with comparable results (Fig. 15) (Hemken et al., 2023; Narasimhan et al., 2021; Takahashi et al., 2023). Moreover, the cPass assay both measures the titre of nAbs and the percentage of neutralization by applying a conversion formula.

Still, the cell-based assays suffer from the cell growth required to obtain the readout. On the contrary, the cPass assays give results in a few hours. Although this is advantageous, it fails to distinguish the wide range of neutralization activity that the cell-based assays provide. A potential strategy to improve the cell-free assay readout and shorten the time required for the other two methods is to couple the enzymatic assay with the measure of other biomarkers. In this sense, circulating miRNAs offer a valid target to be implemented with serological assays, as proposed in the following paragraph.

5.4. miRNAs involved in efficient neutralizing humoral immunity

Since the beginning of the vaccination program against SARS-CoV-2, several studies investigated nAbs-mediated protection (Du et al., 2021; Nie et al., 2020). By the time this thesis was written, the research interest in the third booster dose faded because updated vaccines are available against the latest Omicron VOCs (Abdoli et al., 2024). Focusing the research on other factors that could impact the production and maintenance of nAbs could contribute to improving innovative vaccine platforms with foresight on future pandemics and personalized vaccination approaches.

Three decades passed since the first discovery of microRNAs (Lee et al., 1993) and their role as biomarkers is gaining more importance for rapid diagnostic and prognostic purposes, although the application in the clinical field is still limited due to multiple factors (multifactorial nature of miRNAs, expression variability

in the population, relative quantification) (Huang et al., 2011; Keller et al., 2017; Tribolet et al., 2020). miRNAs are also found in the bloodstream and are therefore called circulating miRNAs (Mitchell et al., 2008). Among the number of these circulating miRNAs, many are also involved in immune system maturation and activation, production of antibodies, and stable immune response (Wigton and Ansel, 2021). Two microRNAs, miR-155-5p and miR-148a-3p, emerged as the perfect object for this research (Y. Liang et al., 2023; Miyashita et al., 2022).

miR-155-5p is involved in several inflammatory processes during infections (Gaytán-Pacheco et al., 2022; Jafarzadeh et al., 2021), including pulmonary viral diseases (Woods et al., 2020; Wu et al., 2013). miR-155 is upregulated in COVID-19 (Giannella et al., 2022; Molinero et al., 2022) and post-acute COVID-19 patients for several days (Eyileten et al., 2022), specifically in PBMCs (Abbasi-Kolli et al., 2022; Donyavi et al., 2021; Garg et al., 2021; Soni et al., 2020) and in plasma (Gaytán-Pacheco et al., 2022). Another study (Gedikbasi et al., 2022) found a descending trend in post-COVID-19 patients, in opposition to the previous cited study. Since contradictory results were reported, it would be interesting to further investigate the role of miR-155-5p in the disease, as it is implied in the regulation of B cell activities (Thai et al., 2007), and potentially, it could directly impact the production of nAbs.

As for miR-155-5p, miR-148a-3p is involved in proinflammatory processes (Miyashita et al., 2022). It also participates in infectious diseases: miR-148a-3p directly targeted the genome of SARS-CoV in a previous study (Mallick et al., 2009). Murine miR-148a-3p is critical for B lymphocyte maturation and activation and prevents apoptosis in B cells (Gonzalez-Martin et al., 2016; Porstner et al., 2015; Pracht et al., 2021). A recent study found the upregulation of miR-148a-3p in COVID-19 patients who required intensive care unit (ICU) hospitalization (de Gonzalo-Calvo et al., 2021). The following works found a direct association between the titre of specific antibodies and the modulation of miR-148a-3p. First, upregulated miR-148a-3p from nasal swabs was correlated with specific antibody titres in water buffaloes after vaccination against BuHV-1 (Lecchi et al., 2023). Secondly, a reduction of circulating miR-148a-3p was inversely proportional to the titre of anti-Spike antibodies in vaccinated subjects (Miyashita et al., 2022).

Given these studies, the investigation on the role of miR-148a-3p in modulating the production and maintenance of nAbs, paired with that of miR-155-5p, could be the first approach to establish a panel of immunologically relevant miRNAs involved in the vaccination against SARS-CoV-2 and future SARS-related CoVs.

I extracted the total circulating RNA from the serum of vaccinated people at the three timepoints and performed RT-qPCR. I also selected a group of gender- and age-matched subjects that never contracted the infection or received the vaccine as a control. I chose miR-191-5p as a normalizer as it is one of the best validated (Peltier and Latham, 2008). First, the non-parametric analysis showed a difference in the quantitative cycle of miR-191-5p between the T5 group and the control group and between the T4 and T5 groups. Possibly, miR-191-5p could be involved in immune responses and vaccination, although it is usually considered a biomarker of cancer or other diseases (He et al., 2015; Kudelova et al., 2022; Vistbakka et al., 2017). A study published after I performed the experiments found that miR-191-5p is downregulated in hospitalized COVID-19 patients (Franco et al., 2024). An alteration could exist also after vaccination. The Cq of miR-155-5p and miR-148a-3p did not differ over time. Unfortunately, miR-155-5p could not be detected in the majority of the subjects. Despite repeating the experiment starting from the RNA isolation, only 5 subjects were actively expressing miR-155-5p. After normalization on miR-191-5p, miR-155-5p expression appears altered over time, consistently with the aforementioned studies. No difference in the expression emerged. Circulating miR-148a-3p also was not detected in some samples. However, the plot in Fig. 16E shows an increased expression level before the time of vaccination, decreased expression at T4 and a slight increase at T5. Also, in this case, no differences that could be attributed to the vaccine were found.

I performed Spearman's correlation analysis to verify whether one of these microRNAs could influence the antibody titre or the neutralizing activity. The dataset of miR-155-5p was insufficient to perform the analysis. miR-148a-3p, on the other hand, showed a significant correlation with the IgG-S titre at T5, and with neutralizing activity against BA.1 at T3 and T5, against BA.2 at T4, against BA.2.75 at T5. It appears that a direct correlation is present after vaccination, and therefore it could be used as a suitable biomarker for effective vaccine response. Yet, this could not be completely asserted because of A) the lack of a sufficiently large number of samples, and B) the exclusion of PI subjects.

Although the data were insufficient, these preliminary results suggest that the titration of nAbs coupled with the measure of circulating miRNAs, which are involved in B cells processes, could be a valid method to monitor the neutralizing immune responses against the virus. A larger number of target miRNAs is necessary to validate a panel which is specific for anti-SARS-CoV-2 immunity since both miR-155-5p and miR-148a-3p are among the first to participate in

inflammatory responses (Tsitsiou and Lindsay, 2009). The major advantages of this approach over the other methods presented in this thesis are that both the miRNA and the cell-free serological assays give readouts in a few hours and that containment conditions for handling PVs or real viruses are not required. Lastly, this strategy can be applied to several other vaccines against other highly-pathogenic viruses.

5.5. The role of miR-28-3p in the shedding of ACE2

COVID-19 induces the critical rise of sACE2 in the circulation of most severe patients (Elemam et al., 2022; Kuba et al., 2005; Mariappan et al., 2022; Nagy et al., 2021). This condition is comparable to the onset of several cardiovascular and pulmonary diseases (Narula et al., 2020). Previous studies (Haga et al., 2010, 2008) on SARS-CoV showed the release of sACE2 is attributable to the direct Spike-ACE2 contact. They found that the release is caused by ADAM17 and that the cytoplasmic tail of ACE2 plays a critical role in the transduction of the Spike-mediated signal. The shedding of ACE2 was abrogated when ADAM17 inhibitors were used, or absent if using PVs of VSV-G or HCoV-NL63, the latter sharing the receptor with SARS-CoV and SARS-CoV-2 (Haga et al., 2010, 2008). Therefore, this mechanism could be one of the major participants in the beginning of the most severe pathological state of SARS and COVID-19.

ADAM17 has been identified as the major responsible for ACE2 shedding in the human organism. First, ADAM17 is constitutively releasing sACE2 to contribute to exploiting its protective function (Lambert et al., 2005). Secondly, the alteration of ADAM17 activity has been studied in tumorigenesis and other pathological processes (Calligaris et al., 2021; Saad et al., 2019; Yang et al., 2021).

A study from 2021 (Xu and Li, 2021) found a potential third participant that could be involved in the mechanism. The incubation of ACE2-overexpressing HEK293T cells with Spike RBD of SARS-CoV-2 reduced the intracellular levels of miR-28-3p and raised the expression levels of ADAM17 in 24 hours. Longer incubation time would revert the process.

With a preliminary experiment, I replicated the reduction of miR-28-3p in HEK-293T cells overexpressing after incubating the HEK293T/A2 cells with SARS-CoV-2 (Wuhan strain) for 6 hours (Fig. 18). No differences were observed when the same cell line was incubated with VSV-G. Therefore, this experiment

confirmed that a reduction of miR-28-3p is specifically induced by the SARS-CoV-2 Spike protein.

This was the first evidence that PVs can be applied to study miRNAs if the expected effect is directly mediated by the viral glycoprotein. The same result was observed by repeating the experiment with Wuhan PVs and including a second SARS-CoV-2 VOC, the Omicron BA.5. This VOC induced a reduction of miR-28-3p expression after 6 hours. The Omicron subfamily uses an ACE2-dependent/TMRPSS2-independent entry pathway (Bruel et al., 2022; Pather et al., 2023). Therefore, the reduction of miR-28-3p should be expected.

In parallel, FACS analysis of ACE2 and ADAM17 alternate regulation was monitored with SARS-CoV-2 PVs (Wuhan and Omicron BA.5), using VSV-G as a control. I chose flow cytometry because A) the process should occur at the surface level, and B) previous studies used either total cellular extracts in WB analysis or cytoplasm, membrane and extracellular protein isolates. Before commenting on the results, it is worth mentioning that HEK293T cells have been transduced to overexpress ACE2 and PMA was used to stimulate ADAM17 surface overexposure to facilitate the surface localization and its detection (Lambert et al., 2005). In fact, in a previous study, they transfected HEK293 and HeLa cell lines with the plasmid constructs of ADAM17 and incubated them with PMA, because of the quick surface turnover of ADAM17 (Lorenzen et al., 2016).

The median number of ACE2+ cells after 6 hours of incubation with the PVs (SARS-CoV-2 Wuhan and Omicron BA.5 variants, and VSV-G as control) did not change. By prolonging the incubation time up to 12 hours, no significant difference was detected. However, it appeared that the BA.5 PV could induce a reduction of ACE2+ cells if visually compared to VSV-G and Wuhan incubated samples.

For the analysis of surface ADAM17, 5-10 minutes of incubation of the cell line with PMA increased the ADAM17-positive median population, as suggested by a previous study (Lorenzen et al., 2016), and was therefore used as a control. Moreover, PMA was capable of reducing miR-28-3p expression, although the statistical analysis revealed no significant difference. ADAM17 was lightly overexposed on the surface of cells incubated with SARS-CoV-2 Wuhan PVs at 6 and 12 hours post-incubation. Interestingly, the BA.5 variant reduced the number of ADAM17-positive cells. Possibly, the altered entry pathway of Omicron, compared to Wuhan, (ACE2-dependent/TMRPSS-2-independent) stimulates different pathways that can induce the expression of other

metalloproteases involved in ACE2-shedding, such as ADAM10 from the same family of ADAM17 (Niehues et al., 2022).

I also performed the correlative analysis of the number of cells expressing the two protein targets, ACE2 and ADAM17, with the expression levels of miR-28-3p, which did not reveal any association.

Major issues and limitations, however, with these experiments are A) the overexpression of ACE2 in HEK293T cells, which could alter intracellular signal pathways, B) the low expression and the rapid turnover of ADAM17 on the cell surface that result in difficult detection, C) the disproportionate increase of miR-28-3p intracellular expression at 12 hours incubation with all the PVs, VSV-G included. A study on HTLV-1 revealed that miR-28-3p directly binds to the genome of the virus (Bai and Nicot, 2015). Possibly, miR-28-3p interacts with the lentiviral vector introduced by the PVs. Also, this bias could be avoided by adopting alternative PV packaging systems.

A piece of additional information to this study could be the analysis of the transcription levels of ADAM17 and ACE2 following exposure to PVs. To date, no study has produced such information. However, it could contribute to the understanding of the differences that arise using different models.

Nonetheless, these are preliminary experiments that could contribute to the study of this pathway using the model of PVs, which is more reliable than the use of a recombinant, monomeric protein (Haga et al., 2010, 2008; Xu and Li, 2021).

From the biological point of view, this phenomenon appears as a first-line alert mechanism against the impairment of the RAS system caused by SARS-CoV and SARS-CoV-2. It is, in fact, well established that A) sACE2 has a protective role in preserving the cardiovascular and pulmonary functions, B) the overall circulating sACE2 setpoint is increased in cardiovascular (Sama et al., 2020) and pulmonary diseases (Imai et al., 2005; Marshall et al., 2002). Thus, sACE2 displays a different function based on the levels of the circulating active form. The fact that SARS-CoVs induce the shedding of ACE2, throughout the pathway described above, represents a protective strategy that the organism adopts to counterbalance the onset of the disease and preserve the cardiovascular and pulmonary functions. However, with the worsening of the disease, the tolerable sACE2 levels are surpassed, resulting in the opposite, destructive effect. This could explain why acute and deceased COVID-19 subjects present high sACE2 levels in the circulation (Elemam et al., 2022; Kuba et al., 2005; Mariappan et al., 2022; Nagy et al., 2021).

To further sustain this hypothesis, it has to be noticed that ADAM17 (Sperrhacke et al., 2023; Wang et al., 2011) is involved in proinflammatory and apoptotic processes, by releasing several immune-related surface cytokines and receptors, such as TNFα and IL-6 (Schumacher and Rose-John, 2022). miR-28-3p is also involved in the initiation of apoptosis and inflammatory processes, and it is downmodulated in several cancer types (Lv et al., 2019; Schneider et al., 2014; Jiabin Zhang et al., 2021), preserving proliferation. In this sense, the observed upregulation of miR-28-3p at 12 hours of incubation with all the analysed PVs (Fig. 19) could be explained as the activation of anti-proliferative mechanisms, that the cell activates sensing the presence of the lentiviral vector.

Therefore, the ACE2/miR-28-3p/ADAM17 interplay could represent a specific pathway that the organism adopts to counteract the infection by ACE2-dependent SARS-CoVs, by signalling the presence of the RAS impairment and initiating proapoptotic and proinflammatory processes, to contrast the viral replication.

6. FINAL CONSIDERATIONS

This thesis presented multiple uses of PVs for serological studies, the investigation of biomarkers for sustained immune protection, and molecular mechanisms that could favour the onset of severe COVID-19. The contributions of this thesis to the basic research and potential applications are several. First, the optimization of methods for the monitoring of serological protection against COVID-19 could contribute to identifying people who are subject to the severe form of the disease, the recurrent infections, and the exposure to new variants. Also, the comparison of different serological assays allows for the evaluation of their points of strength and weakness, stimulating the research for improvements and developing new methods. For example, the simultaneous measure of circulating miRNAs, involved in modulating the production of pathogen-specific antibodies, and cell-free serological assays is an innovative strategy to improve and accelerate the monitoring of immune protection in the population. Secondly, here the technology of PVs has been applied to the study of molecular mechanisms involved in the pathogenesis of COVID-19. In conclusion, it must be considered the vast contribution of SARS-CoV-2 PVs in COVID-19 research, especially showing their potential in the research of new, emerging pandemic pathogens.

7. REFERENCES

Abbasi-Kolli, M., Sadri Nahand, J., Kiani, S.J., Khanaliha, K., Khatami, A., Taghizadieh, M., Torkamani, A.R., Babakhaniyan, K., Bokharaei-Salim, F., 2022. The expression patterns of MALAT-1, NEAT-1, THRIL, and miR-155-5p in the acute to the post-acute phase of COVID-19 disease. Braz J Infect Dis 26, 102354. https://doi.org/10.1016/j.bjid.2022.102354

Abdoli, A., Jamshidi, H., Taqavian, M., Baghal, M.L., Jalili, H., 2024. Omicron-specific and bivalent omicron-containing vaccine candidates elicit potent virus neutralisation in the animal model. Sci Rep 14, 268. https://doi.org/10.1038/s41598-023-50822-w

Aboulela, A., Taha, M., Ghazal, A., Baess, A., Elsheredy, A., 2024. Alternations in miR-155 and miR-200 serum levels can serve as biomarkers for COVID-19 in the post-mass vaccination era. Mol Biol Rep 51, 689. https://doi.org/10.1007/s11033-024-09630-2

ALIMOHAMADI, Y., SEPANDI, M., TAGHDIR, M., HOSAMIRUDSARI, H., 2020. Determine the most common clinical symptoms in COVID-19 patients: a systematic review and meta-analysis. J Prev Med Hyg 61, E304–E312. https://doi.org/10.15167/2421-4248/jpmh2020.61.3.1530

Almeida, M.I., Nicoloso, M.S., Zeng, L., Ivan, C., Spizzo, R., Gafà, R., Xiao, L., Zhang, X., Vannini, I., Fanini, F., Fabbri, M., Lanza, G., Reis, R.M., Zweidler–McKay, P.A., Calin, G.A., 2012. Strand-Specific miR-28-5p and miR-28-3p Have Distinct Effects in Colorectal Cancer Cells. Gastroenterology 142, 886-896.e9. https://doi.org/10.1053/j.gastro.2011.12.047

Andreano, E., Piccini, G., Licastro, D., Casalino, L., Johnson, N.V., Paciello, I., Dal Monego, S., Pantano, E., Manganaro, N., Manenti, A., Manna, R., Casa, E., Hyseni, I., Benincasa, L., Montomoli, E., Amaro, R.E., McLellan, J.S., Rappuoli, R., 2021. SARS-CoV-2 escape from a highly neutralizing COVID-19 convalescent plasma. Proceedings of the National Academy of Sciences 118, e2103154118. https://doi.org/10.1073/pnas.2103154118

Anguiano, L., Riera, M., Pascual, J., Soler, M.J., 2017. Circulating ACE2 in Cardiovascular and Kidney Diseases. CMC 24. https://doi.org/10.2174/0929867324666170414162841

Baggen, J., Vanstreels, E., Jansen, S., Daelemans, D., 2021. Cellular host factors for SARS-CoV-2 infection. Nat Microbiol 6, 1219–1232. https://doi.org/10.1038/s41564-021-00958-0

Bahadur Shrestha, L., Foster, C., Rawlinson, W., Tedla, N., Bull, R.A., Rowena Bull, C.A., 2022. Evolution of the SARS-CoV-2 omicron variants BA.1 to BA.5: Implications for immune escape and transmission. Reviews in Medical Virology e2381. https://doi.org/10.1002/RMV.2381

Bai, X.T., Nicot, C., 2015. miR-28-3p Is a Cellular Restriction Factor That Inhibits Human T Cell Leukemia Virus, Type 1 (HTLV-1) Replication and Virus Infection. J Biol Chem 290, 5381–5390. https://doi.org/10.1074/jbc.M114.626325

Barthe, M., Hertereau, L., Lamghari, N., Osman-Ponchet, H., Braud, V.M., 2023. Receptors and Cofactors That Contribute to SARS-CoV-2 Entry: Can Skin Be an Alternative Route of Entry? Int J Mol Sci 24, 6253. https://doi.org/10.3390/ijms24076253

Bellino, S., 2021. COVID-19 vaccines approved in the European Union: current evidence and perspectives. Expert Review of Vaccines 20, 1195–1199. https://doi.org/10.1080/14760584.2021.1962304

Benedictow, O.J., 2021. The Complete History of the Black Death. Boydell & Brewer. https://doi.org/10.1017/9781787449312

Benhaim, M.A., Lee, K.K., 2020. New Biophysical Approaches Reveal the Dynamics and Mechanics of Type I Viral Fusion Machinery and Their Interplay with Membranes. Viruses 12, 413. https://doi.org/10.3390/v12040413

Bewley, K.R., Coombes, N.S., Gagnon, L., McInroy, L., Baker, N., Shaik, I., St-Jean, J.R., St-Amant, N., Buttigieg, K.R., Humphries, H.E., Godwin, K.J., Brunt, E., Allen, L., Leung, S., Brown, P.J., Penn, E.J., Thomas, K., Kulnis, G., Hallis, B., Carroll, M., Funnell, S., Charlton, S., 2021. Quantification of SARS-CoV-2 neutralizing antibody by wild-type plaque reduction neutralization, microneutralization and pseudotyped virus neutralization assays. Nat Protoc 16, 3114–3140. https://doi.org/10.1038/s41596-021-00536-y

Brisotto, G., Muraro, E., Montico, M., Corso, C., Evangelista, C., Casarotto, M., Caffau, C., Vettori, R., Cozzi, M.R., Zanussi, S., Turetta, M., Ronchese, F., Steffan, A., 2021. IgG antibodies against SARS-CoV-2 decay but persist 4 months after vaccination in a cohort of healthcare workers.

Clinica Chimica Acta; International Journal of Clinical Chemistry 523, 476. https://doi.org/10.1016/j.cca.2021.10.035

Bruel, T., Hadjadj, J., Maes, P., Planas, D., Seve, A., Staropoli, I., Guivel-Benhassine, F., Porrot, F., Bolland, W.-H., Nguyen, Y., Casadevall, M., Charre, C., Péré, H., Veyer, D., Prot, M., Baidaliuk, A., Cuypers, L., Planchais, C., Mouquet, H., Baele, G., Mouthon, L., Hocqueloux, L., Simon-Loriere, E., André, E., Terrier, B., Prazuck, T., Schwartz, O., 2022. Serum neutralization of SARS-CoV-2 Omicron sublineages BA.1 and BA.2 in patients receiving monoclonal antibodies. Nat Med 28, 1297–1302. https://doi.org/10.1038/s41591-022-01792-5

Calligaris, M., Cuffaro, D., Bonelli, S., Spanò, D.P., Rossello, A., Nuti, E., Scilabra, S.D., 2021. Strategies to Target ADAM17 in Disease: From Its Discovery to the iRhom Revolution. Molecules 26, 944. https://doi.org/10.3390/molecules26040944

Cameroni, E., Bowen, J.E., Rosen, L.E., Saliba, C., Zepeda, S.K., Culap, K., Pinto, D., VanBlargan, L.A., De Marco, A., di Iulio, J., Zatta, F., Kaiser, H., Noack, J., Farhat, N., Czudnochowski, N., Havenar-Daughton, C., Sprouse, K.R., Dillen, J.R., Powell, A.E., Chen, A., Maher, C., Yin, L., Sun, D., Soriaga, L., Bassi, J., Silacci-Fregni, C., Gustafsson, C., Franko, N.M., Logue, J., Iqbal, N.T., Mazzitelli, I., Geffner, J., Grifantini, R., Chu, H., Gori, A., Riva, A., Giannini, O., Ceschi, A., Ferrari, P., Cippà, P.E., Franzetti-Pellanda, A., Garzoni, C., Halfmann, P.J., Kawaoka, Y., Hebner, C., Purcell, L.A., Piccoli, L., Pizzuto, M.S., Walls, A.C., Diamond, M.S., Telenti, A., Virgin, H.W., Lanzavecchia, A., Snell, G., Veesler, D., Corti, D., 2022. Broadly neutralizing antibodies overcome SARS-CoV-2 Omicron antigenic shift. Nature 602, 664–670. https://doi.org/10.1038/s41586-021-04386-2

Cantoni, D., Siracusano, G., Mayora-Neto, M., Pastori, C., Fantoni, T., Lytras, S., Di Genova, C., Hughes, J., on behalf of the Ambulatorio Medico San Luca Villanuova Group, Lopalco, L., Temperton, N., 2023a. Analysis of Antibody Neutralisation Activity against SARS-CoV-2 Variants and Seasonal Human Coronaviruses NL63, HKU1, and 229E Induced by Three Different COVID-19 Vaccine Platforms. Vaccines 11, 58. https://doi.org/10.3390/vaccines11010058

Cantoni, D., Wilkie, C., Bentley, E.M., Mayora-Neto, M., Wright, E., Scott, S., Ray, S., Castillo-Olivares, J., Heeney, J.L., Mattiuzzo, G., Temperton,

N.J., 2023b. Correlation between pseudotyped virus and authentic virus neutralisation assays, a systematic review and meta-analysis of the literature. Frontiers in Immunology 14.

Carabelli, A.M., Peacock, T.P., Thorne, L.G., Harvey, W.T., Hughes, J., Peacock, S.J., Barclay, W.S., de Silva, T.I., Towers, G.J., Robertson, D.L., 2023. SARS-CoV-2 variant biology: immune escape, transmission and fitness. Nat Rev Microbiol 21, 162–177. https://doi.org/10.1038/s41579-022-00841-7

Carnell, G.W., Ferrara, F., Grehan, K., Thompson, C.P., Temperton, N.J., 2015. Pseudotype-Based Neutralization Assays for Influenza: A Systematic Analysis. Front Immunol 6, 161. https://doi.org/10.3389/fimmu.2015.00161

Casalino, L., Gaieb, Z., Goldsmith, J.A., Hjorth, C.K., Dommer, A.C., Harbison, A.M., Fogarty, C.A., Barros, E.P., Taylor, B.C., McLellan, J.S., Fadda, E., Amaro, R.E., 2020. Beyond Shielding: The Roles of Glycans in the SARS-CoV-2 Spike Protein. ACS Cent. Sci. 6, 1722–1734. https://doi.org/10.1021/acscentsci.0c01056

Castruita, J.A.S., Schneider, U.V., Mollerup, S., Leineweber, T.D., Weis, N., Bukh, J., Pedersen, M.S., Westh, H., 2023. SARS-CoV-2 spike mRNA vaccine sequences circulate in blood up to 28 days after COVID-19 vaccination. APMIS 131, 128–132. https://doi.org/10.1111/apm.13294

CDC, 2020. Coronavirus Disease 2019 (COVID-19) [WWW Document]. Centers for Disease Control and Prevention. URL https://www.cdc.gov/coronavirus/2019-ncov/variants/variant-classifications.html (accessed 1.29.24).

Cele, S., Jackson, L., Khoury, D.S., Khan, K., Moyo-Gwete, T., Tegally, H., San, J.E., Cromer, D., Scheepers, C., Amoako, D.G., Karim, F., Bernstein, M., Lustig, G., Archary, D., Smith, M., Ganga, Y., Jule, Z., Reedoy, K., Hwa, S.-H., Giandhari, J., Blackburn, J.M., Gosnell, B.I., Abdool Karim, S.S., Hanekom, W., von Gottberg, A., Bhiman, J.N., Lessells, R.J., Moosa, M.-Y.S., Davenport, M.P., de Oliveira, T., Moore, P.L., Sigal, A., 2022. Omicron extensively but incompletely escapes Pfizer BNT162b2 neutralization. Nature 602, 654–656. https://doi.org/10.1038/s41586-021-04387-1

Chakraborty, C., Sharma, A.R., Bhattacharya, M., Lee, S.-S., 2022. A Detailed Overview of Immune Escape, Antibody Escape, Partial Vaccine Escape

of SARS-CoV-2 and Their Emerging Variants With Escape Mutations. Front Immunol 13, 801522. https://doi.org/10.3389/fimmu.2022.801522

Chavda, V.P., Balar, P., Vaghela, D., Solanki, H.K., Vaishnav, A., Hala, V., Vora, L., 2023. Omicron Variant of SARS-CoV-2: An Indian Perspective of Vaccination and Management. Vaccines 11, 160. https://doi.org/10.3390/vaccines11010160

Chen, P., Wu, M., He, Y., Jiang, B., He, M.-L., 2023. Metabolic alterations upon SARS-CoV-2 infection and potential therapeutic targets against coronavirus infection. Sig Transduct Target Ther 8, 1–23. https://doi.org/10.1038/s41392-023-01510-8

Chen, Y., Zhao, X., Zhou, H., Zhu, H., Jiang, S., Wang, P., 2023. Broadly neutralizing antibodies to SARS-CoV-2 and other human coronaviruses. Nat Rev Immunol 23, 189–199. https://doi.org/10.1038/s41577-022-00784-3

Choi, J., Lee, Y.J., Ko, J.-H., Kim, S.-H., Kim, H.-J., Lee, H.W., Jeong, H., Kim, T.-Y., Jang, Y.G., Hong, H., Kim, M.-S., Lee, S.E., Kim, Y.G., Chung, E.J., Lim, H., Jang, S., Kim, K., Kim, S.S., Ahn, J.Y., Choi, J.Y., Kim, Y.C., Park, Y.S., Peck, K.R., Kim, B., 2022. Neutralizing Activity Against SARS-CoV-2 Delta and Omicron Variants Following a Third BNT162b2 Booster Dose According to Three Homologous or Heterologous COVID-19 Vaccination Schedules. Front Cell Infect Microbiol 12, 948014. https://doi.org/10.3389/fcimb.2022.948014

Clemente-Suárez, V.J., Hormeño-Holgado, A., Jiménez, M., Benitez-Agudelo, J.C., Navarro-Jiménez, E., Perez-Palencia, N., Maestre-Serrano, R., Laborde-Cárdenas, C.C., Tornero-Aguilera, J.F., 2020. Dynamics of Population Immunity Due to the Herd Effect in the COVID-19 Pandemic. Vaccines (Basel) 8, 236. https://doi.org/10.3390/vaccines8020236

Colman, P.M., Lawrence, M.C., 2003. The structural biology of type I viral membrane fusion. Nat Rev Mol Cell Biol 4, 309–319. https://doi.org/10.1038/nrm1076

Condrat, C.E., Thompson, D.C., Barbu, M.G., Bugnar, O.L., Boboc, A., Cretoiu, D., Suciu, N., Cretoiu, S.M., Voinea, S.C., 2020. miRNAs as Biomarkers in Disease: Latest Findings Regarding Their Role in Diagnosis and Prognosis. Cells 9, 276. https://doi.org/10.3390/cells9020276

Cosar, B., Karagulleoglu, Z.Y., Unal, S., Ince, A.T., Uncuoglu, D.B., Tuncer, G., Kilinc, B.R., Ozkan, Y.E., Ozkoc, H.C., Demir, I.N., Eker, A., Karagoz, F., Simsek, S.Y., Yasar, B., Pala, M., Demir, A., Atak, I.N., Mendi, A.H., Bengi, V.U., Cengiz Seval, G., Gunes Altuntas, E., Kilic, P., Demir-Dora, D., 2022. SARS-CoV-2 Mutations and their Viral Variants. Cytokine Growth Factor Rev 63, 10–22. https://doi.org/10.1016/j.cytogfr.2021.06.001

cPass™ SARS-CoV-2 Neutralization Antibody Detection Kit (FDA EUA) | GenScript [WWW Document], n.d. URL https://www.genscript.com/covid-19-detection-fda-eua.html (accessed 12.28.23).

Crackower, M.A., Sarao, R., Oudit, G.Y., Yagil, C., Kozieradzki, I., Scanga, S.E., Oliveira-dos-Santos, A.J., da Costa, J., Zhang, L., Pei, Y., Scholey, J., Ferrario, C.M., Manoukian, A.S., Chappell, M.C., Backx, P.H., Yagil, Y., Penninger, J.M., 2002. Angiotensin-converting enzyme 2 is an essential regulator of heart function. Nature 417, 822–828. https://doi.org/10.1038/nature00786

Crotty, S., 2021. Hybrid immunity. Science 372, 1392–1393. https://doi.org/10.1126/science.abj2258

Cui, J., Li, F., Shi, Z.L., 2019. Origin and evolution of pathogenic coronaviruses. Nature Reviews Microbiology 17, 181–192. https://doi.org/10.1038/s41579-018-0118-9

Dalle Carbonare, L., Valenti, M.T., Bisoffi, Z., Piubelli, C., Pizzato, M., Accordini, S., Mariotto, S., Ferrari, S., Minoia, A., Bertacco, J., Li Vigni, V., Dorelli, G., Crisafulli, E., Alberti, D., Masin, L., Tiberti, N., Longoni, S.S., Lopalco, L., Beretta, A., Zipeto, D., 2021. Serology study after BTN162b2 vaccination in participants previously infected with SARS-CoV-2 in two different waves versus naïve. Commun Med 1, 38. https://doi.org/10.1038/s43856-021-00039-7

de GONZALO-CALVO, D., BENÍTEZ, I.D., PINILLA, L., CARRATALÁ, A., MONCUSÍ-MOIX, A., GORT-PANIELLO, C., MOLINERO, M., GONZÁLEZ, J., TORRES, G., BERNAL, M., PICO, S., ALMANSA, R., JORGE, N., ORTEGA, A., BUSTAMANTE-MUNGUIRA, E., GÓMEZ, J.M., GONZÁLEZ-RIVERA, M., MICHELOUD, D., RYAN, P., MARTINEZ, A., TAMAYO, L., ALDECOA, C., FERRER, R., CECCATO, A., FERNÁNDEZ-BARAT, L., MOTOS, A., RIERA, J., MENÉNDEZ, R., GARCIA-GASULLA, D., PEÑUELAS, O.,

TORRES, A., BERMEJO-MARTIN, J.F., BARBÉ, F., 2021. Circulating microRNA profiles predict the severity of COVID-19 in hospitalized patients. Transl Res 236, 147–159. https://doi.org/10.1016/j.trsl.2021.05.004

De Rienzo, M., Foddai, M.L., Conti, L., Mandoj, C., Iaboni, S., Saladini, I., Castilletti, C., Matusali, G., Donno, D.R., Marchioni, L., Ianniello, S., Corpolongo, A., Palange, M., Ciliberto, G., Piaggio, G., De Marco, F., 2021. Long-Term Persistence and Relevant Therapeutic Impact of High-Titer Viral-Neutralizing Antibody in a Convalescent COVID-19 Plasma Super-Donor: A Case Report. Front Immunol 12, 690322. https://doi.org/10.3389/fimmu.2021.690322

Della Polla, G., Miraglia del Giudice, G., Pelullo, C.P., Angelillo, I.F., 2023. Bivalent second booster dose of the COVID-19 vaccine: Eligible populations' reasons for receiving in Italy. Human Vaccines & Immunotherapeutics 19, 2188856. https://doi.org/10.1080/21645515.2023.2188856

Di Genova, C., Sampson, A., Scott, S., Cantoni, D., Mayora-Neto, M., Bentley, E., Mattiuzzo, G., Wright, E., Derveni, M., Auld, B., Ferrara, B.T., Harrison, D., Said, M., Selim, A., Thompson, E., Thompson, C., Carnell, G., Temperton, N., 2021. Production, Titration, Neutralisation, Storage and Lyophilisation of Severe Acute Respiratory Syndrome Coronavirus 2 (SARS-CoV-2) Lentiviral Pseudotypes. Bio Protoc 11, e4236. https://doi.org/10.21769/BioProtoc.4236

Donoghue, M., Hsieh, F., Baronas, E., Godbout, K., Gosselin, M., Stagliano, N., Donovan, M., Woolf, B., Robison, K., Jeyaseelan, R., Breitbart, R.E., Acton, S., 2000. A Novel Angiotensin-Converting Enzyme–Related Carboxypeptidase (ACE2) Converts Angiotensin I to Angiotensin 1-9. Circulation Research 87, e1–e9. https://doi.org/10.1161/01.RES.87.5.e1

Donyavi, T., Bokharaei-Salim, F., Baghi, H.B., Khanaliha, K., Alaei Janat-Makan, M., Karimi, B., Sadri Nahand, J., Mirzaei, H., Khatami, A., Garshasbi, S., Khoshmirsafa, M., Jalal Kiani, S., 2021. Acute and post-acute phase of COVID-19: Analyzing expression patterns of miRNA-29a-3p, 146a-3p, 155-5p, and let-7b-3p in PBMC. Int Immunopharmacol 97, 107641. https://doi.org/10.1016/j.intimp.2021.107641

Du, L., Yang, Y., Zhang, X., 2021. Neutralizing antibodies for the prevention and treatment of COVID-19. Cell Mol Immunol 18, 2293–2306. https://doi.org/10.1038/s41423-021-00752-2

Elemam, N.M., Hasswan, H., Aljaibeji, H., Sharif-Askari, N.S., Halwani, R., Taneera, J., Sulaiman, N., 2022. Profiling Levels of Serum microRNAs and Soluble ACE2 in COVID-19 Patients. Life (Basel) 12, 575. https://doi.org/10.3390/life12040575

Evans, J.P., Liu, S.-L., 2021. Role of host factors in SARS-CoV-2 entry. J Biol Chem 297, 100847. https://doi.org/10.1016/j.jbc.2021.100847

Eyileten, C., Wicik, Z., Simões, S.N., Martins-Jr, D.C., Klos, K., Wlodarczyk, W., Assinger, A., Soldacki, D., Chcialowski, A., Siller-Matula, J.M., Postula, M., 2022. Thrombosis-related circulating miR-16-5p is associated with disease severity in patients hospitalised for COVID-19. RNA Biology 19, 963–979. https://doi.org/10.1080/15476286.2022.2100629

Fantoni, T., Bissoli, M., Stefani, C., Voi, M., Dabija, A., Casula, R., Minafra, D.L., Palmeira, J. da F., Argañaraz, E.R., Mayora-Neto, M., Temperton, N.J., Zipeto, D., Ruggiero, A., 2023. Author Spotlight: Studying Host-Virus Interactions with Pseudotyped Viruses. JoVE (Journal of Visualized Experiments) e65658. https://doi.org/10.3791/65658

Fathizadeh, H., Afshar, S., Masoudi, M.R., Gholizadeh, P., Asgharzadeh, M., Ganbarov, K., Köse, Ş., Yousefi, M., Kafil, H.S., 2021. SARS-CoV-2 (Covid-19) vaccines structure, mechanisms and effectiveness: A review. Int J Biol Macromol 188, 740–750. https://doi.org/10.1016/j.ijbiomac.2021.08.076

Feikin, D.R., Higdon, M.M., Abu-Raddad, L.J., Andrews, N., Araos, R., Goldberg, Y., Groome, M.J., Huppert, A., O'Brien, K.L., Smith, P.G., Wilder-Smith, A., Zeger, S., Deloria Knoll, M., Patel, M.K., 2022. Duration of effectiveness of vaccines against SARS-CoV-2 infection and COVID-19 disease: results of a systematic review and meta-regression. Lancet 399, 924–944. https://doi.org/10.1016/S0140-6736(22)00152-0

Ferrara, F., Del Rosario, J.M.M., da Costa, K.A.S., Kinsley, R., Scott, S., Fereidouni, S., Thompson, C., Kellam, P., Gilbert, S., Carnell, G., Temperton, N., 2021. Development of Lentiviral Vectors Pseudotyped With Influenza B Hemagglutinins: Application in Vaccine

Immunogenicity, mAb Potency, and Sero-Surveillance Studies. Front Immunol 12, 661379. https://doi.org/10.3389/fimmu.2021.661379

Ferrara, F., Temperton, N., 2018. Pseudotype Neutralization Assays: From Laboratory Bench to Data Analysis. Methods and Protocols 1, 8. https://doi.org/10.3390/mps1010008

Ferrari, L., Ruggiero, A., Stefani, C., Benedetti, L., Piermatteo, L., Andreassi, E., Caldara, F., Zace, D., Pagliari, M., Ceccherini-Silberstein, F., Jones, C., Iannetta, M., Geretti, A.M., 2024. Utility of accessible SARS-CoV-2 specific immunoassays in vaccinated adults with a history of advanced HIV infection. Sci Rep 14, 8337. https://doi.org/10.1038/s41598-024-58597-4

Flores-Alanis, A., Sandner-Miranda, L., Delgado, G., Cravioto, A., Morales-Espinosa, R., 2020. The receptor binding domain of SARS-CoV-2 spike protein is the result of an ancestral recombination between the bat-CoV RaTG13 and the pangolin-CoV MP789. BMC Res Notes 13, 398. https://doi.org/10.1186/s13104-020-05242-8

Fountain, J.H., Kaur, J., Lappin, S.L., 2024. Physiology, Renin Angiotensin System, in: StatPearls. StatPearls Publishing, Treasure Island (FL).

Franco, S., Mateu, L., Pluvinet, R., Sanchez-Herrero, J.F., Toledo, R., Sumoy, L., Massanella, M., Martinez, M.A., 2024. Altered Plasma microRNA Signature in Hospitalized COVID-19 Patients Requiring Oxygen Support. Microorganisms 12, 440. https://doi.org/10.3390/microorganisms12030440

Furukawa, K., Tjan, L.H., Kurahashi, Y., Sutandhio, S., Nishimura, M., Arii, J., Mori, Y., 2022. Assessment of Neutralizing Antibody Response Against SARS-CoV-2 Variants After 2 to 3 Doses of the BNT162b2 mRNA COVID-19 Vaccine. JAMA Netw Open 5, e2210780. https://doi.org/10.1001/jamanetworkopen.2022.10780

Garg, A., Seeliger, B., Derda, A.A., Xiao, K., Gietz, A., Scherf, K., Sonnenschein, K., Pink, I., Hoeper, M.M., Welte, T., Bauersachs, J., David, S., Bär, C., Thum, T., 2021. Circulating cardiovascular microRNAs in critically ill COVID-19 patients. Eur J Heart Fail 23, 468–475. https://doi.org/10.1002/ejhf.2096

Gasparello, J., Finotti, A., Gambari, R., 2021. Tackling the COVID-19 “cytokine storm” with microRNA mimics directly targeting the 3’UTR of pro-inflammatory mRNAs. Med Hypotheses 146, 110415. https://doi.org/10.1016/j.mehy.2020.110415

Gaspersic, J., Dolzan, V., 2022. Viral and Host Genetic and Epigenetic Biomarkers Related to SARS-CoV-2 Cell Entry, Infection Rate, and Disease Severity. Biology (Basel) 11, 178. https://doi.org/10.3390/biology11020178

Gaytán-Pacheco, N., Ibáñez-Salazar, A., Herrera-Van Oostdam, A.S., Oropeza-Valdez, J.J., Magaña-Aquino, M., Adrián López, J., Monárrez-Espino, J., López-Hernández, Y., 2022. miR-146a, miR-221, and miR-155 are Involved in Inflammatory Immune Response in Severe COVID-19 Patients. Diagnostics (Basel) 13, 133. https://doi.org/10.3390/diagnostics13010133

Gedikbasi, A., Adas, G., Isiksacan, N., Kart Yasar, K., Canbolat Unlu, E., Yilmaz, R., Hergunsel, G.O., Cukurova, Z., 2022. The Effect of Host miRNAs on Prognosis in COVID-19: miRNA-155 May Promote Severity via Targeting Suppressor of Cytokine Signaling 1 (SOCS1) Gene. Genes (Basel) 13, 1146. https://doi.org/10.3390/genes13071146

Giannella, A., Riccetti, S., Sinigaglia, A., Piubelli, C., Razzaboni, E., Di Battista, P., Agostini, M., Dal Molin, E., Manganelli, R., Gobbi, F., Ceolotto, G., Barzon, L., 2022. Circulating microRNA signatures associated with disease severity and outcome in COVID-19 patients. Frontiers in Immunology 13.

Girl, P., von Buttlar, H., Mantel, E., Antwerpen, M.H., Wölfel, R., Müller, K., 2024. Comparative Analysis of Vaccine-Induced Neutralizing Antibodies against the Alpha, Beta, Delta, and Omicron Variants of SARS-CoV-2. Vaccines 12, 515. https://doi.org/10.3390/vaccines12050515

Goldblatt, D., Alter, G., Crotty, S., Plotkin, S.A., 2022. Correlates of protection against SARS-CoV-2 infection and COVID-19 disease. Immunol Rev 10.1111/imr.13091. https://doi.org/10.1111/imr.13091

Gonzalez-Martin, A., Adams, B.D., Lai, M., Shepherd, J., Salvador-Bernaldez, M., Salvador, J.M., Lu, J., Nemazee, D., Xiao, C., 2016. The microRNA miR-148a functions as a critical regulator of B cell tolerance and autoimmunity. Nat Immunol 17, 433–440. https://doi.org/10.1038/ni.3385

Greinacher, A., Thiele, T., Warkentin, T.E., Weisser, K., Kyrle, P.A., Eichinger, S., 2021. Thrombotic Thrombocytopenia after ChAdOx1 nCov-19 Vaccination. N Engl J Med NEJMoa2104840. https://doi.org/10.1056/NEJMoa2104840

Grunau, B., Prusinkiewicz, M., Asamoah-Boaheng, M., Golding, L., Lavoie, P.M., Petric, M., Levett, P.N., Haig, S., Barakauskas, V., Karim, M.E., Jassem, A.N., Drews, S.J., Sediqi, S., Goldfarb, D.M., 2022. Correlation of SARS-CoV-2 Viral Neutralizing Antibody Titers with Anti-Spike Antibodies and ACE-2 Inhibition among Vaccinated Individuals. Microbiology Spectrum 10, e01315-22. https://doi.org/10.1128/spectrum.01315-22

Haga, S., Nagata, N., Okamura, T., Yamamoto, Norio, Sata, T., Yamamoto, Naoki, Sasazuki, T., Ishizaka, Y., 2010. TACE antagonists blocking ACE2 shedding caused by the spike protein of SARS-CoV are candidate antiviral compounds. Antiviral Res 85, 551–555. https://doi.org/10.1016/j.antiviral.2009.12.001

Haga, S., Yamamoto, Norio, Nakai-Murakami, C., Osawa, Y., Tokunaga, K., Sata, T., Yamamoto, Naoki, Sasazuki, T., Ishizaka, Y., 2008. Modulation of TNF-α-converting enzyme by the spike protein of SARS-CoV and ACE2 induces TNF-α production and facilitates viral entry. Proceedings of the National Academy of Sciences 105, 7809–7814. https://doi.org/10.1073/pnas.0711241105

He, Y., Lin, J., Kong, D., Huang, M., Xu, C., Kim, T.-K., Etheridge, A., Luo, Y., Ding, Y., Wang, K., 2015. Current State of Circulating MicroRNAs as Cancer Biomarkers. Clinical Chemistry 61, 1138–1155. https://doi.org/10.1373/clinchem.2015.241190

Hemken, P.M., Israeli, E., Taylor, R., Jacobson, C., Datwyler, M., Geissler, R., Hadji, A., Jeanblanc, N., Pandya, K., Marcinkus, M., Piktel, R., Bogdan, M.F., Rodgers, M., Anderson, M., Ziemann, R., Tieman, B.C., Hawksworth, D., Moore, J., Otis, K.S., Marohnic, C.C., Corby, J., Tu, B., Lin, Z., Kar, A., Hartnett, J., Strobel, C., Gregory, S., Rae, T., Muerhoff, A.S., Brophy, S., Hackett, J.R., Daghfal, D., Faron, M.L., Cruz, A., Mohr, P., Sokoll, L., Davis, G.J., 2023. Pre-analytical considerations in the development of a prototype SARS-CoV-2 antigen ARCHITECT automated immunoassay. Clinical Chemistry and Laboratory Medicine (CCLM) 61, 1511–1517. https://doi.org/10.1515/cclm-2022-1292

Higashimoto, Y., Kozawa, K., Miura, H., Kawamura, Y., Ihira, M., Hiramatsu, H., Suzuki, R., Haga, K., Takai-Todaka, R., Sawada, A., Katayama, K., Yoshikawa, T., 2022. Correlation between anti-S IgG and neutralizing antibody titers against three live SARS-CoV-2 variants in BNT162b2

vaccine recipients. Human Vaccines & Immunotherapeutics 18, 2105611. https://doi.org/10.1080/21645515.2022.2105611

Hoffmann, M., Kleine-Weber, H., Pöhlmann, S., 2020a. A Multibasic Cleavage Site in the Spike Protein of SARS-CoV-2 Is Essential for Infection of Human Lung Cells. Molecular Cell 78, 779-784.e5. https://doi.org/10.1016/j.molcel.2020.04.022

Hoffmann, M., Kleine-Weber, H., Schroeder, S., Krüger, N., Herrler, T., Erichsen, S., Schiergens, T.S., Herrler, G., Wu, N.H., Nitsche, A., Müller, M.A., Drosten, C., Pöhlmann, S., 2020b. SARS-CoV-2 Cell Entry Depends on ACE2 and TMPRSS2 and Is Blocked by a Clinically Proven Protease Inhibitor. Cell 181, 271-280.e8. https://doi.org/10.1016/j.cell.2020.02.052

Hu, J., Stojanović, J., Yasamineh, S., Yasamineh, P., Karuppannan, S.K., Hussain Dowlath, M.J., Serati-Nouri, H., 2021. The potential use of microRNAs as a therapeutic strategy for SARS-CoV-2 infection. Arch Virol 166, 2649–2672. https://doi.org/10.1007/s00705-021-05152-5

Huang, R.S., Gamazon, E.R., Ziliak, D., Wen, Y., Im, H.K., Zhang, W., Wing, C., Duan, S., Bleibel, W.K., Cox, N.J., Dolan, M.E., 2011. Population differences in microRNA expression and biological implications. RNA Biol 8, 692–701. https://doi.org/10.4161/rna.8.4.16029

HUI, D.S., WONG, P., WANG, C., 2003. SARS: clinical features and diagnosis. Respirology 8, S20–S24. https://doi.org/10.1046/j.1440-1843.2003.00520.x

Hvidt, A.K., Baerends, E.A.M., Søgaard, O.S., Stærke, N.B., Raben, D., Reekie, J., Nielsen, H., Johansen, I.S., Wiese, L., Benfield, T.L., Iversen, K.K., Mustafa, A.B., Juhl, M.R., Petersen, K.T., Ostrowski, S.R., Lindvig, S.O., Rasmussen, L.D., Schleimann, M.H., Andersen, S.D., Juhl, A.K., Dietz, L.L., Andreasen, S.R., Lundgren, J., Østergaard, L., Tolstrup, M., Group, the E.S., 2022. Comparison of vaccine-induced antibody neutralization against SARS-CoV-2 variants of concern following primary and booster doses of COVID-19 vaccines. Front. Med. 9. https://doi.org/10.3389/fmed.2022.994160

Ibarrondo, F.J., Hofmann, C., Fulcher, J.A., Goodman-Meza, D., Mu, W., Hausner, M.A., Ali, A., Balamurugan, A., Taus, E., Elliott, J., Krogstad, P., Tobin, N.H., Ferbas, K.G., Kitchen, S.G., Aldrovandi, G.M., Rimoin, A.W., Yang, O.O., 2021. Primary, Recall, and Decay Kinetics

of SARS-CoV-2 Vaccine Antibody Responses. ACS Nano 15, 11180–11191. https://doi.org/10.1021/acsnano.1c03972

Imai, Y., Kuba, K., Rao, S., Huan, Y., Guo, F., Guan, B., Yang, P., Sarao, R., Wada, T., Leong-Poi, H., Crackower, M.A., Fukamizu, A., Hui, C.-C., Hein, L., Uhlig, S., Slutsky, A.S., Jiang, C., Penninger, J.M., 2005. Angiotensin-converting enzyme 2 protects from severe acute lung failure. Nature 436, 112–116. https://doi.org/10.1038/nature03712

Jafarzadeh, A., Naseri, A., Shojaie, L., Nemati, M., Jafarzadeh, S., Bannazadeh Baghi, H., Hamblin, M.R., Akhlagh, S.A., Mirzaei, H., 2021. MicroRNA-155 and antiviral immune responses. International Immunopharmacology 101, 108188. https://doi.org/10.1016/j.intimp.2021.108188

Jung, J., Rajapakshe, D., Julien, C., Devaraj, S., 2021. Analytical and clinical performance of cPass neutralizing antibodies assay. Clin Biochem 98, 70–73. https://doi.org/10.1016/j.clinbiochem.2021.09.008

Justo Arevalo, S., Castillo-Chávez, A., Uribe Calampa, C.S., Zapata Sifuentes, D., Huallpa, C.J., Landa Bianchi, G., Garavito-Salini Casas, R., Quiñones Aguilar, M., Pineda Chavarría, R., 2023. What do we know about the function of SARS-CoV-2 proteins? Front Immunol 14, 1249607. https://doi.org/10.3389/fimmu.2023.1249607

Kakavandi, S., Zare, I., VaezJalali, M., Dadashi, M., Azarian, M., Akbari, A., Ramezani Farani, M., Zalpoor, H., Hajikhani, B., 2023. Structural and non-structural proteins in SARS-CoV-2: potential aspects to COVID-19 treatment or prevention of progression of related diseases. Cell Commun Signal 21, 1–31. https://doi.org/10.1186/s12964-023-01104-5

Kassif-Lerner, R., Zloto, K., Rubin, N., Asraf, K., Doolman, R., Paret, G., Nevo-Caspi, Y., 2022. miR-155: A Potential Biomarker for Predicting Mortality in COVID-19 Patients. J Pers Med 12, 324. https://doi.org/10.3390/jpm12020324

Keller, A., Rounge, T., Backes, C., Ludwig, N., Gislefoss, R., Leidinger, P., Langseth, H., Meese, E., 2017. Sources to variability in circulating human miRNA signatures. RNA Biol 14, 1791–1798. https://doi.org/10.1080/15476286.2017.1367888

Khare, S., Niharika, Singh, A., Hussain, I., Singh, N.B., Singh, S., 2023. SARS-CoV-2 Vaccines: Types, Working Principle, and Its Impact on Thrombosis and Gastrointestinal Disorders. Appl Biochem Biotechnol 195, 1541–1573. https://doi.org/10.1007/s12010-022-04181-3

Khatami, A., Taghizadieh, M., Nahand, J.S., Karimzadeh, M., Kiani, S.J., Khanaliha, K., Kalantari, S., Chavoshpour, S., Mirzaei, H., Donyavi, T., Bokharaei-Salim, F., 2023. Evaluation of MicroRNA Expression Pattern (miR-28, miR-181a, miR-34a, and miR-31) in Patients with COVID-19 Admitted to ICU and Diabetic COVID-19 Patients. INT 1–1. https://doi.org/10.1159/000529985

Khoury, S., Ajuyah, P., Tran, N., 2014. Isolation of Small Noncoding RNAs from Human Serum. J Vis Exp 51443. https://doi.org/10.3791/51443

Kitikoon, P., Vincent, A.L., 2014. Microneutralization Assay for Swine Influenza Virus in Swine Serum, in: Spackman, E. (Ed.), Animal Influenza Virus, Methods in Molecular Biology. Springer, New York, NY, pp. 325–335. https://doi.org/10.1007/978-1-4939-0758-8_27

Koma, T., Adachi, S., Doi, N., Adachi, A., Nomaguchi, M., 2020. Toward Understanding Molecular Bases for Biological Diversification of Human Coronaviruses: Present Status and Future Perspectives. Front. Microbiol. 11. https://doi.org/10.3389/fmicb.2020.02016

König, S., Vollenberg, R., Tepasse, P.-R., 2023. The Renin–Angiotensin System in COVID-19: Can Long COVID Be Predicted? Life (Basel) 13, 1462. https://doi.org/10.3390/life13071462

Kuba, K., Imai, Y., Rao, S., Gao, H., Guo, F., Guan, B., Huan, Y., Yang, P., Zhang, Y., Deng, W., Bao, L., Zhang, B., Liu, G., Wang, Z., Chappell, M., Liu, Y., Zheng, D., Leibbrandt, A., Wada, T., Slutsky, A.S., Liu, D., Qin, C., Jiang, C., Penninger, J.M., 2005. A crucial role of angiotensin converting enzyme 2 (ACE2) in SARS coronavirus–induced lung injury. Nat Med 11, 875–879. https://doi.org/10.1038/nm1267

Kudelova, E., Holubekova, V., Grendar, M., Kolkova, Z., Samec, M., Vanova, B., Mikolajcik, P., Smolar, M., Kudela, E., Laca, L., Lasabova, Z., 2022. Circulating miRNA expression over the course of colorectal cancer treatment. Oncology Letters 23, 1–15. https://doi.org/10.3892/ol.2021.13136

Kunvariya, A.D., Dave, S.A., Modi, Z.J., Patel, P.K., Sagar, S.R., 2023. Exploration of multifaceted molecular mechanism of angiotensin-converting enzyme 2 (ACE2) in pathogenesis of various diseases. Heliyon 9, e15644. https://doi.org/10.1016/j.heliyon.2023.e15644

La Rosa, G., Iaconelli, M., Veneri, C., Mancini, P., Bonanno Ferraro, G., Brandtner, D., Lucentini, L., Bonadonna, L., Rossi, M., Grigioni, M., Suffredini, E., 2022. The rapid spread of SARS-COV-2 Omicron

variant in Italy reflected early through wastewater surveillance. Sci Total Environ 837, 155767. https://doi.org/10.1016/j.scitotenv.2022.155767

Lambert, D.W., Yarski, M., Warner, F.J., Thornhill, P., Parkin, E.T., Smith, A.I., Hooper, N.M., Turner, A.J., 2005. Tumor Necrosis Factor-α Convertase (ADAM17) Mediates Regulated Ectodomain Shedding of the Severe-acute Respiratory Syndrome-Coronavirus (SARS-CoV) Receptor, Angiotensin-converting Enzyme-2 (ACE2). J Biol Chem 280, 30113–30119. https://doi.org/10.1074/jbc.M505111200

Lan, J., Ge, J., Yu, J., Shan, S., Zhou, H., Fan, S., Zhang, Q., Shi, X., Wang, Q., Zhang, L., Wang, X., 2020. Structure of the SARS-CoV-2 spike receptor-binding domain bound to the ACE2 receptor. Nature 581, 215–220. https://doi.org/10.1038/s41586-020-2180-5

Le, K., Kannappan, S., Kim, T., Lee, J.H., Lee, H.-R., Kim, K.K., 2023. Structural understanding of SARS-CoV-2 virus entry to host cells. Front Mol Biosci 10, 1288686. https://doi.org/10.3389/fmolb.2023.1288686

Lecchi, C., Ceciliani, F., Petrini, S., Cappelli, G., Grassi, C., Balestrieri, A., Galiero, G., DeCarlo, E., Salvi, G., Panzeri, F., Gini, C., Cafiso, A., Agazzi, A., Martucciello, A., 2023. Endogenous and viral microRNAs in nasal secretions of water buffaloes (Bubalus bubalis) after Bubaline alphaherpesvirus 1 (BuHV-1) challenge infection. Veterinary Research 54, 44. https://doi.org/10.1186/s13567-023-01175-9

Lee, R.C., Feinbaum, R.L., Ambros, V., 1993. The C. elegans heterochronic gene lin-4 encodes small RNAs with antisense complementarity to lin-14. Cell 75, 843–854. https://doi.org/10.1016/0092-8674(93)90529-y

Lester, S.N., Stumpf, M., Freeman, B.D., Mills, L., Schiffer, J., Semenova, V., Jia, T., Desai, R., Browning, P., Alston, B., Ategbole, M., Bolcen, S., Chen, A., David, E., Manitis, P., Tatum, H., Qin, Y., Zellner, B., Drobeniuc, J., Tejada-Strop, A., Chatterjee, P., Shrivastava-Ranjan, P., Jenks, M.H., McMullan, L.K., Flint, M., Spiropoulou, C.F., Niemeyer, G.P., Werner, B.J., Bean, C.J., Johnson, J.A., Hoffmaster, A.R., Satheshkumar, P.S., Schuh, A.J., Owen, S.M., Thornburg, N.J., 2024. Examination of SARS-CoV-2 serological test results from multiple commercial and laboratory platforms with an in-house serum panel. Access Microbiol 6, 000463.v4. https://doi.org/10.1099/acmi.0.000463.v4

Levin, E.G., Lustig, Y., Cohen, C., Fluss, R., Indenbaum, V., Amit, S., Doolman, R., Asraf, K., Mendelson, E., Ziv, A., Rubin, C., Freedman, L., Kreiss, Y., Regev-Yochay, G., 2021. Waning Immune Humoral Response to BNT162b2 Covid-19 Vaccine over 6 Months. New England Journal of Medicine 385, e84. https://doi.org/10.1056/NEJMoa2114583

Li, Q., Liu, Q., Huang, W., Li, X., Wang, Y., 2018. Current status on the development of pseudoviruses for enveloped viruses. Rev Med Virol 28, e1963. https://doi.org/10.1002/rmv.1963

Liang, Y., Fang, D., Gao, X., Deng, X., Chen, N., Wu, J., Zeng, M., Luo, M., 2023. Circulating microRNAs as emerging regulators of COVID-19. Theranostics 13, 125–147. https://doi.org/10.7150/thno.78164

Liang, Z., Wu, X., Wu, J., Liu, S., Tong, J., Li, T., Yu, Y., Zhang, L., Zhao, C., Lu, Q., Qin, H., Nie, J., Huang, W., Wang, Y., 2023. Development of an automated, high-throughput SARS-CoV-2 neutralization assay based on a pseudotyped virus using a vesicular stomatitis virus (VSV) vector. Emerging Microbes & Infections 12, e2261566. https://doi.org/10.1080/22221751.2023.2261566

Lim, Y.X., Ng, Y.L., Tam, J.P., Liu, D.X., 2016. Human Coronaviruses: A Review of Virus–Host Interactions. Diseases 4, 26. https://doi.org/10.3390/diseases4030026

LIU, S.-G., QIN, X.-G., ZHAO, B.-S., QI, B., YAO, W.-J., WANG, T.-Y., LI, H.-C., WU, X.-N., 2013. Differential expression of miRNAs in esophageal cancer tissue. Oncol Lett 5, 1639–1642. https://doi.org/10.3892/ol.2013.1251

Lorenzen, I., Lokau, J., Korpys, Y., Oldefest, M., Flynn, C.M., Künzel, U., Garbers, C., Freeman, M., Grötzinger, J., Düsterhöft, S., 2016. Control of ADAM17 activity by regulation of its cellular localisation. Scientific Reports 6. https://doi.org/10.1038/srep35067

Lu, G., Wang, Q., Gao, G.F., 2015. Bat-to-human: spike features determining 'host jump' of coronaviruses SARS-CoV, MERS-CoV, and beyond. Trends in Microbiology 23, 468–478. https://doi.org/10.1016/j.tim.2015.06.003

Luna Buitrago, D., Lovering, R.C., Caporali, A., 2023. Insights into Online microRNA Bioinformatics Tools. Non-Coding RNA 9, 18. https://doi.org/10.3390/ncrna9020018

Lv, Y., Yang, H., Ma, X., Wu, G., 2019. Strand-specific miR-28-3p and miR-28-5p have differential effects on nasopharyngeal cancer cells proliferation, apoptosis, migration and invasion. Cancer Cell International 19, 187. https://doi.org/10.1186/s12935-019-0915-x

Malik, J.A., Ahmed, S., Mir, A., Shinde, M., Bender, O., Alshammari, F., Ansari, M., Anwar, S., 2022. The SARS-CoV-2 mutations versus vaccine effectiveness: New opportunities to new challenges. Journal of Infection and Public Health 15, 228–240. https://doi.org/10.1016/j.jiph.2021.12.014

Mallick, B., Ghosh, Z., Chakrabarti, J., 2009. MicroRNome Analysis Unravels the Molecular Basis of SARS Infection in Bronchoalveolar Stem Cells. PLOS ONE 4, e7837. https://doi.org/10.1371/journal.pone.0007837

Mao, L., Chen, Y., Gu, J., Zhao, Y., Chen, Q., 2023. Roles and mechanisms of exosomal microRNAs in viral infections. Arch Virol 168, 121. https://doi.org/10.1007/s00705-023-05744-3

Mariappan, V., Ranganadin, P., Shanmugam, L., Rao, S.R., Pillai, A.B., 2022. Early shedding of membrane-bounded ACE2 could be an indicator for disease severity in SARS-CoV-2. Biochimie 201, 139. https://doi.org/10.1016/j.biochi.2022.06.005

Markov, P.V., Ghafari, M., Beer, M., Lythgoe, K., Simmonds, P., Stilianakis, N.I., Katzourakis, A., 2023. The evolution of SARS-CoV-2. Nat Rev Microbiol 21, 361–379. https://doi.org/10.1038/s41579-023-00878-2

Marshall, R.P., Webb, S., Bellingan, G.J., Montgomery, H.E., Chaudhari, B., McAnulty, R.J., Humphries, S.E., Hill, M.R., Laurent, G.J., 2002. Angiotensin Converting Enzyme Insertion/Deletion Polymorphism Is Associated with Susceptibility and Outcome in Acute Respiratory Distress Syndrome. Am J Respir Crit Care Med 166, 646–650. https://doi.org/10.1164/rccm.2108086

Mengist, H.M., Kombe Kombe, A.J., Mekonnen, D., Abebaw, A., Getachew, M., Jin, T., 2021. Mutations of SARS-CoV-2 spike protein: Implications on immune evasion and vaccine-induced immunity. Seminars in Immunology, Complexity and diversity of immune responses in COVID-19 55, 101533. https://doi.org/10.1016/j.smim.2021.101533

Millet, J.K., Tang, T., Nathan, L., Jaimes, J.A., Hsu, H.L., Daniel, S., Whittaker, G.R., 2019. Production of pseudotyped particles to study highly

pathogenic coronaviruses in a biosafety level 2 setting. Journal of Visualized Experiments 2019. https://doi.org/10.3791/59010

Mishra, N., Kumar, S., Singh, S., Bansal, T., Jain, N., Saluja, S., Kumar, R., Bhattacharyya, S., Palanichamy, J.K., Mir, R.A., Sinha, S., Luthra, K., 2021. Cross-neutralization of SARS-CoV-2 by HIV-1 specific broadly neutralizing antibodies and polyclonal plasma. PLoS Pathog 17, e1009958. https://doi.org/10.1371/journal.ppat.1009958

Mitchell, P.S., Parkin, R.K., Kroh, E.M., Fritz, B.R., Wyman, S.K., Pogosova-Agadjanyan, E.L., Peterson, A., Noteboom, J., O'Briant, K.C., Allen, A., Lin, D.W., Urban, N., Drescher, C.W., Knudsen, B.S., Stirewalt, D.L., Gentleman, R., Vessella, R.L., Nelson, P.S., Martin, D.B., Tewari, M., 2008. Circulating microRNAs as stable blood-based markers for cancer detection. Proceedings of the National Academy of Sciences 105, 10513–10518. https://doi.org/10.1073/pnas.0804549105

Miyashita, Y., Yoshida, T., Takagi, Y., Tsukamoto, H., Takashima, K., Kouwaki, T., Makino, K., Fukushima, S., Nakamura, K., Oshiumi, H., 2022. Circulating extracellular vesicle microRNAs associated with adverse reactions, proinflammatory cytokine, and antibody production after COVID-19 vaccination. NPJ Vaccines 7, 16. https://doi.org/10.1038/s41541-022-00439-3

Molinero, M., Benítez, I.D., González, J., Gort-Paniello, C., Moncusí-Moix, A., Rodríguez-Jara, F., García-Hidalgo, M.C., Torres, G., Vengoechea, J.J., Gómez, S., Cabo, R., Caballero, J., Bermejo-Martin, J.F., Ceccato, A., Fernández-Barat, L., Ferrer, R., Garcia-Gasulla, D., Menéndez, R., Motos, A., Peñuelas, O., Riera, J., Torres, A., Barbé, F., de Gonzalo-Calvo, D., 2022. Bronchial Aspirate-Based Profiling Identifies MicroRNA Signatures Associated With COVID-19 and Fatal Disease in Critically Ill Patients. Front Med (Lausanne) 8, 756517. https://doi.org/10.3389/fmed.2021.756517

Morales-Núñez, J.J., Muñoz-Valle, J.F., Torres-Hernández, P.C., Hernández-Bello, J., 2021. Overview of Neutralizing Antibodies and Their Potential in COVID-19. Vaccines (Basel) 9, 1376. https://doi.org/10.3390/vaccines9121376

Nagy, B., Fejes, Z., Szentkereszty, Z., Sütő, R., Várkonyi, I., Ajzner, É., Kappelmayer, J., Papp, Z., Tóth, A., Fagyas, M., 2021. A dramatic rise in serum ACE2 activity in a critically ill COVID-19 patient. Int J Infect Dis 103, 412–414. https://doi.org/10.1016/j.ijid.2020.11.184

Naqvi, A.A.T., Fatima, K., Mohammad, T., Fatima, U., Singh, I.K., Singh, A., Atif, S.M., Hariprasad, G., Hasan, G.M., Hassan, Md.I., 2020. Insights into SARS-CoV-2 genome, structure, evolution, pathogenesis and therapies: Structural genomics approach. Biochim Biophys Acta Mol Basis Dis 1866, 165878. https://doi.org/10.1016/j.bbadis.2020.165878

Narasimhan, M., Mahimainathan, L., Araj, E., Clark, A.E., Markantonis, J., Green, A., Xu, J., SoRelle, J.A., Alexis, C., Fankhauser, K., Parikh, H., Wilkinson, K., Reczek, A., Kopplin, N., Yekkaluri, S., Balani, J., Thomas, A., Singal, A.G., Sarode, R., Muthukumar, A., 2021. Clinical Evaluation of the Abbott Alinity SARS-CoV-2 Spike-Specific Quantitative IgG and IgM Assays among Infected, Recovered, and Vaccinated Groups. Journal of Clinical Microbiology 59, 10.1128/jcm.00388-21. https://doi.org/10.1128/jcm.00388-21

Narożna, M., Rubiś, B., 2021. Anti-SARS-CoV-2 Strategies and the Potential Role of miRNA in the Assessment of COVID-19 Morbidity, Recurrence, and Therapy. Int J Mol Sci 22, 8663. https://doi.org/10.3390/ijms22168663

Narula, S., Yusuf, S., Chong, M., Ramasundarahettige, C., Rangarajan, S., Bangdiwala, S.I., van Eikels, M., Leineweber, K., Wu, A., Pigeyre, M., Paré, G., 2020. Plasma ACE2 and risk of death or cardiometabolic diseases: a case-cohort analysis. Lancet 396, 968–976. https://doi.org/10.1016/S0140-6736(20)31964-4

Nassar, A., Ibrahim, I.M., Amin, F.G., Magdy, M., Elgharib, A.M., Azzam, E.B., Nasser, F., Yousry, K., Shamkh, I.M., Mahdy, S.M., Elfiky, A.A., 2021. A Review of Human Coronaviruses' Receptors: The Host-Cell Targets for the Crown Bearing Viruses. Molecules 26, 6455. https://doi.org/10.3390/molecules26216455

Nie, J., Li, Q., Wu, J., Zhao, C., Hao, H., Liu, H., Zhang, L., Nie, L., Qin, H., Wang, M., Lu, Q., Li, X., Sun, Q., Liu, J., Fan, C., Huang, W., Xu, M., Wang, Y., 2020. Establishment and validation of a pseudovirus neutralization assay for SARS-CoV-2. Emerging Microbes & Infections 9, 680–686. https://doi.org/10.1080/22221751.2020.1743767

Niehues, R.V., Wozniak, J., Wiersch, F., Lilienthal, E., Tacken, N., Schumertl, T., Garbers, C., Ludwig, A., Düsterhöft, S., 2022. The collectrin-like part of the SARS-CoV-1 and -2 receptor ACE2 is shed by the metalloproteinases ADAM10 and ADAM17. FASEB J 36, e22234. https://doi.org/10.1096/fj.202101521R

O'Brien, J., Hayder, H., Zayed, Y., Peng, C., 2018. Overview of MicroRNA Biogenesis, Mechanisms of Actions, and Circulation. Frontiers in Endocrinology 9.

Pastorio, C., Zech, F., Noettger, S., Jung, C., Jacob, T., Sanderson, T., Sparrer, K.M.J., Kirchhoff, F., 2022. Determinants of Spike infectivity, processing, and neutralization in SARS-CoV-2 Omicron subvariants BA.1 and BA.2. Cell Host Microbe 30, 1255-1268.e5. https://doi.org/10.1016/j.chom.2022.07.006

Patel, V.B., Clarke, N., Wang, Z., Fan, D., Parajuli, N., Basu, R., Putko, B., Kassiri, Z., Turner, A.J., Oudit, G.Y., 2014. Angiotensin II induced proteolytic cleavage of myocardial ACE2 is mediated by TACE/ADAM-17: A positive feedback mechanism in the RAS. Journal of Molecular and Cellular Cardiology 66, 167–176. https://doi.org/10.1016/j.yjmcc.2013.11.017

Pather, S., Madhi, S.A., Cowling, B.J., Moss, P., Kamil, J.P., Ciesek, S., Muik, A., Türeci, Ö., 2023. SARS-CoV-2 Omicron variants: burden of disease, impact on vaccine effectiveness and need for variant-adapted vaccines. Front Immunol 14, 1130539. https://doi.org/10.3389/fimmu.2023.1130539

Peltier, H.J., Latham, G.J., 2008. Normalization of microRNA expression levels in quantitative RT-PCR assays: Identification of suitable reference RNA targets in normal and cancerous human solid tissues. RNA 14, 844–852. https://doi.org/10.1261/rna.939908

Piubelli, C., Ruggiero, A., Calciano, L., Mazzi, C., Castilletti, C., Tiberti, N., Caldrer, S., Verzè, M., Longoni, S.S., Accordini, S., Bisoffi, Z., Zipeto, D., 2023. Subjects who developed SARS-CoV-2 specific IgM after vaccination show a longer humoral immunity and a lower frequency of infection. eBioMedicine 89, 104471. https://doi.org/10.1016/j.ebiom.2023.104471

Plotkin, S.A., 2010. Correlates of Protection Induced by Vaccination. Clin Vaccine Immunol 17, 1055–1065. https://doi.org/10.1128/CVI.00131-10

Pollet, K., Garnier, N., Szunerits, S., Madder, A., Hober, D., Engelmann, I., 2023. Host miRNAs as biomarkers of SARS-CoV-2 infection: a critical review. Sens. Diagn. 2, 12–35. https://doi.org/10.1039/D2SD00140C

Porstner, M., Winkelmann, R., Daum, P., Schmid, J., Pracht, K., Côrte-Real, J., Schreiber, S., Haftmann, C., Brandl, A., Mashreghi, M.-F., Gelse, K.,

Hauke, M., Wirries, I., Zwick, M., Roth, E., Radbruch, A., Wittmann, J., Jäck, H.-M., 2015. miR-148a promotes plasma cell differentiation and targets the germinal center transcription factors Mitf and Bach2. European Journal of Immunology 45, 1206–1215. https://doi.org/10.1002/eji.201444637

Pracht, K., Meinzinger, J., Schulz, S.R., Daum, P., Côrte-Real, J., Hauke, M., Roth, E., Kindermann, D., Mielenz, D., Schuh, W., Wittmann, J., Jäck, H.-M., 2021. miR-148a controls metabolic programming and survival of mature CD19-negative plasma cells in mice. European Journal of Immunology 51, 1089–1109. https://doi.org/10.1002/eji.202048993

Pramod, R.K., Nair, A.V., Tambare, P.K., Chauhan, K., Kumar, T.V., Rajan, R.A., Mani, B.M., Asaf, M., Pandey, A.K., 2021. Reverse zoonosis of coronavirus disease-19: Present status and the control by one health approach. Vet World 14, 2817–2826. https://doi.org/10.14202/vetworld.2021.2817-2826

Qin, L., Meng, J., Ding, X., Jiang, T., 2022. Mapping Genetic Events of SARS-CoV-2 Variants. Front. Microbiol. 13. https://doi.org/10.3389/fmicb.2022.890590

Raghuvamsi, P.V., Tulsian, N.K., Samsudin, F., Qian, X., Purushotorman, K., Yue, G., Kozma, M.M., Hwa, W.Y., Lescar, J., Bond, P.J., MacAry, P.A., Anand, G.S., 2021. SARS-CoV-2 S protein:ACE2 interaction reveals novel allosteric targets. eLife 10, e63646. https://doi.org/10.7554/eLife.63646

Ruggiero, A., Piubelli, C., Calciano, L., Accordini, Simone, Valenti, M.T., Carbonare, L.D., Siracusano, G., Temperton, N., Tiberti, N., Longoni, S.S., Pizzato, M., Accordini, Silvia, Fantoni, T., Lopalco, L., Beretta, A., Bisoffi, Z., Zipeto, D., 2022. SARS-CoV-2 vaccination elicits unconventional IgM specific responses in naïve and previously COVID-19-infected individuals. eBioMedicine 77. https://doi.org/10.1016/j.ebiom.2022.103888

Saad, M.I., Rose-John, S., Jenkins, B.J., 2019. ADAM17: An Emerging Therapeutic Target for Lung Cancer. Cancers (Basel) 11, 1218. https://doi.org/10.3390/cancers11091218

Salgado, B.B., Barbosa, A.R.C., Arcanjo, A.R., de Castro, D.B., Ramos, T.C.A., Naveca, F., Altmann, D.M., Boyton, R.J., Lalwani, J.D.B., Lalwani, P., 2023. Hybrid Immunity Results in Enhanced and More Sustained Antibody Responses after the Second Sinovac-CoronaVac Dose in a

Brazilian Cohort: DETECTCoV-19 Cohort. Viruses 15, 1987. https://doi.org/10.3390/v15101987

Sama, I.E., Ravera, A., Santema, B.T., van Goor, H., ter Maaten, J.M., Cleland, J.G.F., Rienstra, M., Friedrich, A.W., Samani, N.J., Ng, L.L., Dickstein, K., Lang, C.C., Filippatos, G., Anker, S.D., Ponikowski, P., Metra, M., van Veldhuisen, D.J., Voors, A.A., 2020. Circulating plasma concentrations of angiotensin-converting enzyme 2 in men and women with heart failure and effects of renin–angiotensin–aldosterone inhibitors. European Heart Journal 41, 1810–1817. https://doi.org/10.1093/eurheartj/ehaa373

Schneider, C., Setty, M., Holmes, A.B., Maute, R.L., Leslie, C.S., Mussolin, L., Rosolen, A., Dalla-Favera, R., Basso, K., 2014. microRNA 28 controls cell proliferation and is down-regulated in B-cell lymphomas. Proc Natl Acad Sci U S A 111, 8185–8190. https://doi.org/10.1073/pnas.1322466111

Schumacher, N., Rose-John, S., 2022. ADAM17 orchestrates Interleukin-6, TNFα and EGF-R signaling in inflammation and cancer. Biochimica et Biophysica Acta (BBA) - Molecular Cell Research 1869, 119141. https://doi.org/10.1016/j.bbamcr.2021.119141

Selvavinayagam, S.T., Yong, Y.K., Tan, H.Y., Zhang, Y., Subramanian, G., Rajeshkumar, M., Vasudevan, K., Jayapal, P., Narayanasamy, K., Ramesh, D., Palani, S., Larsson, M., Shankar, E.M., Raju, S., 2022. Factors Associated With the Decay of Anti-SARS-CoV-2 S1 IgG Antibodies Among Recipients of an Adenoviral Vector-Based AZD1222 and a Whole-Virion Inactivated BBV152 Vaccine. Frontiers in Medicine 9.

Shang, R., Lee, S., Senavirathne, G., Lai, E.C., 2023. microRNAs in action: biogenesis, function and regulation. Nat Rev Genet 24, 816–833. https://doi.org/10.1038/s41576-023-00611-y

Shao, Z., Schuster, A., Borowski, A.G., Thakur, A., Li, L., Tang, W.H.W., 2019. Soluble Angiotensin Converting Enzyme 2 Levels in Chronic Heart Failure is Associated with Decreased Exercise Capacity and Increased Oxidative Stress-mediated Endothelial Dysfunction. Transl Res 212, 80–88. https://doi.org/10.1016/j.trsl.2019.06.004

Sharp, P.M., Hahn, B.H., 2010. The evolution of HIV-1 and the origin of AIDS. Philos Trans R Soc Lond B Biol Sci 365, 2487–2494. https://doi.org/10.1098/rstb.2010.0031

Shukla, G.C., Singh, J., Barik, S., 2011. MicroRNAs: Processing, Maturation, Target Recognition and Regulatory Functions. Molecular and cellular pharmacology 3, 83.

Silaghi-Dumitrescu, R., Patrascu, I., Lehene, M., Bercea, I., 2023. Comorbidities of COVID-19 Patients. Medicina (Kaunas) 59, 1393. https://doi.org/10.3390/medicina59081393

Silva, C.M.S., Barros-Filho, M.C., Wong, D.V.T., Mello, J.B.H., Nobre, L.M.S., Wanderley, C.W.S., Lucetti, L.T., Muniz, H.A., Paiva, I.K.D., Kuasne, H., Ferreira, D.P.P., Cunha, M.P.S.S., Hirth, C.G., Silva, P.G.B., Sant'Ana, R.O., Souza, M.H.L.P., Quetz, J.S., Rogatto, S.R., Lima-Junior, R.C.P., 2021. Circulating let-7e-5p, miR-106a-5p, miR-28-3p, and miR-542-5p as a Promising microRNA Signature for the Detection of Colorectal Cancer. Cancers (Basel) 13, 1493. https://doi.org/10.3390/cancers13071493

Sinha, A., Sangeet, S., Roy, S., 2023. Evolution of Sequence and Structure of SARS-CoV-2 Spike Protein: A Dynamic Perspective. ACS Omega 8, 23283–23304. https://doi.org/10.1021/acsomega.3c00944

Siracusano, G., Ruggiero, A., Bisoffi, Z., Piubelli, C., Carbonare, L.D., Valenti, M.T., Mayora-Neto, M., Temperton, N., Lopalco, L., Zipeto, D., 2022. Different decay of antibody response and VOC sensitivity in naïve and previously infected subjects at 15 weeks following vaccination with BNT162b2. Journal of Translational Medicine 20, 22. https://doi.org/10.1186/s12967-021-03208-3

Soni, D.K., Cabrera-Luque, J., Kar, S., Sen, C., Devaney, J., Biswas, R., 2020. Suppression of miR-155 attenuates lung cytokine storm induced by SARS-CoV-2 infection in human ACE2-transgenic mice. https://doi.org/10.1101/2020.12.17.423130

Sperrhacke, M., Leitzke, S., Ahrens, B., Reiss, K., 2023. Breakdown of Phospholipid Asymmetry Triggers ADAM17-Mediated Rescue Events in Cells Undergoing Apoptosis. Membranes 13, 720. https://doi.org/10.3390/membranes13080720

Srinivasan, S., Ghosh, M., Maity, S., Varadarajan, R., 2016. Broadly neutralizing antibodies for therapy of viral infections. ANTI 6, 1–15. https://doi.org/10.2147/ANTI.S92190

Srivastava, K., Carreño, J.M., Gleason, C., Monahan, B., Singh, G., Abbad, A., Tcheou, J., Raskin, A., Kleiner, G., Bakel, H. van, Sordillo, E.M., Alshammary, H., Amoako, A.A., Andre, D., Awawda, M., Bermúdez-

González, M.C., Beach, K.F., Bielak, D., Cai, G.Y., Chernet, R.L., Cognigni, C., Chen, Y., Eaker, L.Q., Ferreri, E.D., Floda, D.L., Fried, M., Hamburger, J.Z., Jurczyszak, D., Kang, H.M., Lyttle, N., Matthews, J.C., Mauldin, J., Mendez, W.A., Mischka, J., Morris, S., Mulder, L.C.F., Nabeel, I., Nardulli, J.R., Polanco, J., Oostenink, A., Rooker, A., Russo, K.T., Salimbangon, A.-B., Saksena, M.S., Shin, A.A., Sominsky, L.A., Stadlbauer, D., Sullivan, L., Kesteren, M. van, Yellin, T., Wajnberg, A., Krammer, F., Simon, V., 2024. SARS-CoV-2-infection- and vaccine-induced antibody responses are long lasting with an initial waning phase followed by a stabilization phase. Immunity 0. https://doi.org/10.1016/j.immuni.2024.01.017

Stefanelli, P., Trentini, F., Guzzetta, G., Marziano, V., Mammone, A., Sane Schepisi, M., Poletti, P., Molina Grané, C., Manica, M., del Manso, M., Andrianou, X., Ajelli, M., Rezza, G., Brusaferro, S., Merler, S., Di Martino, A., Ambrosio, L., Lo Presti, A., Fiore, S., Fabiani, C., Benedetti, E., Di Mario, G., Facchini, M., Puzelli, S., Calzoletti, L., Fontana, S., Venturi, G., Fortuna, C., Marsili, G., Amendola, A., Stuppia, L., Savini, G., Picerno, A., Lopizzo, T., Dell'Edera, D., Minchella, P., Greco, F., Viglietto, G., Atripaldi, L., Limone, A., D'Agaro, P., Licastro, D., Pongolini, S., Sambri, V., Dirani, G., Affanni, P., Colucci, M.E., Capobianchi, M.R., Icardi, G., Bruzzone, B., Lillo, F., Orsi, A., Pariani, E., Baldanti, F., Gismondo, M.R., Maggi, F., Caruso, A., Ceriotti, F., Boniotti, M.B., Barbieri, I., Bagnarelli, P., Menzo, S., Garofalo, S., Scutellà, M., Pagani, E., Collini, L., Ghisetti, V., Brossa, S., Ru, G., Bozzetta, E., Chironna, M., Parisi, A., Rubino, S., Serra, C., Piras, G., Coghe, F., Vitale, F., Tramuto, F., Scalia, G., Palermo, C.I., Mancuso, G., Pollicino, T., Di Gaudio, F., Vullo, S., Reale, S., Cusi, M.G., Rossolini, G.M., Pistello, M., Mencacci, A., Camilloni, B., Severini, S., Di Benedetto, M., Terregino, C., Monne, I., Biscaro, V., 2022. Co-circulation of SARS-CoV-2 Alpha and Gamma variants in Italy, February and March 2021. Euro Surveill 27, 2100429. https://doi.org/10.2807/1560-7917.ES.2022.27.5.2100429

Sun, C., Xie, C., Bu, G.-L., Zhong, L.-Y., Zeng, M.-S., 2022. Molecular characteristics, immune evasion, and impact of SARS-CoV-2 variants. Signal Transduct Target Ther 7, 202. https://doi.org/10.1038/s41392-022-01039-2

Takahashi, T., Ai, T., Saito, K., Nojiri, S., Takahashi, M., Igawa, G., Yamamoto, T., Khasawneh, A., Paran, F.J., Takei, S., Horiuchi, Y., Kanno, T., Tobiume, M., Hiki, M., Wakita, M., Miida, T., Okuzawa, A., Suzuki, T., Takahashi, K., Naito, T., Tabe, Y., 2023. Assessment of antibody dynamics and neutralizing activity using serological assay after SARS-CoV-2 infection and vaccination. PLOS ONE 18, e0291670. https://doi.org/10.1371/journal.pone.0291670

Tam, D., Lorenzo-Leal, A.C., Hernández, L.R., Bach, H., 2023. Targeting SARS-CoV-2 Non-Structural Proteins. Int J Mol Sci 24, 13002. https://doi.org/10.3390/ijms241613002

Tan, C., Wang, N., Deng, S., Wu, X., Yue, C., Jia, X., Lyu, Y., 2023. The development and application of pseudoviruses: assessment of SARS-CoV-2 pseudoviruses. PeerJ 11, e16234. https://doi.org/10.7717/peerj.16234

Taubenberger, J.K., Morens, D.M., 2006. 1918 Influenza: the Mother of All Pandemics. Emerg Infect Dis 12, 15–22. https://doi.org/10.3201/eid1201.050979

Temperton, N.J., 2009a. The Use of Retroviral Pseudotypes for the Measurement of Antibody Responses to SARS Coronavirus. Molecular Biology of the SARS-Coronavirus 279–288. https://doi.org/10.1007/978-3-642-03683-5_17

Temperton, N.J., 2009b. The Use of Retroviral Pseudotypes for the Measurement of Antibody Responses to SARS Coronaviru. Molecular Biology of the SARS-Coronavirus 279–288.

Thai, T.-H., Calado, D.P., Casola, S., Ansel, K.M., Xiao, C., Xue, Y., Murphy, A., Frendewey, D., Valenzuela, D., Kutok, J.L., Schmidt-Supprian, M., Rajewsky, N., Yancopoulos, G., Rao, A., Rajewsky, K., 2007. Regulation of the Germinal Center Response by MicroRNA-155. Science 316, 604–608. https://doi.org/10.1126/science.1141229

Thucydides, History of the Peloponnesian War, THE SECOND BOOK, chapter 47 [WWW Document], n.d. URL https://www.perseus.tufts.edu/hopper/text?doc=Perseus%3Atext%3A1999.01.0247%3Abook%3D2%3Achapter%3D47 (accessed 1.29.24).

Tosta, E., 2022. The adaptation of SARS-CoV-2 to humans. Mem Inst Oswaldo Cruz 116, e210127. https://doi.org/10.1590/0074-02760210127

Tran, T.T., Vaage, E.B., Mehta, A., Chopra, A., Tietze, L., Kolderup, A., Anthi, A., König, M., Nygaard, G., Lind, A., Müller, F., Nissen-Meyer, L.S.,

Magnus, P., Trogstad, L., Mjaaland, S., Søraas, A., Midtvedt, K., Åsberg, A., Barratt-Due, A., Medhus, A.W., Høivik, M.L., Lundin, K., Karlsen, R.F., Dahle, R., Danielsson, K., Thomassen, K.S., Kro, G.B., Cox, R.J., Zhou, F., Langeland, N., Aukrust, P., Melum, E., Åvitsland, T.L., Wiencke, K., Holter, J.C., Munthe, L.A., Grødeland, G., Andersen, J.-T., Vaage, J.T., Lund-Johansen, F., 2022. Titers of antibodies against ancestral SARS-CoV-2 correlate with levels of neutralizing antibodies to multiple variants. npj Vaccines 7, 1–11. https://doi.org/10.1038/s41541-022-00586-7

Tribolet, L., Kerr, E., Cowled, C., Bean, A.G.D., Stewart, C.R., Dearnley, M., Farr, R.J., 2020. MicroRNA Biomarkers for Infectious Diseases: From Basic Research to Biosensing. Front Microbiol 11, 1197. https://doi.org/10.3389/fmicb.2020.01197

Tsitsiou, E., Lindsay, M.A., 2009. microRNAs and the immune response. Current Opinion in Pharmacology, Cancer/Immunomodulation 9, 514–520. https://doi.org/10.1016/j.coph.2009.05.003

Vergori, A., Cozzi Lepri, A., Cicalini, S., Matusali, G., Bordoni, V., Lanini, S., Meschi, S., Iannazzo, R., Mazzotta, V., Colavita, F., Mastrorosa, I., Cimini, E., Mariotti, D., De Pascale, L., Marani, A., Gallì, P., Garbuglia, A., Castilletti, C., Puro, V., Agrati, C., Girardi, E., Vaia, F., Antinori, A., 2022. Immunogenicity to COVID-19 mRNA vaccine third dose in people living with HIV. Nat Commun 13, 4922. https://doi.org/10.1038/s41467-022-32263-7

Verma, J., Subbarao, N., 2021. A comparative study of human betacoronavirus spike proteins: structure, function and therapeutics. Arch Virol 166, 697–714. https://doi.org/10.1007/s00705-021-04961-y

Vicenti, I., Basso, M., Gatti, F., Scaggiante, R., Boccuto, A., Zago, D., Modolo, E., Dragoni, F., Parisi, S.G., Zazzi, M., 2021. Faster decay of neutralizing antibodies in never infected than previously infected healthcare workers three months after the second BNT162b2 mRNA COVID-19 vaccine dose. International Journal of Infectious Diseases 112, 40–44. https://doi.org/10.1016/j.ijid.2021.08.052

Vistbakka, J., Elovaara, I., Lehtimäki, T., Hagman, S., 2017. Circulating microRNAs as biomarkers in progressive multiple sclerosis. Mult Scler 23, 403–412. https://doi.org/10.1177/1352458516651141

von Bülow, S., Sikora, M., Blanc, F.E.C., Covino, R., Hummer, G., 2023. Antibody accessibility determines location of spike surface mutations in

SARS-CoV-2 variants. PLoS Comput Biol 19, e1010822. https://doi.org/10.1371/journal.pcbi.1010822

Walker, L.M., Burton, D.R., 2018. Passive immunotherapy of viral infections: “super-antibodies” enter the fray. Nat Rev Immunol 18, 297–308. https://doi.org/10.1038/nri.2017.148

Walls, A.C., Park, Y.J., Tortorici, M.A., Wall, A., McGuire, A.T., Veesler, D., 2020. Structure, Function, and Antigenicity of the SARS-CoV-2 Spike Glycoprotein. Cell 181, 281-292.e6. https://doi.org/10.1016/j.cell.2020.02.058

Wan, Y., Shang, J., Graham, R., Baric, R.S., Li, F., 2020. Receptor Recognition by the Novel Coronavirus from Wuhan: an Analysis Based on Decade-Long Structural Studies of SARS Coronavirus. Journal of Virology 94, 10.1128/jvi.00127-20. https://doi.org/10.1128/jvi.00127-20

Wang, C., Hu, J., Lu, M., Gu, H., Zhou, X., Chen, X., Zen, K., Zhang, C.-Y., Zhang, T., Ge, J., Wang, J., Zhang, C., 2015. A panel of five serum miRNAs as a potential diagnostic tool for early-stage renal cell carcinoma. Sci Rep 5, 7610. https://doi.org/10.1038/srep07610

Wang, Y., Robertson, J.D., Walcheck, B., 2011. Different Signaling Pathways Stimulate a Disintegrin and Metalloprotease-17 (ADAM17) in Neutrophils during Apoptosis and Activation. J Biol Chem 286, 38980–38988. https://doi.org/10.1074/jbc.M111.277087

Wang, Z., Li, K., Wang, X., Huang, W., 2019. MiR-155-5p modulates HSV-1 replication via the epigenetic regulation of SRSF2 gene expression. Epigenetics 14, 494–503. https://doi.org/10.1080/15592294.2019.1600388

WHO Coronavirus (COVID-19) Dashboard [WWW Document], n.d. URL https://covid19.who.int (accessed 7.1.23).

Wigton, E.J., Ansel, K.M., 2021. Noncoding RNAs in B cell responses. RNA Biology 18, 633–639. https://doi.org/10.1080/15476286.2021.1885876

Wood, C.D., Carvell, T., Gunnell, A., Ojeniyi, O.O., Osborne, C., West, M.J., 2018. Enhancer Control of MicroRNA miR-155 Expression in Epstein-Barr Virus-Infected B Cells. Journal of Virology 92, 10.1128/jvi.00716-18. https://doi.org/10.1128/jvi.00716-18

Woods, P.S., Doolittle, L.M., Rosas, L.E., Nana-Sinkam, S.P., Tili, E., Davis, I.C., 2020. Increased expression of microRNA-155-5p by alveolar type II cells contributes to development of lethal ARDS in H1N1 influenza

A virus-infected mice. Virology 545, 40–52. https://doi.org/10.1016/j.virol.2020.03.005

Wrapp, D., Wang, N., Corbett, K.S., Goldsmith, J.A., Hsieh, C.-L., Abiona, O., Graham, B.S., McLellan, J.S., 2020. Cryo-EM structure of the 2019-nCoV spike in the prefusion conformation. Science 367, 1260–1263. https://doi.org/10.1126/science.abb2507

Wrobel, A.G., Benton, D.J., Xu, P., Roustan, C., Martin, S.R., Rosenthal, P.B., Skehel, J.J., Gamblin, S.J., 2020. SARS-CoV-2 and bat RaTG13 spike glycoprotein structures inform on virus evolution and furin-cleavage effects. Nat Struct Mol Biol 27, 763–767. https://doi.org/10.1038/s41594-020-0468-7

Wu, Z., Hao, R., Li, P., Zhang, X., Liu, N., Qiu, S., Wang, L., Wang, Y., Xue, W., Liu, K., Yang, G., Cui, J., Zhang, C., Song, H., 2013. MicroRNA Expression Profile of Mouse Lung Infected with 2009 Pandemic H1N1 Influenza Virus. PLOS ONE 8, e74190. https://doi.org/10.1371/journal.pone.0074190

Xia, X., 2021. Domains and Functions of Spike Protein in SARS-Cov-2 in the Context of Vaccine Design. Viruses 13, 109. https://doi.org/10.3390/v13010109

Xiang, Q., Li, L., Wu, J., Tian, M., Fu, Y., 2022. Application of pseudovirus system in the development of vaccine, antiviral-drugs, and neutralizing antibodies. Microbiol Res 258, 126993. https://doi.org/10.1016/j.micres.2022.126993

Xu, C., Han, W., Cong, Y., 2023. Cryo-EM and cryo-ET of the spike, virion, and antibody neutralization of SARS-CoV-2 and VOCs. Current Opinion in Structural Biology 82, 102664. https://doi.org/10.1016/j.sbi.2023.102664

Xu, W., Wong, G., Hwang, Y.Y., Larbi, A., 2020. The untwining of immunosenescence and aging. Semin Immunopathol 42, 559–572. https://doi.org/10.1007/s00281-020-00824-x

Xu, Y., Li, Y., 2021. MicroRNA-28-3p inhibits angiotensin-converting enzyme 2 ectodomain shedding in 293T cells treated with the spike protein of severe acute respiratory syndrome coronavirus 2 by targeting A disintegrin and metalloproteinase 17. International Journal of Molecular Medicine 48, 1–10. https://doi.org/10.3892/ijmm.2021.5022

Yang, G., Cui, M., Jiang, W., Sheng, J., Yang, Y., Zhang, X., 2021. Molecular switch in human diseases-disintegrin and metalloproteinases,

ADAM17. Aging (Albany NY) 13, 16859–16872. https://doi.org/10.18632/aging.203200

Ying, H., Ebrahimi, M., Keivan, M., Khoshnam, S.E., Salahi, S., Farzaneh, M., 2021. miRNAs; a novel strategy for the treatment of COVID-19. Cell Biol Int 45, 2045–2053. https://doi.org/10.1002/cbin.11653

Yue, L., Xie, T., Yang, T., Zhou, J., Chen, H., Zhu, H., Li, H., Xiang, H., Wang, J., Yang, H., Zhao, H., Wei, X., Zhang, Y., Xie, Z., 2022. A third booster dose may be necessary to mitigate neutralizing antibody fading after inoculation with two doses of an inactivated SARS-CoV-2 vaccine. J Med Virol 94, 35–38. https://doi.org/10.1002/jmv.27334

Zamagni, G., Armocida, B., Abbafati, C., Ronfani, L., Monasta, L., 2022. COVID-19 Vaccination Coverage in Italy: How Many Hospitalisations and Related Costs Could Have Been Saved If We Were All Vaccinated? Frontiers in Public Health 10.

Zampetaki, A., Kiechl, S., Drozdov, I., Willeit, P., Mayr, U., Prokopi, M., Mayr, A., Weger, S., Oberhollenzer, F., Bonora, E., Shah, A., Willeit, J., Mayr, M., 2010. Plasma MicroRNA Profiling Reveals Loss of Endothelial MiR-126 and Other MicroRNAs in Type 2 Diabetes. Circulation Research 107, 810–817. https://doi.org/10.1161/CIRCRESAHA.110.226357

Zhang, Jun, Xiao, T., Cai, Y., Chen, B., 2021. Structure of SARS-CoV-2 spike protein. Curr Opin Virol 50, 173–182. https://doi.org/10.1016/j.coviro.2021.08.010

Zhang, Jiabin, Yao, Y., Li, H., Ye, S., 2021. miR-28-3p inhibits prostate cancer cell proliferation, migration and invasion, and promotes apoptosis by targeting ARF6. Experimental and Therapeutic Medicine 22, 1–14. https://doi.org/10.3892/etm.2021.10639

Zhang, L., Hom, N., Ojha, A., Lovendahl, K.N., Mou, H., Lee, K.K., Choe, H., 2023. Cytoplasmic Tail Truncation Stabilizes S1-S2 Association and Enhances S Protein Incorporation into SARS-CoV-2 Pseudovirions. Journal of Virology 0, e01650-22. https://doi.org/10.1128/jvi.01650-22

Zhang, S., Wang, K., Wang, W.L., Nguyen, H.T., Chen, S., Lu, M., Go, E.P., Ding, H., Steinbock, R.T., Desaire, H., Kappes, J.C., Sodroski, J., Mao, Y., 2021. Asymmetric Structures and Conformational Plasticity of the Uncleaved Full-Length Human Immunodeficiency Virus Envelope Glycoprotein Trimer. Journal of Virology 95, 10.1128/jvi.00529-21. https://doi.org/10.1128/jvi.00529-21

Zhou, P., Yang, X.L., Wang, X.G., Hu, B., Zhang, L., Zhang, W., Si, H.R., Zhu, Y., Li, B., Huang, C.L., Chen, H.D., Chen, J., Luo, Y., Guo, H., Jiang, R.D., Liu, M.Q., Chen, Y., Shen, X.R., Wang, X., Zheng, X.S., Zhao, K., Chen, Q.J., Deng, F., Liu, L.L., Yan, B., Zhan, F.X., Wang, Y.Y., Xiao, G.F., Shi, Z.L., 2020. A pneumonia outbreak associated with a new coronavirus of probable bat origin. Nature 579, 270–273. https://doi.org/10.1038/s41586-020-2012-7

Zhou, X., Wen, W., Shan, X., Qian, J., Li, H., Jiang, T., Wang, W., Cheng, W., Wang, F., Qi, L., Ding, Y., Liu, P., Zhu, W., Chen, Y., 2016. MiR-28-3p as a potential plasma marker in diagnosis of pulmonary embolism. Thrombosis Research 138, 91–95. https://doi.org/10.1016/j.thromres.2015.12.006

Zipeto, D., Palmeira, J. da F., Argañaraz, G.A., Argañaraz, E.R., 2020. ACE2/ADAM17/TMPRSS2 Interplay May Be the Main Risk Factor for COVID-19. Frontiers in Immunology 11.

8. ATTACHMENTS

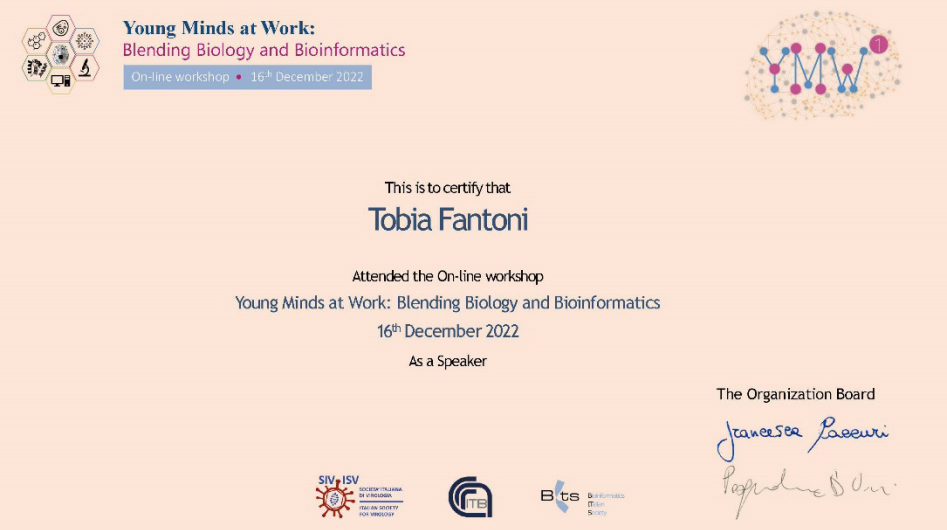

Certificate of Oral Presentation

Online Workshop: Young Minds at Work, 16th December 2022

Is miR-28-3p implicated in the development of severe COVID-19?

Fantoni T.[1], Orlandi E.[1], da Fonseca Palmeira J.[2], Ruggiero A.[1], Gomez-Lira M.[1], Temperton N.[3], Argañaraz E. R.[2], Zipeto D[1].

1 Department of Neuroscience, Biomedicine and Movement, University of Verona, Verona, IT.
2 Laboratory of Molecular Neurovirology, Faculty of Health Science, University of Brasília, Brasília, Brazil.
3 Viral Pseudotype Unit, University of Kent, Chatham, Kent, UK.

BACKGROUND

High levels of soluble ACE2 (sACE2) are correlated to severe COVID-19[1,2]. Physiological low levels of serum sACE2 are maintained by transmembrane proteases, such as A disintegrin and metalloprotease 17 (ADAM17), one of the targets of microRNA-28-3p . It is under debate whether the direct contact between the Spike protein of SARS-CoV-2 and ACE2, with the consequent alternate modulation of miR-28-3p and ADAM17, is one of the main causes of the imbalance in sACE2[3,4]. SARS-CoV-2 pseudoviruses (PVs) are surrogates of the real virus facilitating the study of host-cell interactions in safe conditions. Non-replicating, lentiviral PVs are widely used because of their ability to stably introduce a reporter gene (Luciferase) for facilitating the titration[5].

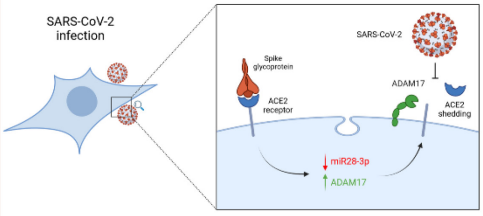

Fig. 1. SARS-CoV-2 induces ACE2 shedding by altering miR-28-3p and ADAM17 expression.

METHODS

PVs of the ancestral SARS-COV-2 strain from Wuhan (Wu), the Omicron BA.2.75 variant (Om BA.2.75), and vesicular stomatitis virus (VSVg) (control of infection) were produced by co-transfecting HEK293T cells. The supernatant was harvested, centrifuged, and filtered after incubating for 72hs. HEK293T/ACE2 target cell line was infected after titrating PVs (Fig.2). Infected cells were collected at 6, 12, and 24 hours after infection and treated with Trizol to extract total RNA. miR-28-3p levels were quantified using qPCR. For the flow cytometry (FACS) assay, cells were infected, collected at 12hs after infection, stained with anti-human ACE2—PE, and analysed (Fig. 3).

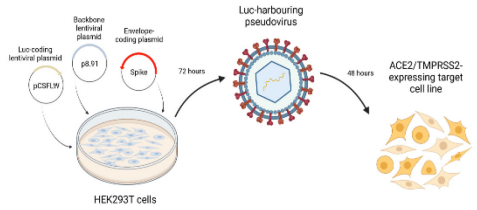

Fig. 2. Experimental workflow for the production of SARS-CoV-2 PVs and the infection of target cells.

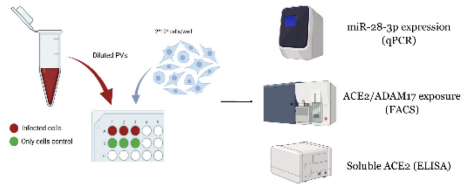

Fig. 3. SARS-CoV-2 PVs can be applied to multiple platform analyses such as the analysis of genes and miRNAs alteration (qPCR), surface protein expression (FACS) and the quantification of proteins released upon infection (ELISA).

RESULTS

miR28-3p levels (normalized to miR-103a) were measured at 6, 12, and 24hs after infection with SARS-CoV-2 PVs. Significant deregulation ($p<0.05$, *) was observed at 12hs after infection (Fig. 4A). Simultaneously, preliminary FACS assays suggested the percentage of ACE2-positive cells is reduced after 12hs when exposed to Wu and Om BA.2.75 PVs compared to the untreated (UT) and infection (VSVg) controls (Fig. 4B).

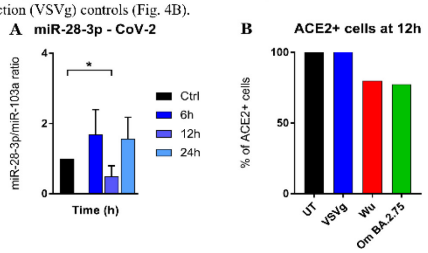

Fig. 4. miR-28-3p has been measured at 6, 12, and 24 hs after infection with SARS-CoV-2 PVs. Its significant downmodulation was observed at 12hs after exposing the target cells to the PVs (A). Preliminary results on ACE2 shedding after incubation of cells with SARS-CoV– PVs. The percentage of ACE2-positive cells is reduced when compared to untreated (UT) and VSVg-infected cells (B).

DISCUSSION

Many COVID-19 patients develop symptoms similar to cardiovascular disorders (hypertension, vascular inflammation, etc.) in addition to lung injuries and consequent failure. The imbalance of the RAS system has been pointed as the main responsible for the increased severity of the disease. In fact, high levels of soluble ACE2, similarly to several cardiovascular disorders, were detected in severe COVID-19 patients. Deregulation of miR-28-3p and consequent upregulation of one of its targets, ADAM17, are thought to mediate the shedding of ACE2 on infected cells, potentially causing COVID-19. Here, we show that exposing ACE2-expressing cells to SARS-CoV-2 PVs induces a reduction of the relative expression of the miR-28-3p. Also, the percentage of ACE-postive cells is reduced when SARS-CoV-2 Wuhan and Omicron BA.2.75 are added to the cell medium. Further analyses aim at measuring the number of ADAM17+ cells that contacted the PVs of CoV-2 and the increased levels of sACE2 in the correspinding cell medium.

This preliminary study is important in two aspects. First, it investigates the effects of the full Spike protein of SARS-CoV-2 on the modulation of a single microRNA, showing that it could be involved in ACE2 shedding, and consequently, in the onset of severe COVID-19. Secondly, it emphasises the role of the technology of pseudoviruses in the research on a real virus (and/or its variants, or similar viruses), under appropriate safety conditions, on multiple platforms, in order to fully understand its interactions with the host organism.

REFERENCES

1. *Nagy et al.*, Int J Infect Dis, 2020. doi: 10.1016/j.ijid.2020.11.184
2. *Mariappan et al.*, Biochimie, 2022. doi: 10.1016/j.biochi.2022.06.005
3. *Xu et al.*, Int J Mol Med, 2021. doi: 10.3892/ijmm.2021.5022
4. *Zipeto et al.*, Front Immunol, 2020. doi: 10.3389/fimmu.2020.576745
5. *Di Genova et al.*, Bio Protoc, 2021. doi: 10.21769/BioProtoc.4236

CONTACTS: tobia.fantoni@univr.it; donato.zipeto@univr.it

PhD Day 2023 - PhD Course in Applied Life and Health Sciences

Poster and Oral Presentation

PhD Day 2023, 25th September 2023, University of Verona

SARS-CoV-2 vaccination elicits unconventional IgM specific responses in naïve and previously COVID-19-infected individuals

Alessandra Ruggiero,[a] Chiara Piubelli,[b] Lucia Calciano,[c] Simone Accordini,[c] Maria Teresa Valenti,[d] Luca Dalle Carbonare,[d] Gabriel Siracusano,[e] Nigel Temperton,[f] Natalia Tiberti,[b] Silvia Stefania Longoni,[b] Massimo Pizzato,[g] Silvia Accordini,[g] A.M.S.L.V. group ,[2] Tobia Fantoni,[a] Lucia Lopalco,[e] Alberto Beretta,[h] Zeno Bisoffi,[b,c,1] and Donato Zipeto [a,1]*

[a]Department of Neurosciences, Biomedicine and Movement Sciences, University of Verona, Verona, Italy
[b]Department of Infectious, Tropical Diseases and Microbiology, IRCCS Sacro Cuore Don Calabria Hospital, Negrar (VR), Italy
[c]Department of Diagnostics and Public Health, University of Verona, Verona, Italy
[d]Department of Medicine, University of Verona, Verona, Italy
[e]Division of Immunology, Transplantation and Infectious Diseases, San Raffaele Scientific Institute, Milan, Italy
[f]Viral Pseudotype Unit, Medway School of Pharmacy, Universities of Kent and Greenwich, UK
[g]Department of Cellular, Computational and Integrative Biology, University of Trento, Povo (TN), Italy
[h]Solongevity Research, Milan, Italy

eBioMedicine 2022;77: 103888
Published online 20 February 2022
https://doi.org/10.1016/j.ebiom.2022.103888

Summary

Background Currently, evaluation of the IgG antibodies specific for the SARS-CoV-2 Spike protein following vaccination is used worldwide to estimate vaccine response. Limited data are available on vaccine-elicited IgM antibodies and their potential implication in immunity to SARS-CoV-2.

Methods We performed a longitudinal study to quantify anti-S SARS-CoV-2 IgG and IgM (IgG-S and IgM-S) in health care worker (HCW) recipients of the BNT162b2 vaccine. Samples were collected before administration (T0), at the second dose (T1) and three weeks after T1 (T2). The cohort included 1584 immunologically naÿve to SARS-CoV-2 (IN) and 289 with history of previous infection (PI).

Findings IN showed three patterns of responses: (a) IgG positive/IgM negative (36.1%), (b) coordinated IgM-S/IgG-S responses appearing at T1 (37.4%) and (c) IgM appearing after IgG (26.3%). Coordinated IgM-S/IgG-S responses were associated with higher IgG titres. In IgM-S positive PI, 64.5% were IgM-S positive before vaccination, whereas 32% and 3.5% developed IgM-S after the first and second vaccine dose, respectively. IgM-S positive sera had higher pseudovirus neutralization titres compared to the IgM-S negative.

Interpretation Coordinated expression of IgG-S and IgM-S after vaccination was associated with a significantly more efficient response in both antibody levels and virus-neutralizing activity. The unconventional IgG-S positive/IgM-S negative responses may suggest a recruitment of cross coronaviruses immunity by vaccination, warranting further investigation.

Funding Italian Ministry of Health under "Fondi Ricerca Corrente"- L1P5 and "Progetto Ricerca Finalizzata COVID-2020-12371675"; FUR 2020 Department of Excellence 2018-2022, MIUR, Italy; The Brain Research Foundation Verona.

Keywords: SARS-CoV-2; COVID-19; BTN162b2 vaccine; IgG; IgM; Spike

Abbreviations: IgM, Immunoglobulins M; IgG, Immunoglobulins G

*Corresponding author.
E-mail address: donato.zipeto@univr.it (D. Zipeto).

[1] These authors contributed equally to this work.

[2] Ambulatorio Medico San Luca Villanuova (Bettini G.L., Bonvicini A., Braga A., Chiappini F., Inverardi F., Ravera S., Rossi M.G., Sas A., Turrini A.), Villanuova sul Clisi (BS), Italy.

Research in context

Evidence before this study

It is generally accepted that IgM antibodies provide an early-stage response during viral infections prior to the maturation of the class-switched, high affinity IgG response for long-term immunity and immunological memory. The humoral response following SARS-CoV-2 vaccination is still under intensive investigation, with the main confounder being previous exposures to SARS-CoV-2 and the resulting presence of pre-existing immunity towards the Spike protein used in the vaccine formulation. Thus, the definition of correlates of protective immunity to SARS-CoV-2 infection and vaccination are urgently needed for guiding vaccine management and informing public health decisions. Nonetheless, most research to date has focused on the development and maintenance of the RBD-specific IgG, with little attention to IgM.

Added value of this study

We investigated a population of 1873 health care worker (HCW) recipients of the BNT162b2 (Comirnaty) vaccine, with 1584 immunologically naïve to SARS-CoV-2 (IN) and 289 with history of previous infection (PI). We performed a longitudinal analysis of the humoral response (IgG and IgM antibodies specific for the SARS-CoV-2 spike protein, IgG-S and IgM-S) in samples collected before administration (T0), at the second dose (T1) and 3 weeks after the second dose (T2). Furthermore, we analysed the vaccine response in a small group of subjects vaccinated with Vaxzevria (Astra Zeneca) or Spikevax (Moderna). We observed three unconventional patterns of antibody response: absence of IgM, development of IgM following IgG appearance and simultaneous presence of IgM and IgG. Among the three, the latter was associated with a more efficient response in both anti-SARS-CoV-2 IgG-S levels and virus-neutralizing activity, following vaccination.

Implications of all the available evidence

Our study highlights the importance of IgM in assessing response after SARS- CoV-2 vaccination. We demonstrated that SARS-CoV-2 vaccination can induce a humoral response that appears to be unconventional. This is suggestive of a response that recalls IgG developed against other coronaviruses. Indeed, only individuals that developed SARS-CoV-2 specific IgM together with SARS-CoV-2 specific IgG showed the better response and probably higher levels of protection, following vaccination. These findings are innovative, timely and significantly improve current knowledge by suggesting a crucial role of IgM in the development of anti-SARS-CoV-2 humoral response, following vaccination.

Introduction

Correlates of protective immunity to SARS-CoV-2 infection are under intensive investigation in COVID-19 patients and vaccinees and are urgently needed for guiding vaccine management and informing public health decisions.[1,2] It is generally accepted that IgM antibodies provide an early-stage response during viral infections prior to the maturation of the class-switched, high affinity IgG response for long-term immunity and immunological memory.[3] During SARS-CoV-2 infection, antigen (Ag)-specific IgM antibodies can be detected as soon as four days after infection with a peak at around 20 days, while Ag-specific IgG increase around 7 days after infection with a peak at approximately 25 days.[4,5] Rapid deployment of SARS-CoV-2 specific IgM was reported to be associated with milder disease course compared with severe cases that experienced a later raise in IgM,[6] although the question remains controversial.[7] Several studies reported that a proportion of patients never develop IgM, while others develop IgG prior to IgM.[2,5,8–12] Overall, these data suggest both a potential role of Ag-specific IgM in preventing severe disease but also the possibility that SARS-CoV-2 infection may trigger unconventional humoral responses, possibly generated by pre-existing immunity to other human coronaviruses.[13,14]

The humoral response following SARS-CoV-2 vaccination is still under intensive investigation, as it is not yet clear the role played by pre-existing immunity in the response to vaccination. Previously infected (PI) individuals have been shown to develop a more efficient antibody response to COVID-19 vaccines than immunologically naÿve individuals (IN).[15] Notably, neutralizing activity 7 days following the first vaccine dose in PI vaccinees was not significantly different from that observed in IN vaccinees 7 days after the second vaccine dose.[15] Furthermore, the kinetic of both anti SARS-CoV-2 receptor-binding domain (RBD) IgG and live-virus neutralization capacity was faster in PI than in IN vaccinees.[15] With regard to IgM, one study reported that about 50% of IN vaccinees did not develop IgM after the first dose of BNT162b2 vaccine.[16]

Nonetheless, most research thus far has concentrated on the development and maintenance of the RBD-specific IgG, with little attention to IgM.

Our group has previously shown that IN vaccinees fail to develop IgM against the SARS-CoV-2 spike glycoprotein (IgM-S) before IgG against the SARS-CoV-2 spike glycoprotein (IgG-S)[14]; more specifically, following the first vaccine dose, we observed the simultaneous development of IgM-S and IgG-S in 54% of the vaccinees, and an unconventional IgG-S response without detectable IgM-S in the remaining 46%. We observed a similar trend in PI vaccinees.

In this study, we analysed a cohort of Health Care Workers (HCW) including 1584 IN and 289 PI vaccinees to study the IgM-S response following BNT162b2 vaccination and assess its association with the development and maintenance of IgG responses. We leveraged the availability of two groups of PI vaccinees who had been infected in the first and the second pandemic wave in Italy to assess the antibody profile at different times after infection. In available subgroups of IN vaccinees, we evaluated humoral response following other types of vaccines, including Vaxzevria (AstraZeneca) and Spikevax (Moderna).

Methods

Population

The sera of 1989 HCW with and without pre-existing infection for SARS-CoV-2 (as per former nasal swab positivity) who had received their first vaccine dose (BNT162b2 mRNA, Pfizer-BioNTech) in January 2021 were analysed. Samples were collected before vaccine administration (T0), at the second dose (T1) and three weeks after T1 (T2) and tested for IgG against the Spike glycoprotein (IgG-S), IgG against the Nucleocapsid protein (IgG-N) and IgM against the Spike glycoprotein (IgM-S). All individuals who had received two doses of BNT162b2 vaccine and had complete serological data were included in the study. Among the 1957 individuals having complete information, 84 were negative at the swab test but had positive serology (IgM-S or IgG-S or IgG-N) at T0; they were considered as false negatives in accordance with a recent study[17] and were not included in the present study. Antibody response analyses were conducted on 1584 IN subjects and 289 PI subjects.

Ethics

Samples were collected and stored in the University of Verona biobank (Ethics Committee approval prot. N. 1538) and in Tropica Biobank of the IRCCS Sacro Cuore Don Calabria Hospital (Ethics Committee approval prot. N. 17985). All participants signed informed consent.

Serology and neutralization

IgM-S and IgG-N were measured using the SARS-CoV-2 IgG-N assay and the SARS-CoV-2 IgM-S assay (Abbott, Ireland); IgG-S(RBD) were tested using the SARS-CoV-2 IgG II Quant assay (Abbott, Ireland) as previously described.[14,17]

Briefly, SARS-CoV-2 IgG-N, IgM and SARS-CoV-2 IgG II Quant (IgG-S) assays (Abbott, Ireland) were performed according to the manufacturer's procedure, using the ARCHITET i System (Abbott). The resulting chemiluminescent reaction was measured as a relative light unit (RLU) by the system optics. The RLU of the sample (S) was automatically compared with the RLU of a specific calibrator (C), resulting in a IgG assay index (S/C). As per manufacturer's instructions, the interpretation of the results were as follow: for IgG-N, index (S/C)<1.4 = negative, index (S/C)≥1.4 = positive. For IgM-S, index (S/C)<1 = negative, index (S/C)≥1 = positive. For IgM-S assay the reported positive predicted value (PPV) is 92.07% (IC 95%: 87.07, 95.24) and the reported negative predicted value (NPV) is 99.82% (IC 95%: 99.47, 99.94).

For IgG-S the Ab quantification was automatically performed by the system using a calibration curve, a fitting system and interpolation with 4 parameters (4PLC, Y weighted). The results in Arbitrary Unit (AU)/mL, is converted in the WHO international binding antibody unit (BAU)/mL according to the following equation: 1BAU = 0.142*AU, with BAU/mL<7.1 = negative and BAU/mL≥7.1 = positive. For IgG II Quant the manufacturer reports a PPV of 92.11% (IC 95%: 85.87, 95.73) and a NPV of 99.97% (IC 95%: 99.76, 100.00). Samples with values >5680 BAU/mL (upper limit of quantification) were diluted 1:2 and measured again. Concentrations were reported considering the dilution factor. Samples were run in single replicate.

Neutralizing activity of sera was tested using lentiviral particles pseudotyped with SARS-CoV-2 spike, as previously described.[14,18]

Statistical analysis

Kruskal-Wallis rank test and Fisher's exact test were used when needed in the descriptive analysis. Pseudovirus neutralization assay expressed as infectious dose (ID50) and IgG-S levels were ln-transformed [ln(ID50) and ln(IgG-S)] to resemble normal distributions. Two-level linear regression models (measurement: level 1 unit; subject: level 2 unit) were used to predict the mean of ln(ID50) and ln(IgG-S) levels according to time of examination (T0, T1, T2) and IgM-S group (for Figs. 1, 4 and 5) or serology group (for Figure 6), separately for IN and PI subjects. The models had a random intercept term at level 2 and time of examination, IgM-S/serology group, their interaction term, age at T0, sex and pandemic wave (1st or 2nd, for PI only) as fixed effect covariates. A first-order autoregressive error was included at level 1 in order to take the correlation of the within-subject observations over time into account. All statistical analyses were performed by using STATA software (release 17; StataCorp, College Station, TX).

Role of funding source

This work was supported by the Italian Ministry of Health under "Fondi Ricerca Corrente"- L1P5 and "Progetto Ricerca Finalizzata COVID-2020-12371675" to IRCCS Sacro Cuore Don Calabria Hospital, by FUR 2020 Department of Excellence 2018-2022, MIUR,

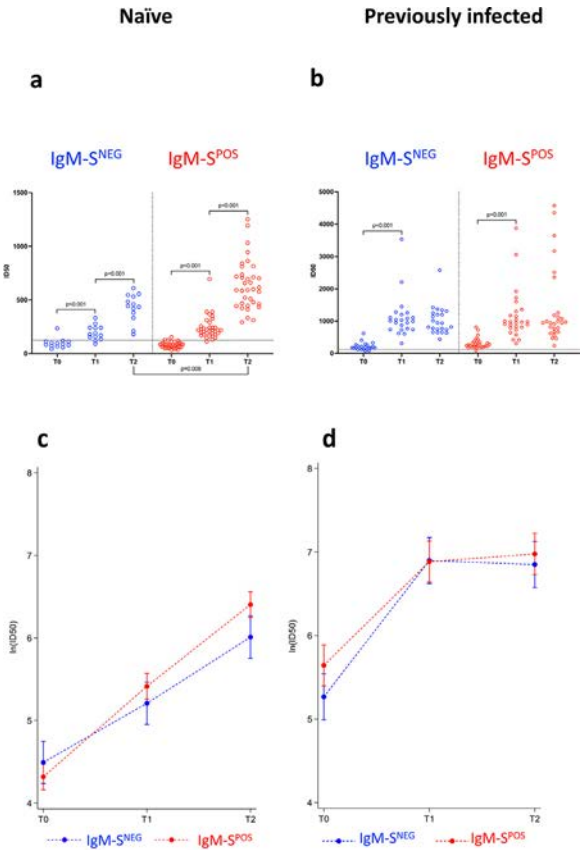

Figure 1. Neutralization assays in naïve and previously infected vaccinees.

Pseudovirus neutralization assay expressed as infectious dose (ID50) in naïve (panel a) and previously infected (panel b) vaccinees according to time of examination (T0, T1 and T2) and IgM-S development after two doses of the BNT162b2 vaccine (IgM-S^{POS}, red dots and lines; IgM-S^{NEG} subjects, blue dots and lines). Predicted means of ln(ID50) levels (with the 95% confidence interval) according to time of examination and IgM-S group in naïve (panel c) and previously infected (panel d) vaccinees were obtained by a two-level linear regression model. Statistically significant p-values of the difference in the predicted means between consecutive times of examination in the same IgM-S group and between IgM-S groups at the same time of examination are reported in panels a and b.

Italy and by The Brain Research Foundation Verona. The funding source had no role in the development of this study.

Results

Development of IgM-S is associated with higher neutralizing activity in naïve vaccinees

We initially tested the neutralizing activity against SARS-CoV-2 of sera from IN (n = 48) and PI (n = 50) vaccinees, in a cohort described in our previous study[14] collected at the time of first vaccine dose (To), at the second dose (T1) and 3 weeks after the second dose (T2). Among IN vaccinees, IgM-S were detected in 35/48 (72.9%) after the two vaccine doses (IgM-S^{POS}) while the remaining 13/48 (27.1%) had undetectable IgM-S (IgM-S^{NEG}) (Figure 1a and c). IgM-S^{POS} IN vaccinees had higher neutralizing activity than IgM-S^{NEG} IN vaccinees (blue dots) at T2 (p = 0.008).

Among PI vaccinees, 22/50 (44.0%) had undetectable IgM-S while the remaining 28/50 (56.0%) resulted positive at any of the timepoints. No significant differences in neutralization activity were observed when comparing the two groups of PI vaccines at each timepoint (Figure 1b and d). This first set of data on a limited number of vaccinees confirmed our previous observation of the absence of detectable IgM-S in a significant fraction of IN vaccinees and expanded on the association of IgM-S responses with higher serum neutralizing activity.

IgM-S development following BNT162b2 vaccine

We further tested these initial observations on a larger cohort of 1989 HCW who had been vaccinated with two doses of BNT162b2 vaccine (Figure 2 depicts a flowchart of the patients' groups that were analysed in this study). The study included longitudinal samples collected at the day the first dose of vaccine was administered (To), at the second dose (3 weeks after the first one, T1) and 3 weeks after the second dose (T2). Among those 1989 subjects, complete information (IgG-S, IgM-S and IgG-N at To, T1 and T2) was available for 1957 vaccinees. Vaccinees with negative swab and no infection history but positive serology at To (n = 84) were considered as false negatives and were not included in this analysis. Of the evaluable 1873 patients, 289 were previously infected (PI), with a history of SARS-CoV-2 infection documented by a positive swab test; 1584 were immunologically naïve (IN) with no documented history of infection, negative swab test and negative serology (IgM-S, IgG-S and IgG-N) at To. For all these patients we had access to serum samples that were used to quantify IgG-S(RBD) as proxy of neutralization activity.[19] We divided the two initial groups (PI and IN) into four sub-groups, according to the time of IgM-S positivity: (a) IgM-S never detected (IgM-S^{NEG}); (b) IgM-S detected before the first vaccine dose (IgM-S$^{POS}{}_{T0}$); (c) IgM-S detected after the first vaccine dose (IgM-S$^{POS}{}_{T1}$); (d) IgM-S detected after the second vaccine dose (IgM-S$^{POS}{}_{T2}$). We further explored whether the development of IgM-S before, after or at the same time of IgG-S could reflect a gain in the load of IgG-S thus providing a putative proxy of protection from future infections in IN or PI.

IgM-S serotyping identifies three patterns of responses in naïve vaccinees

Of the 1584 IN vaccinees, 1011 (63.8%) developed both IgM-S and IgG-S (IgM-S^{POS}), 572 (36.1%) developed IgG-S but not IgM-S (IgM-S^{NEG}), none had IgM-S but

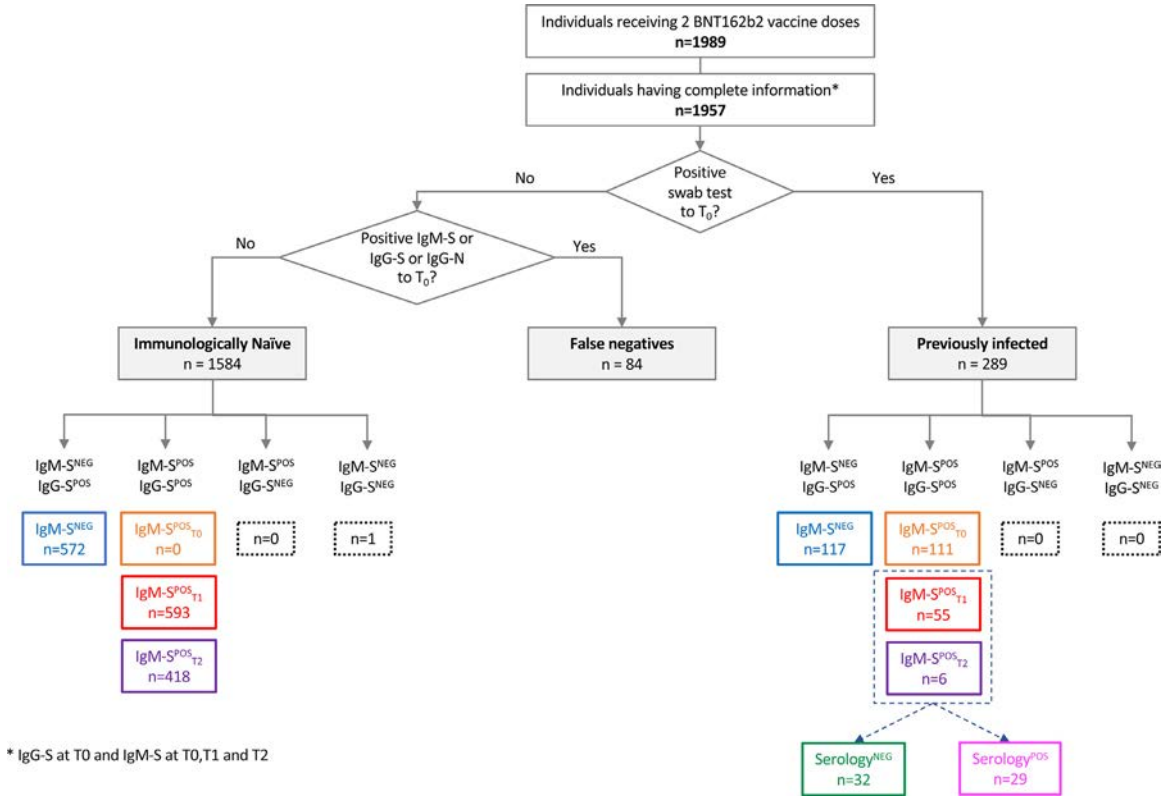

Figure 2. Study population.

Classification and distribution of the different types of IgM-S and IgG-S responses in naïve and previously infected subjects who received the BNT162b2 vaccine. NEG: negative; POS: positive.

not IgG-S and only one (0.1%) was negative for both isotypes (Figure 2). Among the 1011 IgM-S^{POS} vaccinees, 593 (58.7%) developed both IgG-S and IgM-S at T1 (IgM-$S^{POS}{}_{T1}$), 418 (41.3%) developed IgG-S at T1 and IgM-S at T2 (IgM-$S^{POS}{}_{T2}$). Among the 572 IgM-S^{NEG} vaccinees (excluding the single subject who did not elicit IgG-S), 550 (96.2%) developed IgG-S at T1 and the rest (n = 22, 3.8%) at T2 (Figs. 3 and 4a). All vaccinees who were IgM-S positive at T1 were also IgG-S positive at the same time point (Figure 3). Only eight vaccinees with undetectable IgM-S/IgG-S at T1 (Figure 3, row IgM-$S^{POS}{}_{T2}$, column T1) became positive for both at T2. Therefore, the patterns of IgM-S/IgG-S responses can be interpreted as follows: (a) IgM-S negative (IgM-S^{NEG}, 572/1584, 36.1%, blue dots in Figs. 3 and 4), (b) IgG-S/IgM-S coordinated (IgM-$S^{POS}{}_{T1}$, 593/1584, 37.4%, red dots in Figs. 3 and 4); and (c) IgM-S delayed responses (IgM-$S^{POS}{}_{T2}$, 418/1584, 26.4%, purple dots in Figs. 3 and 4). We defined as coordinated (pattern b) the IgG-S and IgM-S responses that appeared in the same time window regardless of whether IgM-S appeared before or at the same time of IgG-S, a pattern that can be considered a canonical primary antibody response. Conversely, patterns (a) and (c) can be considered as non-canonical.

In Figure 4b and c, the IgM-$S^{POS}{}_{T1}$ (red dots) group had statistically significantly higher IgG-S levels than groups IgM-S^{NEG} (blue dots) and IgM-$S^{POS}{}_{T2}$ (purple dots) after both the first ($p < 0.001$) and the second ($p < 0.001$) vaccines dose. Thus, of the three groups of vaccinees identified in our analysis, the IgM-S/IgG-S coordinated group (IgM-$S^{POS}{}_{T1}$) displayed a more efficient response to the vaccine, at least as measured by the levels of IgG-S antibodies elicited by the first and second vaccine dose. Of note, IN vaccinees who displayed the delayed IgM-S pattern (IgM-$S^{POS}{}_{T2}$) were older (median 47 years) and had a higher frequency of males (43%) than the other two groups (Table 1). In all subgroups, we also observed a statistically significant lower IgG-S antibody response with increasing age (difference in ln IgG-S for one-year increase of age = -0.015, $p < 0.001$) and a higher IgG-S response in females (difference in ln IgG-S between females and males = 0.1, $p = 0.007$).

Finally, 28 (1.8%) and 2 (0.1%) IN vaccinees became positive for IgG-N at T1 and T2, respectively (Supplementary Fig. 1). Because the nucleocapsid protein is not present in the BNT162b2 vaccine, these vaccinees most likely were infected during vaccination. The proportion of IgG-N positive vaccinees was not statistically different

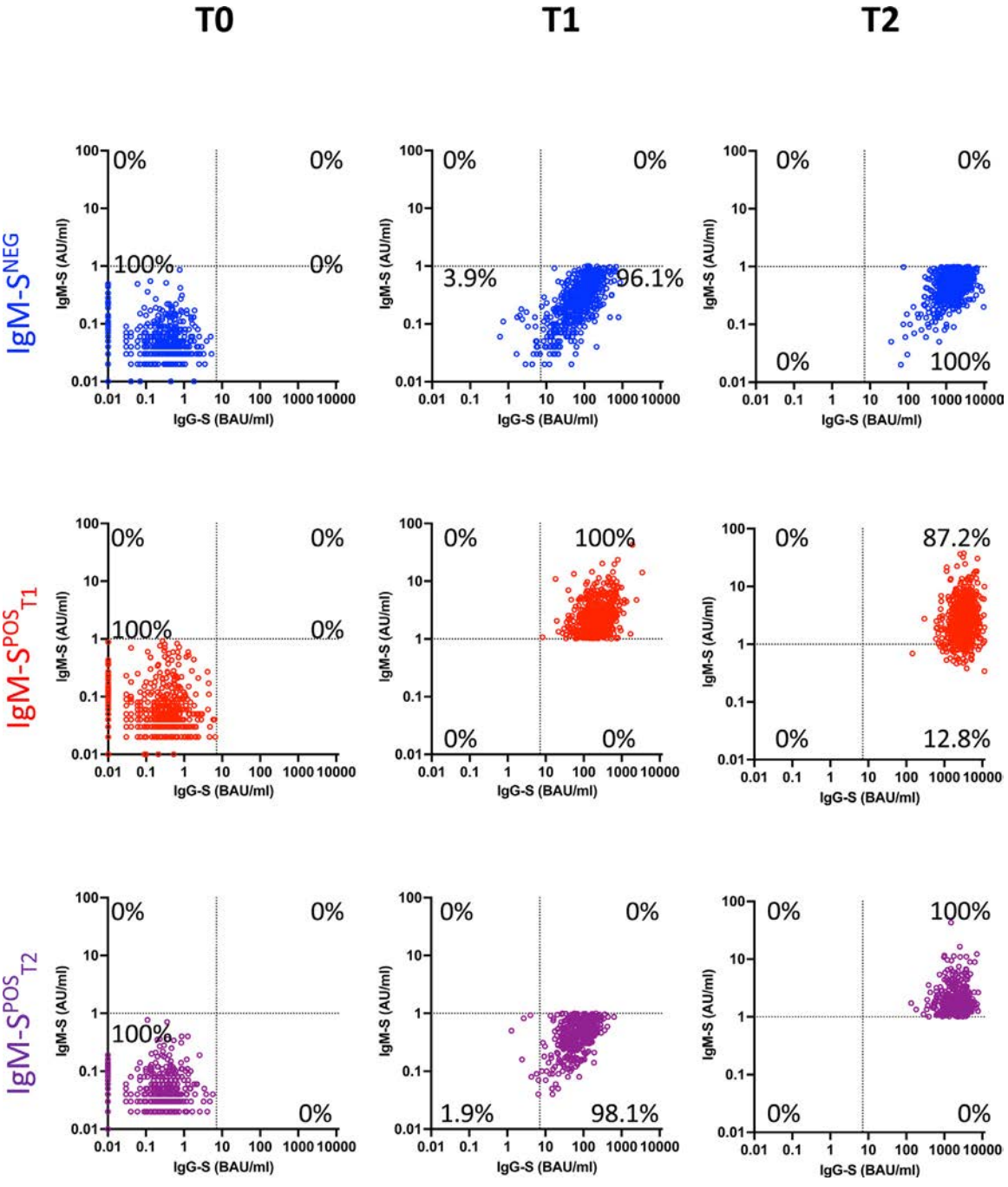

Figure 3. Development of IgM-S and IgG-S following vaccination.

Scatterplots of IgM-S (y axis) and IgG-S (x axis) measures in naïve vaccines according to time of examination (T0, T1 and T2) and time of IgM-S positivity (IgM-S^{NEG}, blue dots; IgM-$S^{POS}{}_{T1}$, red dots; IgM-$S^{POS}{}_{T2}$, purple dots).

in the three IN subgroups (IgM-S^{NEG}, IgM-$S^{POS}{}_{T1}$ and IgM-$S^{POS}{}_{T2}$; $p = 0.200$). We performed a sensitivity analysis by excluding IN vaccinees who became IgG-N positive at T1 or T2, and we observed the same results as in the main analysis ($p < 0.001$).

IgM-S and IgG-S responses in previously infected vaccinees

At T0, 117/289 (40.5%) PI vaccinees were IgM-S negative (IgM-S^{NEG}) and 172/289 (59.5%) were IgM positive (IgM-S^{POS}) (Figure 2). Of these, 111 (64.5%) were

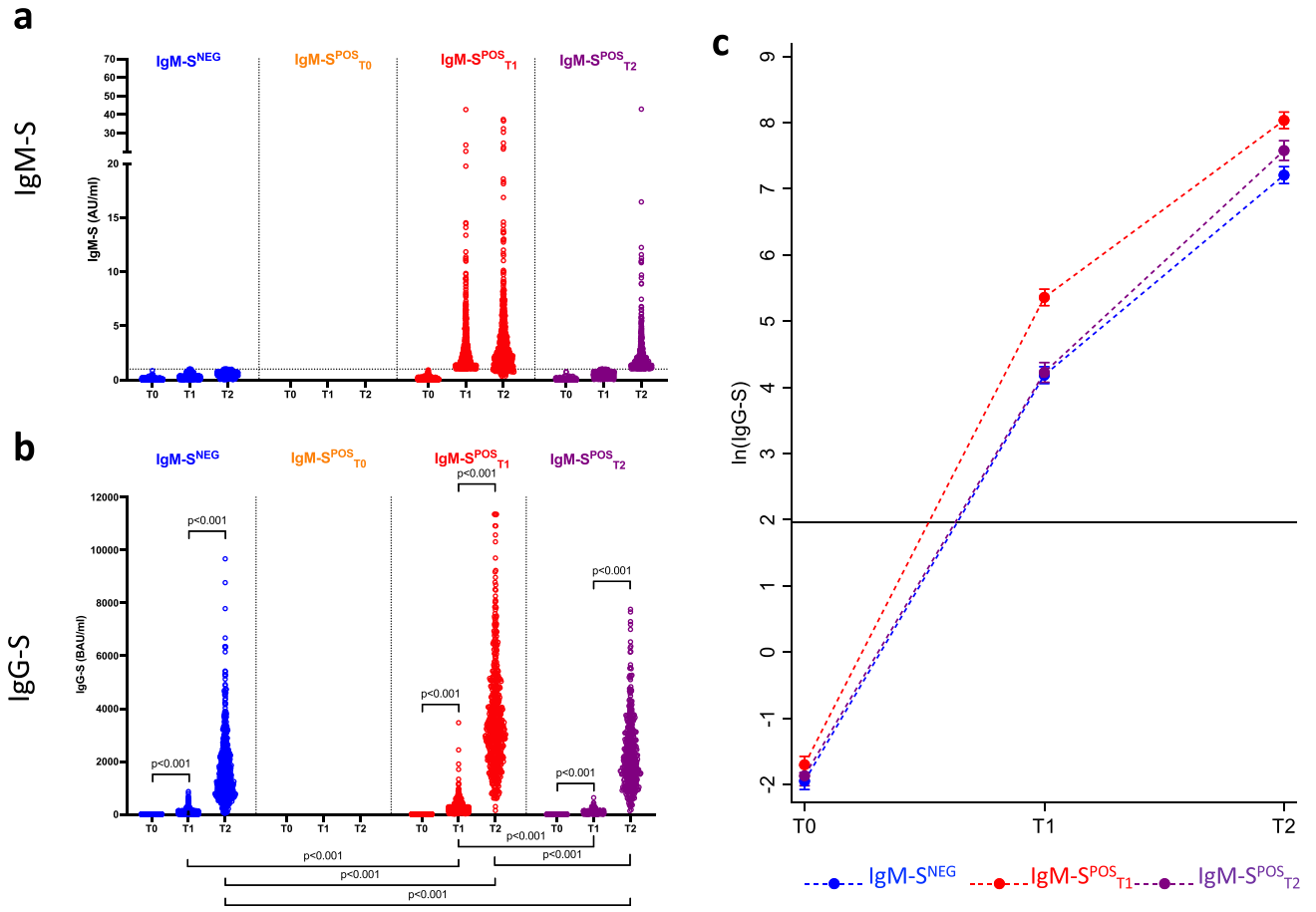

Figure 4. IgG-S response in naïve vaccinees.

IgM-S (panel a) and IgG-S (panel b) measures in naïve vaccinees according to time of examination (T0, T1 and T2) and time of IgM-S positivity (IgM-S^{NEG}, *n* = 572, blue dots; IgM-S^{POS}_{T1}, *n* = 593, red dots; IgM-S^{POS}_{T2}, *n* = 418, purple dots). Being all naïve subjects, no individuals had detectable IgM-S at T0. Predicted means of ln(IgG-S) measures (with the 95% confidence interval) according to time of examination and time of IgM-S positivity (panel c) were obtained by a two-level linear regression model. Statistically significant p-values of the difference in the predicted means between consecutive times of examination at the same time of IgM-S positivity and between different times of IgM-S positivity at the same time of examination are reported in panel b. The horizontal lines indicate the cut-off value to discriminate positive and negative samples for each assay.

	IgM-S^{NEG} (n = 572)	IgM-S$^{POS}_{T0}$ (n = 0)	IgM-S$^{POS}_{T1}$ (n = 593)	IgM-S$^{POS}_{T2}$ (n = 418)	p-value
Age at T0, median	45	-	42	47	<0.001 (Kruskal-Wallis rank test)
Female, % (vs male)	66.4	-	65.1	56.9	<0.001 (Fisher's Exact test)

***Table 1*: Comparison of the main characteristics among the four IgM-S subgroups of naïve subjects.**

positive at T0 (IgM-S$^{POS}_{T0}$), 55 (32.0%) at T1 (IgM-S$^{POS}_{T1}$), and 6 (3.5%) at T2 (IgM-S$^{POS}_{T2}$) (Figure 2). Among IgM-S$^{POS}_{T0}$ vaccinees, 24/111 (21.6%) and 87/111 (78.4%) had been infected during the first and second wave of the pandemic in Italy, respectively. The IgG-S levels significantly increased after both the first ($p < 0.001$) and second doses ($p = 0.002$) in all PI subgroups, except for IgM-S$^{POS}_{T0}$ individuals for whom the second dose did not significantly improve IgG-S levels as compared to the first vaccine dose (p-value=0.49) (Figure 5b). There were no significant differences of IgG-S levels between PI subgroups after the second vaccine dose (Figure 5b and c). The fact that IgM-S$^{POS}_{T2}$ vaccinees reached IgG-S levels similar to the other groups only after the second dose of vaccine (Figure 5c) suggests that in these subjects a single dose of vaccine induces suboptimal antibody levels.

Among the PI vaccinees who developed IgM-S after the first and second vaccine dose (55 IgM-S$^{POS}_{T1}$ and 6 IgM-S$^{POS}_{T2}$), 29 had undetectable IgM-S but were IgG-S and/or IgG-N positive at T0 and were classified as serology positive (Serology^{POS}), whereas 32 were negative at T0 for IgM-S, IgG-S and IgG-N and were therefore classified as serology negative (Serology^{NEG}) (Figure 2). Comparison of the IgG-S levels elicited by the first and second dose of vaccine in these two groups revealed a faster and stronger IgG-S response in PI vaccinees classified as serology positive ($p < 0.001$) (Figure 6a). Next, we compared the two groups with the 1584 IN vaccinees and with the subgroup of PI vaccinees (PI*), from which the Serology^{NEG} and Serology^{POS} PI vaccinees were excluded (Figure 2). Serology^{NEG} vaccinees were different from PI* vaccinees at all time points ($p < 0.001$) but similar to IN (except at T1, $p = 0.011$), while Serology^{POS} were different from IN ($p < 0.001$ at T0 and T1, $p = 0.007$ at T2), and similar to PI* (Figure 6b). Thus, these data revealed the presence among PI vaccinees of subjects (Serology^{NEG}) who displayed a naÿve serological profile and responded to vaccination with a coordinated IgM-S/IgG-S pattern similar to that of a primary response. Of note, these vaccinees were generally younger, had been mostly infected during the second wave and were mostly asymptomatic. In contrast, Serology^{POS} PI vaccinees were generally older, had a slightly higher frequency of males, were mostly infected during the first wave, and reported symptomatic COVID-19 (Table 2).

The majority of Serology^{POS} subjects (18/29) had IgG-N at T0. The remaining where IgG-S positive. Serology^{NEG} subjects, on the contrary, did not present IgG-N at T0, which instead appeared at T1 in as many as 11/32 (34%) subjects (Supplementary Fig. 2). In IN subjects, however, we observed only 28/1584 subjects (1.8%) positive for IgG-N at T1 (Supplementary Fig. 1a).

Together these data defined three patterns of IgM-S responses in PI vaccinees (Figure 5): (a) negative IgM-S (IgM-S^{NEG}) (b) persistent IgM-S (IgM-S$^{POS}_{T0}$) and (c) delayed IgM-S (IgM-S detected at T1, IgM-S$^{POS}_{T1}$ or at T2, IgM-S$^{POS}_{T2}$). Pattern (a) was consistent with that of a canonical anamnestic response after the natural decay of IgM-S that follows infection. Pattern (b) was observed in 21.6% of PI vaccinees who had been infected almost one year before vaccination and it was someway unexpected since IgM responses are usually short lived. There are however reports on the persistence of long-lived memory IgM B cells in other viral infections including influenza.[20–23] Pattern (c) revealed a proportion of PI vaccinees who may had experienced only a transient infection which was not sufficient to induce a fully matured class-switched response and responded to vaccination with a pattern typical of a primary response.

IgM response in naïve subjects vaccinated with Vaxzevria and Spikevax vaccines

We analysed a limited numbers of available naÿve individuals vaccinated with the Vaxzevria (Astra Zeneca) and with the Spikevax (Moderna) vaccines. Among the 37 subjects vaccinated with Vaxzevria, all developed IgG-S following vaccination, but only 6 (16.2%) had detectable IgM-S (Table 3). Similarly, among the 15 subjects vaccinated with Spikevax, all elicited IgG-S and only 2 also had evidence of detectable IgM-S (13.3%), thus confirming, in albeit smaller numbers, a consistently non-canonical IgM response in other types of vaccinations as well.

Discussion

The serological response to vaccination shows a relatively rapid decay as observed in natural infection/immunization.[24,25] The extent of this decay is so pronounced that the vaccine efficacy itself has been questioned and a booster dose of BNT162b2 vaccine has been recently authorized by FDA. In this context, it is of paramount importance to gain further information on the patterns of antibody responses that are associated to protective immunity. Most studies have concentrated the attention on IgG responses, while a few have

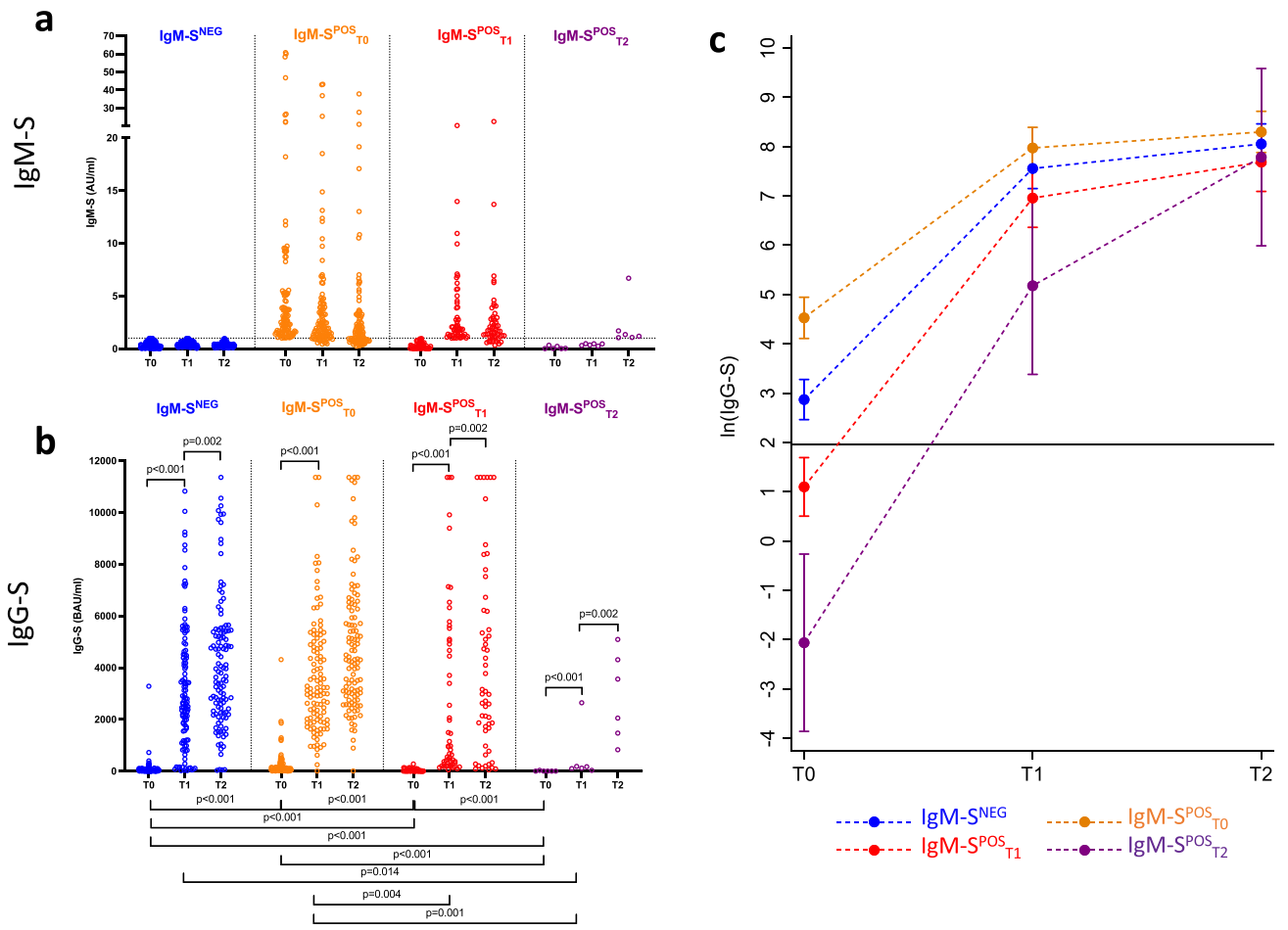

Figure 5. IgG-S response in previously infected vaccinees.

IgM-S (panel a) and IgG-S (panel b) measures in previously infected vaccinees according to time of examination (T0, T1 and T2) and time of IgM-S positivity (IgM-S^{NEG}, *n* = 117, blue dots; IgM-S^{POS}_{T0}, *n* = 111, orange dots; IgM-S^{POS}_{T1}, *n* = 55, red dots; IgM-S^{POS}_{T2}, *n* = 6, purple dots). Predicted means of ln(IgG-S) measures (with the 95% confidence interval) according to time of examination and time of IgM-S positivity (panel c) were obtained by a two-level linear regression model. Statistically significant p-values of the difference in the predicted means between consecutive times of examination at the same time of IgM-S positivity and between different times of IgM-S positivity at the same time of examination are reported in panel b. The horizontal lines indicate the cut-off value to discriminate positive and negative samples for each assay.

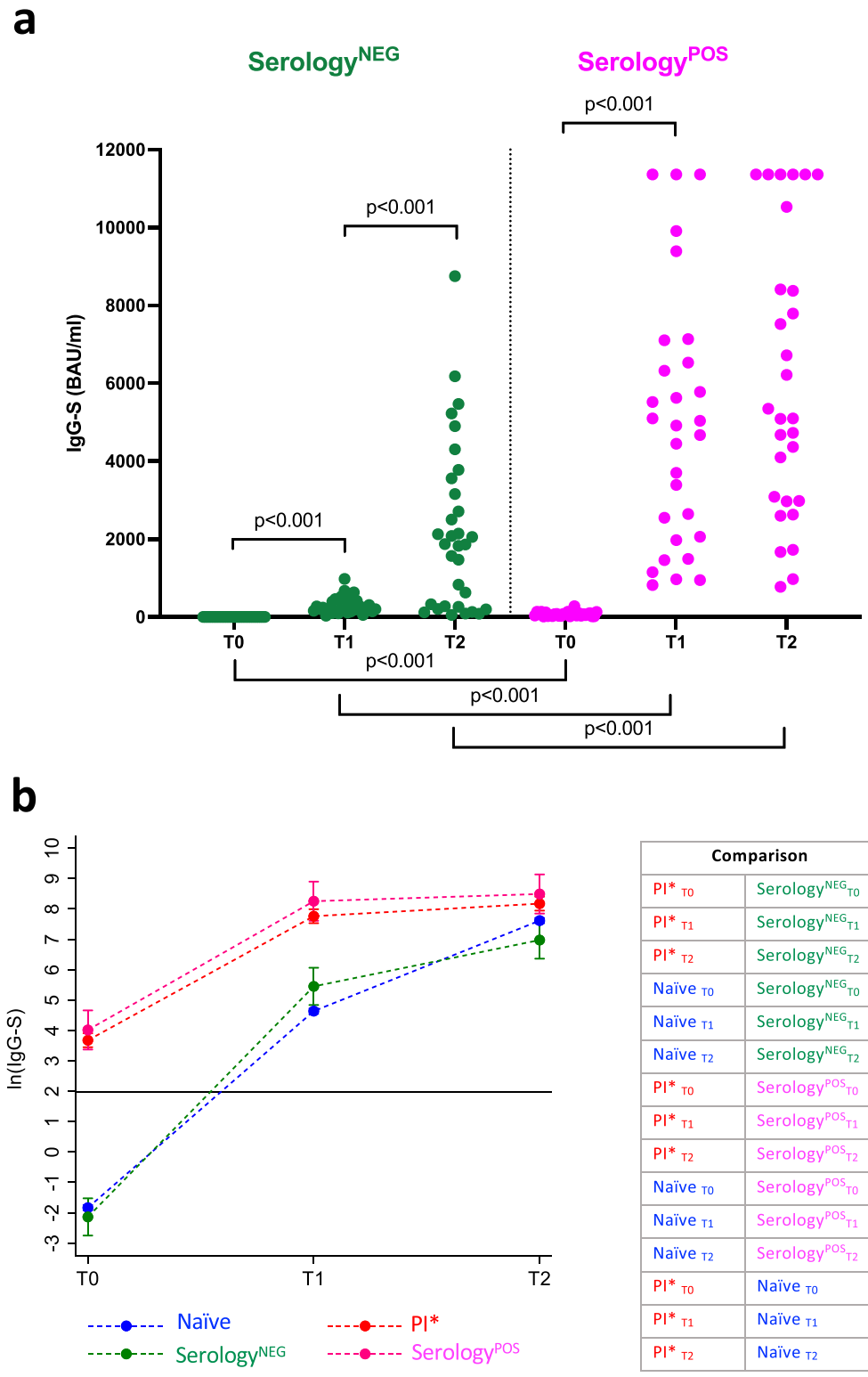

Comparison		p-value
PI* $_{T0}$	Serology$^{NEG}{}_{T0}$	p<0.001
PI* $_{T1}$	Serology$^{NEG}{}_{T1}$	p<0.001
PI* $_{T2}$	Serology$^{NEG}{}_{T2}$	p<0.001
Naïve $_{T0}$	Serology$^{NEG}{}_{T0}$	ns
Naïve $_{T1}$	Serology$^{NEG}{}_{T1}$	p=0.011
Naïve $_{T2}$	Serology$^{NEG}{}_{T2}$	ns
PI* $_{T0}$	Serology$^{POS}{}_{T0}$	ns
PI* $_{T1}$	Serology$^{POS}{}_{T1}$	ns
PI* $_{T2}$	Serology$^{POS}{}_{T2}$	ns
Naïve $_{T0}$	Serology$^{POS}{}_{T0}$	p<0.001
Naïve $_{T1}$	Serology$^{POS}{}_{T1}$	p<0.001
Naïve $_{T2}$	Serology$^{POS}{}_{T2}$	p=0.007
PI* $_{T0}$	Naïve $_{T0}$	p<0.001
PI* $_{T1}$	Naïve $_{T1}$	p<0.001
PI* $_{T2}$	Naïve $_{T2}$	p<0.001

Figure 6. IgG-S response in previously infected vaccinees producing IgM-S.

IgG-S measures (panel a) in previously infected vaccinees who produced IgM-S at T1 or at T2 following BNT162b2 vaccination according to time of examination (T0, T1 and T2) and negative or positive serology at T0 (Serology^{NEG}, *n* = 32, green dots; Serology^{POS}, *n* = 29 magenta dots). Predicted means of ln(IgG-S) measures (with the 95% confidence interval) according to time of

	IgM-S^{NEG} (n = 117)	IgM-S$^{POS}_{T0}$ (n = 111)	IgM-S$^{POS}_{T1}$ (n = 55)$_1$	IgM-S$^{POS}_{T2}$ (n = 6)	p-value
Age, median	43.0	47.0	46.0	35	0.219 (Kruskal-Wallis rank test)
Female, % (vs male)	70.9	62.2	56.4	33.3	0.086 (Fisher's exact test)
2nd wave, % (vs 1st wave)	44.4	78.4	65.5	66.7	<0.001 (Fisher's exact test)
Symptoms, % (vs no symptoms)	80.3	88.3	70.4	50	0.008 (Fisher's exact test)

***Table 2*: Comparison of the main characteristics among the four IgM-S subgroups of previously infected subjects.**

	IgM-S^{NEG}	IgM-S^{POS}	Total
BNT162b2 -Pfizer/BionTech	573 (36.2%)	1011 (63.8%)	1584
Vaxzevria-AstraZeneca	31 (83.8%)	6 (16.2%)	37
Spikevax-Moderna	13 (86.7%)	2 (13.3%)	15

***Table 3*: IgM-S and IgG-S development following the two doses vaccination with BNT162b2, Vaxveria and Spikevax vaccines.**

addressed the role of IgM in virus neutralization. One such study[26] reported that in adults recovered from mild COVID-19, while IgG were maintained for long periods of time, the neutralization capacity decayed more rapidly and was most strongly associated with anti-S trimer IgM. Prevost et al.[27] also reported that the virus neutralization capacity decreases significantly 6 weeks after the onset of symptoms, following a similar trend as anti-RBD IgM and found a stronger correlation with neutralization for IgM than IgG and IgA, suggesting that at least part of the neutralizing activity is mediated by IgM. There are limited data on the kinetic of appearance of IgM after vaccination and its association with virus neutralizing activity.[16]

Here we report that following BNT162b2 vaccination, higher neutralization activity correlates with the presence of both IgG-S and IgM-S in IN vaccinees, suggesting that IgM-S may contribute to protective immunity. On the other hand, we found that 36.1% of IN vaccinees responded to vaccination with IgG-S but not IgM-S. In addition, in vaccinees who responded with both isotypes, 41.3% developed IgM-S after IgG-S. Of note, of the three isotype patterns that we identified, only that with coordinated IgM-S/IgG-S responses, could be considered as a bona fide primary immune response pattern but it was represented in only 37.4% vaccine recipients while the others were either IgM-S negative (36.1%) or developed IgM-S after IgG-S (26.4%). More importantly, vaccinees exhibiting IgG-S without IgM-S or IgM-S after IgG-S had significantly lower IgG-S levels compared to those with coordinated IgM-S/IgG-S responses; this suggests that coordinated IgM-S/IgG-S responses are associated with increased immunity. Also, in the small group of HCW who received the adenovirus-based vaccine Vaxzevria (Astra Zeneca) or the RNA vaccine Spikevax (Moderna), as many as 80% did not develop IgM-S after vaccination. Thus, the unconventional isotype pattern follows SARS-CoV-2 spike vaccination regardless of the type of vaccine used.

Taken together our data suggest that vaccination elicits either a canonical primary response with coordinated IgM-S/IgG-S, associated with higher levels of IgG-S antibodies, or a non-canonical IgM-S negative response. We propose that these non-canonical responses may leverage on pre-existing immunity to cross-reactive human coronaviruses, or even both types of responses where the first to appear is the anamnestic cross-reactive response[28,29] followed by the later appearance of IgM after recruitment of naÿve B cells specific to SARS-CoV-2 epitopes.

There is accumulating evidence that the immune response to SARS-CoV-2 is influenced by cross-coronavirus immunity, with some data pointing to the risk of immunopathogenic responses due to low affinity cross-reactive antibodies generated by an original antigenic sin[30] and other data pointing to a potential protective role of cross-reactive antibodies. Chaudhury et al. recently reported[12] that the IgM response is highly specific for SARS-CoV-2, while the IgG response is more cross-reactive. The same authors hypothesize that the IgM response is naÿve-derived, while the IgG response is memory-derived, thus explaining the simultaneous appearance of IgM and IgG. Furthermore, Kaplonek et al. recently reported[13] the near simultaneous evolution of IgG and IgM specific for the S2 subunit of SARS-CoV-2 spike at

examination in (i) previously infected subjects who did not elicit IgM-S or had IgM-S at T0 (PI*, red line), (ii) subjects who did not have detectable IgM-S at T0 but produced them at T1 or at T2 following vaccination, and who had detectable IgG-S and/or IgG-N at T0 (Serology^{POS}, magenta line), (iii) subjects as the previous ones, but with negative serology at T0 (Serology^{NEG}, green line), and (iv) naïve vaccinees (blue line) (panel B) were obtained by a two-level linear regression model. For Serology^{NEG} and Serology^{POS} subjects, statistically significant p-values of the difference in the predicted means between consecutive times of examination in the same subject group and between different subject groups at the same time of examination are reported in panel b. For all four group of subjects, statistically significant p-values of the difference in the predicted means between different groups of subjects at the same time of examination are reported in panel b table. The horizontal lines indicate the cut-off value to discriminate positive and negative samples for each assay.

early time points in a cohort of COVID-19 survivors and proposed that it could be a reflection of expansion of pre-existing cross-coronavirus immunity to the conserved S2-domain. Furthermore, there is evidence that SARS-CoV-2 infection reactivates hCoVs-specific memory B cells[29,31] concomitantly with the recruitment of SARS-CoV-2 naÿve B cells and the appearance of virus-neutralizing antibodies specific for the RBD of the SARS-CoV-2 Spike protein. Our observation of IgM-S/IgG-S isotype patterns consistent with those of an anamnestic response following vaccination of naÿve individuals is highly suggestive of the recruitment by the vaccine of cross-coronavirus immunity. Whether this would reflect in higher or lower vaccine efficacy remains speculative. However, the established safety of current SARS-CoV-2 vaccines with few signals of immunopathogenic events suggest that cross-coronavirus immunity may play, if any, a protective rather than a pathogenic role following vaccination.

The IgM-S response to vaccination of PI vaccinees also displayed some interesting features. Of the subgroup of PI vaccinees who were IgM-S positive at baseline, 21.6% had been infected during the first pandemic wave in Italy, almost one year before vaccination. While the persistence of IgM-S in these subjects was unexpected, there are reports that IgM antibodies may persist for long period of times after natural infection owing to the persistence of long-lived memory IgM positive B cells.[21,22] Our data suggest that at least a subset of PI vaccinees developed these types of long-lived IgM responses. Of note, the presence of IgM-S before vaccination was associated to the most rapid kinetic of IgG-S responses when compared to those of vaccinees who were either IgM-S negative or had a delayed IgM-S response.

Unexpectedly, we observed a group of PI vaccinees who elicited IgM-S following vaccination. Among them, a subgroup classified as serology negative at baseline (Serology^{NEG}) showed an IgG-S response similar to that of IN vaccinees. These subjects may therefore have had a false-positive swab result. Of these, a consistent fraction (34%) displayed IgG-N after vaccination, suggestive of an infection event. However, in our cohort, only 1.8% of truly IN subjects showed evidence of infection (IgG-N positivity), providing a crude estimate of the occurrence of infection during the vaccination schedule. We speculate that the serology negative vaccinees who became IgG-N positive after vaccination may have experienced a recall response to cross reactive N epitopes similar to that reported in a study by Dobaño et al.,[32] which suggests that anti-N antibodies may be produced following spike-based vaccines resulting from a cross-reactive response.

This observation deserves further investigation because it suggests that not all individuals with a previous history of SARS-CoV-2 infection develop an immunological memory sufficient to ensure a rapid class-switched response to a single dose of vaccine.

While the correlates of protection from SARS-CoV-2 infection have not yet been fully established, it is generally accepted that antibody-mediated neutralization of the virus is a key determinant.[33] Assessing the presence of IgM before and after vaccination may therefore provide useful information on vaccine efficacy and, to some extent, guide decisions on the vaccine regimens in previously infected persons or in IgM non responder individuals. The combined examination of all three branches of adaptive immunity at the level of SARS-CoV-2-specific CD4+ and CD8+ T cell, as well as neutralizing antibody responses in COVID-19 patients, provided evidence that coordinated CD4+ T cell, CD8+ T cell, and antibody responses are protective, but uncoordinated responses may fail to control disease.[34] Thus, while antibodies still represent the strongest correlate of immunity, it is plausible that coordinated T and B cell responses are needed to confer protection. In this context, studies assessing the expression of the different antibody isotypes may provide useful insights for the understanding of protective immunity in both natural infection and vaccination.

This study presents some limitations. Due to limited amount of serum samples collected, we could not determine which specific antibody subclasses correlates with neutralization. For the same reason, we did not address the fine specificity of IgG and IgM antibodies. Therefore, we cannot conclude on a potential priming effect of previous exposures to common human coronaviruses on the response to vaccination. Furthermore, we did not have access to cellular samples, and we could not determine the effect of the pre-existing cellular immunity on the development of the humoral response, following vaccination. The sensitivity of the assays detecting IgM-S and IgG-S could also be argued to be an issue, even though the assays that we used are fully validated and routinely used for clinical screening.[35,36] It must be noted that the assays we used for IgG and IgM quantification is designed to measure Spike S1-specific immunoglobulins, and does not allow the detection of IgG and IgM against other epitopes. Finally, this study focuses on the humoral response within the first weeks following vaccination and a longer follow up is needed to confirm the current observations.

Declaration of interests

The authors declare no competing interests.

Contributors

A.R., D.Z., A.B., L.L. conceived the paper design, analysed and discussed data and wrote the manuscript; C. P. and Z.B. designed the study, enrolled patients, collected and managed clinical data; L.C. and Sim. A. performed statistical analysis; M.T.V., L.D.C., G.S., Ni. Te., and AMSLV collected samples and clinical data for Vaxveria and Spikevax vaccines; Sil. A. and M.P. performed pseudovirus neutralization assays; Na. Ti., S.S.L. and T. F. participated in data collection and analysis. All

authors read, critically revised, and approved the manuscript. D.Z., A.R., L.C., Sim. A. and C.P. have verified the underlying data.

Acknowledgments

We acknowledge the generous contribution of our health-care worker's colleagues, whose sera samples were essential to this study. We thank Dr. Stefania Tremolada for assistance in bleeding subjects vaccinated with Vaxzevria and Spikevax.

Data sharing statement

Raw data are available upon request.

Funding

Italian Ministry of Health under "Fondi Ricerca Corrente"- L1P5 and "Progetto Ricerca Finalizzata COVID-2020-12371675"; FUR 2020 Department of Excellence 2018-2022, MIUR, Italy; The Brain Research Foundation Verona.

Supplementary materials

Supplementary material associated with this article can be found in the online version at doi:10.1016/j.ebiom.2022.103888.

References

1 Krammer F, Srivastava K, Alshammary H, et al. Antibody responses in seropositive persons after a single dose of SARS-CoV-2 mRNA vaccine. *N Engl J Med*. 2021;384(14):1372–1374.
2 Li K, Huang B, Wu M, et al. Dynamic changes in anti-SARS-CoV-2 antibodies during SARS-CoV-2 infection and recovery from COVID-19. *Nat Commun*. 2020;11(1):6044.
3 Gong S, Ruprecht RM. Immunoglobulin M: an ancient antiviral weapon – rediscovered. *Front Immunol*. 2020;11(1943).
4 Jin Y, Wang M, Zuo Z, et al. Diagnostic value and dynamic variance of serum antibody in coronavirus disease 2019. *Int J Infect Dis*. 2020;94:49–52.
5 Long QX, Liu BZ, Deng HJ, et al. Antibody responses to SARS-CoV-2 in patients with COVID-19. *Nat Med*. 2020;26(6):845–848.
6 Liu X, Wang J, Xu X. Patterns of IgG and IgM antibody response in COVID-19 patients. *Emerg Microbes Infect*. 2020;9(1):1269–1274.
7 Al-Jighefee HT, Yassine HM, Nasrallah GK. Evaluation of antibody response in symptomatic and asymptomatic COVID-19 patients and diagnostic assessment of new IgM/IgG ELISA kits. *Pathogens*.. 2021;10(2).
8 Xu X, Sun J, Nie S, et al. Seroprevalence of immunoglobulin M and G antibodies against SARS-CoV-2 in China. *Nat Med*. 2020;26(8):1193–1195.
9 Pan Y, Li X, Yang G, et al. Serological immunochromatographic approach in diagnosis with SARS-CoV-2 infected COVID-19 patients. *J Infect*. 2020;81(1):e28–e32.
10 Qu J, Wu C, Li X, et al. Profile of Immunoglobulin G and IgM antibodies against severe acute respiratory syndrome coronavirus 2 (SARS-CoV-2). *Clin Infect Dis*. 2020;71(16):2255–2258.
11 Du Z, Zhu F, Guo F, Yang B, Wang T. Detection of antibodies against SARS-CoV-2 in patients with COVID-19. *J Med Virol*. 2020;92(10):1735–1738.
12 Chaudhury S, Hutter J, Bolton JS, et al. Serological profiles of pan-coronavirus-specific responses in COVID-19 patients using a multiplexed electro-chemiluminescence-based testing platform. *PLoS One*. 2021;16:(6) e0252628.
13 Kaplonek P, Wang C, Bartsch Y, et al. Early cross-coronavirus reactive signatures of humoral immunity against COVID-19. *Sci Immunol*. 2021;6(64):eabj2901.
14 Dalle Carbonare L, Valenti MT, Bisoffi Z, et al. Serology study after BTN162b2 vaccination in participants previously infected with SARS-CoV-2 in two different waves versus naÿve. *Commun Med*. 2021;1(1):38.
15 Gobbi F, Buonfrate D, Moro L, et al. Antibody response to the BNT162b2 mRNA COVID-19 vaccine in subjects with prior SARS-CoV-2 infection. *Viruses*. 2021;13(3):422.
16 Naaber P, Tserel L, Kangro K, et al. Dynamics of antibody response to BNT162b2 vaccine after six months: a longitudinal prospective study. *Lancet Reg Health Eur*. 2021;10: 100208.
17 Buonfrate D, Piubelli C, Gobbi F, et al. Antibody response induced by the BNT162b2 mRNA COVID-19 vaccine in a cohort of health-care workers, with or without prior SARS-CoV-2 infection: a prospective study. *Clin Microbiol Infect*. 2021;27(12):1845–1850.
18 Pizzato M, McCauley SM, Neagu MR, et al. Lv4 is a capsid-specific antiviral activity in human blood cells that restricts viruses of the SIVMAC/SIVSM/HIV-2 lineage prior to integration. *PLoS Pathog*. 2015;11:(7) e1005050.
19 Salazar E, Kuchipudi SV, Christensen PA, et al. Convalescent plasma anti-SARS-CoV-2 spike protein ectodomain and receptor-binding domain IgG correlate with virus neutralization. *J Clin Invest*. 2020;130(12):6728–6738.
20 Throsby M, van den Brink E, Jongeneelen M, et al. Heterosubtypic neutralizing monoclonal antibodies cross-protective against H5N1 and H1N1 recovered from human IgM+ memory B cells. *PLoS One*. 2008;3(12):e3942.
21 Bohannon C, Powers R, Satyabhama L, et al. Long-lived antigen-induced IgM plasma cells demonstrate somatic mutations and contribute to long-term protection. *Nat Commun*. 2016;7(1):11826.
22 Skountzou I, Satyabhama L, Stavropoulou A, et al. Influenza virus-specific neutralizing IgM antibodies persist for a lifetime. *Clin Vaccine Immunol*. 2014;21(11):1481–1489.
23 Auladell M, Jia X, Hensen L, et al. Recalling the future: immunological memory toward unpredictable influenza viruses. *Front Immunol*. 2019;10(1400):1400.
24 Vicenti I, Basso M, Gatti F, et al. Faster decay of neutralizing antibodies in never infected than previously infected healthcare workers three months after the second BNT162b2 mRNA COVID-19 vaccine dose. *Int J Infect Dis*. 2021;112:40–44.
25 Ibarrondo FJ, Hofmann C, Fulcher JA, et al. Primary, recall, and decay kinetics of SARS-CoV-2 vaccine antibody responses. *ACS Nano*. 2021.
26 Harrington WE, Trakhimets O, Andrade DV, et al. Rapid decline of neutralizing antibodies is associated with decay of IgM in adults recovered from mild COVID-19. *Cell Rep Med*. 2021;2:(4) 100253.
27 Prevost J, Gasser R, Beaudoin-Bussieres G, et al. Cross-sectional evaluation of humoral responses against SARS-CoV-2 spike. *Cell Rep Med*. 2020;1:(7) 100126.
28 Beretta A, Cranage M, Zipeto D. Is cross-reactive immunity triggering COVID-19 immunopathogenesis? *Front Immunol*. 2020;11:(2695) 567710.
29 Nguyen-Contant P, Embong AK, Kanagaiah P, et al. S protein-reactive IgG and memory B cell production after human SARS-CoV-2 infection includes broad reactivity to the S2 subunit. *mBio*. 2020;11(5). 2020.07.20.213298.
30 Vatti A, Monsalve DM, Pacheco Y, Chang C, Anaya JM, Gershwin ME. Original antigenic sin: a comprehensive review. *J Autoimmun*. 2017;83:12–21.
31 Song G, He WT, Callaghan S, et al. Cross-reactive serum and memory B-cell responses to spike protein in SARS-CoV-2 and endemic coronavirus infection. *Nat Commun*. 2021;12(1):2938.
32 Dobano C, Jimenez A, Rubio R, et al. Spike-based COVID-19 immunization increases antibodies to nucleocapsid antigen. *Transl Res*. 2022;240:26–32.
33 Khoury DS, Cromer D, Reynaldi A, et al. Neutralizing antibody levels are highly predictive of immune protection from symptomatic SARS-CoV-2 infection. *Nat Med*. 2021;27(7):1205–1211.
34 Rydyznski Moderbacher C, Ramirez SI, Dan JM, et al. Antigen-specific adaptive immunity to SARS-CoV-2 in acute COVID-19 and associations with age and disease severity. *Cell*. 2020;183(4):996–1012. e19.
35 Higgins V, Fabros A, Wang XY, Bhandari M, Daghfal DJ, Kulasingam V. Anti-SARS-CoV-2 IgM improves clinical sensitivity early in disease course. *Clin Biochem*. 2021;90:1–7.
36 Maine GN, Lao KM, Krishnan SM, et al. Longitudinal characterization of the IgM and IgG humoral response in symptomatic COVID-19 patients using the abbott architect. *J Clin Virol*. 2020;133: 104663.

life

MDPI

Review

HIV and SARS-CoV-2 Co-Infection: From Population Study Evidence to In Vitro Studies

Chiara Stefani [1,†], Tobia Fantoni [1,†], Michele Bissoli [1], Jordan Thomas [2,*] and Alessandra Ruggiero [1,*]

[1] Section of Biology and Genetics, Department of Neurosciences, Biomedicine and Movement Sciences, University of Verona, 37134 Verona, Italy
[2] Department of Clinical Infection, Microbiology and Immunology, Institute of Veterinary and Ecological Sciences, University of Liverpool, Liverpool L69 3BX, UK
* Correspondence: hljthom2@liverpool.ac.uk (J.T.); alessandra.ruggiero@univr.it (A.R.)
† These authors contributed equally to this work.

Abstract: Human immunodeficiency virus type 1 (HIV-1) and severe acute respiratory syndrome coronavirus 2 (SARS-CoV-2) have caused two major viral outbreaks during the last century. Two major aspects of HIV-1 and SARS-CoV-2 co-infection have been extensively investigated and deserve attention. First, the impact of the co-infection on the progression of disease caused by HIV-1 or SARS-CoV-2. Second, the impact of the HIV-1 anti-retroviral treatment on SARS-CoV-2 infection. In this review, we aim to summarize and discuss the works produced since the beginning of the SARS-CoV-2 pandemic ranging from clinical studies to in vitro experiments in the context of co-infection and drug development.

Keywords: HIV-1; SARS-CoV-2; co-infections; anti-retroviral drugs

Citation: Stefani, C.; Fantoni, T.; Bissoli, M.; Thomas, J.; Ruggiero, A. HIV and SARS-CoV-2 Co-Infection: From Population Study Evidence to In Vitro Studies. *Life* **2022**, *12*, 2089. https://doi.org/10.3390/life12122089

Academic Editor: Julien Van Grevenynghe

Received: 10 November 2022
Accepted: 8 December 2022
Published: 13 December 2022

1. Introduction

Human immunodeficiency virus type 1 (HIV-1) and severe acute respiratory syndrome coronavirus 2 (SARS-CoV-2) are two of the most impactful viral outbreaks of the past century. Both outbreaks have caused substantial global mortality as well as significant and far reaching social and economic consequences.

HIV-1 and SARS-CoV-2 are RNA viruses that induce an excessive inflammatory status with a high risk of mortality, albeit with a different magnitude between the two viruses, for vulnerable individuals, including the elderly, newborns, pregnant women and immunocompromised subjects [1,2]. The pathogenesis of the two viruses is on opposite fronts: HIV-1 targets the cells of the immune system with an initial latent infection that induces the progressive depletion of CD4+ T lymphocytes, thus compromising the coordination of the immune system. This results in acquired immunodeficiency syndrome (AIDS) if the infection is not treated in time. On the other hand, SARS-CoV-2 induces predominantly acute infections of respiratory tract tissues, resulting in the development of pneumonia and acute respiratory distress syndrome (ARDS) in the most severe cases [3]. The main characteristics of the two examined viruses are reported in Table 1.

1.1. Human Immunodeficiency Virus-1 (HIV-1)

HIV-1 belongs to the *Retroviridae* family, a group of viruses characterized by their ability to convert their RNA genome into double-stranded DNA through their retro-transcribing polymerase [4]. The primary target cells of HIV-1—CD4+ T lymphocytes—are essential participants in cell-mediated adaptive immune responses.

HIV-1 gp120 protein binds the CD4 receptor and one of the co-receptors (CCR5/CXCR4) on the target cell, facilitating virus and cell membrane fusion and subsequent entry into the target cell, starting the process of reverse transcription and integration into the host

DNA [4]. HIV-1 infection begins with an acute phase, initiated within the first week following infection, during which the patient presents flu-like symptoms and high viremia, with substantial depletion of memory T cells in gut-associated T lymphoid tissue (GALT) and lymph nodes. After this acute phase, the viremia reaches a set point and the chronic infection is initiated, resulting in the progressive loss of T helper lymphocytes [5]. The patient reaches AIDS when the CD4+ T cells count is less than 200 cell/mm^3 in the blood. AIDS is characterized by recurring opportunistic infections that can lead to the patient's death [6]. Up to now, the only treatment available to limit HIV infection is the use of anti-retroviral drugs, molecules that can inhibit different HIV life-cycle steps, entry inhibitors (prevent membrane fusion and HIV entry, such as CCR5 inhibitors), the reverse-transcriptase inhibitors (block the reverse transcriptase process, such as nucleotide/nucleoside or non-nucleotide/nucleoside inhibitors), integrase inhibitors and protease inhibitors (prevent HIV genome integration and HIV protein cleavage) [7]. Combination anti-retroviral therapy (cART) prevents the emergence of drug resistance within HIV infected patients and is therefore more effective than single-drug-based therapies. Following the advent of cART, the life expectancy of people living with HIV (PLWH) is substantially improved; however, neither a cure to eradicate HIV nor an effective vaccine exist [8,9]. Further, global statistics on HIV-1 in 2021 reported that there were 38.4 million PLWH (1.5 million newly infected), yet only 28.7 million people globally had access to cART [10].

1.2. Severe Acute Respiratory Syndrome-Coronavirus-2 (SARS-CoV-2)

SARS-CoV-2 is a novel coronavirus isolated for the first time in the province of Wuhan, Hubei, China at the end of 2019. The virus is highly transmissible and therefore rapidly became pandemic with, until now, 550 million confirmed cases and almost 6.3 million deaths [11]. SARS-CoV-2 is a respiratory virus that predominantly infects the upper respiratory tract, albeit some variants show high affinity for the lower respiratory tract and, as such, a greater propensity to induce pneumonia. The spike protein trimers on its envelope mediates virus entry via interaction with the human angiotensin-converting enzyme 2 (ACE2) which acts as receptor for spike. After binding, virus entry is completed when the virus fusion complex is induced by an enzymatic cleavage performed by the human transmembrane serine protease 2 (TMPRSS) [12]. After the uncoating event, the single stranded positive RNA genome is replicated and translated into protein, after which viral assembly leads to the release of complete virus particles. SARS-CoV-2 infection is associated with a cytokine storm that causes massive inflammation of lung tissue with the development of interstitial pneumonia and the presentation of the coronavirus disease, named COVID-19 [1,3]. Patients with overactivated immune responses suffer from the most severe respiratory conditions, thus requiring artificial ventilation to survive [13]. Due to its RNA genome and the absence of a proofreading activity in the viral RNA-dependent RNA polymerase, the SARS-CoV-2 genome has accumulated substantial diversity since its outbreak into the human population. In particular, mutations in the spike protein coding region potentially confer immune escape and can result in a decreased vaccine-mediated protection, even leading to non-protection [14–16]. Owing to the substantial prevalence of SARS-CoV-2 in the general population, co-infection with SARS-CoV-2 amongst PLWH is likely common, though the consequences of this condition are less understood than mono-infection with either virus. In this review, we will provide an overview of the clinical studies to discuss the implications associated with HIV-1 and SARS-CoV-2 co-infection. Furthermore, we will focus on the co-infection event and the clinical outcomes, with a few examples to further understand the pharmaceutical therapy that PLWH must follow and some possible cross action in the SARS-CoV-2 infection.

Table 1. Sum up of differences and similarities between HIV-1 and SARS-CoV-2.

Disease Caused by the Virus	HIV-1	SARS-CoV-2
	AIDS	COVID-19
Genome organization and translation mechanism	RNA genome with a cDNA intermediate followed by integration in the host genome [4]	ssRNA positive genome translated in protein immediately after the infection [2]
Target cells	T cells, macrophages, astrocytes, microglia cells [17]	Respiratory tissues, kidneys, small intestines, pancreas, blood vessels [18]
Target receptor/coreceptor	CD4/CCR5 and CXCR4	ACE2/TMPRSS2
Viral persistence	Lifelong infection that can be managed with cART [5]	From 10 to 17 days [19]
Suggested treatment	Combination of anti-retroviral drugs to avoid the adaptation of HIV-1 to the treatment [8]	Antipyretics, corticosteroids, immunomodulatory agents, mAbs, antivirals, based on the disease severity [20]

2. Population Studies on HIV-1 and SARS-CoV-2 Co-Infections: A Global Overview

The COVID-19 pandemic has had a profound impact on the healthcare system with regard to the treatment of other morbidities and infections. It has been reported that 60% of infectious disease physicians were working on COVID-19 patients, resulting in about 70% of HIV-1 treatment facilities in Central and Eastern Europe not being operative, reducing the ability to offer appropriate treatment and care to PLWH [21,22]. Therefore, access to anti-retroviral therapies and facilities dedicated to HIV-1 became more difficult for PLWH.

It is still debated whether PLWH have a higher risk of infection or severe complications due to SARS-CoV-2 or if they are protected by cART or by the immune suppression status as a result of HIV-1 infection. Comorbidities derived from HIV-1 infection such as diabetes, hypertension, obesity, cardiovascular, renal and lung diseases could represent risk factors for severe SARS-CoV-2 infection. Conversely, the reduced immune response that characterizes advanced HIV-1 infection could be protective against severe complications of SARS-CoV-2 infection [23]. In a cohort of 30 PLWH hospitalized for SARS-CoV-2 complications in France, 90% of them were virologically suppressed and had comorbidities such as cardiovascular and renal diseases, hypertension and diabetes. The authors concluded that HIV-1 is not an independent risk factor for SARS-CoV-2 infection [24]. Other groups explored SARS-CoV-2 seroprevalence in the HIV-1 population. Noe et al. performed a study on a German 'hot-spot' area that included a population of 500 PLWH and concluded that the rate of seroprevalence in PLWH does not seem to exceed previous reports from the general population [25]. In a retrospective study conducted in Germany, a group of 33 PLWH undergoing cART with mainly reverse transcriptase inhibitors who were co-infected with SARS-CoV-2 were evaluated for COVID-19 symptomatology. They found the following most common comorbidities: hypertension (10 out of 33 patients), chronic obstructive pulmonary disease (6 out of 33 patients), diabetes (4 out of 33), cardiovascular disease (3 out of 33) and renal insufficiency (2 out of 33). The most frequent symptoms included: cough, fever and arthralgia. Only 24% of these patients were classified as severe cases and three patients died. The study concluded that there is not an increased risk of mortality and morbidities in cART-treated PLWH with symptomatic COVID-19 infection. However, the authors of these studies underlined some important limitations such as the lack of asymptomatic cases, the absence of transmission and exposure information as well as the limited data on the onset, intensity and duration of symptoms [26]. Another study analyzed 51 PLWH diagnosed with COVID-19 in 2020 in Spain. The rate of COVID-19 infection among PLWH periodically followed up was 1.8%. Moreover, an increased incidence of comorbidities was found in HIV-1- and SARS-CoV-2-positive patients compared with only HIV-1-positive or SARS-CoV-2-positive subjects. Since 25% of patients had severe COVID-19 disease and 12% were admitted to the intensive care unit, the authors concluded

that PLWH might have worse outcomes. Moreover, they did not identify an association between cART and COVID-19 severity [27]. A large English study compared data from 207 different centers located in UK. Among the 47,592 analyzed subjects, only 0.26% were HIV-1 positive. Importantly, the authors concluded that mortality rate was increased in PLWH under 60 years old compared with HIV-1 uninfected individuals [28]. Another large study included 77,590 PLWH undergoing cART in Spain. This work suggested that whilst HIV-1-positive men over 70 years old showed a higher risk for COVID-19 diagnosis, the use of non-nucleoside reverse transcription inhibitors (NNRTIs) TDF/FTC appeared to be protective for COVID-19 hospitalization [29].

This latter evidence paves the way for further debate on the use of anti-retrovirals against HIV-1 and their use in COVID-19 therapy [30]. For example, the role of protease inhibitors (PIs) has been evaluated. It has been reported that the treatment using ritonavir/lopinavir in combination with oseltamivir (a drug used in flu treatment) had a positive effect on a 71-year-old woman with a severe SARS-CoV-2 infection in Thailand [30]. However, this drug regimen failed in a trial performed in China on 199 SARS-CoV-2 patients. The subjects were divided into two groups: one taking the standard drug regimen, the other taking the standard drug regimen and PIs (ritonavir/lopinavir). The study concluded that there is no difference in the SARS-CoV-2 disease outcome between the two study groups and that the observed mortality rate was similar [31]. Another study on the effectiveness of ritonavir/lopinavir in 47 patients in China demonstrated that PIs in combination with adjuvant drugs have positive effects on recovery, including decreasing body temperature and on recovering physiological mechanisms [32]. Other drug regimens that have been studied through phase 2/3 clinical trials to test their efficacy in reducing COVID-19 mortality and morbidity are paxlovid (nirmatrelvir/ritonavir) and molnupiravir. Paxlovid is composed of a protease inhibitor and a pharmacokinetic enhancer and was tested in a phase 2/3 clinical trial. This study, performed on a cohort of 2246 patients, found that the treatment with nirmatrelvir and ritonavir reduced the risk of severe COVID-19 [33]. Another phase 3 clinical trial, performed on a cohort of 1433 patients, tested the efficacy of molnupiravir (a nucleoside analogue) and identified a reduced risk of hospitalization or death in early treated patients [34]. Other studies investigated the impact of IL-10 in SARS-CoV-2 infection. For example, a study performed in Italy on 85 PLWH found that they do not develop higher clinical severity or demonstrate increased risk for COVID-19. Moreover, HIV-1- and SARS-CoV-2-positive patients have higher levels of IL-10, thus suggesting an IL-10-mediated role in SARS-CoV-2 infection in PLWH [35]. Another important issue that has been poorly addressed is the prevalence of long-COVID-19 in PLWH taking cART. In a study conducted in India with a cohort of 94 PLWH, they found that the frequency of long-COVID-19 was 43.6% and that this is associated with moderate-severe SARS-CoV-2 infection [36]. Another study conducted in Italy on 123 PLWH with SARS-CoV-2 infection showed that the risk factors which can result in the development of post-acute COVID-19 syndrome are similar to those experienced by the general population such as severe COVID-19 and polypharmacy [37]. The discussed studies are summarized and reported in Table 2.

Table 2. Summary of relevant in vivo studies studying HIV-1 and SARS-CoV-2 co-infections.

First Author and Year	Country	Studied Cohorts	Results
Isernia et al., 2020 [24]	France	30 HIV-1 and SARS-CoV-2 positive patients	HIV is not an independent risk factor for SARS-CoV-2.
Noe et al., 2021 [25]	Germany	500 PLWH	HIV-1 is not associated with elevated probability of SARS-CoV-2 infection
Härter et al., 2020 [26]	Germany	33 HIV-1 and SARS-CoV-2 positive patients	PLWH on cART regimen did not show increased risk of mortality and morbidities when experiencing symptomatic COVID-19 infection

Table 2. *Cont.*

First Author and Year	Country	Studied Cohorts	Results
Vizcarra et al., 2020 [27]	Spain	51 HIV-1 and SARS-CoV-2 positive patients	HIV-1 infection is not associated with protection and lower risk of severe SARS-CoV-2 infection
Geretti et al., 2021 [28]	United Kingdom	47,592 SARS-CoV-2 patients (0.26% PLWH)	There is an association between PLWH under 60 years old and an increased SARS-CoV-2 mortality compared with the HIV-1 uninfected group
Vanetti et al., 2021 [35]	Italy	85 PLWH among whom 4 had SARS-CoV-2 infection	HIV-1 is not associated with increased risk and severity of SARS-CoV-2 infection. Moreover, higher levels of IL-10 in HIV-1 and SARS-CoV-2 positive patients were observed, thus suggesting an IL-10 role in SARS-CoV-2 infection in PLWH
Del Amo et al., 2020 [29]	Spain	77,590 PLWH under cART regimen among whom 236 with SARS-CoV-2 infection	HIV-1 positive man older than 70 years old possess a higher risk for COVID-19 diagnosis. TDF/FTC cART regimen seems to be protective for COVID-19 and COVID-19-related hospitalization
Cao et al., 2020 [31]	China	199 SARS-CoV-2 patients to test efficacy of PIs	There is no improvement in SARS-CoV-2 infection in patients taking standard drug regimen supplemented with ritonavir/lopinavir compared with patients taking the standard drug regimen. Ritonavir/lopinavir treatment had no antiviral effect on SARS-CoV-2-infected patients
Ye et al., 2020 [32]	China	47 SARS-CoV-2 patients to test efficacy of PIs	The protease inhibitors ritonavir/lopinavir in combination with pneumonia adjuvant drugs have beneficial effects in the management of COVID-19 symptoms.

3. HIV-1 Therapy and SARS-CoV-2 Treatment

As mentioned in the previous section, the benefit of cART in PLWH who contract SARS-CoV-2 infection is still under investigation. A recent study compared a small number of PLWH infected with SARS-CoV-2 on cART with those not on cART. This paper found that COVID-19 infection had similar outcomes and inflammatory markers were high in both the studied groups [38]. In silico analyses indicate the potential of cART drugs binding SARS-CoV-2 protein targets [39].

Mahdi et al. tested the efficacy of various HIV-1 PIs, using a dark-to-bright fluorescent reporter gene for in vitro and cell-based assays. This strategy allows direct measurement of the activity of the analyzed protein; the reporter is quenched by a C-terminal region which is linked to the GFP via the protease substrate. The reporter gains fluorescence if the protease is active. All the drugs tested demonstrated inhibition efficacy in the micromolar range. HIV-1 PIs such as saquinavir, darunavir and atazanavir showed the best inhibitory activity, even though they all failed to completely inhibit the activity of the main protease of SARS-CoV-2 (M^{pro}) in vitro [40]. Saquinavir also showed cytotoxic effect at high concentrations in comparison with the others.

A cytidine analogue, azvudine or FNC, is known for anti-retroviral activity and it has been recently approved for HIV-1 treatment in China [41,42]. FNC is active against viral proteins only upon phosphorylation (FNC-triphosphate). CL236 was used as an analogous of FNC-MP; it showed a reduction of coronavirus RNA production in vitro [42].

Some data suggested that drugs targeting HIV-1 reverse transcriptase (RT), or integrase (IN), could potentially inhibit SARS-CoV-2 entry. Using a receptor–anti-receptor binding

assay (NanoLuc binary technology (NanoBiT), Lee et al. found that the RT inhibitor etravirine has an affinity for the receptor binding domain (RBD) of spike, blocking the binding of SARS-CoV-2 to the human ACE2 receptor [43]. A similar effect was observed with the IN inhibitor dolutegravir, but with a weaker efficacy compared with etravirine. However, these preliminary data were not confirmed in an in vitro infection system to test lentiviral-based pseudotyped virus neutralization due to inherent restrictions of lentiviral vector infection systems in the presence of IN and RT inhibitors [43]. Interestingly, treatment with another protease inhibitor, nelfinavir mesylate, showed considerable cell-to-cell fusion inhibition in vitro [44]. Indeed, it has been demonstrated that SARS-CoV-2 infection induces the formation of syncytia that may be driving the rapid spread of the virus in lung tissue [45]. These data on the efficacy of nelfinavir could potentially suggest new potential drug regimens to slow down the SARS-CoV-2 disease progression [44].

4. Novel Drugs to Resolve Co-Infections and Potentially to Guide the Development of Novel Anti-SARS-CoV-2 Therapies

Although limited information is currently known on SARS-CoV-2/HIV-1 co-infection due to the relative paucity of cases, this group of rare patients represents the opportunity to expand the discovery of currently used antiviral drugs and/or new ones with a broader spectrum of activity and to enhance the knowledge of the immunology of PLWH. Many anti-HIV-1 drugs were also repurposed for COVID-19 treatment as a first means to address the emergency.

Lopinavir and ritonavir (HIV-1 protease inhibitors), usually prescribed in combination, have been tested directly on patients since their positive effects against SARS-CoV and MERS-CoV infections. However, these studies have been abandoned since no clinical improvement was observed when compared with control groups [31,46,47]. In particular, ritonavir showed insufficient inhibitory activity [40]. Other HIV-1 PIs, nelfinavir and atazanavir, have also been proposed and tested in cellular models and showed better inhibition of the viral replication cycle [46]. However, data showed that nelfinavir requires a high dose to obtain inhibition of viral proteins. Atazanavir, on the other hand, is better tolerated by cells, although it also requires high concentrations [40]. Therefore, new drugs against SARS-CoV-2 in the presence or absence of HIV-1 infection are urgently required. The first step could be the identification of a possible cross-reactive virus target for drug development.

4.1. In Silico and In Vitro Identification of Viral Target to Resolve Co-Infections and Potentially to Guide the Development of Novel Anti-SARS-CoV-2 Drugs

Modern drug development usually uses in silico approaches to identify virus proteins that could possibly act as drug targets. In the case of SARS-CoV-2, potential targets are represented by the virus entry mechanism (spike-ACE2 interaction/fusion core blockade), the viral replication (RNA-dependent RNA polymerase, or RdRp) or the maturation processes (viral proteases) [48].

SARS-CoV-2, as with other coronaviruses, expresses a trimeric fusion protein on its envelope (spike protein, or S) [49,50]. The single monomer has separate subunits, namely S1 and S2. The N-terminal segment in the S1 region contains the RBD, which directly binds the ACE2 receptor on the host cells. The S2 region harbors the substrate sequence of proteases such as TMPRSS2, which promotes the fusion between the membranes [51,52]. The infectivity of the virus can be minimized or hindered by blocking its access to ACE2 and/or by preventing the formation of the fusion core by blocking the S1/S2 interface [43,53].

SARS-CoV-2 also requires RdRp to replicate its own genome into new copies for progeny virions [54]. SARS-CoV-2 RdRp is constituted by three domains. The drugs that interfere with the replication of the genome are designed to dock into the nucleotide binding cleft and to prevent RNA production, limiting the formation of replication competent virus particles [55].

The SARS-CoV-2 genome also encodes a long polyprotein that is subsequently processed into single functional proteins. Among these, the proteases PL^{pro} and $3CL^{pro}$ (or

M^{pro}) are fundamental in each of the maturation steps of the viral life cycle. PL^{pro} is also involved in deubiquitination to preserve viral proteins. M^{pro} has a pivotal role in polyprotein processing since viral maturation depends on M^{pro} activity [40,56].

Besides the identification of new potential drug targets, in the case of SARS-CoV-2, HIV-1 cART represented a starting point for virtual molecular analyses, molecular docking and interaction energies to predict interactions between viral proteins and available drugs to shorten the time required for the discovery of new therapies [57]. A small group of anti-HIV-1 drugs showed a cross-reaction to SARS-CoV-2, with clinically relevant results.

The envelope complex of HIV-1, gp160, contains a structure characterized by the presence of two heptad repeats (HRs), HR 1 in gp120 and HR2 in gp41. Once the envelope binds to the receptor, the subsequent conformational change induces the pairing of the HRs, promoting the fusion between membranes. From a structural point of view, the S1 and S2 subunits of the spike protein display a similar function [53,58]. Therefore, the effects of anti-HIV-1 drugs that abrogate the membrane fusion have been investigated. As an example, enfuvirtide (Enf) is one of the most common anti-fusion drugs administered for HIV-1 treatment. Since the emergence of SARS-CoV, it has been proposed as an anti-betacoronavirus drug due to evident similarities between SARS-CoV and HIV-1 envelopes. Enf showed high association levels with the structures of S2, since several residues that are relevant for enfuvirtide docking are conserved between gp41 and S2 [53]. A previous molecular study revealed the interaction between this drug and the spike protein of SARS-CoV-2, based on previous evidence from SARS-CoV. The study shows that the molecule impairs the transition from the pre-fusion to the fusion stage by docking in the interface between monomers [59].

The inhibitory potential of HIV-1 protease blockers against SARS-CoV-2 protease (M^{pro}) was also investigated. MD studies revealed that TMB607 and TMC310911 (in combination with ritonavir, a drug usually included in cART therapy) could be candidates for SARS-CoV-2 M^{pro} blockade for future therapeutic applications [60,61]. Other anti-HIV-1 compounds were also tested for SARS-CoV-2 inhibition/interference based on molecular docking studies. Abacavir, fosamprenavir, indinavir and raltegravir resulted to better interact with SARS-CoV-2 fundamental proteins. Moreover, the group analyzed other predicted biological parameters, such as toxicity, sensitivity and mutagenicity, highlighting that the majority of these were non-mutagenic but potentially toxic [62]. Recently, a study by Y. Wu et al. investigated the binding energies and molecular docking properties of saquinavir, a direct HIV-1 protease inhibitor, on SARS-CoV-2 M^{pro}. The group discovered that saquinavir is predicted as one of the best binders of M^{pro} [48].

4.2. Attempts to Resolve Co-Infection by Enhancing a Humoral Response: The Identification of Possible Broadly Neutralizing Antibodies against HIV-1 and SARS-CoV-2

Previous studies revealed shared motifs in the structure of HIV-1 and SARS-CoV-2 envelope viral proteins [49,58]. Recent studies have aimed to identify antibodies against SARS-CoV-2 in PLWH. Broadly neutralizing antibodies (bnAbs), which produce highly neutralizing responses, are under evaluation for cross-reactivity against SARS-CoV-2. In one study, by adopting an enzyme-linked immunoassay (ELISA) screening approach, six bnAbs were selected to test their neutralization ability in vitro through SARS-CoV-2 pseudotyped virus neutralization assay (PVNA). Only one bnAb showed a sufficient neutralization capacity against SARS-CoV-2, but failed to block infection in a live-virus assay [63]. In another study, a cohort of SARS-CoV-2-recovered patients were enrolled and screened to identify the presence of nAbs through PVNA. In this case, the isolated nAbs were also tested in vivo in a Syrian hamster animal model. The study concluded that only a portion of the tested nAbs confer protection against the SARS-CoV-2 disease [64].

A recent study reported a similar finding. In this case, the group found cross-reactivity against an HIV-1 envelope in sera from SARS-CoV-2-spike immunized mice via ELISA. The opposite situation (anti-HIV-1 Env antibodies against SARS-CoV-2 spike) was also confirmed by ELISA analyses. However, while anti-SARS-CoV-2 sera neutralized the live

virus, they failed to induce strong infectivity reduction against the HIV-1-pseudotyped virus. Moreover, the anti-HIV-1 sera failed to block the entry of live SARS-CoV-2 in a cytopathic effect (CPE) assay [65].

A recent study investigated the cross-reactivity of monoclonal anti-HIV-1 antibodies against the epitopes of SARS-CoV-2 spike glycans [66]. Cross-reactivity against viral proteins that carry host's glycans is rare but possible. Part of the tested antibodies resulted cross-reactively in ELISA tests and Western-blot analysis (both native and denatured substrates) but failed at neutralizing the SARS-CoV-2-pseudotyped virus. The group concluded that the cross-reactivity was mediated by glycan moieties, since the use of glycan-rich casein-based buffers abrogated the cross-reaction [66].

5. Conclusions

Following two years of the outbreak of SARS-CoV-2, there is a solid and wide body of the literature that explores the risk of SARS-CoV-2 infection and/or COVID-19 disease progression in the general population. On the other hand, studies on the risk of infection and severe disease in the presence of persistent co-infections such as HIV-1 are less abundant and therefore deserve particular attention [67,68]. In parallel, the development of in vitro studies to provide robust methodological approaches to study co-infections is still ongoing. In this review, we have provided a global overview on the implications and clinical management of SARS-CoV-2 and HIV-1 co-infection, as well as in the field of novel anti-retroviral drug development. This study of the literature seems to suggest that HIV-1 infection is not an independent factor of a higher risk of SARS-CoV-2 infection or a worse clinical outcome compared with the HIV-1-negative population. Whilst the putative protective role of cART against a more severe COVID-19 clinical outcome still needs to be confirmed, it seems clear that the past 20 years of research in the HIV-1 field have set a solid ground for drug development studies.

Author Contributions: Literature search and writing C.S. and T.F.; writing of the introduction M.B.; Conceptualization, writing and supervision A.R. and J.T. All authors have read and agreed to the published version of the manuscript.

Funding: This research was supported by FUR 2020 Department of Excellence 2018-2022 (MIUR, Italy); the Brain Research Foundation Verona. The founding sources had no role in the development of this study.

Institutional Review Board Statement: Not applicable.

Informed Consent Statement: Not applicable.

Data Availability Statement: Not applicable.

Conflicts of Interest: The authors declare no conflict of interest.

References

1. Soy, M.; Keser, G.; Atagündüz, P.; Tabak, F.; Atagündüz, I.; Kayhan, S. Cytokine Storm in COVID-19: Pathogenesis and Overview of Anti-Inflammatory Agents Used in Treatment. *Clin. Rheumatol.* **2020**, *39*, 2085–2094. [CrossRef] [PubMed]
2. Illanes-álvarez, F.; Márquez-Ruiz, D.; Márquez-Coello, M.; Cuesta-Sancho, S.; Girón-González, J.A. Similarities and Differences between HIV and SARS-CoV-2. *Int. J. Med. Sci.* **2021**, *18*, 846. [CrossRef] [PubMed]
3. Attaway, A.H.; Scheraga, R.G.; Bhimraj, A.; Biehl, M.; Hatipoğ Lu, U. Severe COVID-19 Pneumonia: Pathogenesis and Clinical Management. *BMJ* **2021**, *372*, n436. [CrossRef] [PubMed]
4. Wilen, C.B.; Tilton, J.C.; Doms, R.W. HIV: Cell Binding and Entry. *Cold Spring Harb. Perspect. Med.* **2012**, *2*, a006866. [CrossRef]
5. Moir, S.; Chun, T.W.; Fauci, A.S. Pathogenic Mechanisms of HIV Disease. *Annu. Rev. Pathol.* **2011**, *6*, 223–248. [CrossRef]
6. Orser, L.; O'Byrne, P.; Holmes, D. AIDS Cases in Ottawa: A Review of Simultaneous HIV and AIDS Diagnoses. *Public Health Nurs.* **2022**, *39*, 909–916. [CrossRef]
7. Akanbi, M.O.; Scarci, K.; Taiwo, B.; Murphy, R.L. Combination Nucleoside/ Nucleotide Reverse Transcriptase Inhibitors. *Expert Opin. Pharmacother.* **2012**, *13*, 65. [CrossRef]
8. Campbell, L.A.; Mocchetti, I. Extracellular Vesicles and HIV-Associated Neurocognitive Disorders: Implications in Neuropathogenesis and Disease Diagnosis. *Neurotox. Res.* **2021**, *39*, 2098–2107. [CrossRef]

9. Thomas, J.; Ruggiero, A.; Paxton, W.A.; Pollakis, G. Measuring the Success of HIV-1 Cure Strategies. *Front. Cell. Infect. Microbiol.* **2020**, *10*, 134. [CrossRef]
10. UNAIDS. Global HIV & AIDS Statistics—Fact Sheet. Available online: https://www.unaids.org/en/resources/fact-sheet (accessed on 15 December 2021).
11. Zhou, P.; Yang, X.L.; Wang, X.G.; Hu, B.; Zhang, L.; Zhang, W.; Si, H.R.; Zhu, Y.; Li, B.; Huang, C.L.; et al. Addendum: A Pneumonia Outbreak Associated with a New Coronavirus of Probable Bat Origin. *Nature* **2020**, *588*, E6. [CrossRef]
12. V'kovski, P.; Kratzel, A.; Steiner, S.; Stalder, H.; Thiel, V. Coronavirus Biology and Replication: Implications for SARS-CoV-2. *Nat. Rev. Microbiol.* **2021**, *19*, 155–170. [CrossRef]
13. Hu, B.; Guo, H.; Zhou, P.; Shi, Z.L. Characteristics of SARS-CoV-2 and COVID-19. *Nat. Rev. Microbiol.* **2021**, *19*, 141–154. [CrossRef]
14. Biswas, B.; Chattopadhyay, S.; Hazra, S.; Hansda, A.K.; Goswami, R. COVID-19 Pandemic: The Delta Variant, T-Cell Responses, and the Efficacy of Developing Vaccines. *Inflamm. Res.* **2022**, *71*, 377. [CrossRef]
15. Presti, A.L.; Coghe, F.; Di Martino, A.; Fais, S.; Cappai, R.; Marra, M.; Carollo, M.; Crescenzi, M.; Orrù, G.; Rezza, G.; et al. First Detection of SARS-CoV-2 Lineage A.27 in Sardinia, Italy. *Ann. Ist. Super. Sanita* **2022**, *58*, 1–5. [CrossRef]
16. Nutini, A.; Zhang, J.; Sohail, A.; Arif, R.; Nofal, T.A. Forecasting of the Efficiency of Monoclonal Therapy in the Treatment of CoViD-19 Induced by the Omicron Variant of SARS-CoV2. *Results Phys.* **2022**, *35*, 105300. [CrossRef]
17. Valcour, V.; Sithinamsuwan, P.; Letendre, S.; Ances, B. Pathogenesis of HIV in the Central Nervous System. *Curr. HIV/AIDS Rep.* **2011**, *8*, 54. [CrossRef]
18. Liu, J.; Li, Y.; Liu, Q.; Yao, Q.; Wang, X.; Zhang, H.; Chen, R.; Ren, L.; Min, J.; Deng, F.; et al. SARS-CoV-2 Cell Tropism and Multiorgan Infection. *Cell Discov.* **2021**, *7*, 17. [CrossRef]
19. Cao, C.; Cai, Z.; Xiao, X.; Rao, J.; Chen, J.; Hu, N.; Yang, M.; Xing, X.; Wang, Y.; Li, M.; et al. The Architecture of the SARS-CoV-2 RNA Genome inside Virion. *Nat. Commun.* **2021**, *12*, 3917. [CrossRef]
20. ECDC-Treatment and Pharmaceutical Prophylaxis of COVID-19. Available online: https://www.ecdc.europa.eu/en/covid-19/latest-evidence/treatment (accessed on 15 December 2021).
21. Squillace, N.; Ricci, E.; Colella, E.; Bonfanti, P. HIV and SARS-CoV-2 Co-Infection: What Are the Risks? *Infect. Drug Resist.* **2021**, *14*, 3991. [CrossRef]
22. Chilot, D.; Woldeamanuel, Y.; Manyazewal, T. COVID-19 Burden on HIV Patients Attending Antiretroviral Therapy in Addis Ababa, Ethiopia: A Multicenter Cross-Sectional Study. *Front. Med.* **2022**, *9*, 741862. [CrossRef]
23. Lesko, C.R.; Bengtson, A.M. HIV and COVID-19: Intersecting Epidemics with Many Unknowns. *Am. J. Epidemiol.* **2021**, *190*, 10–16. [CrossRef] [PubMed]
24. Isernia, V.; Julia, Z.; Le Gac, S.; Bachelard, A.; Landman, R.; Lariven, S.; Joly, V.; Deconinck, L.; Rioux, C.; Lescure, X.; et al. SARS-COV2 Infection in 30 HIV-Infected Patients Followed-up in a French University Hospital. *Int. J. Infect. Dis.* **2020**, *101*, 49–51. [CrossRef] [PubMed]
25. Noe, S.; Schabaz, F.; Heldwein, S.; Mayer, W.; Ruecker, K.; Tiller, F.W.; von Krosigk, A.; Wiese, C.; Balogh, A.; Gersbacher, E.; et al. HIV and SARS-CoV-2 Co-Infection: Cross-Sectional Findings from a German 'Hotspot'. *Infection* **2021**, *49*, 313–320. [CrossRef] [PubMed]
26. Härter, G.; Spinner, C.D.; Roider, J.; Bickel, M.; Krznaric, I.; Grunwald, S.; Schabaz, F.; Gillor, D.; Postel, N.; Mueller, M.C.; et al. COVID-19 in People Living with Human Immunodeficiency Virus: A Case Series of 33 Patients. *Infection* **2020**, *48*, 1. [CrossRef] [PubMed]
27. Vizcarra, P.; Pérez-Elías, M.J.; Quereda, C.; Moreno, A.; Vivancos, M.J.; Dronda, F.; Casado, J.L.; Moreno, S.; Fortún, J.; Navas, E.; et al. Description of COVID-19 in HIV-Infected Individuals: A Single-Centre, Prospective Cohort. *Lancet. HIV* **2020**, *7*, e554. [CrossRef] [PubMed]
28. Geretti, A.M.; Stockdale, A.J.; Kelly, S.H.; Cevik, M.; Collins, S.; Waters, L.; Villa, G.; Docherty, A.; Harrison, E.M.; Turtle, L.; et al. Outcomes of Coronavirus Disease 2019 (COVID-19) Related Hospitalization Among People With Human Immunodeficiency Virus (HIV) in the ISARIC World Health Organization (WHO) Clinical Characterization Protocol (UK): A Prospective Observational Study. *Clin. Infect. Dis. An Off. Publ. Infect. Dis. Soc. Am.* **2021**, *73*, e2095. [CrossRef]
29. del Amo, J.; Polo, R.; Moreno, S.; Díaz, A.; Martínez, E.; Arribas, J.R.; Jarrín, I.; Hernán, M.A. Incidence and Severity of COVID-19 in HIV-Positive Persons Receiving Antiretroviral Therapy: A Cohort Study. *Ann. Intern. Med.* **2020**, *173*, 536–541. [CrossRef]
30. Costanzo, M.; De Giglio, M.A.R.; Roviello, G.N. SARS-CoV-2: Recent Reports on Antiviral Therapies Based on Lopinavir/Ritonavir, Darunavir/Umifenovir, Hydroxychloroquine, Remdesivir, Favipiravir and Other Drugs for the Treatment of the New Coronavirus. *Curr. Med. Chem.* **2020**, *27*, 4536–4541. [CrossRef]
31. Cao, B.; Wang, Y.; Wen, D.; Liu, W.; Wang, J.; Fan, G.; Ruan, L.; Song, B.; Cai, Y.; Wei, M.; et al. A Trial of Lopinavir-Ritonavir in Adults Hospitalized with Severe Covid-19. *N. Engl. J. Med.* **2020**, *382*, 1787–1799. [CrossRef]
32. Ye, X.T.; Luo, Y.L.; Xia, S.C.; Sun, Q.F.; Ding, J.G.; Zhou, Y.; Chen, W.; Wang, X.F.; Zhang, W.W.; Du, W.J.; et al. Clinical Efficacy of Lopinavir/Ritonavir in the Treatment of Coronavirus Disease 2019. *Eur. Rev. Med. Pharmacol. Sci.* **2020**, *24*, 3390–3396. [CrossRef]
33. Hammond, J.; Leister-Tebbe, H.; Gardner, A.; Abreu, P.; Bao, W.; Wisemandle, W.; Baniecki, M.; Hendrick, V.M.; Damle, B.; Simón-Campos, A.; et al. Oral Nirmatrelvir for High-Risk, Nonhospitalized Adults with COVID-19. *N. Engl. J. Med.* **2022**, *386*, 1397–1408. [CrossRef]

34. Jayk Bernal, A.; Gomes da Silva, M.M.; Musungaie, D.B.; Kovalchuk, E.; Gonzalez, A.; Delos Reyes, V.; Martín-Quirós, A.; Caraco, Y.; Williams-Diaz, A.; Brown, M.L.; et al. Molnupiravir for Oral Treatment of COVID-19 in Nonhospitalized Patients. *N. Engl. J. Med.* **2022**, *386*, 509–520. [CrossRef]
35. Vanetti, C.; Trabattoni, D.; Stracuzzi, M.; Amendola, A.; Fappani, C.; Rubinacci, V.; Fenizia, C.; Gianolio, L.; Biasin, M.; Dighera, A.; et al. Immunological Characterization of HIV and SARS-CoV-2 Coinfected Young Individuals. *Cells* **2021**, *10*, 3187. [CrossRef]
36. Pujari, S.; Gaikwad, S.; Chitalikar, A.; Dabhade, D.; Joshi, K.; Bele, V. Long-Coronavirus Disease among People Living with HIV in Western India: An Observational Study. *Immunity Inflamm. Dis.* **2021**, *9*, 1037–1043. [CrossRef]
37. Mazzitelli, M.; Trunfio, M.; Sasset, L.; Leoni, D.; Castelli, E.; Menzo, S.L.; Gardin, S.; Putaggio, C.; Brundu, M.; Garzotto, P.; et al. Factors Associated with Severe COVID-19 and Post-Acute COVID-19 Syndrome in a Cohort of People Living with HIV on Antiretroviral Treatment and with Undetectable HIV RNA. *Viruses* **2022**, *14*, 493. [CrossRef]
38. Lee, K.W.; Yap, S.F.; Ngeow, Y.F.; Lye, M.S. Covid-19 in People Living with Hiv: A Systematic Review and Meta-Analysis. *Int. J. Environ. Res. Public Health* **2021**, *18*, 3554. [CrossRef]
39. Gatechompol, S.; Avihingsanon, A.; Putcharoen, O.; Ruxrungtham, K.; Kuritzkes, D.R. COVID-19 and HIV Infection Co-Pandemics and Their Impact: A Review of the Literature. *AIDS Res. Ther.* **2021**, *18*, 28. [CrossRef]
40. Mahdi, M.; Mótyán, J.A.; Szojka, Z.I.; Golda, M.; Miczi, M.; Tőzsér, J. Analysis of the Efficacy of HIV Protease Inhibitors against SARS-CoV-2's Main Protease. *Virol. J.* **2020**, *17*, 190. [CrossRef]
41. Wang, R.R.; Yang, Q.H.; Luo, R.H.; Peng, Y.M.; Dai, S.X.; Zhang, X.J.; Chen, H.; Cui, X.Q.; Liu, Y.J.; Huang, J.F.; et al. Azvudine, a Novel Nucleoside Reverse Transcriptase Inhibitor Showed Good Drug Combination Features and Better Inhibition on Drug-Resistant Strains than Lamivudine in Vitro. *PLoS ONE* **2014**, *9*, e105617. [CrossRef]
42. Zhang, J.L.; Li, Y.H.; Wang, L.L.; Liu, H.Q.; Lu, S.Y.; Liu, Y.; Li, K.; Liu, B.; Li, S.Y.; Shao, F.M.; et al. Azvudine Is a Thymus-Homing Anti-SARS-CoV-2 Drug Effective in Treating COVID-19 Patients. *Signal Transduct. Target. Ther.* **2021**, *6*, 414. [CrossRef]
43. Lee, R.K.L.; Li, T.N.; Chang, S.Y.; Chao, T.L.; Kuo, C.H.; Pan, M.Y.C.; Chiou, Y.T.; Liao, K.J.; Yang, Y.; Wu, Y.H.; et al. Identification of Entry Inhibitors against Delta and Omicron Variants of SARS-CoV-2. *Int. J. Mol. Sci.* **2022**, *23*, 4050. [CrossRef] [PubMed]
44. Musarrat, F.; Chouljenko, V.; Dahal, A.; Nabi, R.; Chouljenko, T.; Jois, S.D.; Kousoulas, K.G. The Anti-HIV Drug Nelfinavir Mesylate (Viracept) Is a Potent Inhibitor of Cell Fusion Caused by the SARSCoV-2 Spike (S) Glycoprotein Warranting Further Evaluation as an Antiviral against COVID-19 Infections. *J. Med. Virol.* **2020**, *92*, 2087–2095. [CrossRef] [PubMed]
45. Buchrieser, J.; Dufloo, J.; Hubert, M.; Monel, B.; Planas, D.; Rajah, M.M.; Planchais, C.; Porrot, F.; Guivel-Benhassine, F.; Van der Werf, S.; et al. Syncytia Formation by SARS-CoV-2-Infected Cells. *EMBO J.* **2020**, *39*, e106267. [CrossRef]
46. Citarella, A.; Scala, A.; Piperno, A.; Micale, N. SARS-CoV-2 Mpro: A Potential Target for Peptidomimetics and Small-Molecule Inhibitors. *Biomolecules* **2021**, *11*, 607. [CrossRef]
47. Mótyán, J.A.; Mahdi, M.; Hoffka, G.; Tőzsér, J. Potential Resistance of SARS-CoV-2 Main Protease (Mpro) against Protease Inhibitors: Lessons Learned from HIV-1 Protease. *Int. J. Mol. Sci.* **2022**, *23*, 3507. [CrossRef]
48. Wu, Y.; Chang, K.Y.; Lou, L.; Edwards, L.G.; Doma, B.K.; Xie, Z.R. In Silico Identification of Drug Candidates against COVID-19. *Inform. Med. Unlocked* **2020**, *21*, 100461. [CrossRef]
49. Harrison, S.C. Mechanism of Membrane Fusion by Viral Envelope Proteins. *Adv. Virus Res.* **2005**, *64*, 231–261. [CrossRef]
50. Plemper, R.K. Cell Entry of Enveloped Viruses. *Curr. Opin. Virol.* **2011**, *1*, 92. [CrossRef]
51. Walls, A.C.; Park, Y.J.; Tortorici, M.A.; Wall, A.; McGuire, A.T.; Veesler, D. Structure, Function, and Antigenicity of the SARS-CoV-2 Spike Glycoprotein. *Cell* **2020**, *181*, 281–292.e6. [CrossRef]
52. Hoffmann, M.; Kleine-Weber, H.; Schroeder, S.; Krüger, N.; Herrler, T.; Erichsen, S.; Schiergens, T.S.; Herrler, G.; Wu, N.H.; Nitsche, A.; et al. SARS-CoV-2 Cell Entry Depends on ACE2 and TMPRSS2 and Is Blocked by a Clinically Proven Protease Inhibitor. *Cell* **2020**, *181*, 271–280.e8. [CrossRef]
53. Ahmadi, K.; Farasat, A.; Rostamian, M.; Johari, B.; Madanchi, H. Enfuvirtide, an HIV-1 Fusion Inhibitor Peptide, Can Act as a Potent SARS-CoV-2 Fusion Inhibitor: An in Silico Drug Repurposing Study. *J. Biomol. Struct. Dyn.* **2022**, *40*, 5566–5576. [CrossRef] [PubMed]
54. Astuti, I. Ysrafil Severe Acute Respiratory Syndrome Coronavirus 2 (SARS-CoV-2): An Overview of Viral Structure and Host Response. *Diabetes Metab. Syndr.* **2020**, *14*, 407–412. [CrossRef] [PubMed]
55. Vicenti, I.; Zazzi, M.; Saladini, F. SARS-CoV-2 RNA-Dependent RNA Polymerase as a Therapeutic Target for COVID-19. *Expert Opin. Ther. Pat.* **2021**, *31*, 325–337. [CrossRef] [PubMed]
56. Razali, R.; Asis, H.; Budiman, C. Structure-Function Characteristics of SARS-CoV-2 Proteases and Their Potential Inhibitors from Microbial Sources. *Microorganisms* **2021**, *9*, 2481. [CrossRef]
57. Chukwudozie, O.S.; Duru, V.C.; Ndiribe, C.C.; Aborode, A.T.; Oyebanji, V.O.; Emikpe, B.O. The Relevance of Bioinformatics Applications in the Discovery of Vaccine Candidates and Potential Drugs for COVID-19 Treatment. *Bioinform. Biol. Insights* **2021**, *15*, 11779322211002168. [CrossRef]
58. Zhang, X.W.; Yap, Y.L. Structural Similarity between HIV-1 Gp41 and SARS-CoV S2 Proteins Suggests an Analogous Membrane Fusion Mechanism. *Theochem* **2004**, *677*, 73–76. [CrossRef]
59. Calligari, P.; Bobone, S.; Ricci, G.; Bocedi, A. Molecular Investigation of SARS-CoV-2 Proteins and Their Interactions with Antiviral Drugs. *Viruses* **2020**, *12*, 445. [CrossRef]

60. Ancy, I.; Sivanandam, M.; Kumaradhas, P. Possibility of HIV-1 Protease Inhibitors-Clinical Trial Drugs as Repurposed Drugs for SARS-CoV-2 Main Protease: A Molecular Docking, Molecular Dynamics and Binding Free Energy Simulation Study. *J. Biomol. Struct. Dyn.* **2021**, *39*, 5368–5375. [CrossRef]
61. Ibrahim, M.A.A.; Abdelrahman, A.H.M.; Allemailem, K.S.; Almatroudi, A.; Moustafa, M.F.; Hegazy, M.E.F. In Silico Evaluation of Prospective Anti-COVID-19 Drug Candidates as Potential SARS-CoV-2 Main Protease Inhibitors. *Protein J.* **2021**, *40*, 296–309. [CrossRef]
62. Mathew, S.M.; Benslimane, F.; Althani, A.A.; Yassine, H.M. Identification of Potential Natural Inhibitors of the Receptor-Binding Domain of the SARS-CoV-2 Spike Protein Using a Computational Docking Approach. *Qatar Med. J.* **2021**, *2021*, 12. [CrossRef]
63. Mishra, N.; Kumar, S.; Singh, S.; Bansal, T.; Jain, N.; Saluja, S.; Kumar, R.; Bhattacharyya, S.; Palanichamy, J.K.; Mir, R.A.; et al. Cross-Neutralization of SARS-CoV-2 by HIV-1 Specific Broadly Neutralizing Antibodies and Polyclonal Plasma. *PLoS Pathog.* **2021**, *17*, e1009958. [CrossRef] [PubMed]
64. Rogers, T.F.; Zhao, F.; Huang, D.; Beutler, N.; Burns, A.; He, W.T.; Limbo, O.; Smith, C.; Song, G.; Woehl, J.; et al. Isolation of Potent SARS-CoV-2 Neutralizing Antibodies and Protection from Disease in a Small Animal Model. *Science* **2020**, *369*, 956–963. [CrossRef] [PubMed]
65. Perween, R.; PraveenKumar, M.; Shrivastava, T.; Parray, H.A.; Singh, V.; Singh, S.; Chiranjivi, A.; Jakhar, K.; Sonar, S.; Tiwari, M.; et al. The SARS CoV-2 Spike Directed Non-Neutralizing Polyclonal Antibodies Cross-React with Human Immunodeficiency Virus (HIV-1) Gp41. *Int. Immunopharmacol.* **2021**, *101*, 108187. [CrossRef] [PubMed]
66. Mannar, D.; Leopold, K.; Subramaniam, S. Glycan Reactive Anti-HIV-1 Antibodies Bind the SARS-CoV-2 Spike Protein but Do Not Block Viral Entry. *Sci. Rep.* **2021**, *11*, 12448. [CrossRef]
67. Nomah, D.K.; Reyes-Urueña, J.; Llibre, J.M.; Ambrosioni, J.; Ganem, F.S.; Miró, J.M.; Casabona, J. HIV and SARS-CoV-2 Co-Infection: Epidemiological, Clinical Features, and Future Implications for Clinical Care and Public Health for People Living with HIV (PLWH) and HIV Most-at-Risk Groups. *Curr. HIV/AIDS Rep.* **2021**, *18*, 518–526. [CrossRef]
68. Dadashi, M.; Dadashi, A.; Sameni, F.; Sayadi, S.; Goudarzi, M. *Since January 2020 Elsevier Has Created a COVID-19 Resource Centre with Free Information in English and Mandarin on the Novel Coronavirus COVID-19. The COVID-19 Resource Centre Is Hosted on Elsevier Connect, the Company's Public News and Information*; Elsevier Inc.: Amsterdam, The Netherlands, 2020.

vaccines

MDPI

Article

Analysis of Antibody Neutralisation Activity against SARS-CoV-2 Variants and Seasonal Human Coronaviruses NL63, HKU1, and 229E Induced by Three Different COVID-19 Vaccine Platforms

Diego Cantoni [1,†], Gabriel Siracusano [2,†], Martin Mayora-Neto [1], Claudia Pastori [2], Tobia Fantoni [3], Spyros Lytras [4], Cecilia Di Genova [1], Joseph Hughes [4], on behalf of the Ambulatorio Medico San Luca Villanuova Group [5,‡], Lucia Lopalco [2,*] and Nigel Temperton [1,*]

1 Viral Pseudotype Unit, Medway School of Pharmacy, The Universities of Kent and Greenwich at Medway, Chatham ME4 4TB, UK
2 Division of Immunology, Transplantation and Infectious Disease, Immunobiology of HIV Group, San Raffaele Scientific Institute, 20132 Milan, Italy
3 Department of Neurosciences, Biomedicine and Movement Sciences, University of Verona, 37129 Verona, Italy
4 MRC-Centre for Virus Research, University of Glasgow, Glasgow G12 BQQ, UK
5 Ambulatorio Medico San Luca Villanuova, Villanuova sul Clisi, 25089 Brescia, Italy
* Correspondence: lopalco.lucia@hsr.it (L.L.); n.temperton@kent.ac.uk (N.T.)
† These authors contributed equally to this work.
‡ Collaborators/Membership of the Group/Team Name is provided in the Acknowledgements.

Abstract: Coronaviruses infections, culminating in the recent severe acute respiratory syndrome coronavirus 2 (SARS-CoV-2) pandemic beginning in 2019, have highlighted the importance of effective vaccines to induce an antibody response with cross-neutralizing activity. COVID-19 vaccines have been rapidly developed to reduce the burden of SARS-CoV-2 infections and disease severity. Cross-protection from seasonal human coronaviruses (hCoVs) infections has been hypothesized but is still controversial. Here, we investigated the neutralizing activity against ancestral SARS-CoV-2 and the variants of concern (VOCs) in individuals vaccinated with two doses of either BNT162b2, mRNA-1273, or AZD1222, with or without a history of SARS-CoV-2 infection. Antibody neutralizing activity to SARS-CoV-2 and the VOCs was higher in BNT162b2-vaccinated subjects who were previously infected with SARS-CoV-2 and conferred broad-spectrum protection. The Omicron BA.1 variant was the most resistant among the VOCs. COVID-19 vaccination did not confer protection against hCoV-HKU1. Conversely, antibodies induced by mRNA-1273 vaccination displayed a boosting in their neutralizing activity against hCoV-NL63, whereas AZD1222 vaccination increased antibody neutralization against hCoV-229E, suggesting potential differences in antigenicity and immunogenicity of the different spike constructs used between various vaccination platforms. These data would suggest that there may be shared epitopes between the HCoVs and SARS-CoV-2 spike proteins.

Keywords: SARS-CoV-2; seasonal; HKU1; 229E; NL63; neutralisation

Citation: Cantoni, D.; Siracusano, G.; Mayora-Neto, M.; Pastori, C.; Fantoni, T.; Lytras, S.; Di Genova, C.; Hughes, J.; on behalf of the Ambulatorio Medico San Luca Villanuova Group; Lopalco, L.; et al. Analysis of Antibody Neutralisation Activity against SARS-CoV-2 Variants and Seasonal Human Coronaviruses NL63, HKU1, and 229E Induced by Three Different COVID-19 Vaccine Platforms. *Vaccines* **2023**, *11*, 58. https://doi.org/10.3390/vaccines11010058

Academic Editor: Seth Pincus

Received: 4 November 2022
Revised: 20 December 2022
Accepted: 22 December 2022
Published: 27 December 2022

1. Introduction

In December 2019, the outbreak of a novel coronavirus named severe acute respiratory syndrome coronavirus 2 (SARS-CoV-2) rapidly spread around the world, resulting in a global pandemic [1]. Since then, international efforts to generate a suitable therapeutic have resulted in the development of multiple vaccination platforms and other antiviral pharmaceuticals. The gradual rise of variants has had a reduced impact on the efficacy of neutralising antibodies raised either by previous infection of SARS-CoV-2 or by vaccination [2,3]. The World Health Organisation (WHO) has categorised the troubling variants as variants of concern (VOC), whereas other variants that do not meet the same criteria

fall under variants of interest (VOI) or variants under investigation (VUI). There has been a substantial amount of focus on variants and their characteristics, such as antibody evasion and replication rates, with many studies comparing variants and their ability to be neutralised [4–8], as the pandemic continues to progress.

SARS-CoV-2 belongs to the *Coronaviridae* family that includes SARS-CoV-1 [9], middle eastern respiratory virus (MERS) [10] and four human coronaviruses 229E, HKU-1, NL63, and OC43 [11] (Figure 1A). Whilst SARS-CoV-1 and MERS have had outbreaks that caused severe disease in humans [12], the four other coronaviruses, commonly referred to as seasonal or human coronaviruses (HCoVs), typically cause mild disease similar to a common cold [11,13]. On rare occasions, however, the HCoVs may cause severe diseases [14–16]. SARS-CoV-2, together with NL63, use angiotensin-converting enzyme 2 (ACE2) as their major cell entry receptor [17,18]. Despite HKU1 and OC43 being more closely related to SARS-CoV-2, they bind to sialic acids as a mode of entry [19], whereas more distantly related 229E uses human aminopeptidase (hAPN) [20]. (Figure 1B).

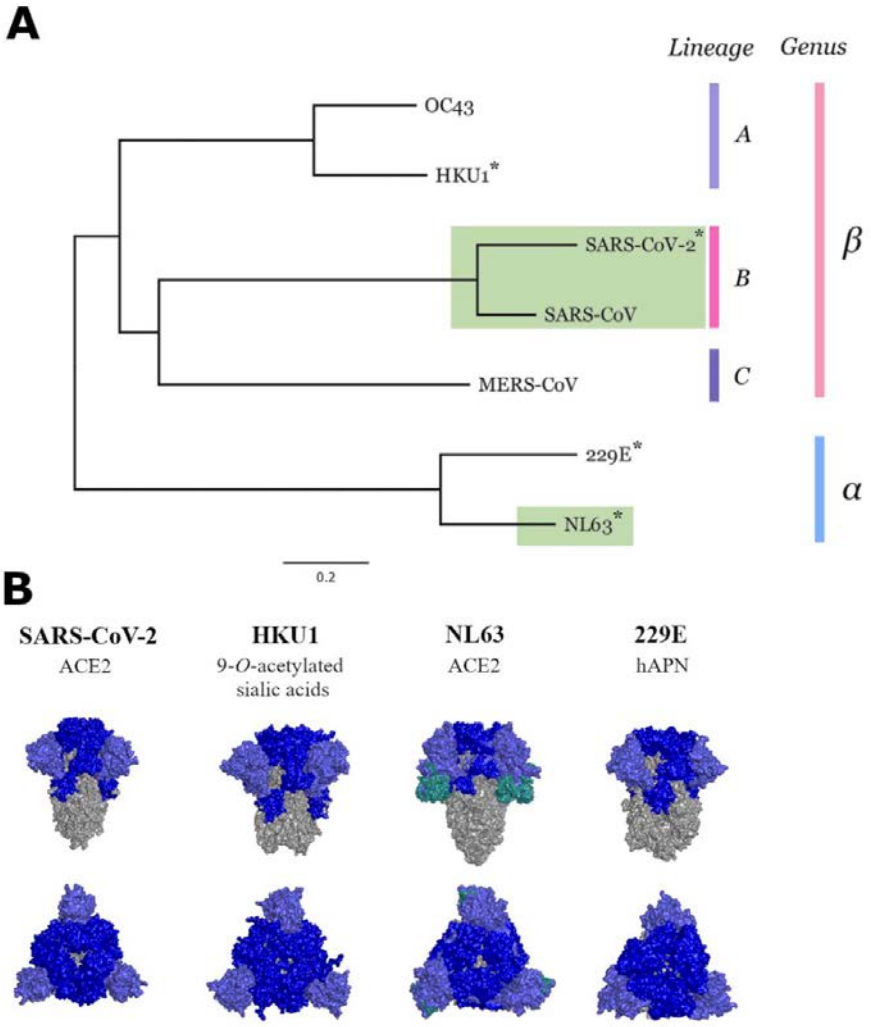

Figure 1. Phylogenetic tree of the members in the *Coronaviridae* family. * denotes spike proteins that were used in this study (**A**). Structures of spike proteins of SARS-CoV-2, and three of the seasonal HCoVs; HKU1, NL63 and 229E, which were used in this study (**B**). (PDB codes: 6VXX, 60HW, 6U7H, 5I08, and 5SZS). Grey denotes the S2 domain, whereas light blue is the N-terminal domain of S1 subunit, and dark blue represents the remaining S1 subunit. NL63 has an additional teal coloured section representing a unique region in the S1 domain not observed in other coronaviruses [21].

At the start of the pandemic, there was a debate as to the possibility that antibodies raised against the HCOVs had any role in protection against SARS-CoV-2 [22–25]. Since then, rising interest in HCoVs has led to an increase in understanding of the immune response they generate. Several publications that investigated the effect of HCoVs relied on the use of binding assays such as enzyme linked immunosorbent assays (ELISA) that measure antibody binding but did not elucidate their neutralising capabilities. Moreover, successful generation of various vaccine platforms have been used to protect individuals from infection and severe disease [26], though their effectiveness is diminished as newer and more immune evasive variants arise [27]. Here, we use lentiviral-based pseudotyped viruses of SARS-CoV-2, the VOCs/VOI, and HCoVs, to measure the strength of neutralising antibodies induced by two doses of either BNT162b2 (Pfizer), AZD1222 (Astrazeneca), or mRNA-1273 (Moderna) against SARS-CoV-2 and variants B.1.1.7 (Alpha), B.1.351 (Beta), P.1 (Gamma), B.1.617.2 (Delta), B.1.525 (Eta), and B.1.1.529 (Omicron BA.1) (Figure 2), and whether any of these vaccines are able to augment neutralising antibodies against HCoVs 229E, HKU1, or NL63.

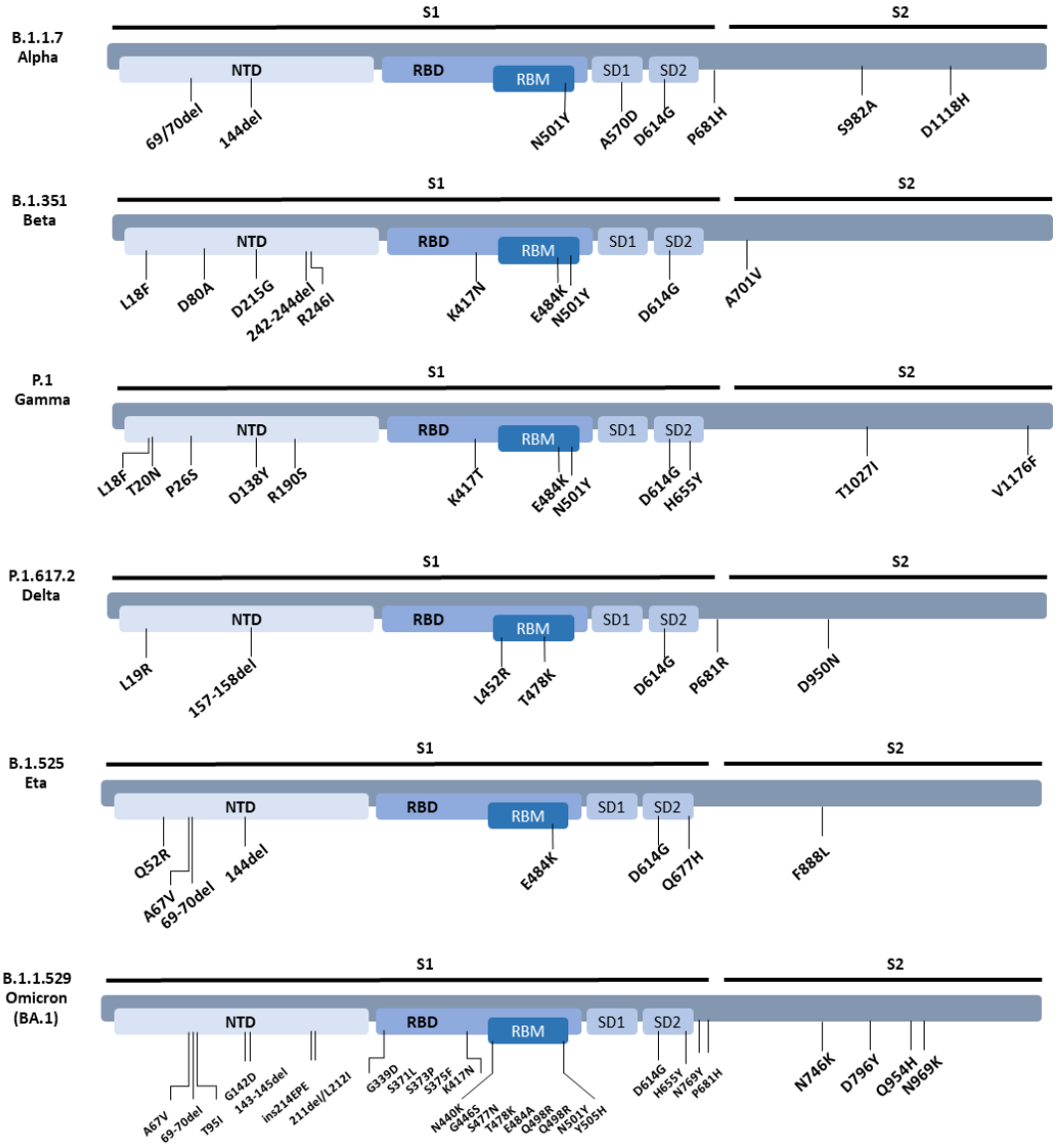

Figure 2. SARS-CoV-2 variants spike mutations used in this study.

2. Materials and Methods

2.1. Patient Serum Collection/Ethics Information

Sera samples were collected from 36 healthy vaccinated subjects. The study was approved by San Raffaele Scientific Hospital Ethical Committee (protocol number 68/INT/2020). All enrolled patients gave written, informed consent.

2.2. Phylogenetic Tree and Similarity Plot

A maximum likelihood phylogenetic reconstruction based on the spike gene codon alignment, was constructed using iqtree (version 1.6.12) [28] with 10,000 ultra-fast bootstrap replicates [29] and a TVM+F+I+G4 substitution model, selected using ModelFinder [30]. The sequence similarity plot was constructed by aligning spike protein sequences of SARS-CoV-2 (QHD43416.1), HKU1 (YP_173238.1) 229E (NP_073551.1) and NL63 (YP_003767.1), using mafft (version 7.453) [31] (genafpair option) and visualised using the D3 JavaScript package implemented in observable (https://observablehq.com/@spyros-lytras/seasonal-cov-spike accessed on 3 November 2022).

2.3. Tissue Culture

Human embryonic kidney 293T/17 (HEK293T/17) cells and human hepatocytes Huh-7 cells were maintained in DMEM supplemented with 10% foetal bovine serum and 1% penicillin/streptomycin. Chinese ovarian hamster (CHO) cells were maintained in Ham's F12 supplemented with 10% foetal bovine serum and 1% penicillin/streptomycin. Cells were routinely passaged to prevent confluency by washing with phosphate-buffered saline solution and detached with trypsin-EDTA. All cells were incubated at 37 °C and 5% CO_2.

2.4. Pseudotype Virus Production

All pseudotypes (PVs) were generated as previously described [32]. Briefly, 1000 ng of pc-DNA 3.1+ plasmid bearing the spike of ancestral SARS-CoV-2, variants Alpha, Beta, Delta, Gamma, Eta, Omicron Ba.1, or HCoVs 229E, HKU1, and NL63 was mixed with 1000 ng of p8.91 plasmid encoding the HIV Gag-pol and 1500 ng of pCSFLW plasmid containing the *Renilla firefly* luciferase reporter gene, and co-transfected onto HEK293T cells at 50% confluency in T-75 flasks using FuGENE-HD. HKU-1 required an additional step of adding 1.5 U of exogenous neuraminidase (Sigma) in 10 mL of replenished DMEM 24 h after transfection. To harvest the pseudotyped viruses, media was aspirated 48 h after day of transfection and filtered using a 0.45 µm cellulose acetate filter. All PVs were aliquoted and stored at −80 °C for storage. After repeated attempts, we were unable to pseudotype HCoV OC43.

2.5. Pseudotype Virus Titration

All PVs were titrated as previously described [32]. Target cells for SARS-CoV-2, variants, and HCoV NL63 were prepared the day before titration by transfecting ACE-2 and TRSSMP2. CHO cells were used as target cells for HKU-1, and Huh-7 cells were used as target cells for 229E. Briefly, 50 µL of harvested PV were added in the top row of a white F-bottom 96-well plate (Nunc), and serially diluted using DMEM or Ham's F-12 for HKU-1 PVs in half steps to the bottom row of the plate prior to addition of 10,000 target cells in each well. Plates were returned to the incubator for 48 h prior to lysis with Bright-Glo reagent and assaying luciferase reporter gene activity in relative line units (RLU) using a Glo-Max luminometer. PV titres are reported in RLU/mL.

2.6. Pseudotype Microneutralisation (pMN) Assays

The pMN assay was carried out as previously described. Briefly, convalescent sera were mixed with either DMEM or Ham's F-12 at an initial 1:40 dilution and then serially diluted 2-fold in a white flat-bottomed 96-well plate to a final dilution of 1:5120. All samples were repeated in duplicate. PVs were then added to each well at an input of 1×10^6 RLU/mL. Plates were returned to the tissue culture incubator for 1 h, prior to

addition of pre-transfected ACE-2/TRSSMP2 HEK293T target cells or CHO cells for HKU-1 and Huh-7 cells for 229E, at a density of 1×10^4 cells per well. Plates were returned to the incubator for 48 h prior to lysis with Bright-Glo reagent and assaying luciferase reporter gene activity in relative line units (RLU) using a Glo-Max luminometer. IC50s were calculated using GraphPad Prism 8 software using a non-linear regression curve as described in [33].

2.7. Statistical Analysis

Wilcoxon matched-pair ranked tests were used to assess significance in matched subjects. Kruskal–Wallis ANOVA test was used to assess significance when comparing IC50 titres between three vaccine platforms. All tests were used on Graphpad Prism 8 software.

3. Results

3.1. Cohort Characteristics

To assess the neutralizing potential of SARS-CoV-2 specific antibodies against SARS-CoV-2 VOCs and hCoVs, sera obtained from double-dosed BNT162b2-vaccinated (n = 13), AZD1222-vaccinated (n = 16) and mRNA-1273-vaccinated (n = 7) individuals with and without an history of SARS-CoV-2 infection were inspected (Table 1).

Table 1. Demographic and clinical characteristics of the cohort.

Total	**36**
Demographics	
Age (median [IQR], Range)	49 [43.5, 55.25] (24–62)
Sex (Male/Female)	8/28
SARS-CoV-2 Prior Infection (Yes/No)	11/28
BNT162b2 Samples (1st dose/2nd Dose)	13/13
mRNA-1273 Samples (1st dose/2nd Dose)	7/7
AZD1222 Samples (1st dose/2nd Dose)	16/16
Time of bleed after 1st dose	21 days (BNT162b2 and mRNA-1273) 12 weeks (AZD1222)
Time of bleed after 2nd dose	15 weeks

3.2. Neutralisation of SARS-CoV-2 Variants

We first carried out pMN assays to analyse the magnitude of neutralising antibody responses against ancestral SARS-CoV-2 and variants, irrespective of vaccine type (Figure 3A). Our results showed that Omicron BA.1 was the least neutralised VOC (24-fold decrease, $p =< 0.0001$). As expected, we observed the samples from individuals with prior infection had higher neutralisation titres compared with immunological naïve subjects.

The serum from previously infected individuals (Figure 3B), neutralized the Alpha variant more effectively compared with the ancestral strain, as it showed a 1.3-fold decrease in median IC_{50} titre, followed by Eta and Delta variants, (3.4- and 4.5-fold decrease, respectively). Beta and Gamma variants were more resistant to neutralization (10.9- and 9.7-fold decrease, respectively), and Omicron BA.1 reached a 16.1-fold decrease compared with ancestral SARS-CoV-2. Notably, the majority of these subjects had received the BNT162b2 vaccine.

Taken together, these results suggested that in vaccinated subjects the pre-existing immunity raised by natural infection with SARS-CoV-2, or a VOC is more effective in protecting against the spectrum of variants that emerged later over time, compared with immunity triggered by vaccination only. However, the recently emerged variants evolved mechanisms to evade the neutralizing antibody response.

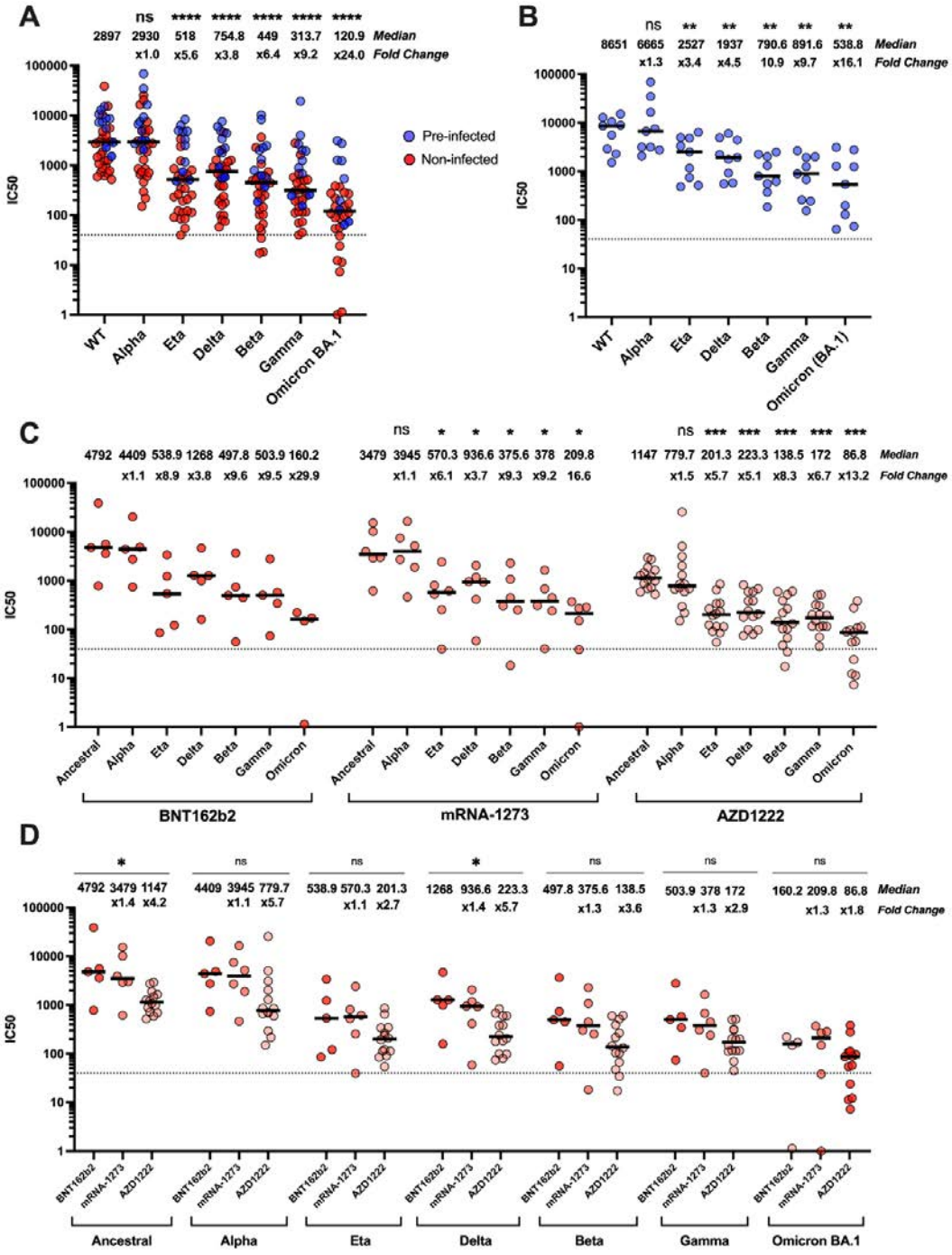

Figure 3. Ability of serum antibodies to neutralise SARS-CoV-2 and VOCs from individuals vaccinated with two doses of either BNT162b2, AZD1222, or mRNA-1273. Neutralizing antibody response against the ancestral SARS-CoV-2 and variants, in previously infected individuals (blue) and non-infected individuals (red) receiving two doses of either BNT162b2, AZD1222, or mRNA-1273 vaccines (**A**). Wilcoxon matched-pairs signed rank tests statistical analysis was used to compare ancestral SARS-CoV-2 against each variant (**A**). Neutralisation profiles of sera from BNT162b2-vaccinated subjects with a history of prior infection. No statistical test was used for BNT162b2 in panel C due to small sample size with large variation. (**B**). Neutralisation profiles of the three vaccine types against variants (**C**) and compared between vaccine platforms. (**D**) Wilcoxon matched-pairs signed rank tests statistical analysis was used to compare ancestral SARS-CoV-2 against each variant in panel C. Kruskal–Wallis ANOVA was used for statistical analysis in panel D. ns = not significant, * $p < 0.05$, ** $p < 0.01$, *** $p < 0.001$, **** $p \leq 0.0001$.

We then analysed subjects who had not experienced SARS-CoV-2 infection before vaccine administration (Figure 3C). The efficacy of each vaccine platform was analysed with respect to the capability to neutralize both the ancestral strain and its variants. We observed that the sera from BNT162b2-vaccinated subjects had high median IC_{50} titres compared with those obtained from mRNA-1273- and AZD1222-vaccinated individuals. Whereas the Alpha variant did not show immune escape in any of the vaccinated subjects, all the VOCs were resistant to antibody neutralization to different degrees (Figure 3C). We were unable to extract meaningful significance scores from the BNT162b2 samples due to few samples (n = 5) with very large spread in IC_{50} titres.

We did not observe any statistically significant difference between the three vaccine platforms with respect to their abilities to neutralize the Alpha, Eta, Beta, Gamma, and BA.1 variants. Conversely, the biggest difference between the three vaccine types was observed with ancestral and Delta variant, as mRNA-1273 showed a 1.6- and 1.4-fold decrease in median IC_{50} titres, respectively, compared with BNT162b2, whereas AZD1222 showed a 3.8- and 4.1-fold decrease (Figure 3D).

3.3. Neutralisation of Seasonal HCoVs

To determine whether vaccination against SARS-CoV-2 may cross-protect against seasonal HCoVs, we asked whether a prior infection with SARS-CoV-2 had any impact on antibody-mediated neutralisation of the HCoVs (Figure 4A). We observed no statistically significant increases in neutralizing titres against either 229E or HKU-1 between previously SARS-CoV-2 infected and naïve individuals. Conversely, a statistically significant decrease in neutralizing titres against NL63 after the second dose administration was found in vaccinated subjects who experienced SARS-CoV-2 infection ($p = 0.033$) compared with the naïve ($p = 0.063$).

We then assessed whether one or more of the vaccine platforms would boost titres against the HCoVs in all subjects, irrespective of their previous infection status (Figure 4B). Overall, in vaccinated subjects, the median antibody neutralization titres against NL63 were higher compared with those against 229E and HKU1, irrespective of the vaccine platform (Figure 4B). Notably, NL63 uses ACE2 as entry receptor into the target cells, as does SARS-CoV-2.

The type of vaccine did not have an impact in boosting the neutralizing activities against the three seasonal coronaviruses we studied after the second dose administration, with the exception of NL63 and HKU1. IC_{50} titres against NL63 increased after the second dose using mRNA-1273 ($p = 0.03$), whereas 229E showed a statistically significant increase in IC_{50} titre in only AZD1222-vaccinated individuals ($p =< 0.001$). Conversely, after the second boost of BNT162b2 vaccine, neutralization titres against HCoV HKU-1 decreased, probably due to the selection of antigen-specific plasma cells with lower affinity for the HKU1 spike.

To better understand the impact of COVID-19 vaccination on the protection from seasonal HCoVs in subjects with or without a history of SARS-CoV-2 infection, we analysed the spike protein similarity of HCoVs HKU1, NL63, 229E and SARS-CoV-2 to investigate whether a particular region could explain the neutralisation differences (Figure 4C). The similarity plot generated by comparing pairwise similarity showed HKU1 had higher similarity in all spike regions to SARS-CoV-2 spike compared with 229E and NL63, consistent with the viruses' taxonomy. However, HKU1 seems to have extra insertions at the C-terminal end of the RBD compared with the other two seasonals and SARS-CoV-2. Furthermore, the S2 region shows much higher similarity to SARS-CoV-2 in all three HCoVs compared with the S1 region (Figure 4C).

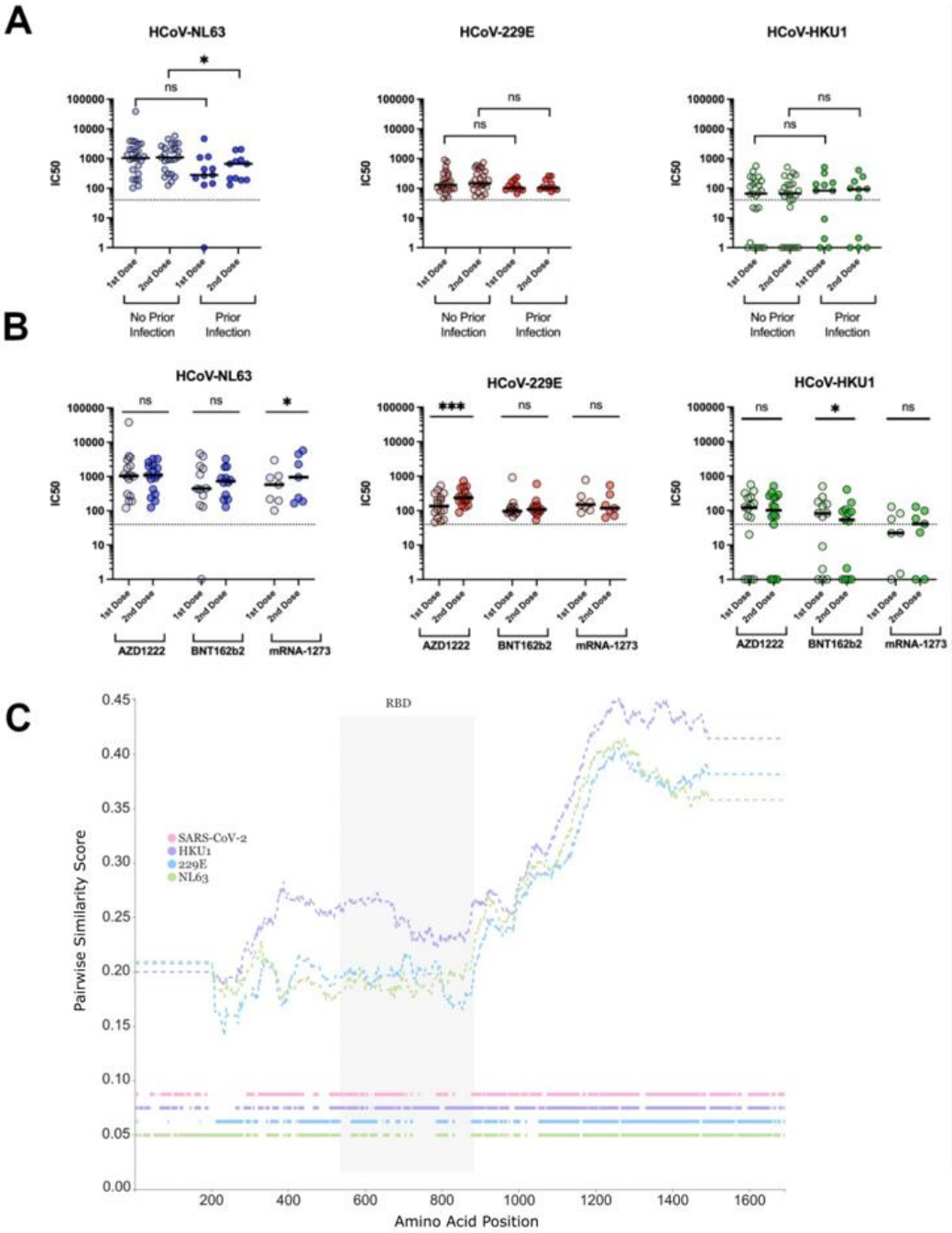

Figure 4. Comparing neutralising responses in HCoVs NL63, 229E, and HKU1 between first- and second-dose vaccination against SARS-CoV-2. Neutralization profile against HCoVs NL63, 229E, and HKU1 in double-dosed BNT162b2, mRNA-1273 or AZD1222 –vaccinated subjects with or without a history of SARS-CoV-2 infection. (**A**). Neutralizing antibody titres against the aforementioned HCoVs after the first and second dose administration of BNT162b2, mRNA-1273 or AZD1222 vaccines. (**B**). Wilcoxon matched-pairs signed rank tests statistical analysis was used in A and B. Similarity plots (**C**) show HKU-1 spike as having more similar amino acid sequence to SARS-CoV-2 compared with both NL63 and 229E in all regions of the spike protein. Dashed lines on the top show amino acid pairwise similarity between SARS-CoV-2 and the 3 HCoV Spike proteins, plotted using a 400 amino acid window size and a step of 1. Positions with gaps were excluded from the windows. Horizontal lines on the bottom indicate residue presence for each of the 4 aligned coronaviruses across the alignment length (colour presence = amino acid presence; colour absence = gap). ns = not significant, * $p < 0.05$, *** $p < 0.001$.

4. Discussion

In this study, we were able to directly compare the antibody neutralisation titres induced by two m-RNA-based vaccines, BNT162b2 and mRNA-1273, and an adenoviral-based vaccine, AZD1222, against SARS-CoV-2, its emerged variants, and three seasonal HCoVs.

Our data on antibody neutralization against SARS-CoV-2 and its variants in vaccinated subjects, with or without a history of previous infection, agree with what is reported in the literature [2,4,5,7,34–38]. We confirmed that vaccination with two doses of vaccines induced antibodies able to neutralize SARS-CoV-2 and VOCs, with BNT162b2 eliciting the highest neutralization titres, followed by mRNA-1273 and AZD1222. Despite their differences in neutralization titres, all three vaccines have been reported to have high efficacy at preventing severe COVID-19 [39–41]. The Omicron BA.1 variant was the most evasive of all VOCs analysed in this study (Figure 3). Indeed, the heavily mutated spike protein of BA.1 variant posed challenges to the effectiveness of the current vaccines to protect against COVID-19 and pointed out the need to monitor the protection conferred against this and the newly emerged SARS-CoV-2 variants, namely Omicron BA.4 and BA.5. Bivalent formulations of mRNA-based vaccines, containing both the mRNA of the spike of the ancestral SARS-CoV-2 and the one in common between the BA.4 and BA.5 lineages have been designed and authorized in order to counteract the evasion of the immune response elicited by the original vaccine design.

HCoVs are globally distributed and believed to induce short-lasting protective antibodies [42]. Therefore, there is a high likelihood of reinfection remaining elevated, especially during the winter periods [13,43–45] despite high seroprevalence [43,45,46]. It is currently debated whether prior infection with seasonal HCoVs elicits cross-reactive antibodies against SARS-CoV-2, and more importantly, if this translates into protection against SARS-CoV-2. Cross-reactive antibodies [47–54] and T-cell responses [55–61] were detected in pre-pandemic sera and healthy donors; however, similar experimental approaches have shown the opposite to be true by other investigators [62]. In addition, in many of the aforementioned articles that revealed cross-reactive antibodies in pre-pandemic samples, the number of cross-reactive samples was a small portion of the total sera analysed, suggesting that cross-reactivity, whilst it exists, is low.

The same question has been raised about antibodies elicited by COVID-19 vaccines, with studies showing cross-reactive antibodies to some but not all the seasonal HCoVs [63–65]. SARS-CoV-2 spike protein vaccination was shown to induce cross-reactive antibodies to both *Alpha-* and *Betacoronaviruses* in macaques [66]. It is important to deduce whether cross-reactive antibodies translate into protective, neutralising antibodies against SARS-CoV-2. Some reports suggested that whilst there is a small boost in antibodies towards HCoVs during SARS-CoV-2 infection, they are not associated with protection [67]. Similarly, studies showed that prior infection with HCoVs did not protect against SARS-CoV-2 infection and disease [68,69].

We did not find any boost of neutralizing antibody titres against HKU1 in our cohort of SARS-CoV-2-vaccinated subjects, irrespective of their SARS-CoV-2 pre-infectious status, with the exception of subjects administered with BNT162b2. This is in contrast with two reports that observed a boost in HKU-1 titres post vaccination against SARS-CoV-2 by BNT162b2 [63,64]. Hicks et al. showed that antibodies reacting to HCoV-OC43 and HCoV-HKU1 had minimal cross-reactivity with SARS-CoV-2, in accordance with the sequence homology of these proteins [54]. Moreover, a previous SARS-CoV-2 infection did not boost the cross-neutralization against either HKU1 or the more phylogenetically related HCoV-229E (Figure 4A). One report suggested that HKU1 may have another candidate receptor that has yet to be identified, due to the presence of a putative RBD, distant from the sialic acid binding regions [70,71]. It should also be noted that neutralising ability might not only be dependent on the pairwise similarity between amino acids in the protein, but also short insertions and deletions that can alter the protein's structural conformation. For

instance, the HKU-1-specific insertion at the C-terminal end of the RBD (Figure 4C) might partly explain our neutralisation results.

Conversely, we found that the second dose administration in naïve subjects increased the protective antibody response against NL63 compared with that obtained in previously infected subjects receiving the same dose. This was probably due to the fact that additional exposures to the spike antigen did not have an effect on antibody neutralization against NL63.

The differences in antibody neutralization between the HCoVs may be due to the differences in the spikes used by the vaccination platforms. BNT162b27 encodes full-length spike with the K986P and V987P mutation sites to stabilize the pre-fusion conformation of the protein [72]. The mRNA-1273 vaccine contains the coding sequence for a spike glycoprotein stabilized by the same proline substitutions used in the BNT162b2 vaccine, with a transmembrane anchor and an intact S1-S2 cleavage site. The pre-fusion conformation is stabilized by the consecutive proline substitutions, which are located in the S2 subunit at the top of the central helix [73]. Conversely, a native-like spike is expressed by the AZD1222 vaccine. As our naïve subjects were administered with the AZD1222 vaccine, we can speculate that the native form of the spike protein triggered the development of higher neutralizing antibodies titres compared with that induced by the pre-fusion-stabilized protein.

Conversely, the second immunogenic exposure to SARS-CoV-2 spike boosted the neutralizing response against NL63 or 229E (Figure 4B), as has been previously reported [67], depending on the vaccine platform, irrespective of the pre-infection status. Interestingly, another report observed the same cross-neutralizing activity, though this was irrespective of vaccine platform [74]. We speculate that cross reactivity can arise due to similarity in epitopes in the receptor-binding motif (RBM) of NL63 to SARS-CoV-2, since both viruses share ACE-2 as their entry receptor [75]. Similarly, an epitope overlapping the S2 fusion peptide in 229E has been reported to elicit cross-reactivity against SARS-CoV-2 [48]. Song et al. described protective neutralizing antibodies targeting the S2 subdomain [53]. Furthermore, a report during the original SARS-CoV-1 outbreak also found cross reactive antibodies against NL63 and 229E [76], strengthening the hypothesis of shared epitopes between *Alphacoronaviruses* and *Betacoronaviruses*. The S protein of NL63 does not contain the furin-recognition site and is not cleaved during biogenesis [77]. Similarly, the spike protein expressed by the mRNA1273 vaccine lacks the cleavage site; therefore, the conformation of the protein might be similar and might trigger neutralizing antibodies against shared epitopes and that are boosted after a second exposure to the same antigen.

The antigenic nature of the spike protein expressed by the different vaccines, together with multiple conformations they can acquire, might affect the development of neutralizing antibodies with different affinities towards several epitopes in the spike protein. Since the AZD-1222 spike does not contain the two proline mutations to stabilise its spike into a trimeric pre fusion structure [78,79], the presence of a post fusion spike could potentially elicit a larger immune response towards epitopes in the S2 domain. This may explain why we did not observe any boost in neutralizing titres against 229E in either mRNA-based, pre-fusion-stabilized immunogen, vaccinated samples. Ultimately, despite observing a boost in titres, it is impossible for us to state whether this translates into protective titres since correlates of protection against SARS-CoV-2 have yet to be defined.

There are several limitations in our study to consider. Our data would have benefitted from larger numbers of samples in all vaccine platform types, and control samples of non-vaccinated individuals who either have been infected with SARS-CoV-2 or not. Furthermore, we did not analyse the baseline levels of cross-reactive neutralizing antibodies against seasonal coronaviruses in our cohort of vaccinated subjects.

A pan-coronavirus vaccine would elicit antibodies that recognise and neutralise a broad range of coronaviruses. This is challenging because of the genetic nature of these RNA viruses that frequently mutate and induce an immunity that wanes over time, increasing the likelihood of reinfection. Therefore, identifying the key epitopes located at the most

conserved regions of the spike protein, especially at the S2 subunit, is relevant to potentially induce neutralizing antibodies with broader affinity to the cellular receptors that mediate viral entry. Several vaccine candidates have been formulated, and some are based on dual antigens including both spike and nucleocapsid (N) components [80]. These formulations are at the pre-clinical stage as they might provide broader and more durable humoral and cellular immune responses against coronaviruses [80].

Author Contributions: Conceptualization, D.C., G.S., L.L. and N.T.; methodology, D.C, G.S, L.L. and N.T.; investigation, D.C., G.S., M.M.-N., C.P., T.F., S.L., C.D.G. and J.H.; data curation, D.C.; writing—original draft preparation, D.C and G.S.; writing—review and editing, D.C., G.S., M.M.-N., C.P., T.F., S.L., C.D.G., J.H., L.L., N.T. and Ambulatorio Medico San Luca Villanuova Group; funding acquisition, L.L. and N.T. All authors have read and agreed to the published version of the manuscript.

Funding: The Temperton group (N.T., D.C., C.D.G. and M.M.N.) is funded by the Wellcome Trust (GB-CHC-210183), the MRC (MC_PC_19060) and MRC/NIHR (MC_PC_20016). S.L. and J.H. are funded by MC_UU_12014/12. L.L. was supported by the Scientific Direction of San Raffaele Scientific Institute (Immuno-COVID) and ANR France (MUCOLUNG).

Institutional Review Board Statement: The study was conducted in accordance with the Declaration of Helsinki and approved by the Institutional Review Board (or Ethics Committee) of San Raffaele Scientific Hospital Ethical Committee (protocol number 68/INT/2020).

Informed Consent Statement: Informed consent was obtained from all subjects involved in the study.

Data Availability Statement: All datasets are available by contacting the corresponding author upon kind request.

Acknowledgments: We would like to acknowledge the Ambulatorio Medico San Luca Villanuova Group members (Bettini, G.L., Bonvicini, A., Braga, A., Chappini, F., Inverardi, F., Ravera, S., Rossi, M.G., Sas, A., Tuttini, A.) and patients who enrolled in this study.

Conflicts of Interest: The authors declare no conflict of interest.

References

1. Zhu, N.; Zhang, D.; Wang, W.; Li, X.; Yang, B.; Song, J.; Zhao, X.; Huang, B.; Shi, W.; Lu, R.; et al. A Novel Coronavirus from Patients with Pneumonia in China, 2019. *N. Engl. J. Med.* **2020**, *382*, 727–733. [CrossRef] [PubMed]
2. Altmann, D.M.; Boyton, R.J.; Beale, R. Immunity to SARS-CoV-2 Variants of Concern. *Science* **2021**, *371*, 1103–1104. [CrossRef] [PubMed]
3. Burki, T. Understanding Variants of SARS-CoV-2. *Lancet* **2021**, *397*, 462. [CrossRef] [PubMed]
4. Garcia-Beltran, W.F.; Lam, E.C.; St. Denis, K.; Nitido, A.D.; Garcia, Z.H.; Hauser, B.M.; Feldman, J.; Pavlovic, M.N.; Gregory, D.J.; Poznansky, M.C.; et al. Multiple SARS-CoV-2 Variants Escape Neutralization by Vaccine-Induced Humoral Immunity. *Cell* **2021**, *184*, 2372–2383. [CrossRef] [PubMed]
5. Hoffmann, M.; Arora, P.; Groß, R.; Seidel, A.; Hörnich, B.F.; Hahn, A.S.; Krüger, N.; Graichen, L.; Hofmann-Winkler, H.; Kempf, A.; et al. SARS-CoV-2 Variants B.1.351 and P.1 Escape from Neutralizing Antibodies. *Cell* **2021**, *184*, 2384–2393. [CrossRef]
6. Cantoni, D.; Mayora-Neto, M.; Nadesalingam, A.; Wells, D.A.; Carnell, G.W.; Ohlendorf, L.; Ferrari, M.; Palmer, P.; Chan, A.C.Y.; Smith, P.; et al. Neutralisation Hierarchy of SARS-CoV-2 Variants of Concern Using Standardised, Quantitative Neutralisation Assays Reveals a Correlation With Disease Severity; Towards Deciphering Protective Antibody Thresholds. *Front. Immunol.* **2022**, *13*, 773982. [CrossRef]
7. Planas, D.; Bruel, T.; Grzelak, L.; Guivel-Benhassine, F.; Staropoli, I.; Porrot, F.; Planchais, C.; Buchrieser, J.; Rajah, M.M.; Bishop, E.; et al. Sensitivity of Infectious SARS-CoV-2 B.1.1.7 and B.1.351 Variants to Neutralizing Antibodies. *Nat. Med.* **2021**, *27*, 917–924. [CrossRef]
8. Lustig, Y.; Zuckerman, N.; Nemet, I.; Atari, N.; Kliker, L.; Regev-Yochay, G.; Sapir, E.; Mor, O.; Alroy-Preis, S.; Mendelson, E.; et al. Neutralising Capacity against Delta (B.1.617.2) and Other Variants of Concern Following Comirnaty (BNT162b2, BioNTech/Pfizer) Vaccination in Health Care Workers, Israel. *Eurosurveillance* **2021**, *26*, 2100557. [CrossRef]
9. Ksiazek, T.G.; Erdman, D.; Goldsmith, C.S.; Zaki, S.R.; Peret, T.; Emery, S.; Tong, S.; Urbani, C.; Comer, J.A.; Lim, W.; et al. A Novel Coronavirus Associated with Severe Acute Respiratory Syndrome. *N. Engl. J. Med.* **2003**, *348*, 1953–1966. [CrossRef]
10. Zaki, A.M.; van Boheemen, S.; Bestebroer, T.M.; Osterhaus, A.D.M.E.; Fouchier, R.A.M. Isolation of a Novel Coronavirus from a Man with Pneumonia in Saudi Arabia. *N. Engl. J. Med.* **2012**, *367*, 1814–1820. [CrossRef]

11. Liu, D.X.; Liang, J.Q.; Fung, T.S. Human Coronavirus-229E, -OC43, -NL63, and -HKU1 (Coronaviridae). In *Encyclopedia of Virology*, 4th ed.; Bamford, D.H., Zuckerman, M., Eds.; Academic Press: Oxford, UK, 2021; pp. 428–440. ISBN 978-0-12-814516-6.
12. de Wit, E.; van Doremalen, N.; Falzarano, D.; Munster, V.J. SARS and MERS: Recent Insights into Emerging Coronaviruses. *Nat. Rev. Microbiol.* **2016**, *14*, 523–534. [CrossRef]
13. Gaunt, E.R.; Hardie, A.; Claas, E.C.J.; Simmonds, P.; Templeton, K.E. Epidemiology and Clinical Presentations of the Four Human Coronaviruses 229E, HKU1, NL63, and OC43 Detected over 3 Years Using a Novel Multiplex Real-Time PCR Method. *J. Clin. Microbiol.* **2010**, *48*, 2940–2947. [CrossRef]
14. Da Veiga, A.B.G.; Martins, L.G.; Riediger, I.; Mazetto, A.; Debur, M.d.C.; Gregianini, T.S. More than Just a Common Cold: Endemic Coronaviruses OC43, HKU1, NL63, and 229E Associated with Severe Acute Respiratory Infection and Fatality Cases among Healthy Adults. *J. Med. Virol.* **2021**, *93*, 1002–1007. [CrossRef]
15. Arden, K.E.; Nissen, M.D.; Sloots, T.P.; Mackay, I.M. New Human Coronavirus, HCoV-NL63, Associated with Severe Lower Respiratory Tract Disease in Australia. *J. Med. Virol.* **2005**, *75*, 455–462. [CrossRef]
16. Hand, J.; Rose, E.B.; Salinas, A.; Lu, X.; Sakthivel, S.K.; Schneider, E.; Watson, J.T. Severe Respiratory Illness Outbreak Associated with Human Coronavirus NL63 in a Long-Term Care Facility. *Emerg. Infect. Dis.* **2018**, *24*, 1964–1966. [CrossRef]
17. Hoffmann, M.; Kleine-Weber, H.; Schroeder, S.; Krüger, N.; Herrler, T.; Erichsen, S.; Schiergens, T.S.; Herrler, G.; Wu, N.-H.; Nitsche, A.; et al. SARS-CoV-2 Cell Entry Depends on ACE2 and TMPRSS2 and Is Blocked by a Clinically Proven Protease Inhibitor. *Cell* **2020**, *181*, 271–280.e8. [CrossRef]
18. Hofmann, H.; Pyrc, K.; van der Hoek, L.; Geier, M.; Berkhout, B.; Pöhlmann, S. Human Coronavirus NL63 Employs the Severe Acute Respiratory Syndrome Coronavirus Receptor for Cellular Entry. *Proc. Natl. Acad. Sci. USA* **2005**, *102*, 7988–7993. [CrossRef]
19. Hulswit, R.J.G.; Lang, Y.; Bakkers, M.J.G.; Li, W.; Li, Z.; Schouten, A.; Ophorst, B.; van Kuppeveld, F.J.M.; Boons, G.-J.; Bosch, B.-J.; et al. Human Coronaviruses OC43 and HKU1 Bind to 9-O-Acetylated Sialic Acids via a Conserved Receptor-Binding Site in Spike Protein Domain A. *Proc. Natl. Acad. Sci. USA* **2019**, *116*, 2681–2690. [CrossRef]
20. Yeager, C.L.; Ashmun, R.A.; Williams, R.K.; Cardellichio, C.B.; Shapiro, L.H.; Look, A.T.; Holmes, K.V. Human Aminopeptidase N Is a Receptor for Human Coronavirus 229E. *Nature* **1992**, *357*, 420–422. [CrossRef]
21. Wu, K.; Li, W.; Peng, G.; Li, F. Crystal Structure of NL63 Respiratory Coronavirus Receptor-Binding Domain Complexed with Its Human Receptor. *Proc. Natl. Acad. Sci. USA* **2009**, *106*, 19970–19974. [CrossRef]
22. Meyerholz, D.K.; Perlman, S. Does Common Cold Coronavirus Infection Protect against Severe SARS-CoV-2 Disease? *J. Clin. Investig.* **2021**, *131*. [CrossRef] [PubMed]
23. Ringlander, J.; Martner, A.; Nilsson, S.; Westin, J.; Lindh, M.; Hellstrand, K. Incidence and Severity of Covid-19 in Patients with and without Previously Verified Infections with Common Cold Coronaviruses. *J. Infect. Dis.* **2021**, *223*, 1831–1832. [CrossRef]
24. Schnierle, B.S. Reply to Ringlander et al. *J. Infect. Dis.* **2021**, *223*, 1833. [CrossRef] [PubMed]
25. Beretta, A.; Cranage, M.; Zipeto, D. Is Cross-Reactive Immunity Triggering COVID-19 Immunopathogenesis? *Front. Immunol.* **2020**, *11*, 2695. [CrossRef] [PubMed]
26. Creech, C.B.; Walker, S.C.; Samuels, R.J. SARS-CoV-2 Vaccines. *JAMA* **2021**, *325*, 1318–1320. [CrossRef]
27. Tao, K.; Tzou, P.L.; Nouhin, J.; Gupta, R.K.; de Oliveira, T.; Kosakovsky Pond, S.L.; Fera, D.; Shafer, R.W. The Biological and Clinical Significance of Emerging SARS-CoV-2 Variants. *Nat. Rev. Genet.* **2021**, *22*, 757–773. [CrossRef]
28. Nguyen, L.-T.; Schmidt, H.A.; von Haeseler, A.; Minh, B.Q. IQ-TREE: A Fast and Effective Stochastic Algorithm for Estimating Maximum-Likelihood Phylogenies. *Mol. Biol. Evol.* **2015**, *32*, 268–274. [CrossRef]
29. Hoang, D.T.; Chernomor, O.; von Haeseler, A.; Minh, B.Q.; Vinh, L.S. UFBoot2: Improving the Ultrafast Bootstrap Approximation. *Mol. Biol. Evol.* **2018**, *35*, 518–522. [CrossRef]
30. Kalyaanamoorthy, S.; Minh, B.Q.; Wong, T.K.F.; von Haeseler, A.; Jermiin, L.S. ModelFinder: Fast Model Selection for Accurate Phylogenetic Estimates. *Nat. Methods* **2017**, *14*, 587–589. [CrossRef]
31. Katoh, K.; Standley, D.M. MAFFT Multiple Sequence Alignment Software Version 7: Improvements in Performance and Usability. *Mol. Biol. Evol.* **2013**, *30*, 772–780. [CrossRef]
32. Genova, C.D.; Sampson, A.; Scott, S.; Cantoni, D.; Mayora-Neto, M.; Bentley, E.; Mattiuzzo, G.; Wright, E.; Derveni, M.; Auld, B.; et al. Production, Titration, Neutralisation, Storage and Lyophilisation of Severe Acute Respiratory Syndrome Coronavirus 2 (SARS-CoV-2) Lentiviral Pseudotypes. *Bio-Protocol* **2021**, *11*, e4236. [CrossRef]
33. Ferrara, F.; Temperton, N. Pseudotype Neutralization Assays: From Laboratory Bench to Data Analysis. *Methods Protoc.* **2018**, *1*, 8. [CrossRef]
34. Liu, C.; Ginn, H.M.; Dejnirattisai, W.; Supasa, P.; Wang, B.; Tuekprakhon, A.; Nutalai, R.; Zhou, D.; Mentzer, A.J.; Zhao, Y.; et al. Reduced Neutralization of SARS-CoV-2 B.1.617 by Vaccine and Convalescent Serum. *Cell* **2021**, *184*, 4220–4236.e13. [CrossRef]
35. Shen, X.; Tang, H.; Pajon, R.; Smith, G.; Glenn, G.M.; Shi, W.; Korber, B.; Montefiori, D.C. Neutralization of SARS-CoV-2 Variants B.1.429 and B.1.351. *N. Engl. J. Med.* **2021**, *384*, 2352–2354. [CrossRef]
36. Shen, X.; Tang, H.; McDanal, C.; Wagh, K.; Fischer, W.; Theiler, J.; Yoon, H.; Li, D.; Haynes, B.F.; Sanders, K.O.; et al. SARS-CoV-2 Variant B.1.1.7 Is Susceptible to Neutralizing Antibodies Elicited by Ancestral Spike Vaccines. *Cell Host Microbe* **2021**, *29*, 529–539. [CrossRef]
37. Willett, B.J.; Grove, J.; MacLean, O.A.; Wilkie, C.; De Lorenzo, G.; Furnon, W.; Cantoni, D.; Scott, S.; Logan, N.; Ashraf, S.; et al. SARS-CoV-2 Omicron Is an Immune Escape Variant with an Altered Cell Entry Pathway. *Nat. Microbiol.* **2022**, *7*, 1161–1179. [CrossRef]

38. Siracusano, G.; Ruggiero, A.; Bisoffi, Z.; Piubelli, C.; Carbonare, L.D.; Valenti, M.T.; Mayora-Neto, M.; Temperton, N.; Lopalco, L.; Zipeto, D. Different Decay of Antibody Response and VOC Sensitivity in Naïve and Previously Infected Subjects at 15 Weeks Following Vaccination with BNT162b2. *J. Transl. Med.* **2022**, *20*, 22. [CrossRef]
39. Polack, F.P.; Thomas, S.J.; Kitchin, N.; Absalon, J.; Gurtman, A.; Lockhart, S.; Perez, J.L.; Pérez Marc, G.; Moreira, E.D.; Zerbini, C.; et al. Safety and Efficacy of the BNT162b2 MRNA Covid-19 Vaccine. *N. Engl. J. Med.* **2020**, *383*, 2603–2615. [CrossRef]
40. Baden, L.R.; El Sahly, H.M.; Essink, B.; Kotloff, K.; Frey, S.; Novak, R.; Diemert, D.; Spector, S.A.; Rouphael, N.; Creech, C.B.; et al. Efficacy and Safety of the MRNA-1273 SARS-CoV-2 Vaccine. *N. Engl. J. Med.* **2021**, *384*, 403–416. [CrossRef]
41. Emary, K.R.W.; Golubchik, T.; Aley, P.K.; Ariani, C.V.; Angus, B.; Bibi, S.; Blane, B.; Bonsall, D.; Cicconi, P.; Charlton, S.; et al. Efficacy of ChAdOx1 NCoV-19 (AZD1222) Vaccine against SARS-CoV-2 Variant of Concern 202012/01 (B.1.1.7): An Exploratory Analysis of a Randomised Controlled Trial. *Lancet* **2021**, *397*, 1351–1362. [CrossRef]
42. Edridge, A.W.D.; Kaczorowska, J.; Hoste, A.C.R.; Bakker, M.; Klein, M.; Loens, K.; Jebbink, M.F.; Matser, A.; Kinsella, C.M.; Rueda, P.; et al. Seasonal Coronavirus Protective Immunity Is Short-Lasting. *Nat. Med.* **2020**, *26*, 1691–1693. [CrossRef] [PubMed]
43. Aldridge, R.W.; Lewer, D.; Beale, S.; Johnson, A.M.; Zambon, M.; Hayward, A.C.; Fragaszy, E.B. Seasonality and Immunity to Laboratory-Confirmed Seasonal Coronaviruses (HCoV-NL63, HCoV-OC43, and HCoV-229E): Results from the Flu Watch Cohort Study. *Wellcome Open Res* **2020**, *5*, 52. [CrossRef] [PubMed]
44. Zhang, S.-F.; Tuo, J.-L.; Huang, X.-B.; Zhu, X.; Zhang, D.-M.; Zhou, K.; Yuan, L.; Luo, H.-J.; Zheng, B.-J.; Yuen, K.-Y.; et al. Epidemiology Characteristics of Human Coronaviruses in Patients with Respiratory Infection Symptoms and Phylogenetic Analysis of HCoV-OC43 during 2010-2015 in Guangzhou. *PLoS ONE* **2018**, *13*, e0191789. [CrossRef] [PubMed]
45. Byington, C.L.; Ampofo, K.; Stockmann, C.; Adler, F.R.; Herbener, A.; Miller, T.; Sheng, X.; Blaschke, A.J.; Crisp, R.; Pavia, A.T. Community Surveillance of Respiratory Viruses Among Families in the Utah Better Identification of Germs-Longitudinal Viral Epidemiology (BIG-LoVE) Study. *Clin. Infect. Dis.* **2015**, *61*, 1217–1224. [CrossRef] [PubMed]
46. Wells, D.A.; Cantoni, D.; Mayora-Neto, M.; Genova, C.D.; Sampson, A.; Ferrari, M.; Carnell, G.; Nadesalingam, A.; Smith, P.; Chan, A.; et al. Human Seasonal Coronavirus Neutralization and COVID-19 Severity. *J. Med. Virol.* **2022**, *94*, 4820–4829. [CrossRef]
47. Shrwani, K.; Sharma, R.; Krishnan, M.; Jones, T.; Mayora-Neto, M.; Cantoni, D.; Temperton, N.J.; Dobson, S.L.; Subramaniam, K.; McNamara, P.S.; et al. Detection of Serum Cross-Reactive Antibodies and Memory Response to SARS-CoV-2 in Prepandemic and Post–COVID-19 Convalescent Samples. *J. Infect. Dis.* **2021**, *224*, 1305–1315. [CrossRef]
48. Ng, K.W.; Faulkner, N.; Cornish, G.H.; Rosa, A.; Harvey, R.; Hussain, S.; Ulferts, R.; Earl, C.; Wrobel, A.G.; Benton, D.J.; et al. Preexisting and de Novo Humoral Immunity to SARS-CoV-2 in Humans. *Science* **2020**, *370*, 1339–1343. [CrossRef]
49. Woudenberg, T.; Pelleau, S.; Anna, F.; Attia, M.; Donnadieu, F.; Gravet, A.; Lohmann, C.; Seraphin, H.; Guiheneuf, R.; Delamare, C.; et al. Humoral Immunity to SARS-CoV-2 and Seasonal Coronaviruses in Children and Adults in North-Eastern France. *EBioMedicine* **2021**, *70*, 103495. [CrossRef]
50. Tso, F.Y.; Lidenge, S.J.; Peña, P.B.; Clegg, A.A.; Ngowi, J.R.; Mwaiselage, J.; Ngalamika, O.; Julius, P.; West, J.T.; Wood, C. High Prevalence of Pre-Existing Serological Cross-Reactivity against Severe Acute Respiratory Syndrome Coronavirus-2 (SARS-CoV-2) in Sub-Saharan Africa. *Int. J. Infect. Dis.* **2021**, *102*, 577–583. [CrossRef]
51. Laing, E.D.; Sterling, S.L.; Richard, S.A.; Phogat, S.; Samuels, E.C.; Epsi, N.J.; Yan, L.; Moreno, N.; Coles, C.; Mehalko, J.; et al. A Betacoronavirus Multiplex Microsphere Immunoassay Detects Early SARS-CoV-2 Seroconversion and Controls for Pre-Existing Seasonal Human Coronavirus Antibody Cross-Reactivity. *medRxiv* **2020**. [CrossRef]
52. Ladner, J.T.; Henson, S.N.; Boyle, A.S.; Engelbrektson, A.L.; Fink, Z.W.; Rahee, F.; D'ambrozio, J.; Schaecher, K.E.; Stone, M.; Dong, W.; et al. Epitope-Resolved Profiling of the SARS-CoV-2 Antibody Response Identifies Cross-Reactivity with Endemic Human Coronaviruses. *Cell Rep. Med.* **2021**, *2*, 100189. [CrossRef]
53. Song, G.; He, W.; Callaghan, S.; Anzanello, F.; Huang, D.; Ricketts, J.; Torres, J.L.; Beutler, N.; Peng, L.; Vargas, S.; et al. Cross-Reactive Serum and Memory B-Cell Responses to Spike Protein in SARS-CoV-2 and Endemic Coronavirus Infection. *Nat. Commun.* **2021**, *12*, 2938. [CrossRef]
54. Hicks, J.; Klumpp-Thomas, C.; Kalish, H.; Shunmugavel, A.; Mehalko, J.; Denson, J.-P.; Snead, K.R.; Drew, M.; Corbett, K.S.; Graham, B.S.; et al. Serologic Cross-Reactivity of SARS-CoV-2 with Endemic and Seasonal Betacoronaviruses. *J. Clin. Immunol.* **2021**, *41*, 906–913. [CrossRef]
55. Grifoni, A.; Weiskopf, D.; Ramirez, S.I.; Mateus, J.; Dan, J.M.; Moderbacher, C.R.; Rawlings, S.A.; Sutherland, A.; Premkumar, L.; Jadi, R.S.; et al. Targets of T Cell Responses to SARS-CoV-2 Coronavirus in Humans with COVID-19 Disease and Unexposed Individuals. *Cell* **2020**, *181*, 1489–1501.e15. [CrossRef]
56. Mateus, J.; Grifoni, A.; Tarke, A.; Sidney, J.; Ramirez, S.I.; Dan, J.M.; Burger, Z.C.; Rawlings, S.A.; Smith, D.M.; Phillips, E.; et al. Selective and Cross-Reactive SARS-CoV-2 T Cell Epitopes in Unexposed Humans. *Science* **2020**, *370*, 89–94. [CrossRef]
57. Sekine, T.; Perez-Potti, A.; Rivera-Ballesteros, O.; Strålin, K.; Gorin, J.-B.; Olsson, A.; Llewellyn-Lacey, S.; Kamal, H.; Bogdanovic, G.; Muschiol, S.; et al. Robust T Cell Immunity in Convalescent Individuals with Asymptomatic or Mild COVID-19. *Cell* **2020**, *183*, 158–168.e14. [CrossRef]
58. Schulien, I.; Kemming, J.; Oberhardt, V.; Wild, K.; Seidel, L.M.; Killmer, S.; Sagar; Daul, F.; Salvat Lago, M.; Decker, A.; et al. Characterization of Pre-Existing and Induced SARS-CoV-2-Specific CD8+ T Cells. *Nat Med* **2021**, *27*, 78–85. [CrossRef]
59. Reynolds, C.J.; Swadling, L.; Gibbons, J.M.; Pade, C.; Jensen, M.P.; Diniz, M.O.; Schmidt, N.M.; Butler, D.K.; Amin, O.E.; Bailey, S.N.L.; et al. Discordant Neutralizing Antibody and T Cell Responses in Asymptomatic and Mild SARS-CoV-2 Infection. *Sci. Immunol.* **2020**, *5*, eabf3698. [CrossRef]

60. Low, J.S.; Vaqueirinho, D.; Mele, F.; Foglierini, M.; Jerak, J.; Perotti, M.; Jarrossay, D.; Jovic, S.; Perez, L.; Cacciatore, R.; et al. Clonal Analysis of Immunodominance and Cross-Reactivity of the CD4 T Cell Response to SARS-CoV-2. *Science* **2021**, *372*, 1336–1341. [CrossRef]
61. Echeverría, G.; Guevara, Á.; Coloma, J.; Ruiz, A.M.; Vasquez, M.M.; Tejera, E.; de Waard, J.H. Pre-Existing T-Cell Immunity to SARS-CoV-2 in Unexposed Healthy Controls in Ecuador, as Detected with a COVID-19 Interferon-Gamma Release Assay. *Int. J. Infect. Dis.* **2021**, *105*, 21–25. [CrossRef]
62. Poston, D.; Weisblum, Y.; Wise, H.; Templeton, K.; Jenks, S.; Hatziioannou, T.; Bieniasz, P. Absence of Severe Acute Respiratory Syndrome Coronavirus 2 Neutralizing Activity in Prepandemic Sera From Individuals With Recent Seasonal Coronavirus Infection. *Clin. Infect. Dis.* **2020**, *73*, e1208–e1211. [CrossRef] [PubMed]
63. Amanat, F.; Thapa, M.; Lei, T.; Ahmed, S.M.S.; Adelsberg, D.C.; Carreño, J.M.; Strohmeier, S.; Schmitz, A.J.; Zafar, S.; Zhou, J.Q.; et al. SARS-CoV-2 MRNA Vaccination Induces Functionally Diverse Antibodies to NTD, RBD, and S2. *Cell* **2021**, *184*, 3936–3948.e10. [CrossRef]
64. Angyal, A.; Longet, S.; Moore, S.C.; Payne, R.P.; Harding, A.; Tipton, T.; Rongkard, P.; Ali, M.; Hering, L.M.; Meardon, N.; et al. T-Cell and Antibody Responses to First BNT162b2 Vaccine Dose in Previously Infected and SARS-CoV-2-Naive UK Health-Care Workers: A Multicentre Prospective Cohort Study. *Lancet Microbe* **2022**, *3*, e21–e31. [CrossRef] [PubMed]
65. Skelly, D.T.; Harding, A.C.; Gilbert-Jaramillo, J.; Knight, M.L.; Longet, S.; Brown, A.; Adele, S.; Adland, E.; Brown, H.; Tipton, T.; et al. Two Doses of SARS-CoV-2 Vaccination Induce Robust Immune Responses to Emerging SARS-CoV-2 Variants of Concern. *Nat. Commun.* **2021**, *12*, 5061. [CrossRef] [PubMed]
66. Grobben, M.; van der Straten, K.; Brouwer, P.J.; Brinkkemper, M.; Maisonnasse, P.; Dereuddre-Bosquet, N.; Appelman, B.; Lavell, A.A.; van Vught, L.A.; Burger, J.A.; et al. Cross-Reactive Antibodies after SARS-CoV-2 Infection and Vaccination. *eLife* **2021**, *10*, e70330. [CrossRef]
67. Anderson, E.M.; Goodwin, E.C.; Verma, A.; Arevalo, C.P.; Bolton, M.J.; Weirick, M.E.; Gouma, S.; McAllister, C.M.; Christensen, S.R.; Weaver, J.; et al. Seasonal Human Coronavirus Antibodies Are Boosted upon SARS-CoV-2 Infection but Not Associated with Protection. *Cell* **2021**, *184*, 1858–1864.e10. [CrossRef]
68. Sermet-Gaudelus, I.; Temmam, S.; Huon, C.; Behillil, S.; Gajdos, V.; Bigot, T.; Lurier, T.; Chrétien, D.; Backovic, M.; Delaunay-Moisan, A.; et al. Prior Infection by Seasonal Coronaviruses, as Assessed by Serology, Does Not Prevent SARS-CoV-2 Infection and Disease in Children, France, April to June 2020. *Eurosurveillance* **2021**, *26*, 2001782. [CrossRef]
69. Gombar, S.; Bergquist, T.; Pejaver, V.; Hammarlund, N.E.; Murugesan, K.; Mooney, S.; Shah, N.; Pinsky, B.A.; Banaei, N. SARS-CoV-2 Infection and COVID-19 Severity in Individuals with Prior Seasonal Coronavirus Infection. *Diagn. Microbiol. Infect. Dis.* **2021**, *100*, 115338. [CrossRef]
70. Qian, Z.; Ou, X.; Góes, L.G.B.; Osborne, C.; Castano, A.; Holmes, K.V.; Dominguez, S.R. Identification of the Receptor-Binding Domain of the Spike Glycoprotein of Human Betacoronavirus HKU1. *J. Virol.* **2015**, *89*, 8816–8827. [CrossRef]
71. Ou, X.; Guan, H.; Qin, B.; Mu, Z.; Wojdyla, J.A.; Wang, M.; Dominguez, S.R.; Qian, Z.; Cui, S. Crystal Structure of the Receptor Binding Domain of the Spike Glycoprotein of Human Betacoronavirus HKU1. *Nat Commun* **2017**, *8*, 15216. [CrossRef]
72. Vogel, A.B.; Kanevsky, I.; Che, Y.; Swanson, K.A.; Muik, A.; Vormehr, M.; Kranz, L.M.; Walzer, K.C.; Hein, S.; Güler, A.; et al. BNT162b Vaccines Protect Rhesus Macaques from SARS-CoV-2. *Nature* **2021**, *592*, 283–289. [CrossRef]
73. Jackson, L.A.; Anderson, E.J.; Rouphael, N.G.; Roberts, P.C.; Makhene, M.; Coler, R.N.; McCullough, M.P.; Chappell, J.D.; Denison, M.R.; Stevens, L.J.; et al. An MRNA Vaccine against SARS-CoV-2—Preliminary Report. *N. Engl. J. Med.* **2020**, *383*, 1920–1931. [CrossRef]
74. Lawrenz, J.; Xie, Q.; Zech, F.; Weil, T.; Seidel, A.; Krnavek, D.; van der Hoek, L.; Münch, J.; Müller, J.A.; Kirchhoff, F. Severe Acute Respiratory Syndrome Coronavirus 2 Vaccination Boosts Neutralizing Activity Against Seasonal Human Coronaviruses. *Clin. Infect. Dis.* **2022**, *75*, e653–e661. [CrossRef]
75. Simula, E.R.; Manca, M.A.; Jasemi, S.; Uzzau, S.; Rubino, S.; Manchia, P.; Bitti, A.; Palermo, M.; Sechi, L.A. HCoV-NL63 and SARS-CoV-2 Share Recognized Epitopes by the Humoral Response in Sera of People Collected Pre- and during CoV-2 Pandemic. *Microorganisms* **2020**, *8*, 1993. [CrossRef]
76. Chan, K.H.; Cheng, V.C.C.; Woo, P.C.Y.; Lau, S.K.P.; Poon, L.L.M.; Guan, Y.; Seto, W.H.; Yuen, K.Y.; Peiris, J.S.M. Serological Responses in Patients with Severe Acute Respiratory Syndrome Coronavirus Infection and Cross-Reactivity with Human Coronaviruses 229E, OC43, and NL63. *Clin. Vaccine Immunol.* **2005**, *12*, 1317–1321. [CrossRef]
77. Lin, H.-X.; Feng, Y.; Tu, X.; Zhao, X.; Hsieh, C.-H.; Griffin, L.; Junop, M.; Zhang, C. Characterization of the Spike Protein of Human Coronavirus NL63 in Receptor Binding and Pseudotype Virus Entry. *Virus Res.* **2011**, *160*, 283–293. [CrossRef]
78. Heinz, F.X.; Stiasny, K. Distinguishing Features of Current COVID-19 Vaccines: Knowns and Unknowns of Antigen Presentation and Modes of Action. *npj Vaccines* **2021**, *6*, 1–13. [CrossRef]
79. Martínez-Flores, D.; Zepeda-Cervantes, J.; Cruz-Reséndiz, A.; Aguirre-Sampieri, S.; Sampieri, A.; Vaca, L. SARS-CoV-2 Vaccines Based on the Spike Glycoprotein and Implications of New Viral Variants. *Front. Immunol.* **2021**, *12*. [CrossRef]
80. Dolgin, E. Pan-Coronavirus Vaccine Pipeline Takes Form. *Nat. Rev. Drug Discov.* **2022**, *21*, 324–326. [CrossRef]

jove

Pseudotyped Viruses As a Molecular Tool to Monitor Humoral Immune Responses Against SARS-CoV-2 Via Neutralization Assay

Tobia Fantoni[*,1], **Michele Bissoli**[*,1], **Chiara Stefani**[1], **Mauro Voi**[1], **Alexandrina Dabija**[1], **Rebecca Casula**[1], **Domenico Luca Minafra**[1], **Julys da Fonseca Palmeira**[2], **Enrique Roberto Argañaraz**[2], **Martin Mayora-Neto**[3], **Nigel J. Temperton**[3], **Donato Zipeto**[1], **Alessandra Ruggiero**[1]

[1] Department of Neuroscience, Biomedicine and Movement, University of Verona [2] Laboratory of Molecular Neurovirology, Faculty of Health Science, University of Brasília [3] Viral Pseudotype Unit, Medway School of Pharmacy, Universities of Kent and Greenwich at Medway

[*] These authors contributed equally

Corresponding Author

Alessandra Ruggiero
Alessandra.Ruggiero@univr.it

Citation

Fantoni, T., Bissoli, M., Stefani, C., Voi, M., Dabija, A., Casula, R., Minafra, D.L., da Fonseca Palmeira, J., Argañaraz, E.R., Mayora-Neto, M., Temperton, N.J., Zipeto, D., Ruggiero, A. Pseudotyped Viruses As a Molecular Tool to Monitor Humoral Immune Responses Against SARS-CoV-2 Via Neutralization Assay. *J. Vis. Exp.* (201), e65658, doi:10.3791/65658 (2023).

Date Published

November 21, 2023

DOI

10.3791/65658

URL

jove.com/video/65658

Abstract

Pseudotyped viruses (PVs) are molecular tools that can be used to study host-virus interactions and to test the neutralizing ability of serum samples, in addition to their better-known use in gene therapy for the delivery of a gene of interest. PVs are replication defective because the viral genome is divided into different plasmids that are not incorporated into the PVs. This safe and versatile system allows the use of PVs in biosafety level 2 laboratories. Here, we present a general methodology to produce lentiviral PVs based on three plasmids as mentioned here: (1) the backbone plasmid carrying the reporter gene needed to monitor the infection; (2) the packaging plasmid carrying the genes for all the structural proteins needed to generate the PVs; (3) the envelope surface glycoprotein expression plasmid that determines virus tropism and mediates viral entry into the host cell. In this work, SARS-CoV-2 Spike is the envelope glycoprotein used for the production of non-replicative SARS-CoV-2 pseudotyped lentiviruses.

Briefly, packaging cells (HEK293T) were co-transfected with the three different plasmids using standard methods. After 48 h, the supernatant containing the PVs was harvested, filtered, and stored at -80 °C. The infectivity of SARS-CoV-2 PVs was tested by studying the expression of the reporter gene (luciferase) in a target cell line 48 h after infection. The higher the value for relative luminescence units (RLUs), the higher the infection/transduction rate. Furthermore, the infectious PVs were added to the serially diluted serum samples to study the neutralization process

of pseudoviruses' entry into target cells, measured as the reduction in RLU intensity: lower values corresponding to high neutralizing activity.

Introduction

Pseudotyped viruses (PVs) are molecular tools used in microbiology to study host-virus and pathogen-pathogen interactions[1,2,3,4]. PVs consist of an inner part, the viral core that protects the viral genome, and an outer part, the envelope glycoproteins on the surface of the virus that defines the tropism[5]. A pseudovirus is replication-incompetent in the target cell because it does not contain all the genetic information to generate new viral particles. This combination of peculiar features makes PVs a safe alternative to a wildtype virus. Wildtype viruses, on the other hand, are highly pathogenic and cannot be used in BSL 2 laboratories for analysis[6].

The infectivity of PVs can be monitored by a reporter gene, usually coding for a fluorescent protein (GFP, RFP, YFP) or an enzyme that produces chemiluminescent products (luciferase). This is contained in one of the plasmids used for PV production and incorporated in the genome of the pseudovirus[7].

Several types of PV cores currently exist, including lentiviral-derived particles based on the HIV-1 genome. The great advantage of HIV-1-based PVs over other platforms is their intrinsic integration process in the target cell genome[8]. Although HIV-1 is a highly contagious virus and is the causative agent of AIDS, these lentiviral vectors are safe to use because of the extensive optimization steps over the years. Optimal safety conditions were achieved with the introduction of 2nd-generation lentiviral vectors, in which viral genes were depleted without influencing transduction capabilities[9]. The 3rd and 4th generations contributed to the increased safety of lentiviral vector handling with the further splitting of the viral genome into separate plasmids[10, 11]. The latest generations of PVs are generally employed to produce lentiviral vectors for gene therapy.

PVs can be used to study interactions between viruses and host cells, during both the production and the infection phases. PVs are especially employed in pseudovirus neutralization assays (PVNA). PVNAs are widely validated to assess the neutralization potential of serum or plasma by targeting the viral glycoprotein on the PV's envelope[12,13]. Neutralization activity, expressed as the inhibitory concentration 50 (IC50), is defined as the dilution of serum/plasma that blocks 50% of viral particle entry[14]. In this protocol, we described the set-up of a PVNA to test the antibody activity against Severe Acute Respiratory Syndrome - Coronavirus 2 (SARS-CoV-2) in sera collected before and after receiving a booster vaccine dose.

Protocol

The present protocol has been approved by and follows the guidelines of the Ethical Committee of the University of Verona (approval protocol number 1538). Informed written consent was obtained from the human subjects participating in the study. Whole blood samples were collected from healthcare worker (HCW) volunteers who were in the process of receiving anti-SARS-CoV-2 vaccines. These samples were collected in plastic tubes containing anticoagulants for the subsequent isolation of serum[15].

All the following processes must be performed in a Class-2 biological hood, working under sterile conditions. Virus handling must be performed with care, and all waste products must be neutralized in a diluted bleach solution. An overview of the protocol is displayed in **Figure 1**.

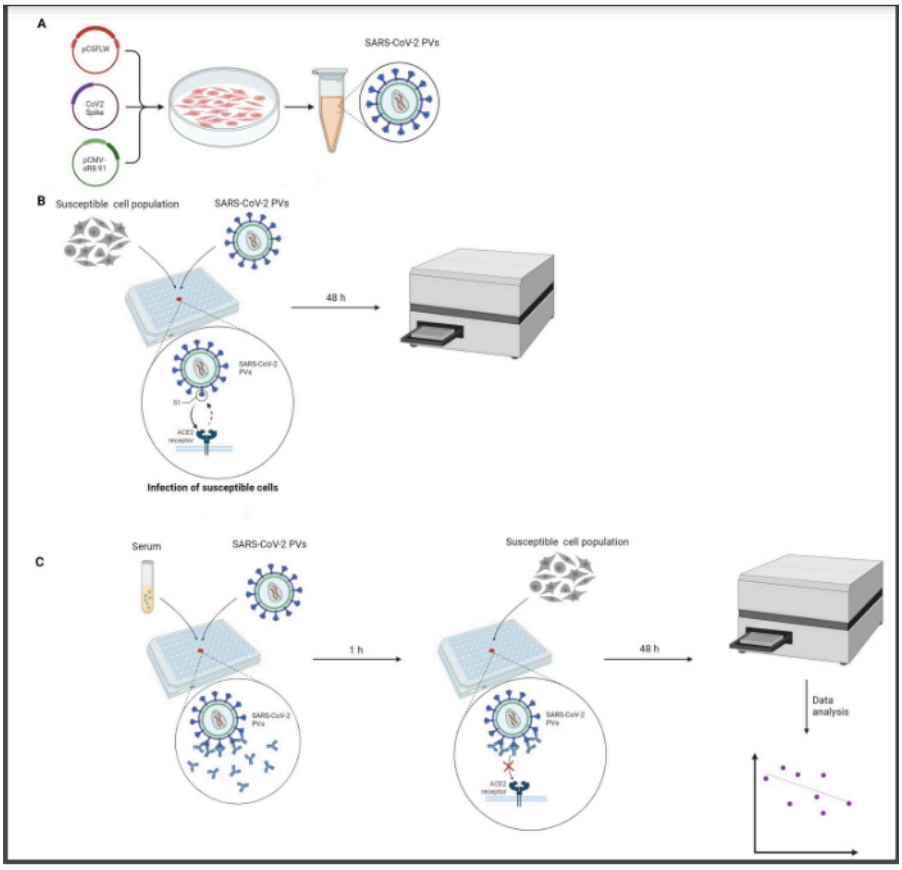

Figure 1: Graphical representation of a neutralization assay. (**A**) PV production, (**B**) PV titration, and (**C**) neutralization assay. All the procedures are performed in a class-2 biological hood under sterile conditions. Titration step (B) needs to be performed to standardize the infectivity levels of PVs before use in the neutralization assay (C). This figure was created with BioRender. Please click here to view a larger version of this figure.

1. SARS-CoV-2 PVs production and infectivity test

1. Seed 5 x 10^5 HEK293T cells in complete Dulbecco's Modified Eagle Medium (DMEM, high-glucose, 10% foetal bovine serum (FBS), 1% L-glutamine, 1% penicillin/streptomycin) in a 6-well plate (6WP) to reach a suitable cell density compatible with the transfection reagent used. In the case of performing transfection with polyehtylenimine (PEI) (prepare the reagent following the manufacturer instructions), ensure that the cells reach 40-60% density on the day of transfection (step 1.3). Keep the cells in a humidified incubator at 37 °C and 5% CO_2.

2. Prior to transfection, replace the spent cell medium with fresh medium without antibiotics (DMEM, high-glucose, 10% FBS, 1% L-glutamine) to achieve higher transfection efficiency.
   NOTE: The day after seeding, HEK293T cells are ready to be transfected.
3. Transfect adherent HEK293T cells with a suitable transfection reagent according to the manufacturer's instructions. If using PEI, prepare two mixes and follow the steps below.
   1. To prepare mix A, add 500 ng of pCMV-dR8.91 packaging plasmid[16], 750 ng of pCSFLW reporter plasmid[16], and 450 ng of SARS-CoV-2 Spike expressing plasmid in 100 µL of reduced serum medium.
   2. To prepare mix B, add 17.5 µL of PEI (concentration: 1 mg/mL) to 100 µL of the reduced serum medium.
   3. Allow both mixes to incubate at room temperature (RT) for 5 min. Next, mix the contents of both tubes together by adding the PEI mix B to DNA mix A.
   4. Incubate the tube for 20-30 min at RT. Flick the tube gently every 3-4 min to enhance the mixing. Finally, add the mixture to the HEK293T cells.
4. 16-20 h after the transfection, replace the culture medium with fresh, complete DMEM. Incubate at 37 °C and 5% CO_2, to allow for the production of PVs by transfected cells.
5. 72 h after the transfection, harvest the supernatant containing PVs. Then centrifuge at 1600 x *g* for 7 min at room temperature to remove cell debris and dead cells and filter it through a 0.45 µm cellulose acetate filter.
6. OPTIONAL STEP: To increase the final yield of PV titer, perform multiple transfections, pool the cell media containing PVs, and concentrate it using concentrating tubes.
7. Proceed directly with the next steps ("PVs titration", section 2) or aliquot the PV-containing medium in suitable tubes to store at -80 °C until use. Prepare an additional aliquot (400-500 µL) to be used for titration.
   NOTE: Making multiple aliquots will guarantee reproducibility between experiments by avoiding excessive thaw-freeze cycles.

2. PVs titration

1. Use the fresh PV-containing medium for the next steps or thaw the testing aliquot (step 1.7) to perform the titration of the new viral stock. Freezing aliquots of the same PV stock will guarantee reproducibility.
2. Add 50 µL of complete DMEM (or complete medium compatible with the target cell line in usage) in all the wells of a 96 well-plate (96WP) necessary to test in duplicate the PV stock, leaving row "A" empty. Add 100 µL of PVs stock to row "A". Based on the number of preparations to be tested, leave one column without the virus as a "cell only" control (**Figure 2**).
3. Pipette 50 µL from row A to row B and repeat this process up to row G to obtain serial dilutions of the initial stock. Discard the excess volume from the last row.
4. Detach cellsusing trypsin/ethylenediaminetetraacetic acid 1x (EDTA) in Dulbecco's phosphate buffer saline 1x (DPBS 1x), after removing the spent medium and washing cells with DPBS 1x twice. Prepare cells to a density of 4 x 10^5 cells/mL.

NOTE: In this protocol, PVs infection was tested on the susceptible cell line HEK293T/ACE2; such cells were derived from HEK293T, transduced using a lentiviral vector to express ACE2 receptor.

5. Add 50 µL of the cell suspension into each well to ensure a cell count of 2 x 10^4 cells per well.
6. Incubate at 37 °C and 5% CO_2, for 48 h.
7. After the incubation, perform the Luciferase assay to obtain the reading as per the manufacturer's instructions. Add 100 µL of the luciferase reagent to the wells and incubate in the dark at RT for 2 min. Move the content of each well to a black 96 well plate (compatible with the available plate reader) and read the plates in a 96 well plate reader.

NOTE: The luminometer used for the luciferase readout will produce a spreadsheet file with the raw, unprocessed data that will be used for downstream analysis (in this case, an Excel file). The virus' infectivity will be expressed as relative luminescence units (RLU) (described in paragraph 4.1).

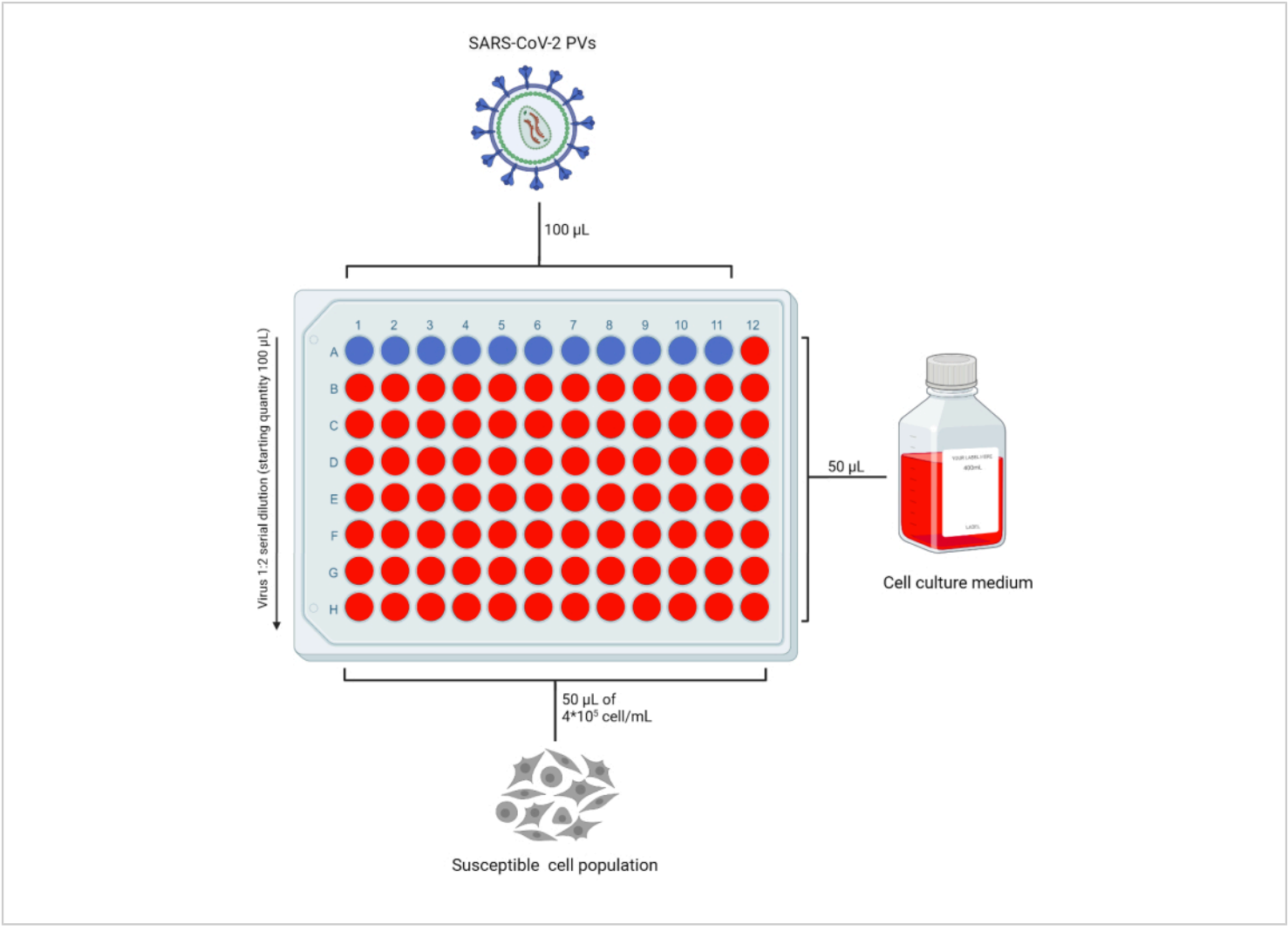

Figure 2: Representative layout of a 96 well plate for PVs titration. A fixed volume of PV-containing supernatant is added to row A, columns 1-11, and serially diluted. The last column is left as the "cell only" control. This figure was created with BioRender. Please click here to view a larger version of this figure.

3. Neutralization assay

1. Thaw patients' sera on ice. Inactivate serum samples by incubating them at 56 °C for 30 min.
2. In a 96 well plate, add 50 µL of the fresh, complete DMEM (or complete medium compatible with the target cell line used)in each of the following wells: from row B (columns 1-10) to row H (columns 1-10). Put 95 µL of the fresh, complete DMEM in row A (columns 1-10). Add 50 µL and 100 µL of complete DMEM into the wells of columns 11 and 12, respectively. These will be the infected (virus control, or VC) and uninfected (cell only, or CC) controls, respectively (**Figure 3**).
3. Add 5 µL of heat-inactivated serum/plasma samples in row A (columns 1-10). Each sample will be in duplicate. With a multichannel pipette, mix the samples in the first row and move 50 µL of medium containing serum from row A to row B. Repeat this process up to the last row (**Figure 3**). Discard the remaining 50 µL.
4. Thaw the necessary number of PVs' aliquots and dilute to ≥ 10^4 RLU/mL. Add 50 µL of the diluted PV-containing medium to each well (from column 1 to column 11) using a multichannel pipette to reach a 1:1 dilution of heat inactivated serum/plasma to virus. Incubate at 37 °C and 5% CO_2, for 1 h to allow the antibodies in the serum samples to bind to the SARS-CoV-2 spike protein on the PVs.
5. Prepare at least 5 mL suspension of susceptible cells (HEK293T/ACE2) at a cell density of 4 x 10^5 cells/mL. Add 50 µL of the cell suspension to each well and incubate at 37 °C and 5% CO_2, for 48 h.
6. After the incubation, perform the luciferase assay reading according to the manufacturer's instructions, as described in step 2.7.

   NOTE: The luminometer used for luciferase readout will produce a spreadsheet file (in this case, .xlsx) with the raw, unprocessed data that will be used for downstream analysis (the Luciferase assay file).

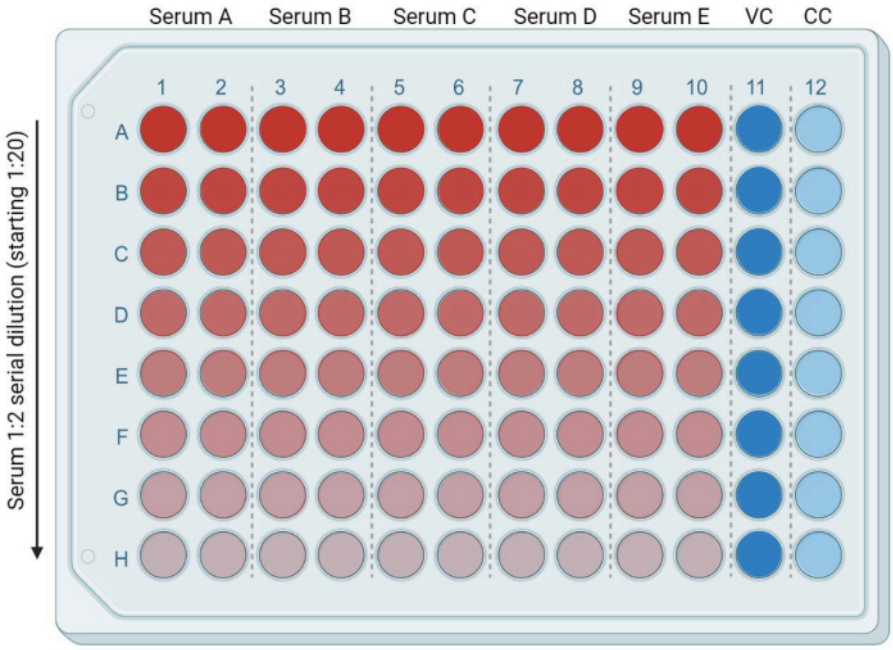

Figure 3: Plate representation based on serum dilution. Bright red corresponds to a higher quantity of serum, and bright blue lane (column 11) corresponds to infected cell control (VC, virus control). Light blue lane (column 12) corresponds to uninfected cells (CC, cell control). This figure was created with BioRender. Please click here to view a larger version of this figure.

4. Titration analysis

1. On the Luciferase assay file, assign the names/titles to the corresponding samples.
2. Multiply the RLU measure by the dilution factors (from the top to the bottom of the grid: 20x, 40x, 80x, 160x, 320x, 640x, 1,280x, 2,560x) to obtain RLU/mL. If different dilution factors are used, change the multiplication factors accordingly.
3. Calculate the average RLU/mL for each PV preparation.

5. PVs neutralization assay analysis

1. On the Luciferase assay spreadsheet file (in this case, .xlsx), assign the corresponding titles to the tested samples. Enter the dilution factor of the sample (40s, 80x, 160x, 320x, 640x, 1,280x, 2,560x, 5,120x). Calculate the Log10 of the dilution factors.
2. Calculate the average RLU of uninfected and infected control (**Figure 3**, columns 11 and 12, respectively). These values will be useful for the normalization in step 5.5.

3. Open a new document for data analysis. Select **X/Y analysis**, input X as **Numbers** and Y as **Enter 2 replicate values in side-by-side sub-columns**.
4. Enter Log10 (dilution) values as X numbers. Enter the duplicate RLU of the samples.
5. Go to **Analyze > Normalize > Flag all** the samples on the same sheet. Input the average VC and CC values in **How is 0% defined?**, and **How is 100% defined?**, respectively. Click **OK**.
6. On the normalized data sheet, go to **Analyze > XY analyses > Nonlinear analyses (curve fit)**. Flag all the samples and click **OK**. For the **Dose-response - Inhibition**, select **log(inhibitor) vs normalized response - variable slope**.
7. Under **Constrain**, change **HillSlope** to **Must be less than 0**.
8. Under **Output**, flag **Create summary table and graph**. Click on **OK** to obtain the final analyses. A working sheet with a template for the analysis is provided in **Supplementary File 1**.

Representative Results

This protocol describes the production of SARS-CoV-2 PVs and a downstream application of these PVs to analyze the neutralization activity of serum/plasma of subjects receiving anti-COVID-19 vaccination[17]. Furthermore, this protocol can be applied to produce pseudotypes of each SARS-CoV-2 variant of concern (VOC) to test the evolution of the neutralizing response. Despite this protocol facilitating the study of humoral immune response after COVID-19 vaccination, it can be adapted to easily test the neutralization of different sera/plasma against different viruses[13,18,19].

Figure 4A represents the increment of the dilution of serum (Log(dilution)) corresponding to the increase of the RLU signal. Thus, the higher the dilution of the sample, the less blocked the virus entry is (**Figure 4A**). This is further expressed as a percentage of neutralization (**Figure 4B**).

The IC50 result shows the neutralization capacity of a single vaccine serum over time. In the example reported in **Figure 4C**, the subject developed a strong humoral activity against the virus at four weeks after vaccination; however, after 16 weeks the IC50 is similar to the one prior to vaccine administration. In this case, the PVNA showed the loss of neutralization potential over time.

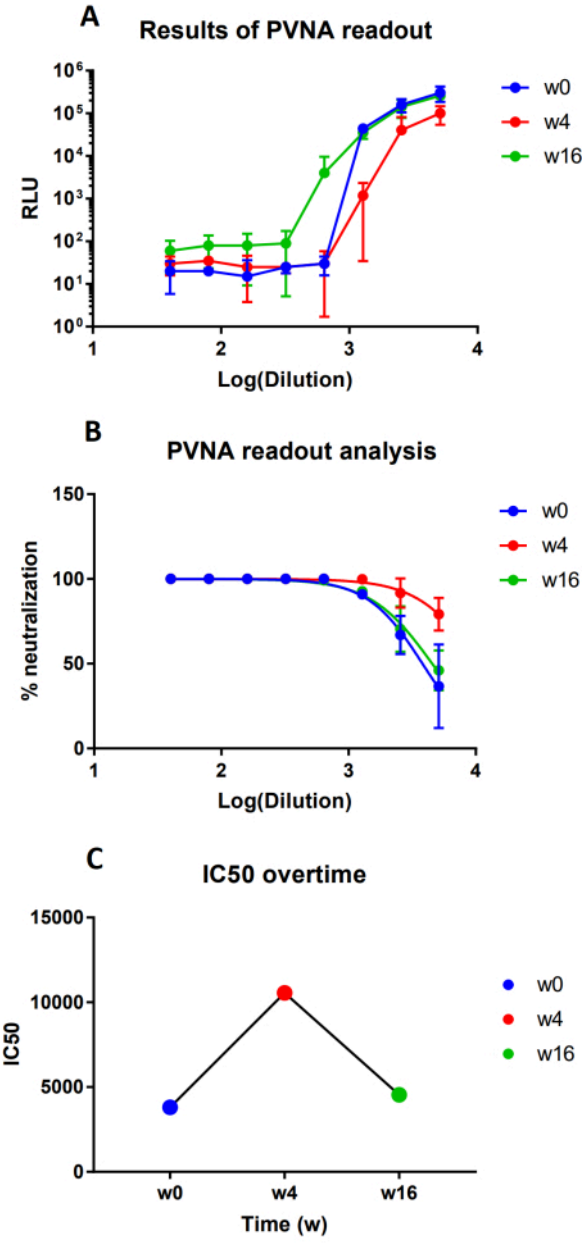

Figure 4: Representative results of PVNA. (**A**) Infectivity (RLU, and (**B**) percentage of neutralization are shown at week 0 (W0, before the vaccination); W4 (four weeks after vaccination); W16 (sixteen weeks after W0). (**C**) IC50 values at the same time points. Please click here to view a larger version of this figure.

Supplementary File 1: Neutralization analysis template. A working sheet with a template for conducting the neutralization analysis. Please click here to download this File.

Discussion

Although using a wildtype virus simulates the actual infection, lentiviral PVs are a safer option to study the mechanisms associated with viral entry and infection without the strict safety requirements necessary to work with pathogenic viruses[4,20,21]. PVs are composed of a replication-defective viral core surrounded by the surface envelope glycoprotein of a pathogenic virus which is the objective of the study.

HIV-1-based PVs are one of the most widely used platforms and these have been employed in this protocol for the production of SARS-CoV-2 pseudoviral particles. The reporter gene can be different as per the use of the PVs; in this case, the choice of the luciferase reporter gene provides an easy, fast, and sensitive readout of the infectivity of the produced PVs.

PVs based on lentiviruses are widely applied to study anti-HIV-1 humoral response[22]. The PV technology was instantly applied during the recent COVID-19 pandemic, caused by SARS-CoV-2. SARS-CoV-2 is a highly pathogenic human *Betacoronavirus*, identified for the first time in China (Wu Han) which became rapidly pandemic, causing more than 6 million deaths worldwide[23,24]. Because of the validation of vaccine strategies, the pandemic has been largely controlled; nonetheless, in most vulnerable people, such as cancer patients or people living with HIV, it does still pose a risk[25,26,27]. In this context, there is still a need for validated assays to monitor the anti-vaccine humoral response in terms of neutralizing activity. In this article we have described a simple protocol that can be easily be performed in laboratories with no access to category-3 containment. Furthermore, the PV platform is a versatile system to study different SARS-COV-2 virus variants. Indeed, by changing the envelope-expressing plasmid with different spikes, it is possible to generate PVs of SARS-CoV-2 new variants or of any other coronaviruses[28]. These virus portfolios can be used to assess the reactivity of vaccine-induced humoral response against the different variants of concern[15, 29,30,31,32]. This information can guide the generation of new and more effective vaccines.

Three major obstacles could be encountered while following this protocol concerning transfection conditions, titration failure and/or neutralization assay. First, the packaging cells may not be sufficiently confluent at the time of transfection. This may be due to the lack of nutrients. Ensure that step 1.1. is properly followed. Otherwise, perform seeding in the morning of the day before transfection and transfect the packaging cells later the next day to increase the growth time. A recurring problem is the potential contamination of the cell medium between transfection and medium replacement the next day. In this case, repeat the procedure by increasing the sterilization procedure before use when working under the BSL2 hood or include antibiotics to avoid unwanted contaminations. Second, an undetected luciferase signal may occur that can be attributed to various stages of PVs production or the characteristics of the target cell line. Plasmids should be extracted with endotoxin-free kits. The transfection step is critical for the outcome of the protocol. PEI reagent must be prepared at the correct concentration of 1 mg/mL. Gently flicking the tube during the preparation of transfection mixes enhances the formation of DNA-PEI complexes. To verify that the cells have been transfected correctly, it is recommended to perform the luciferase assay immediately after harvesting the cells. In addition, include a control virus envelope glycoprotein such as VSV: VSV-PVs give strong RLU signals on human cell lines. Moreover, it is necessary to mention that the target cell line must express

the receptor, which is easily verified via western blot or flow cytometry.

This method has been previously optimized[16] with respect to the experimental conditions, including the selection of the transfection reagent, the determination of the ratios between the different plasmids needed for the generation of the PV, and the selection of the target cell lines, the use of luciferase as reporter genes. Nonetheless, each laboratory will need to validate the proposed methods according to the available equipment. For example, (step 2.7) requires the addition of 100 µL of Luciferase substrate as suggested by the producer: this is optimal for the readout of the luciferase assay with the plate reader that is currently available. On the other hand, other laboratories that are equipped with a different plate reader may adapt the protocol using different luciferase substrates or volumes of the reagent[33]. Furthermore, other authors have proposed the use of the green fluorescent protein (GFP) as a reporter gene instead of the luciferase. This could be considered if a laboratory is fully equipped for GFP readout but not luciferase[34,35].

To conclude, PVs are a flexible and straightforward system that allows quantifying the infection by using a simple detection method. It represents a cost-effective approach that is more accessible for many research groups and allows avoiding the use of pathogenic viruses that require a biosafety level 3 laboratory[21]. The use of PVs represents a well-characterized and safe approach to studying antibody-mediated neutralization in individuals who experienced SARS-CoV-2 infection and/or vaccination.

Disclosures

The authors declare to have no conflict of interest.

Acknowledgments

We acknowledge the contribution of the health-care workers volunteers. This project was supported by the Department of Excellence 2023/2027, MUR, Italy. AR and DZ were supported by PRIN2022 (EU fundings; NextGenerationEU)

References

1. Ozaki, D. A. et al. International technology transfer of a GCLP-compliant HIV-1 neutralizing antibody assay for human clinical trials. *Plos One.* **7** (1), e30963 (2012).
2. Pouget, M. et al. Generation of liposomes to study the effect of Mycobacterium tuberculosis lipids on HIV-1 cis- and trans-infections. *International Journal of Molecular Sciences.* **22** (4), 1945 (2021).
3. McKay, L. G. A. et al. The HCV envelope glycoprotein down-modulates NF-κB signalling and associates with stimulation of the host endoplasmic reticulum stress pathway. *Frontiers in Immunology.* **13**, 831695 (2022).
4. Xiang, Q., Li, L., Wu, J., Tian, M., Fu, Y. Application of pseudovirus system in the development of vaccine, antiviral-drugs, and neutralizing antibodies. *Microbiological Research.* **258**, 126993 (2022).
5. Li, Q., Liu, Q., Huang, W., Li, X., Wang, Y. Current status on the development of pseudoviruses for enveloped viruses. *Reviews in Medical Virology.* **28** (1), e1963 (2018).
6. D'Apice, L. et al. Comparative analysis of the neutralizing activity against SARS-CoV-2 Wuhan-Hu-1 strain and variants of concern: Performance evaluation of a pseudovirus-based neutralization assay. *Frontiers in Immunology.* **13**, 981693 (2022).

7. Falzarano, D., Groseth, A., Hoenen, T. Development and application of reporter-expressing mononegaviruses: current challenges and perspectives. *Antiviral Research.* **103**, 78-87 (2014).
8. Gutierrez-Guerrero, A., Cosset, F.-L., Verhoeyen, E. Lentiviral vector pseudotypes: Precious tools to improve gene modification of hematopoietic cells for research and gene therapy. *Viruses.* **12** (9), 1016 (2020).
9. Zufferey, R., Nagy, D., Mandel, R. J., Naldini, L., Trono, D. Multiply attenuated lentiviral vector achieves efficient gene delivery in vivo. *Nature Biotechnology.* **15** (9), 871-875 (1997).
10. Dull, T. et al. A third-generation lentivirus vector with a conditional packaging system. *Journal of Virology.* **72** (11), 8463-8471 (1998).
11. Berkhout, B. A Fourth generation lentiviral Vector: Simplifying genomic gymnastics. *Molecular Therapy.* **25** (8), 1741-1743 (2017).
12. Wu, X. et al. Development and evaluation of a pseudovirus-luciferase assay for rapid and quantitative detection of neutralizing antibodies against Enterovirus 71. *Plos One.* **8** (6), e64116 (2013).
13. Ferrara, F. et al. Development of lentiviral vectors pseudotyped with Influenza B hemagglutinins: application in vaccine immunogenicity, mAb potency, and sero-surveillance studies. *Frontiers in Immunology.* **12**, 661379 (2021).
14. Hu, J. et al. Development of cell-based pseudovirus entry assay to identify potential viral entry inhibitors and neutralizing antibodies against SARS-CoV-2. *Genes & Diseases.* **7** (4), 551-557 (2020).
15. Dalle Carbonare, L. et al. Serology study after BTN162b2 vaccination in participants previously infected with SARS-CoV-2 in two different waves versus naïve. *Communications Medicine.* **1** (1), 38 (2021).
16. Di Genova, C. et al. Production, titration, neutralisation, storage and lyophilisation of severe acute respiratory syndrome coronavirus 2 (SARS-CoV-2) lentiviral pseudotypes. *Bio-protocol.* **11** (21), e4236 (2021).
17. Chmielewska, A. M., Czarnota, A., Bieńkowska-Szewczyk, K., Grzyb, K. Immune response against SARS-CoV-2 variants: The role of neutralization assays. *NPJ Vaccines.* **6** (1), 1-8 (2021).
18. Chen, Q. et al. Development and optimization of a sensitive pseudovirus-based assay for HIV-1 neutralizing antibodies detection using A3R5 cells. *Human Vaccines & Immunotherapeutics.* **14** (1), 199-208 (2018).
19. Gauger, P. C., Vincent, A. L. Serum virus neutralization assay for detection and quantitation of serum neutralizing antibodies to influenza A virus in swine. *Methods in Molecular Biology (Clifton, N.J.).* **2123**, 321-333 (2020).
20. Miglietta, R., Pastori, C., Venuti, A., Ochsenbauer, C., Lopalco, L. Synergy in monoclonal antibody neutralization of HIV-1 pseudoviruses and infectious molecular clones. *Journal of Translational Medicine.* **12** (1), 346 (2014).
21. Chen, M., Zhang, X.-E. Construction and applications of SARS-CoV-2 pseudoviruses: A mini review. *International Journal of Biological Sciences.* **17** (6), 1574-1580 (2021).
22. Zipeto, D. et al. Induction of human immunodeficiency virus neutralizing antibodies using fusion complexes. *Microbes and Infection.* **8** (6), 1424-1433 (2006).

23. *WHO Coronavirus (COVID-19) Dashboard.* at <https://covid19.who.int>. (2023).
24. Zhou, P. et al. A pneumonia outbreak associated with a new coronavirus of probable bat origin. *Nature.* **579** (7798), 270-273 (2020).
25. Chen, X., Huang, H., Ju, J., Sun, R., Zhang, J. Impact of vaccination on the COVID-19 pandemic in U.S. states. *Scientific Reports.* **12** (1), 1554 (2022).
26. Stefani, C., Fantoni, T., Bissoli, M., Thomas, J., Ruggiero, A. HIV and SARS-CoV-2 Co-Infection: From Population Study Evidence to In Vitro Studies. *Life.* **12** (12), 2089 (2022).
27. Watson, O. J. et al. Global impact of the first year of COVID-19 vaccination: a mathematical modelling study. *The Lancet Infectious Diseases.* **22** (9), 1293-1302 (2022).
28. Cantoni, D. et al. Analysis of antibody neutralisation activity against SARS-CoV-2 variants and seasonal human coronaviruses NL63, HKU1, and 229E induced by three different COVID-19 vaccine olatforms. *Vaccines.* **11** (1), 58 (2023).
29. Siracusano, G. et al. Different decay of antibody response and VOC sensitivity in naïve and previously infected subjects at 15 weeks following vaccination with BNT162b2. *Journal of Translational Medicine.* **20** (1), 22 (2022).
30. Ruggiero, A. et al. SARS-CoV-2 vaccination elicits unconventional IgM specific responses in naïve and previously COVID-19-infected individuals. *eBioMedicine.* **77** (2022).
31. Piubelli, C. et al. Subjects who developed SARS-CoV-2 specific IgM after vaccination show a longer humoral immunity and a lower frequency of infection. *eBioMedicine.* **89**, 104471 (2023).
32. Zhang, G. F. et al. Infectivity of pseudotyped SARS-CoV-2 variants of concern in different human cell types and inhibitory effects of recombinant spike protein and entry-related cellular factors. *Journal of Medical Virology.* **95** (1), e28437 (2023).
33. da Costa, K. A. S. et al. Influenza A (N1-N9) and Influenza B (B/Victoria and B/Yamagata) neuraminidase pseudotypes as tools for pandemic preparedness and improved influenza vaccine design. *Vaccines.* **10** (9), 1520 (2022).
34. Condor Capcha, J. M. et al. Generation of SARS-CoV-2 spike pseudotyped virus for viral entry and neutralization assays: a 1-week protocol. *Frontiers in Cardiovascular Medicine.* **7**, 618651 (2021).
35. Diomede, L. et al. Doxycycline inhibition of a pseudotyped virus transduction does not translate to inhibition of SARS-CoV-2 infectivity. *Viruses.* **13** (9), 1745 (2021).

Journal of Translational Medicine

RESEARCH

Open Access

Immune signature in vaccinated versus non-vaccinated aged people with COVID-19 pneumonia

Ruggiero Alessandra[1†], Caldrer Sara[2†], Pastori Claudia[3], Gianesini Natasha[1], Cugnata Federica[4], Brombin Chiara[4], Fantoni Tobia[1], Tais Stefano[2], Rizzi Eleonora[2], Matucci Andrea[2], Mayora-Neto Martin[5], Uberti-Foppa Caterina[6], Temperton Nigel[5], Di Serio Mariaclelia Stefania[4], Lopalco Lucia[3*†] and Piubelli Chiara[2†]

Abstract

Background A definition of the immunological features of COVID-19 pneumonia is needed to support clinical management of aged patients. In this study, we characterized the humoral and cellular immune responses in presence or absence of SARS-CoV-2 vaccination, in aged patients admitted to the IRCCS San Raffaele Hospital (Italy) for COVID-19 pneumonia between November 2021 and March 2022.

Methods The study was approved by local authorities. Disease severity was evaluated according to WHO guidelines. We tested: (A) anti-SARS-CoV-2 humoral response (anti-RBD-S IgG, anti-S IgM, anti-N IgG, neutralizing activity against Delta, BA1, BA4/5 variants); (B) Lymphocyte B, CD4 and CD8 T-cell phenotype; (C) plasma cytokines. The impact of vaccine administration and different variants on the immunological responses was evaluated using standard linear regression models and Tobit models for censored outcomes adjusted for age, vaccine doses and gender.

Result We studied 47 aged patients (median age 78.41), 22 (47%) female, 33 (70%) older than 70 years (elderly). At hospital admission, 36% were unvaccinated (VAC_{no}), whilst 63% had received 2 (VAC_2) or 3 doses (VAC_3) of vaccine. During hospitalization, WHO score > 5 was higher in unvaccinated (14% in VAC_3 vs. 43% in VAC_2 and 44% VACno). Independently from vaccination doses and gender, elderly had overall reduced anti-SARS-CoV-2 humoral response (IgG-RBD-S, $p = 0.0075$). By linear regression, the anti-RBD-S ($p = 0.0060$), B ($p = 0.0079$), CD8 ($p = 0.0043$) and Th2 cell counts ($p = 0.0131$) were higher in VAC_{2+3} compared to VAC_{no}. Delta variant was the most representative in VAC_2 ($n = 13/18$, 72%), detected in 41% of VAC_{no}, whereas undetected in VAC_3, and anti-RBD-S production was higher in VAC_2 vs. VAC_{no} ($p = 0.0001$), alongside neutralization against Delta ($p = 0141$), BA1 ($p = 0.0255$), BA4/5 ($p = 0.0162$). Infections with Delta also drove an increase of pro-inflammatory cytokines (IFN-α, $p = 0.0463$; IL-6, $p = 0.0010$).

Conclusions Administration of 3 vaccination doses reduces the severe symptomatology in aged and elderly. Vaccination showed a strong association with anti-SARS-CoV-2 humoral response and an expansion of Th2 T-cells

†Ruggiero Alessandra, Caldrer Sara, Lopalco Lucia and Piubelli Chiara equally contributing authors.

*Correspondence:
Lopalco Lucia
lopalco.lucia@hsr.it

Full list of author information is available at the end of the article

populations, independently of age. Delta variants and number of vaccine doses affected the magnitude of the humoral response against the original SARS-CoV-2 and emerging variants. A systematic surveillance of the emerging variants is paramount to define future vaccination strategies.

Keywords Elderly, COVID-19 vaccine, Non-vaccinated, SARS-CoV-2 variants, Immunological response, Plasma cytokines, COVID-19 disease severity, Th2, Pneumonia

Introduction

SARS-CoV-2 infection can lead to COVID-19 pneumonia. The risk of death in the general population is low but it dramatically increases in elder individuals with comorbid chronic conditions such as hypertension, cardiovascular diseases, type 2 diabetes, and with obesity, smoking habits, and male gender [1, 2]. Furthermore the immune system undergoes remarkable changes known as immunosenescence during aging. A low-grade chronic inflammation, known as "inflamm-aging", causes a progressive decline in the ability to produce effective humoral and cellular responses against infections or upon vaccination [3, 4]. In aged individuals, a hyper-inflammatory condition is favoured by the chronic activation of monocytes, which generates a pro-thrombotic environment, contributing to the negative outcomes observed in severe COVID-19 [5, 6]. Moreover, the alteration of T lymphocytes repertoire with aging [6] can affect the accessibility of naïve T cells to SARS-CoV-2 antigens, reducing the activation of specific cells [7]. Also, long-lived B cell repertoire, important in maintaining immunity elicited by vaccines [8–10] is affected by immunosenescence and a particular sign of this impairment is the expansion of the atypical non-functional B cells that is associated with suboptimal humoral responses to vaccine [11].

Despite ongoing immunosenescence in elderly population, the administration of COVID-19 vaccine has demonstrated efficacy [8, 12–15] with an incredible impact on the prevention of severe disease [16–19]. A milder course of the disease is a reflection of a prompt anti-SARS-CoV-2 immune response elicited by the vaccine, which decreases the progression of the infection and supports a quicker virus clearance, preventing the raise of COVID-19 complications. There are scarce data reporting comprehensive immunological characterization in elderly patients. One previous study described the immune features in 31 aged patients with severe SARS-CoV-2 infection (mean age: 76.4 years), compared to 33 adult patients at the same stage of infection (mean age: 49.8 years) in absence of vaccination [6]. Whilst success of vaccination is not questioned, it still remains to better characterize the immunological mechanisms associated with severe COVID-19, even after SARS-CoV-2 vaccination.

In this study, we provided a fine characterization of the humoral and cellular immune responses in aged patients who were admitted to the IRCCS San Raffaele Hospital (Italy) for COVID-19 pneumonia, between November 2021 and March 2022, during Delta/Omicron variants of concern (VOC) waves. We compared unvaccinated patients with subjects receiving two or three doses, to evaluate the impact of vaccination on the immunological humoral, cellular and pro-inflammatory response. This population is unique, having a group of patients that were naïve to vaccination or infection.

Methods

Study population

This study included a total of 47 patients (median age 78.41, ranging from 60 to 94 years old) admitted to the IRCCS San Raffaele Hospital (Milan, Italy) for pneumonia between November 2021 and March 2022. All patients had proven evidence of SARS-CoV-2 infection with nasopharyngeal swab tested positive for SARS-CoV-2 nucleic acid using reverse-transcriptase real-time PCR assay [20, 21], and they were treated with corticosteroids according to common clinical practice. Disease severity was evaluated according to WHO guidelines [22]: score (s) ≤ 5 = moderate; s > 5 = severe. The study group included vaccinated and non-vaccinated patients. Information about vaccine type is available only for 18/30 (60%). Patients receiving 2 doses were vaccinated with Pfizer Comirnaty vaccine (8/16, 50%), or with Astra Zeneca Vaxzevria (5/16, 31%), or with Moderna Spikevax (3/16, 19%). Information about the booster dose were available only for two patients (one received two doses of Astra Zeneca Vaxzevria and one Pfizer Comirnaty dose; the other received 3 Pfizer Comirnaty doses). Individuals that needed intensive care unit (ICU) support at admission were excluded. Two patients were admitted with score = 6 and included in the study, but they experienced a severe curse the infection and died during hospitalization.

SARS-COV-2 VOC genomic characterization

SARS-COV-2 sequences were obtained using Menarini Diagnostics CoronaMeltVAR Real Time PCR kit (Firenze, Italia). Viral genome characterization of the SARS-CoV-2 VOC driving the pneumonia was available for only 17 subjects. For the other patients, we estimated the probable VOC based on the genomic epidemiological data of the Italian National Institute of Health [23]. According to Lombardy epidemiological data, Omicron surpassed Delta and became the most prevalent VOC at the beginning of January 2022 [24]. Considering a reasonable

time-lag between infection and hospitalization of about 7–10 days [25], patients hospitalized after the 15 of January 2022 were considered as Omicron-infected.

Sample collection and storage

EDTA-venous blood and serum were collected within 3 days after hospital admission, with all patients having received corticosteroids. Plasma was isolated from EDTA-blood and stored at -80^{0}C for further use. Peripheral blood mononuclear cells (PBMCs) were isolated using Ficoll density gradient and cryopreserved in FBS 10% DMSO until analysis, in liquid nitrogen. Serum was aliquoted and stored at -80^{0}C until use.

Anti-SARS-CoV-2 humoral response

All individuals were tested for IgG recognizing the RBD domain of the Spike glycoprotein (IgG-RBD-S), IgG against the Nucleocapsid protein (IgG-N) and IgM against the Spike glycoprotein (IgM-S). IgM-S and IgG-N were measured using the SARSCoV-2 IgG-N and the SARS-CoV-2 IgM-S assays (Abbott, Ireland), respectively, and IgG-RBD-S were tested using the SARS-CoV-2 IgG II Quant assay (Abbott, Ireland). Samples were run in single replicate according to the manufacturer's instructions, using the ARCHITECT i2000 System (Abbott), as previously described [26–28]. For IgG-N and IgM-S, the results were reported as assay index (S/C) with a positive cut-off ≥1.4 for IgG-N and ≥1 for IgM-S. For IgG-RBD-S results were reported as binding antibody Unit/mL (BAU/mL, cut-off ≥7.1) [29]. Samples with values>5680 BAU/mL (upper limit of quantification) were diluted 1:2 and measured again. Concentrations were reported considering the dilution factor.

SARS-CoV-2 neutralizing activity against virus variants Delta, BA1, BA4/5

Neutralizing activity of sera was tested using lentiviral pseudotypes of SARS-CoV-2, as previously described [30–32]. SARS-CoV-2 pseudotypes with Spike variants were produced in HEK293T/17 cells (human embryonic kidney 293 cells, ATCC CRL-11268) by co-transfecting with the Spike variant-coding plasmids, packaging plasmid p8.91 and pCSFLW reporter plasmid using the FuGENE HD Transfection Reagent (Promega) according to the manufacturer's instructions. Supernatants containing the virus were harvested 72 h after transfection, centrifuged at 500xg for 5 min to clear it from cell debris and filtered with a 0.45-µm filter before storage at −80 °C. Before neutralization, all virus stocks were titrated by infection of Chinese Hamster Ovary (CHO) cells that stably expressed human ACE2/TMPRSS2 proteins (CHO ACE2/TMPRSS2, herein referred to as CHO/A2/T2) which are the cellular targets of SARS-CoV-2 infection, as described previously [30, 33]. Sera neutralizing potency was assayed on CHO/A2/T2 cells. Endpoint two-fold serial dilutions of heat-inactivated sera samples (56 °C for 30 min) were incubated with 106 RLU of pseudotyped viruses at 37 °C 5%, CO2 for 1 h before addition of 104 CHO/A2/T2 cells per well (96 well plate format) and incubation for 48 h. Following incubation, cells were lysed in Luciferase Assay System (Promega) and luciferase activity was measured using a Glo-Max luminometer (Promega). The neutralization rates were expressed as IC50 values, defined as the inhibitory dilution at which the half-maximal neutralization is achieved. To set up the neutralization assay the International Standard for anti-SARS-CoV-2 antibody (NIBSC code 20/136) and WHO Reference Panel were included as controls, as established previously [30].

Immune cell phenotype (B, CD4 and CD8)

Cellular markers were measured by staining frozen PBMCs. For B and T cell populations DURAClone IM B cell tube and DURAClone IM T cell (both from Beckman Coulter, Research Use Only RUO) were used as we previously described [34]. Using surface marker staining, we assessed the frequencies of B and T cell maturation stage distribution. Therefore, we examined the exhausted or senescent phenotype of T cells, by measuring respectively the Programmed cell death protein 1 (PD-1) and CD57 expression on the cells' surface. Moreover, we designed two panels for helper (Th) and regulatory (Treg) T cells, as previously published [27]. Data acquisition was performed using a CytoFlex flow cytometer with CytExpert v2.3 software (Beckman Coulter). The stopping rule was set at 10,000 events in the T cells (CD3+) panel and 1,000 events in the B-cells (CD19+). Data were analysed with Kaluza v2.1 software (Beckman Coulter) and the Cytobank Premim software (Beckman Coulter). The list of Ab and gating strategies applied were described in Supplementary Tables 1 and Supplementary Figs. 1, 2, 3.

Plasma cytokine profile

MACSPlex Cytokine 12 kit human (MACS Miltenyi Biotec) was used as indicated by the manufacturer to specifically detect: GM-CSF, IFN- α, IFN-γ, IL-2, IL-4, IL-5, IL-6, IL-9, IL-10, IL-12p70, IL-17α e TNF- α. Data were acquired on a CytoFlex flow cytometer (Beckman Coulter) at a flow rate of 20 µL/minute. The acquisition stopping rule was set to 4.000 events in the bead gate or 180 µl of acquired sample. The exported data were analyzed with Flowlogic software (Inivai Technologies). Cytokines' concentration (pg/ml) was obtained by interpolation with the standard curve provided by the kit.

Statistical analysis

Results for continuous variables were summarized using median and IQR while categorical variables using

frequencies and percentages. Nonparametric tests were applied to compare patients receiving different vaccine doses for relevant demographic/clinical characteristics and immunological responses: in particular, Fisher's exact test was used with categorical variables, while the Mann-Whitney test was applied in continuous variables. Spearman's partial correlation coefficient was calculated to evaluate, within patients receiving 0 or 2/3 doses of vaccine, the presence of a monotonic relationship between two immunological responses after adjusting for age. The false discovery rate (FDR) approach was used to adjust *p*-values thus addressing arising multiplicity issues. Multiple regression models were performed to evaluate differences among groups defined either (i) on received dose or (ii) on age (>70 yrs vs. ≤ 70 yrs) on immunological response adjusting for potential confounding variables. In particular, along with standard linear regression models, Tobit models have been estimated in the presence of censored dependent outcome variables. To satisfy underlying model assumptions, outcome variables were transformed using standard transformations (e.g., logarithm, power transformation, square root, ordered quantile normalization). All the analyses were performed using R statistical software (version 4.2.2, https://cran.r-project.org/index.html). In all the analyses, the significance level was set at 0.05.

Results

Patients' population characteristics according to vaccination doses and age

The study cohort included 47 patients hospitalized for COVID-19 pneumonia resulting from SARS-CoV-2 infection, during Delta and Omicron waves. Patients' characteristics are shown in Table 1. Overall, median age was 78.41 years [IQR 68–84], 22/47 (47%) were female, and 12/47 (29%) had history of cancer. Based on the WHO clinical progression scale [22], 25/47 (57%) patients were classified as moderate (score 4 and 5, s≤5) and 19/47 (43%) as severe patients (score 6, s>5). Patients that appeared critically ill at admission and needed ICU were not included in the study. Apart from 2 patients (age>80 years), who experienced a negative progression of the disease and died (at admission s>5; at death s=10), all the other patients achieved a full remission.

At hospital admission, 17/47 (36%) individuals were not vaccinated (VAC_{no}), whilst the remaining 30/47 (64%) had received 2 doses (18/30, 60%, VAC_2) or 3 doses (12/30, 40%, VAC_3) of anti-SARS-CoV-2 vaccine, designed *versus (vs.)* the original Wuhan strain. Comparing general characteristics of vaccinated and unvaccinated patients, the ratio male/female was similar in the two groups (VAC_{no}vs. VAC_{2+3}), while the VAC_{2+3} one was relatively older than the VAC_{no} (medians years 80 vs. 71, respectively). The older group (VAC_{2+3}) was more likely to have experienced some comorbidities compared to the younger one (VAC_{no}), including obesity (19% vs. 0%), chronic obstructive pulmonary disease (COPD, 4% vs. 0), diabetes (12% vs. 6%), cancer (31% vs. 25%), or other diseases (31% vs. 13%, specified in Table 1), albeit none of the difference was statistically significant. Both VAC_{2+3} and VAC_{no} experienced pulmonary arterial hypertension (PAH) with similar frequency (39% vs. 38%). Within VAC_{2+3} group, individuals who received 3 vaccination doses were less likely to have experienced PAH (10% of cases in VAC_3 vs. 56% in VAC_2). With regards to the percentage of severe patients (s>5), this was lower in VAC_{2+3} group (39%) than in VAC_{no} (50%) and among the vaccinated, those with three doses were less likely to have experienced severe symptoms (30% of s>5 in VAC_3 vs. 44% in VAC_2) (Table 1).

Anti-SARS-CoV-2 response in elderly versus aged patients

Further, we explored the impact of age on the disease outcome and immune response in the context of COVID-19 pneumonia in presence or absence of vaccination. We thus divided the population into two strata: one below 70 years of age (≤70y, $n=14$) and one over 70 (>70y, $n=33$) and the characteristics of these 2 groups are provided in Supplementary Table 2. As it could be expected, the individuals>70y were more likely to have experienced comorbidities associated with aging such as PAH (29% in ≤70y vs. 36% in >70y), diabetes (absent in ≤70 vs. 12% in >70y), cancer (21% in ≤70y vs. 27% in >70y) and other diseases (14% in ≤70 vs. 24% in >70y). Lack of vaccination was more frequent in younger individuals, with 50% of ≤70y and 30% of >70y subjects being VAC_{no}. Of note, in the elderly group, administration of three doses of vaccination resulted in a lower proportion of severe cases (14% severe cases in VAC_3 vs. 43% in VAC_2 and 44% in VAC_{no}). We further run a multivariable regression model comparing subjects≤70 yrs and >70 yrs of age adjusted for vaccine doses and gender (Table 2). We found that elderly had an overall lower anti-SARS-CoV-2 humoral response (IgG-RBD-S) with an expansion of CD28null CD4 populations. Of note, none of the individuals who received 3 doses experienced death, whilst the two people who died were both >70y: one was VAC_2 and the other was VAC_{no} (Supplementary Table 2).

Vaccination was associated with increased anti-SARS-CoV-2 humoral response and neutralizing activity

Humoral response was evaluated by measuring circulating IgG-N, IgM-S, IgG-RBD-S Antibodies (Ab) (Table 3; Fig. 1). Overall, IgG-N were detectable in 33/47 (70%), IgM-S in 26/47 (55%) and IgG-RBD-S in 30/47 (81%). By linear regression models adjusted for gender, age and cancer, comparing individuals that received or not the vaccine, we reported that IgG-RBD-S Ab levels

Table 1 Patients' characteristics

		All	VAC_{no}	VAC_{2+3}		VAC_2		VAC_3	
		47	*17*	*30*	p-value (2 + 3 vs. no)	*18*	p-value (2 vs. no)	*12*	p-value (3 vs. 0)
WHO classification, n (%)	**Moderate, s ≤ 5**	25 (56.8)	8 (50.0)	17 (60.7)	0.54	10 (55.6)	1	7 (70.0)	0.428
	Severe, s > 5	19 (43.2)	8 (50.0)	11 (39.3)		8 (44.4)		3 (30.0)	
	NA, n	3	1	2				2	
PAH, n (%)	**No**	26 (61.9)	10 (62.5)	16 (61.5)	1	7 (43.8)	0.479	9 (90.0)	0.19
	Yes	16 (38.1)	6 (37.5)	10 (38.5)		9 (56.2)		1 (10.0)	
	NA, n	5	1	4		2		2	
Obesity, n (%)	**No**	37 (88.1)	16 (100.0)	21 (80.8)	0.138	11 (68.8)	0.043	10 (100.0)	1
	Yes	5 (11.9)	0 (0.0)	5 (19.2)		5 (31.2)		0	
	NA, n	5	1	4		2		2	
COPD, n (%)	**No**	41 (97.6)	16 (100.0)	25 (96.2)	1	16 (100.0)	1	9 (90.0)	0.385
	Yes	1 (2.4)	0 (0.0)	1 (3.8)		0		1 (10.0)	
	NA, n	5	1	4		2		2	
Diabetes, n (%)	**No**	38 (90.5)	15 (93.8)	23 (88.5)	1	13 (81.2)	0.6	10 (100.0)	1
	Yes	4 (9.5)	1 (6.2)	3 (11.5)		3 (18.8)		0	
	NA, n	5	1	4		2		2	
Cancer, n (%)[a]	**No**	30 (71.4)	12 (75.0)	18 (69.2)	0.74	13 (81.2)	1	5 (50.0)	0.234
	Yes	12 (28.6)	4 (25.0)	8 (30.8)		3 (18.8)		5 (50.0)	
	NA, n	5	1	4		2		2	
Other diseases, n (%)[b]	**No**	32 (76.2)	14 (87.5)	18 (69.2)	0.27	12 (75.0)	0.654	6 (60.0)	0.163
	Yes	10 (23.8)	2 (12.5)	8 (30.8)		4 (25.0)		4 (40.0)	
	NA, n	5	1	4		2		2	
Gender, n (%)	**F**	22 (46.8)	9 (52.9)	13 (43.3)	0.558	7 (38.9)	0.505	6 (50.0)	1
	M	25 (53.2)	8 (47.1)	17 (56.7)		11 (61.1)		6 (50.0)	
Outcome, n (%)	**RE**	45 (95.7)	16 (94.1)	29 (96.7)	1	17 (94.4)	1	12 (100.0)	1
	DE	2 (4.3)	1 (5.9)	1 (3.3)		1 (5.6)		0 (0.0)	
SARS-CoV-2 VOC, n (%)	**Delta**	20 (42.6)	7 (41.2)	13 (43.3)	1	13 (72.2)	0.092	0 (0.0)	0.023
	Omicron	27 (57.4)	10 (58.8)	17 (56.7)		5 (27.8)		12 (100.0)	
age (median [IQR])		78.41 [68.31, 84.04]	71.32 [66.78, 79.51]	79.80 [74.15, 84.27]	0.163	79.24 [74.15, 82.28]	0.276	80.78 [74.58, 84.37]	0.184

NA = not available data; RE: remission, DE: death. PAH: pulmonary arterial hypertension. COPD: chronic obstructive pulmonary disease. [a]Type of cancer in the population were: chronic lymphatic leukaemia ($n=2$), lymphoma ($n=1$), multiple myeloma ($n=1$), myelofibrosis ($n=1$), breast cancer ($n=2$), pancreatic cancer ($n=1$), lung cancer ($n=1$), colorectal cancer ($n=1$), prostatic cancer ($n=1$), adenoid cystic carcinoma ($n=1$). [b]other disease included: cardiovascular ($n=2$), pulmonary ($n=2$), metabolic (other than diabetes and obesity, $n=1$), renal ($n=1$), neurologic ($n=4$). p-values referred to Fisher's exact test in presence of categorical outcomes, while Mann-Whitney test was applied in the presence of continuous variables

were higher in VAC_{2+3} compared to VAC_{no} ($p=0.0026$, Table 3; Fig. 1) conversely to what was observed for IgG-N Ab levels which were lower in (VAC_{2+3} compared to VAC_{no} ($p=0.0408$, Table 3; Fig. 1. IgM-S levels did not vary across the groups.

In a separate regression model, using the same adjustments described above, we evaluated the impact of one or two doses of vaccine, and we compared the humoral response in VAC_{no} vs. VAC_2 or VAC_3 (Supplementary Table 3). We observed that both VAC_2 and VAC_3 had higher levels of IgG-RBD-S compared to VAC_{no}, but this was only significant for VAC_2 ($p=0.0001$). On the other hand, anti-N IgG levels decrease with the number of vaccine doses, with the highest level detected in VAC_{no} group ($p=0.0014$ compared with VAC_3), as showed in Fig. 1; Table 3.

Further, we explored the impact of vaccination on the Ab neutralization activity during natural infection driving pneumonia. We tested neutralizing antibodies against both circulating variants Delta, BA.1 and BA.4/5 and human seasonal coronaviruses (HCOVs, 229E, HKU1, NL63). Overall, individuals who received vaccination (VAC_{2+3}) showed significantly higher levels of neutralizing activity against the circulating variants compared to VAC_{no} ($p=0.0.34$ Delta; $p=0.044$ BA.1 and $p=0.038$ BA.4/5; Table 3). Of note, this difference was mainly driven by VAC_2, rather than VAC_3 (Supplementary Table 3). Activity versus seasonal coronaviruses was not different between the groups.

Cellular immune response was elevated in individuals who received vaccination, regardless to age, gender or cancer history.

Table 2 Multiple regressions for comparison of subjects > 70 yrs of age and subjects ≤ 70 yrs of age, adjusted for vaccine doses and gender. Tobit regression models for IgG-N (index), IgM-S (index) and IgG-RBD-S (BAU/mL). Linear regression models for the other outcomes

	> 70 yrs vs. ≤ 70 yrs		
Outcome	**Estimate**	**Std.er.**	***p*-value**
IgG-N (index)	-2.0165	0.7431	0.0067
IgM-S (index)	-1.2085	0.7847	0.1236
IgG-RBD-S (BAU/mL)	-2.2159	0.8287	0.0075
IC50 229E	0.2193	0.3314	0.5119
IC50 HKU1	0.1482	0.3278	0.6535
IC50 NL63	-0.1728	0.3452	0.6193
IC50 DELTA	-0.7378	0.2877	0.0141
IC50 BA1	-0.5189	0.3042	0.0956
IC50 BA4/5	-0.5859	0.2954	0.0541
GM-CSF pg/ml	-0.2694	0.4097	0.5148
IFN-α pg/ml	-0.1027	0.3306	0.7577
IFN-γ pg/ml	0.0584	0.3191	0.8558
IL-4 pg/ml	-4.3309	13.8644	0.7565
IL-5 pg/ml	-0.1588	0.3146	0.6168
IL-6 pg/ml	0.5311	0.3135	0.0985
IL-10 pg/ml	0.2305	0.7504	0.7604
IL-12p70 pg/ml	-0.1541	0.4480	0.7327
IL-17 A pg/ml	-0.1109	0.4508	0.8070
TNF-α pg/ml	-0.0881	0.3039	0.7733
leukocytes	-0.3116	0.3455	0.3727
B cells count	-0.2466	0.3113	0.4330
B cells (% on CD45+)	-0.5055	0.6985	0.4736
B activated (CD19+/CD27+/IgD-/CD21-)	0.6580	0.3130	0.0440
B resting (CD19+/CD27+/IgD-/CD21+)	0.7319	0.5651	0.2051
CD21low/CD38 low (CD19+/ $CD21^{low}$/$CD38^{low}$)	-0.3782	0.3683	0.3127
DN (CD19+/CD27-/IgD-)	0.4236	0.4014	0.2998
Marginal Zone (MZ) (CD19+/CD27+/IgD+)	0.0240	0.2882	0.9341
Memory B cells (MB) (CD19+/CD27+/IgD-)	0.9430	0.5817	0.1154
Naive B cells (CD19+/CD27-/IgD+/CD21-)	-13.0766	8.8247	0.1488
Plasmablast (CD19+/CD27+/IgM-/IgG-/$CD38^{high}$)	7.6308	4.9079	0.1305
SWI (CD19+/CD27+/IgM-/IgG-)	0.8061	0.6244	0.2065
TLM (CD19+/CD27-/CD21-)	-0.3157	0.4136	0.4512
Trans B (CD19+/CD27-/ $CD38^{high}$/$CD24^{high}$)	-0.5682	0.3394	0.1045
UNSWI (CD19+/CD27+/IgM+/IgG+)	0.0692	0.5991	0.9089
CD4 + T cells count	0.0321	0.3353	0.9242
CD4+ (% of CD3+)	-4.9385	6.4672	0.4497
CM-CD4 (CD4+/CD45RA-/CCR7+)	-3.5265	4.4790	0.4364
N-CD4 (CD4+/ CD45RA+ /CCR7+)	-2.6626	4.1079	0.5211
EM-CD4 (CD4+/ CD45RA-/ CCR7-)	4.5056	4.3223	0.3044
TEMRA CD4 (CD4+/ CD45RA+/ CCR7+)	0.6308	0.5071	0.2218
CD4+/PD1-/CD57-	-5.6604	5.7776	0.3340
CD4+/PD1-/CD57+	0.3004	0.3344	0.3750
CD4+/PD1+/CD57-	0.1981	5.1764	0.9697
CD4+/PD1+/CD57+	0.7492	0.4763	0.1247
CD4+/CD27-/CD28-	0.7354	0.3063	0.0218
CD4+/CD27-/CD28+	0.2070	0.2981	0.4921
CD4+/CD27+/CD28-	0.7004	0.3400	0.0469
CD4+/CD27+/CD28+	-8.2945	5.1942	0.1193
CD8 + T cells count	1291.8860	632.4504	0.0479
CD8+ (%of CD3+)	0.0853	0.1746	0.6280

Table 2 (continued)

	> 70 yrs vs. ≤ 70 yrs		
Outcome	**Estimate**	**Std.er.**	***p*-value**
N-CD8 (CD8+/ CD45RA+ /CCR7+)	-0.3726	0.2208	0.1001
CM-CD8 (CD8+/CD45RA-/CCR7+)	-8.0210	6.3046	0.2114
EM-CD8 (CD8+/ CD45RA-/ CCR7-)	7.8387	5.3385	0.1507
TEMRA-CD8 (CD8+/ CD45RA+/ CCR7+)	0.9748	0.6742	0.1568
CD8+/CD57-/PD1-	0.2013	2.9723	0.9464
CD8+/CD57-/PD1+	-0.1358	0.1691	0.4273
CD8+/CD57+/PD1-	0.6822	0.5927	0.2574
CD8+/CD57+/PD1+	1.7821	5.0780	0.7277
CD8+/CD27-/CD28-	4.4434	6.7942	0.5173
CD8+/CD27-/CD28+	0.4703	0.2475	0.0655
CD8+/CD27+/CD28-	1.4167	1.7725	0.4294
CD8+/CD27+/CD28+	-8.8544	6.4304	0.1770
Th1 (CD4+/CCR6- /CXCR3+);	4.1130	4.3099	0.3463
Th17 (CD4+/CCR6+/ CCR4+)	0.1043	0.3537	0.7698
Th17-1 (CD4+/CCR6+/CXCR3+)	-0.4384	0.4224	0.3062
Th2 (CD4+/CCR6-/CCR4+)	-0.2955	0.3311	0.3781
Treg (CD4+/CD25+/CD127^{low})	0.1662	0.1639	0.3175

At admission, extensive phenotypic profiling was also performed to evaluate the immune activation in the B and T (CD4, CD8) cell compartments. All the cellular subpopulations were included in the linear regression models and reported in Table 3 and Supplementary Table 3.

With regards to B-cells, we observed only that the total B count was higher in VAC_{2+3} compared to VAC_{no} ($p=0.0079$), meanwhile none of the activated populations were different (Table 3 and Supplementary Table 3). This data was probably driven mostly by the comparison VAC_2 vs. VAC_0 (Supplementary Table 3, $p=0.0028$). When looking at the CD4 sub-populations in the three vaccination groups, levels of Th1 lymphocytes (CCR6-/CXCR3+) appeared to be the most abundant compared to the other Th subtypes (Th2, Th17-1, Th17) (Fig. 2A-B, Supplementary Table 3). Of note, the proportion of the Th2 cell varied across the groups, with the VAC_{2+3} showing higher levels compared to VAC_{no} ($p=0.009$, Fig. 2A; adjusted value in Table 3). This difference remained significant also when the number of vaccine doses was considered. Indeed, both VAC_2 ($p=0.0233$) and VAC_3 ($p=0.0241$) had higher levels compared to VAC_{no} (adjusted values in Supplementary Table 3, Fig. 2B). We did not observe significant differences regarding the other CD4 populations, a part of an increase of the effector memory CD4 in the VAC_3 compared to VAC_{no} (EM-CD4+, $p=0.0325$, Supplementary Table 3).

Finally, we explored the CD8 population and we found an increase of the proportion of CD8 in VAC_{2+3} compared to VAC_{no} ($p=0.008$, Table 3) and this association persisted only when comparing separately VAC_{no} to VAC_3 ($p=0.0319$, Supplementary Table 3); furthermore, individuals who received 3 vaccine doses also had higher total CD8 counts ($p=0.0002$) compared to unvaccinated (Supplementary Table 3). When looking at the CD4/CD8 lymphocytes ratio (Fig. 2C), consistently with the multivariable adjusted analysis, we observed an expansion of the CD8 in VAC_3 group.

Soluble cytokines levels during COVID-19 pneumonia varied according to vaccination doses

Alongside the characterization of humoral and cellular responses of our cohort, we also profiled the serum levels of cytokines and included the data within the multivariable linear regression models (Table 3, Supplementary Table 3). Probably in response to COVID-19 pneumonia and independently from vaccine administration, cytokines levels appeared overall strongly correlated with each other, in the three VAC groups (Fig. 3). No statistically significant differences were observed between vaccinated and not vaccinated patients (VAC_{2+3} vs. VAC_{no}). When considering the number of vaccination doses (Supplementary Table 3), we found higher levels of GM-CSF in VAC_2 vs. VAC_{no} ($p=0.0250$), meanwhile the pro-inflammatory cytokine IFN-α appeared to be reduced in VAC_3 vs. VAC_{no} ($p=0.0388$).

Both humoral and cellular immune response is influenced by the virus variants driving pneumonia

Overall, Delta variant was the most representative in VAC_2 ($n=13/18$, 72%), detected in 41% of VAC_0, whereases undetected in VAC_3 (Table 1). We then evaluated the impact of the type of variants (Delta vs. Omicron, Table 4) using a multiple regression adjusted for vaccine dose, age, gender and cancer. Delta infections were able

Table 3 Multiple regressions for comparison of groups VAC_{2+3} vs. VAC_{no} adjusted for age, gender and cancer. Tobit regression models for IgG-N (index), IgM-S (index) and IgG-RBD-S (BAU/mL). Linear regression models for the other outcomes

	VAC_{2+3} vs. VAC_{no}		
	Estimate	**Std.er.**	***p*-value**
IgG-N (index)	-1.6287	0.7961	0.0408
IgM-S (index)	0.2484	0.8002	0.7563
IgG-RBD-S (BAU/mL)	2.8312	0.9397	0.0026
IC50 229E	-0.304	0.342	0.381
IC50 HKU1	0.021	0.351	0.952
IC50 NL63	0.110	0.382	0.775
IC50 DELTA	0.685	0.311	0.034
IC50 BA1	1.982	0.949	0.044
IC50 BA4/5	0.678	0.315	0.038
GM-CSF pg/ml	0.527	0.484	0.284
IFN-α pg/ml	-0.391	0.366	0.294
IFN-γ pg/ml	0.036	0.339	0.915
IL-4 pg/ml	9.587	14.513	0.513
IL-5 pg/ml	0.291	0.350	0.411
IL-6 pg/ml	-0.068	0.350	0.848
IL-10 pg/ml	0.053	0.839	0.950
IL-12p70 pg/ml	0.132	0.498	0.792
IL-17 A pg/ml	0.150	0.518	0.774
TNF-α pg/ml	0.099	0.334	0.768
leukocytes	13.392	8.054	0.106
B cells count	700.739	233.339	0.005
B cells (% on CD45+)	1.651	0.637	0.014
B activated (CD19+/CD27+/IgD-/CD21-)	0.404	0.314	0.209
B resting (CD19+/CD27+/IgD-/CD21+)	-0.277	0.643	0.670
CD21low/CD38 low (CD19+/ $CD21^{low}$/$CD38^{low}$)	0.027	0.427	0.950
DN (CD19+/CD27-/IgD-)	0.076	0.461	0.871
Marginal Zone (MZ) (CD19+/CD27+/IgD+)	0.107	0.299	0.724
Memory B cells (MB) (CD19+/CD27+/IgD-)	-0.132	0.663	0.843
Naive B cells (CD19+/CD27-/IgD+/CD21-)	6.012	9.631	0.538
Plasmablast (CD19+/CD27+/IgM-/IgG-/$CD38^{high}$)	2.318	5.566	0.681
SWI (CD19+/CD27+/IgM-/IgG-)	-0.070	0.703	0.921
TLM (CD19+/CD27-/CD21-)	-0.123	0.482	0.800
Trans B (CD19+/CD27-/ $CD38^{high}$/$CD24^{high}$)	0.253	0.369	0.500
UNSWI (CD19+/CD27+/IgM+/IgG+)	-0.296	0.661	0.658
CD4 + T cells count	889.308	900.969	0.331
CD4+ (% of CD3+)	-2.434	7.447	0.746
CM-CD4 (CD4+/CD45RA-/CCR7+)	-4.022	4.497	0.378
N-CD4 (CD4+/ CD45RA+ /CCR7+)	-0.093	0.371	0.804
EM-CD4 (CD4+/ CD45RA-/ CCR7-)	1.461	5.256	0.783
TEMRA CD4 (CD4+/ CD45RA+/ CCR7+)	0.106	0.531	0.844
CD4+/PD1-/CD57-	119.221	456.438	0.796
CD4+/PD1-/CD57+	-0.072	0.271	0.791
CD4+/PD1+/CD57-	2.501	5.742	0.666
CD4+/PD1+/CD57+	0.085	0.563	0.880
CD4+/CD27-/CD28-	-0.281	0.546	0.610
CD4+/CD27-/CD28+	3.481	4.064	0.399
CD4+/CD27+/CD28-	0.259	0.377	0.498
CD4+/CD27+/CD28+	-2.927	5.969	0.627
CD8 + T cells count	1966.495	702.269	0.008
CD8+ (%of CD3+)	5.442	7.070	0.447
N-CD8 (CD8+/ CD45RA+ /CCR7+)	-0.247	0.231	0.294

Table 3 (continued)

	VAC_{2+3} vs. VAC_{no}		
	Estimate	**Std.er.**	***p*-value**
CM-CD8 (CD8+/CD45RA-/CCR7+)	-5.938	6.537	0.371
EM-CD8 (CD8+/ CD45RA-/ CCR7-)	3.330	5.416	0.543
TEMRA-CD8 (CD8+/ CD45RA+/ CCR7+)	0.496	0.677	0.469
CD8+/CD57-/PD1-	2.609	3.056	0.400
CD8+/CD57-/PD1+	-3.202	6.384	0.619
CD8+/CD57+/PD1-	0.128	0.701	0.857
CD8+/CD57+/PD1+	-2.653	5.087	0.606
CD8+/CD27-/CD28-	-1.105	7.444	0.883
CD8+/CD27-/CD28+	-0.402	0.271	0.148
CD8+/CD27+/CD28-	-0.745	1.936	0.703
CD8+/CD27+/CD28+	4.998	7.074	0.485
Th1 (CD4+/CCR6- /CXCR3+);	-3.974	4.653	0.400
Th17 (CD4+/CCR6+/ CCR4+)	-0.178	0.393	0.654
Th17-1 (CD4+/CCR6+/CXCR3+)	0.627	0.422	0.148
Th2 (CD4+/CCR6-/CCR4+)	0.975	0.351	0.009
Treg (CD4+/CD25+/$CD127^{low}$)	0.008	0.159	0.961

to elicit a higher humoral response in terms of IgM-S ($p=0.0301$) and IC50 vs. Delta ($p=0.0123$), with a trend for higher IgG-RBD-S ($p=0.0715$). Further, infections with Delta also increased pro-inflammatory cytokines, such as IFN-α ($p=0.0463$) and IL-6 ($p=0.0010$). Alongside a trend for higher IgG-RBD-S in Delta, we also observed an expansion in the B cells compartments, including resting B cells (CD27+IgD-CD21+, $p=0.0400$) and Switched B cells (CD27+IgD-IgM-, $p=0.0176$). Together with an increase of pentamer a-specific IgM-S in Delta infections, we reported higher levels of the naïve CD4 T cells ($p=0.0025$) and a decrease of the CD27- (memory) CD4 T cells ($p=0.0147$). Helper CD4 and CD8 populations did not appear to be affected by type of variants.

Discussion

In this work, we explored the humoral, cellular and soluble markers of immune response in aged patients with COVID-19 pneumonia caused by Delta/Omicron variants. We showed that vaccination supported an elevated anti-SARS-CoV-2 humoral and cellular response, regardless to age, gender or cancer history. The administration of three doses of vaccine, rather than two or none, was more frequent in elderly individuals above 70 years of age and was highly associated with less severe symptomatology and higher survival rate. The virus variants driving pneumonia played a central role in supporting both the cellular and humoral response. Our study provides comprehensive immunological profiling of a cohort of aged patients, which is unique because it does also include non-vaccinated subjects that were hospitalized for COVID-19 pneumonia.

A previous work explored the immunological features during COVID-19 pneumonia in a population of 33 vaccine naïve subjects above 70 years old compared to younger individuals (<60 years) [6]. The authors found that elderly population showed reduced capacity to mount a proper anti-viral response that could drive to more severe outcomes. In our cohort, we confirmed that older individuals who did not receive vaccination or only 2 doses experienced worse clinical outcome an higher probability of death. On the other hand, we confirmed that completion of the vaccine schedule (3 vaccination doses at the time of the study) was associated with an efficient immune response and milder clinical outcome, confirming general guidelines that seek to prioritise the elderly population for vaccination to avoid severe COVID-19 symptoms [15].

Patients within our cohort experienced respiratory distress syndrome (ARDS) caused by SARS-CoV-2 infection. All had a positive clinical outcome, excluding two patients over 70 years, one non-vaccinated and one that did not complete the vaccination schedule, who did not survive the infection, despite being initially assigned a score in the range of the study group. Despite the similar clinical course, we observed differences driven by the vaccination status (VAC_{no}, VAC_2, VAC_3,) that affected the immune responses during natural infection.

Vaccinated individuals also had elevated levels of Th2 cells, which are known to prevent immune-driven lung damage [35, 36]; this data is in line with others confirming the protective role of the vaccines towards worse clinical outcomes [37–40]. Whilst plasma cytokines appeared to be similar between vaccinated and non-vaccinated individuals, when stratifying the population according to the number of vaccine doses, we could make

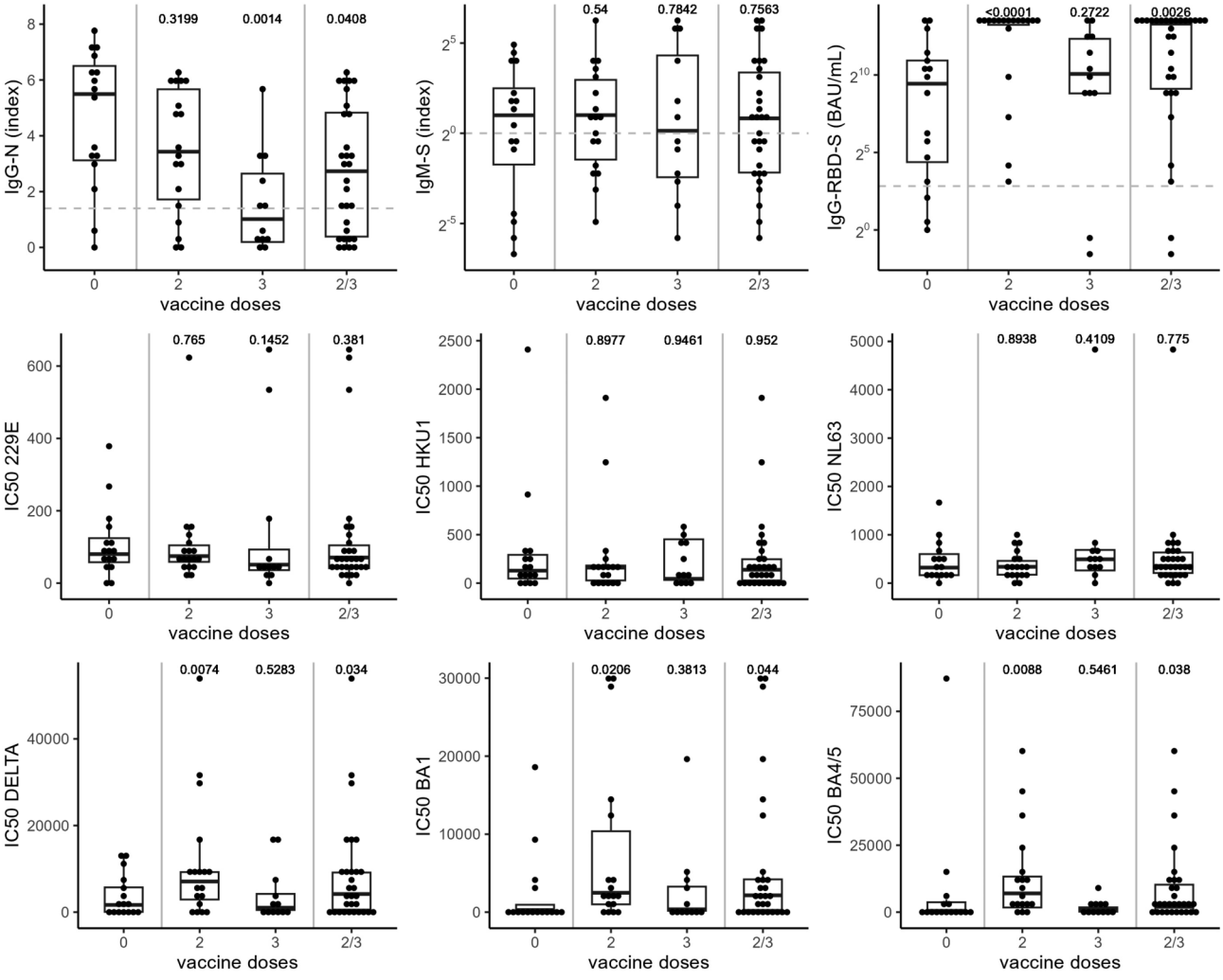

Fig. 1 Levels of SARS-CoV-2 specific antibodies and neutralizing activity. The dashed lines represent the cutoff values. p-values correspond to the comparison against the group VACno adjusted for age, gender and cancer. Tobit regression models for IgG-N (index), IgM-S (index) and IgG-RBD-S (BAU/mL). Linear regression models for the other outcomes. Full statistics report is available in Table 2 and Supplementary Table 2.

some observations. First, the levels of GM-CSF, which is known to be associated with virus clearance from lungs, [36] were significantly higher in VAC_2 but not in VAC_3 compared to VAC_{no}. Second, the levels of the pro-inflammatory cytokine IFN-α were significantly reduced in VAC_3 vs. VAC_{no}. As an expected consequence of the vaccination, VAC_{2+3} individuals showed higher anti-SARS-CoV-2 humoral response levels and expansion of B and CD8 cell populations, which appeared to be independent of age, gender or cancer history.

Neither vaccination nor variants driving infection had an impact on the neutralization activity vs. human seasonal coronaviruses. On the other hand, we observed differences in the anti-SARS-CoV2 humoral response when looking independently at VAC_2 and VAC_3 vs. VAC_{no}, which could be explained by the intrinsic variability of the group, vaccine doses or it could be attributed to the variants driving pneumonia, considering that majority of VAC_2 were infected with Delta virus and VAC_3 with Omicron virus. Thus, we explored whether virus variants driving pneumonia could impact the immune responses, including humoral, cellular and soluble markers. Compared to VAC_{no}, VAC_2 group (Delta infections) but not VAC_3 (Omicron infections) showed higher anti-SARS-CoV-2 IgG levels. Whilst this could be attributed to possible immune tolerance driven by multiple doses [14], we previously demonstrated that Delta viruses are associated with anti-RBD-IgG/neutralizing antibodies against Wuhan [34]. Our analysis confirmed that infections with Delta are not only capable of eliciting a higher immune humoral response, but they also support an increase in the B cell compartments (resting and switched).

In line with previous studies, we found that Omicron variant (mainly detected in VAC_3) had proportionally lower production of circulating anti-RBD-S IgG and higher levels of IgG-N antibodies. This could be a

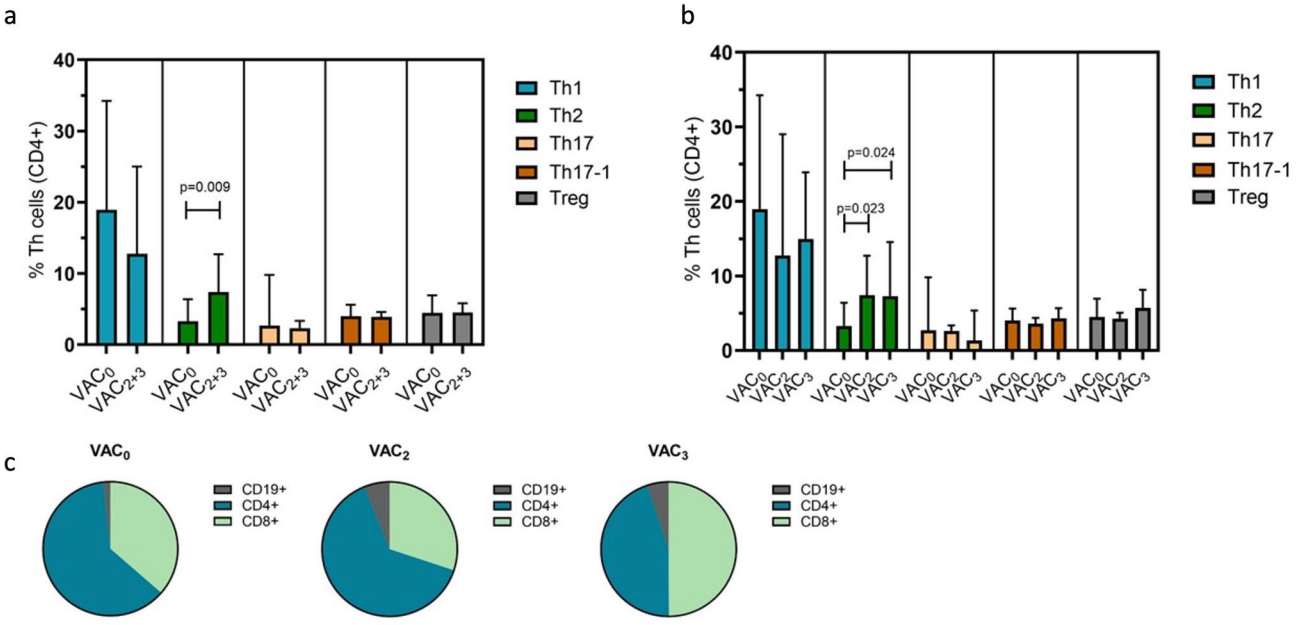

Fig. 2 The relative frequencies of T Helper subpopulation and Treg lymphocyte in the different groups of subjects. Bar plot representing the median and 95% IC of Th cells relative frequencies in non vaccinated (VAC0) or vaccinated (VAC2 + 3) (**a**) or depending on the number of doses (**b**). Pie-chart showing the relative frequency of CD19 + B cells, CD8 and CD4 T-cells sub-populations on CD3 + lymphocytes in VAC0, VAC2 and VAC3 (**c**). p-alues were obtained using non-parametric Spearman test. Levels of statistical significance was set at $p < 0.05$

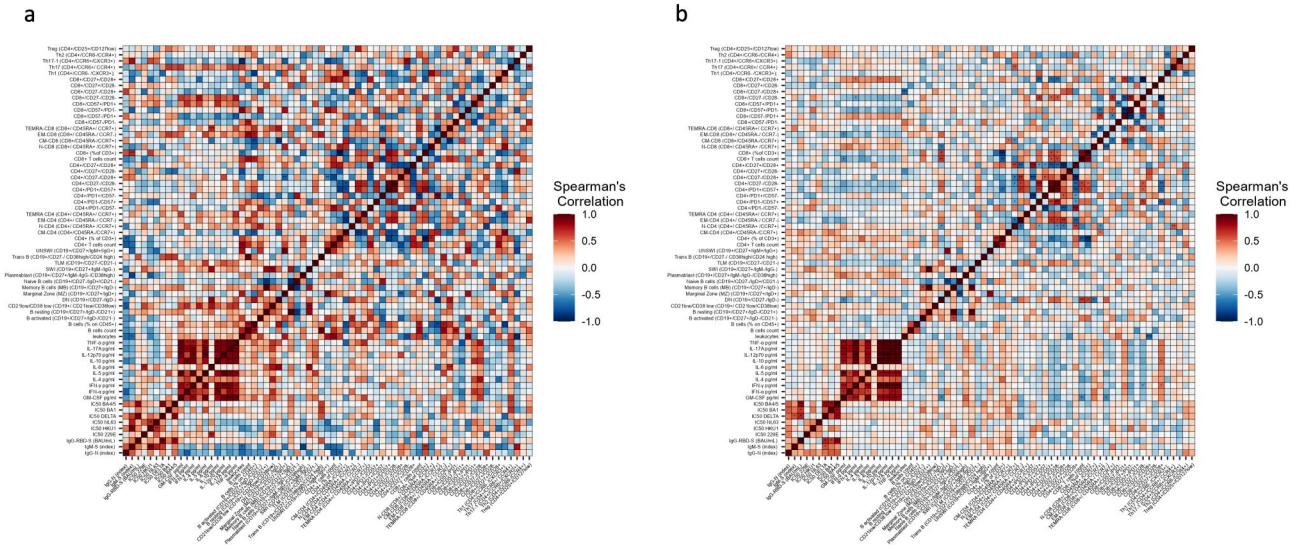

Fig. 3 Spearman's correlations between immunological responses in VACno ($n = 17$ in a) and VAC2 + 3 ($n = 30$ in b). The magnitude of each correlation is denoted with a colour, whereby the red colour indicates a positive correlation and the blue colour represents a negative correlation, such that the deeper the colour, the stronger the correlation. Levels of statistical significance with false discovery rate (FDR) correction are denoted as: $p < 0.05$, *$p < 0.01$, ***$p < 0.001$

reflection of the spike epitope immune escape mechanisms adopted by Omicron virus, which does also lead to an increment of CD8 T-cells (mainly cytotoxic) that we observed consistently with others [40, 41]. Consistently with the knowledge that Delta is more aggressive towards lung tissue than Omicron [42–44], we found that GM-CSF and IFN-α levels are higher in Delta vs. Omicron. Furthermore, whilst we reported above that variants could have an impact on the distribution of some cell populations, we observed that Th2 cells, which are associated with prevention from lung damage, were not affected by virus variants, but only a consequence of the vaccination, confirming again the protective role of vaccination against worse clinical outcome.

Table 4 Multiple regressions for comparison of Omicron and Delta, adjusted for vaccine doses, age, gender and cancer. Tobit regression models for IgG-N (index), IgM-S (index) and IgG-RBD-S (BAU/mL). Linear regression models for the other outcomes

	Delta vs. Omicron		
Outcome	Estimate	Std.er.	p-value
IgG-N (index)	0.6217	0.7509	0.4077
IgM-S (index)	1.5062	0.6943	0.0301
IgG-RBD-S (BAU/mL)	1.5130	0.8395	0.0715
IC50 229E	0.2817	0.3223	0.3879
IC50 HKU1	0.4711	0.3242	0.1551
IC50 NL63	0.3086	0.3594	0.3963
IC50 DELTA	0.7124	0.2698	0.0123
IC50 BA1	-0.5759	0.8979	0.5254
IC50 BA4/5	1.2422	0.9360	0.1931
GM-CSF pg/ml	0.4751	0.3420	0.1744
IFN-α pg/ml	0.6852	0.3305	0.0463
IFN-γ pg/ml	0.1774	0.3240	0.5879
IL-4 pg/ml	14.1453	13.7252	0.3105
IL-5 pg/ml	0.2850	0.3324	0.3976
IL-6 pg/ml	1.6181	0.4454	0.0010
IL-10 pg/ml	1.3452	0.7703	0.0903
IL-12p70 pg/ml	0.5763	0.4677	0.2269
IL-17 A pg/ml	0.8790	0.4731	0.0724
TNF-α pg/ml	0.3995	0.3129	0.2109
leukocytes	-2.9011	7.8949	0.7156
B cells count	269.8776	224.3362	0.2375
B cells (% on CD45+)	0.7588	0.6113	0.2232
B activated (CD19+/CD27+/IgD-/CD21-)	-0.0173	0.3028	0.9548
B resting (CD19+/CD27+/IgD-/CD21+)	0.9019	0.4162	0.0400
CD21low/CD38 low (CD19+/ $CD21^{low}$/$CD38^{low}$)	0.6866	0.3888	0.0896
DN (CD19+/CD27-/IgD-)	0.4834	0.4337	0.2757
Marginal Zone (MZ) (CD19+/CD27+/IgD+)	-0.1516	0.2872	0.6024
Memory B cells (MB) (CD19+/CD27+/IgD-)	0.6686	0.3927	0.1011
Naive B cells (CD19+/CD27-/IgD+/CD21-)	-7.1532	9.1820	0.4433
Plasmablast (CD19+/CD27+/IgM-/IgG-/$CD38^{high}$)	7.5426	5.1543	0.1558
SWI (CD19+/CD27+/IgM-/IgG-)	0.9232	0.3633	0.0176
TLM (CD19+/CD27-/CD21-)	-0.7770	0.4384	0.0885
Trans B (CD19+/CD27-/ $CD38^{high}$/$CD24^{high}$)	-0.0005	0.3564	0.9988
UNSWI (CD19+/CD27+/IgM+/IgG+)	-1.7455	4.7323	0.7154
CD4 + T cells count	786.8960	874.3323	0.3746
CD4+ (% of CD3+)	10.6719	7.0755	0.1410
CM-CD4 (CD4+/CD45RA-/CCR7+)	0.2753	4.3295	0.9497
N-CD4 (CD4+/ CD45RA+ /CCR7+)	13.4578	4.0624	0.0025
EM-CD4 (CD4+/ CD45RA-/ CCR7-)	-12.8855	4.4594	0.0072
TEMRA CD4 (CD4+/ CD45RA+/ CCR7+)	-0.2333	0.5096	0.6505
CD4+/PD1-/CD57-	14.5185	5.5581	0.0141
CD4+/PD1-/CD57+	-0.3390	0.2534	0.1913
CD4+/PD1+/CD57-	-9.2431	5.2551	0.0891
CD4+/PD1+/CD57+	-0.8698	0.5173	0.1034
CD4+/CD27-/CD28-	-0.9335	0.4966	0.0702
CD4+/CD27-/CD28+	-9.1499	3.5254	0.0147
CD4+/CD27+/CD28-	-0.3853	0.3559	0.2879
CD4+/CD27+/CD28+	15.2394	5.0018	0.0049
CD8 + T cells count	-1262.3090	653.8846	0.0622
CD8+ (%of CD3+)	-8.1591	6.7983	0.2386
N-CD8 (CD8+/ CD45RA+ /CCR7+)	0.0348	0.2200	0.8753

Table 4 (continued)

	Delta vs. Omicron		
CM-CD8 (CD8+/CD45RA-/CCR7+)	-8.3449	6.0393	0.1772
EM-CD8 (CD8+/ CD45RA-/ CCR7-)	0.5504	5.1589	0.9157
TEMRA-CD8 (CD8+/ CD45RA+/ CCR7+)	0.7101	0.6322	0.2703
CD8+/CD57-/PD1-	-1.1609	2.9039	0.6922
CD8+/CD57-/PD1+	1.2502	6.0777	0.8384
CD8+/CD57+/PD1-	-0.2581	0.6660	0.7011
CD8+/CD57+/PD1+	1.8455	4.8351	0.7054
CD8+/CD27-/CD28-	-5.2644	7.0267	0.4596
CD8+/CD27-/CD28+	-0.4830	0.2425	0.0555
CD8+/CD27+/CD28-	-1.2794	1.8300	0.4899
CD8+/CD27+/CD28+	9.8105	6.4971	0.1415
Th1 (CD4+/CCR6- /CXCR3+);	-1.9562	4.4188	0.6612
Th17 (CD4+/CCR6+/ CCR4+)	-0.1706	0.3736	0.6512
Th17-1 (CD4+/CCR6+/CXCR3+)	0.3190	0.3979	0.4290
Th2 (CD4+/CCR6-/CCR4+)	0.0029	0.3346	0.9931
Treg (CD4+/CD25+/CD127^{low})	-0.0103	0.1517	0.9463

This study presents some limitations that deserve discussion. First, the sample size was small and analysed cross-sectionally, thus subjected to casualties. Second, our study lacked a control group of vaccinated/non vaccinated subjects with COVID-19 mild disease without pneumonia, which could have helped to better define the impact of vaccination on preventing severe clinical outcome. Third, which is common to other similar studies, is the lack of clinical history before hospitalisation and thus the inability to accurately estimate timing of infection which can have an impact on the humoral response dynamic. Further and similarly to other studies, patients were treated with corticosteroids which may have an impact on the measured immune markers; however, administration was provided according to clinical practice to all patients and blood was collected after maximum 2 days. It is reasonable to think that the exposure to corticosteroids was similar in all patients and thus the putative impact of corticosteroids was negligible. Last point that deserves to be mentioned is that would have been interesting to explore in vitro activation towards SARS-CoV-2 specific peptides but considering that patients were treated with corticosteroids before sample collection, this approach was not feasible due to poor viability of the cells after resting.

Conclusions

The present study indicates that vaccination was protective of worse clinical outcome in individuals older than 70 years, that virus variants driving infection has a direct impact on the shape of the immune response and the set of data presented in this work can guide future studies on the impact of variants on the disease progression and outcome.

Supplementary Information

The online version contains supplementary material available at https://doi.org/10.1186/s12967-024-05556-2.

Supplementary Material 1

Supplementary Material 2

Acknowledgements

We are grateful to the staff of the Ospedale San Raffaele (Italy) and to the participants for their generous contribution. We thank Gabriel Siracusano for contributing to data collection.

Author contributions

AR, CP supervised data collection and analysis and wrote the manuscript. LL designed the study, supervised data collection and analysis, and revised the manuscript. CS and NG performed the flow cytometry data, with the contribution of AM. CPa processed samples and contributed to data collection. FC and CB performed the statistical analysis, under the supervision of MSdS. TF, MMN, NT produced the neutralizing assays. ST and ER processing samples. CUF managed patients' recruitment and data collection. All authors provided input into the analysis and revised the manuscript.

Funding

AR is supported by the Fondo Universitario della Ricerca (FUR, 2023), the MUR 2023/2027 Department of Excellence and the PRIN 2022 (NextGenerationEU, MUR n. 972, CUP B53D23003290001). LL was supported by the Scientific Direction of San Raffaele Scientific Institute (Immuno-COVID) and ANR France (MUCOLUNG). IRCCS Sacro Cuore Don Calabria Hospital was supported by EU funding within the MUR PNRR Extended Partnership initiative on Emerging Infectious Diseases (Project no. PE00000007, INF-ACT), and by Italian Ministry of Health "Fondi Ricerca Corrente" project L1P6. The funding sources had no role in the development of this study.

Data availability

Complete data set is available in Zenodo upon request.

Declarations

Ethics approval and consent to participate

The study was approved by San Raffaele Institutional Ethical Committee in date 14/04/2020, within the non-interventional study "ImmCOVID" and all patients were treated according to Institutional programs upon written informed consent.

Consent for publication
All authors have read and approved the manuscript.

Competing interests
Authors have no interests to declare.

Author details
[1]Department of Neuroscience, Biomedicine and Movement Sciences, University of Verona, Verona, Italy
[2]Department of Infectious, Tropical Diseases and Microbiology, IRCCS Sacro Cuore Don Calabria Hospital, Verona, Negrar, Italy
[3]Division of Immunology, Transplantation and Infectious Disease, Immunobiology of HIV Group, IRCCS San Raffaele Scientific Institute, Milan, Italy
[4]University Centre of Statistics in the Biomedical Sciences, Vita-Salute San Raffaele University, Milan, Italy
[5]Viral Pseudotype Unit, Medway School of Pharmacy, Universities of Kent and Greenwich, Chatham, UK
[6]Infectious Diseases Clinic, IRCCS San Raffaele Scientific Institute, Milan, Italy

Received: 5 June 2024 / Accepted: 29 July 2024
Published online: 12 August 2024

References

1. Billingsley S, Brandén M, Aradhya S, Drefahl S, Andersson G, Mussino E. COVID-19 mortality across occupations and secondary risks for elderly individuals in the household: a population register-based study. Scand J Work Environ Health. 2022;48:52–60.
2. Brandén M, Aradhya S, Kolk M, Härkönen J, Drefahl S, Malmberg B, et al. Residential context and COVID-19 mortality among adults aged 70 years and older in Stockholm: a population-based, observational study using individual-level data. Lancet Healthy Longev. 2020;1:e80–8.
3. Crooke SN, Ovsyannikova IG, Poland GA, Kennedy RB, Immunosenescence. A systems-level overview of immune cell biology and strategies for improving vaccine responses. Exp Gerontol. 2019;124:110632.
4. Fulop T, Larbi A, Dupuis G, Le Page A, Frost EH, Cohen AA, et al. Immunosenescence and Inflamm-Aging as two sides of the same Coin: friends or foes? Front Immunol. 2018;8:1960.
5. Cunha LL, Perazzio SF, Azzi J, Cravedi P, Riella LV. Remodeling of the Immune Response with Aging: Immunosenescence and its potential impact on COVID-19 Immune response. Front Immunol. 2020;11:1748.
6. Lo Tartaro D, Neroni A, Paolini A, Borella R, Mattioli M, Fidanza L, et al. Molecular and cellular immune features of aged patients with severe COVID-19 pneumonia. Commun Biol. 2022;5:590.
7. Yu M, Charles A, Cagigi A, Christ W, Österberg B, Falck-Jones S, et al. Delayed generation of functional virus-specific circulating T follicular helper cells correlates with severe COVID-19. Nat Commun. 2023;14:2164.
8. Ferreira IATM, Lee CYC, Foster WS, Abdullahi A, Dratva LM, Tuong ZK, et al. Atypical B cells and impaired SARS-CoV-2 neutralization following heterologous vaccination in the elderly. Cell Rep. 2023;42:112991.
9. Mazzoni A, Vanni A, Spinicci M, Lamacchia G, Kiros ST, Rocca A, et al. SARS-CoV-2 infection and vaccination trigger long-lived B and CD4 + T lymphocytes with implications for booster strategies. J Clin Invest. 2022;132:e157990.
10. Jeffery-Smith A, Burton AR, Lens S, Rees-Spear C, Davies J, Patel M, et al. SARS-CoV-2–specific memory B cells can persist in the elderly who have lost detectable neutralizing antibodies. J Clin Invest. 2022;132:e152042.
11. Yam-Puc JC, Hosseini Z, Horner EC, Gerber PP, Beristain-Covarrubias N, Hughes R, et al. Age-associated B cells predict impaired humoral immunity after COVID-19 vaccination in patients receiving immune checkpoint blockade. Nat Commun. 2023;14:3292.
12. Hoang TNA, Quach H-L, Hoang VN, Tran VT, Pham QT, Vogt F. Assessing the robustness of COVID-19 vaccine efficacy trials: systematic review and meta-analysis, January 2023. Eurosurveillance [Internet]. 2023 [cited 2024 Jan 22];28. https://www.eurosurveillance.org/content/10.2807/1560-7917.ES.2023.28.22.2200706.
13. Van Ewijk CE, Kooijman MN, Fanoy E, Raven SF, Middeldorp M, Shah A et al. COVID-19 vaccine effectiveness against SARS-CoV-2 infection during the Delta period, a nationwide study adjusting for chance of exposure, the Netherlands, July to December 2021. Eurosurveillance [Internet]. 2022 [cited 2024 Jan 22];27. https://www.eurosurveillance.org/content/10.2807/1560-7917.ES.2022.27.45.2200217.
14. Liu H-H, Xie Y, Yang B-P, Wen H-Y, Yang P-H, Lu J-E, et al. Safety, immunogenicity and protective effect of sequential vaccination with inactivated and recombinant protein COVID-19 vaccine in the elderly: a prospective longitudinal study. Sig Transduct Target Ther. 2024;9:129.
15. Collier DA, Ferreira IATM, Kotagiri P, Datir RP, Lim EY, Touizer E, et al. Age-related immune response heterogeneity to SARS-CoV-2 vaccine BNT162b2. Nature. 2021;596:417–22.
16. Singh C, Naik BN, Pandey S, Biswas B, Pati BK, Verma M, et al. Effectiveness of COVID-19 vaccine in preventing infection and disease severity: a case-control study from an Eastern State of India. Epidemiol Infect. 2021;149:e224.
17. Rahmani K, Shavaleh R, Forouhi M, Disfani HF, Kamandi M, Oskooi RK, et al. The effectiveness of COVID-19 vaccines in reducing the incidence, hospitalization, and mortality from COVID-19: a systematic review and meta-analysis. Front Public Health. 2022;10:873596.
18. Bajpai J, Kant S, Verma A, Patwa AK, Atam V, Chaudhary SC et al. The Severity of COVID 19 Pneumonia in Vaccinated vs. Non-vaccinated Patients in the Second Wave: An Experience From a Tertiary Care Center in India. Cureus [Internet]. 2022 [cited 2024 Jan 22]; https://www.cureus.com/articles/96590-the-severity-of-covid-19-pneumonia-in-vaccinated-vs-non-vaccinated-patients-in-the-second-wave-an-experience-from-a-tertiary-care-center-in-india
19. Balducci M, Locatelli E, Barbieri MG, Ferrighi E, Scardina S, Barrile G et al. SARS-CoV-2 vaccination and risk of infectious diseases in hospitalized older patients. Eur Geriatr Med [Internet]. 2024 [cited 2024 Jan 22]; https://link.springer.com/https://doi.org/10.1007/s41999-023-00902-x
20. https://www.who.int/publications/i/item/diagnostic-testing-for-sars-cov-2.WHO/2019-nCoV/laboratory/20206
21. Marcolungo L, Beltrami C, Degli Esposti C, Lopatriello G, Piubelli C, Mori A, et al. ACoRE: Accurate SARS-CoV-2 genome reconstruction for the characterization of intra-host and inter-host viral diversity in clinical samples and for the evaluation of re-infections. Genomics. 2021;113:1628–38.
22. Marshall JC, Murthy S, Diaz J, Adhikari NK, Angus DC, Arabi YM, et al. A minimal common outcome measure set for COVID-19 clinical research. Lancet Infect Dis. 2020;20:e192–7.
23. https://www.epicentro.iss.it/coronavirus/sars-cov-2-monitoraggio-varianti-rapporti-periodici
24. https://www.iss.it/documents/20126/0/Report_flashVarianti_14gennaio22.pdf/b44b1a7d-a0c1-67fd-44b7-34c8b775c088?t=1642159062435
25. Chia WN, Zhu F, Ong SWX, Young BE, Fong S-W, Le Bert N, et al. Dynamics of SARS-CoV-2 neutralising antibody responses and duration of immunity: a longitudinal study. Lancet Microbe. 2021;2:e240–9.
26. Piubelli C, Ruggiero A, Calciano L, Mazzi C, Castilletti C, Tiberti N, et al. Subjects who developed SARS-CoV-2 specific IgM after vaccination show a longer humoral immunity and a lower frequency of infection. eBioMedicine. 2023;89:104471.
27. Caldrer S, Mazzi C, Bernardi M, Prato M, Ronzoni N, Rodari P, et al. Regulatory T Cells as predictors of clinical course in hospitalised COVID-19 patients. Front Immunol. 2021;12:789735.
28. Ruggiero A, Piubelli C, Calciano L, Accordini S, Valenti MT, Carbonare LD, et al. SARS-CoV-2 vaccination elicits unconventional IgM specific responses in naïve and previously COVID-19-infected individuals. EBioMedicine. 2022;77:103888.
29. Xue J-H, Wang Y-J, Li W, Li Q-L, Xu Q-Y, Niu J-J, et al. Anti–receptor-binding domain immunoglobulin G antibody as a predictor of Seropositivity for Anti–SARS-CoV-2 neutralizing antibody. Arch Pathol Lab Med. 2022;146:814–21.
30. Siracusano G, Ruggiero A, Bisoffi Z, Piubelli C, Carbonare LD, Valenti MT, et al. Different decay of antibody response and VOC sensitivity in naïve and previously infected subjects at 15 weeks following vaccination with BNT162b2. J Transl Med. 2022;20:22.
31. Ferrara F, Temperton N. Pseudotype neutralization assays: from Laboratory Bench to Data Analysis. Methods Protocols. 2018;1:8.
32. Genova C, Sampson A, Scott S, Cantoni D, Neto M, Bentley E et al. Production, Titration, Neutralisation, Storage and Lyophilisation of Severe Acute Respiratory Syndrome Coronavirus 2 (SARS-CoV-2) Lentiviral Pseudotypes. BIO-PROTOCOL [Internet]. 2021 [cited 2024 Jan 22];11. https://bio-protocol.org/e4236
33. Ranzenigo M, Pastori C, Siracusano G, Pariani E, Uberti-Foppa C, Lopalco L. Virological and serological discordant profiles in COVID-19 pneumonia: two atypical clinical cases. Front Immunol. 2020;11:580867.

34. Caldrer S, Accordini S, Mazzi C, Tiberti N, Deiana M, Matucci A, et al. Changes in the Adaptive Cellular Repertoire after infection with different SARS-CoV-2 VOCs in a cohort of Vaccinated Healthcare workers. Vaccines. 2024;12:230.
35. Liu X, Han J, Cui R, Peng M, Song H, Li R, et al. The Promotion of Humoral Immune responses in humans via SOCS1-Mediated Th2-Bias following SARS-CoV-2 vaccination. Vaccines. 2023;11:1730.
36. Leavis HL, Van De Veerdonk FL, Murthy S. Stimulating severe COVID-19: the potential role of GM-CSF antagonism. Lancet Respiratory Med. 2022;10:223–4.
37. Aspinall R. Age-related changes in the function of T cells. Microscopy Res Technique. 2003;62:508–13.
38. Schmitt V, Rink L, Uciechowski P. The Th17/Treg balance is disturbed during aging. Exp Gerontol. 2013;48:1379–86.
39. Bajaj V, Gadi N, Spihlman AP, Wu SC, Choi CH, Moulton VR. Aging, immunity, and COVID-19: how Age influences the host Immune Response to Coronavirus infections? Front Physiol. 2021;11:571416.
40. De Marco L, D'Orso S, Pirronello M, Verdiani A, Termine A, Fabrizio C, et al. Assessment of T-cell reactivity to the SARS-CoV-2 Omicron variant by immunized individuals. JAMA Netw Open. 2022;5:e2210871.
41. Müller TR, Sekine T, Trubach D, Niessl J, Olofsson A, Gao Y, et al. Anamnestic expansion of Omicron-reactive CD8 + T cells after booster SARS-CoV-2 mRNA vaccination across different immunocompromised states. J Immunol. 2023;210:7516–7516.
42. Sigal A, Milo R, Jassat W. Estimating disease severity of Omicron and Delta SARS-CoV-2 infections. Nat Rev Immunol. 2022;22:267–9.
43. Hui KPY, Ho JCW, Cheung M, Ng K, Ching RHH, Lai K, et al. SARS-CoV-2 Omicron variant replication in human bronchus and lung ex vivo. Nature. 2022;603:715–20.
44. Meng B, Abdullahi A, Ferreira IATM, Goonawardane N, Saito A, Kimura I, et al. Altered TMPRSS2 usage by SARS-CoV-2 omicron impacts infectivity and fusogenicity. Nature. 2022;603:706–14.

Publisher's Note